DOCTOR OF PHILOSOPHY

Variations and trends in the sensitivity of machair soils and coastal landforms to erosion, South Uist, Outer Hebrides

Young, Elizabeth

Award date:
2015

The University of Dundee

College of Arts and Social Sciences

Geography (School of the Environment)

VARIATIONS AND TRENDS IN THE SENSITIVITY OF MACHAIR SOILS AND COASTAL LANDFORMS TO EROSION, SOUTH UIST, OUTER HEBRIDES

A Thesis in
Geography

by
Elizabeth Jane Young

Submitted in Complete Fulfillment
of the Requirements
for the Degree of

Doctor of Philosophy

July 2015

ABSTRACT

The machair is a coastal grassland system found only in parts of northern and western Scotland and Ireland. Despite its limited geographic distribution, machair landscapes have high ecological, geomorphological, and cultural significance, as recognised by numerous conservation designations and legislation. In January 2005 a severe storm caused extensive damage in the Outer Hebrides, drawing attention to the sensitivity of the machair coast to erosion. The aim of this research was to investigate variations and trends in the sensitivity of three field sites within the South Uist machair to soil and coastal erosion, and to interpret measured change alongside analysis of historic climate data. Two of the sites selected, Cille Pheadair and Staoinebrig, experienced some of the most dramatic geomorphological changes associated with the 2005 storm, while the third site, Milton, appeared to be more resistant to change. A combination of fieldwork, laboratory tests, and archive work was used to obtain and analyse information about sediment budgets, shoreline indicator change, and sediment erodibility, along with contextual climatic information.

A key result of this work is the provision of a detailed framework of short-medium term cyclical changes and fluctuations in the coastal change, which provides a context for interpreting and responding to longer term trends in erosion and/or accretion. Results indicated high spatial and temporal variability in the erodibility of machair soils and landforms, with no clear relationship between climatic factors and rates of erosion. Considerable short-term variations in beach volume and the position of dynamic shoreline indicators caution against the relaibility of using ‘snap-shot’ historic datasets to infer long-term rates of change. It is proposed that the machair landscape currently functions in a state of highly dynamic equilibrium, which has been maintained over the last ~130 years. While storm events such as the January 2005 storm have locally dramatic consequences, they do not appear to have disrupted the overally physical and ecological functions of the system. This contribution is particularly timely given current concerns for the future of the machair landscape under predicted sea-level and climate change scenarios, and the potential for inappropriate hard-engineering responses to the perceived risk.

DECLARATION

I declare that I, Elizabeth Jane Young, am the author of this thesis. All references cited, unless otherwise stated, have been consulted by myself. The work of which this thesis is a record has been done by myself, and it has not previously been accepted for a higher degree.

ACKNOWLEDGEMENTS

I thank my supervisors, Dr Sue Dawson (Geography, University of Dundee) and Dr Blair McKenzie (Environmental and Biochemical Sciences, the James Hutton Institute), who have provided support and guidance throughout my PhD. Thank you for helping me to find resources, putting me in touch with many interesting and helpful people, and for challenging me.

From the University of Dundee I thank: Mr Craig Phillips (Laboratory Technician, Frankland Laboratory) for showing me how to use lots of lab equipment and for helping me get through many particle size analyses; and Mr Alan Long (Field Technician, Frankland Laboratory) for helping me with the RTK-dGPS and many cups of tea.

From the James Hutton Institute I thank: Dr Jean Robertson (Environmental and Biochemical Sciences) for her interest in my research, and assistance with organising and interpreting FTIR analysis of my soil samples; Dr Rachael Hill and Dr Angela Main for assistance with FTIR analysis; Dr Barry Thornton for assistance with stable isotope analysis; Dr Charlie Shand and Renate Wendler for assistance with XRF analysis; Dr Jayne Smith for assistance on fieldwork; Dr Paul Hallett for assistance with setting up and interpreting experiments associated with water repellency and infiltration rates; and Mr Jim McNichol for his invaluable assistance with statistics.

From Comhairle nan Eilean Siar: Mr David Muir for providing me with a great deal of very helpful information on the Outer Hebrides; and Mr Donald John MacDonald for providing me with technical information and drawings of the ridge at Stoneybridge.

From the University of Aberdeen: Prof Ali Dawson for his interest in my thesis and provision of historic weather data.

From the Meteorological Office: Lynn Chambers for helping me to find useful weather records.

Additionally I thank Diana Bell, Alan Bell, Iain Woolley, and Neil Milton, Frankie and Jess, for their assistance and company on field trips. I also thank Neil Milton for proof-reading this thesis.

TABLE OF CONTENTS

LIST OF FIGURES

Figure 5.9. Storm and gale day frequencies from 1867-2014. A) annual totals, B) decadal totals. A 5th order polynomial trend line is fitted to the annual total number of gales.

Figure 5.10. Wind rose showing wind direction gale and storm events (events where wind speed ≥ 34 kts) (n=5,933). Wind rose generated using WindRose Pro (Enviroware).

Figure 5.11. The annual no. of storms plotted against the annual total number of storm and gale events for the period from 1867-2014.

Figure 5.12. Mean annual wind speed from A) 1929-1945, B) 1957-2014.

Figure 5.13. Highest monthly gust speeds (October-March).

Figure 5.14. Wind roses for A) 1928-2014; B) 1928-1939; C)1940-1950; D)1957-1985; E) 1986-2014. Note that for A) the frequency counts for each wind direction from 1957-2014 were divided by 40 so that the number of readings per year was comparable in order of magnitude to the earlier period when measurements were less frequent.

Figure 5.15. Annual mean atmospheric pressure (hPa). Data from 1867-1956 is from the Monach Isles; data from 1957-2013 is from Benbecula. On average, annual mean air pressure values from the Monach Isles were found to be 0.3 hPa higher than those from Benbecula.

Figure 5.16. Mean annual tide gauge levels from Stornoway, 1976-2013.

Figure 5.17. Annual NAO index values from 1867-2013. 1867-1949 values are from the Climate Research Unit; 1950-2013 values are from the Climate Prediction Centre.

Figure 5.18. JFM and OND storminess from 1867-2013.

Figure 6.1. Map of transect positions and polylines digitised from the position of MHWOST on OS maps at Cille Pheadair.

Figure 6.2. Maps of the island of South Uist with location of field sites marked by black boxes (locations approximate on map A). A) Blau 1654 map; B) Bald 1805 estate map; C) Ordnance Survey 2010 map. Maps A and B reproduced by courtesy of the National Map Library of Scotland. Map C contains Ordnance Survey data. (c) Crown copyright and database right 2010. Data provided by Digimap OpenStream, an EDINA, University of Edinburgh Service.

Figure 6.3. Maps of each of the three field sites in 1805 (Blau) and 2010 (Ordnance Survey). The 1805 Blau map is reproduced by courtesy of the National Map Library of Scotland. The 2010 map contains Ordnance Survey data. (c) Crown copyright and

database right 2010. Data provided by Digimap OpenStream, an EDINA, University of Edinburgh Service.

Figure 6.4. Changes in the position of MHWOST between 1878-2002. The 0 line represents the position of MHWOST in 1878. Vertical axis indicates transect number (profile no. x 10 = distance (m) from northern end of site). A. Staoinebrig. B. Milton. C. Cille Pheadair.

Figure 6.5. Temporal variations in EPR. A. Staoinebrig. B. Milton. C. Cille Pheadair.

Figure 6.6. EPR (1878-2002) at Staoinebrig (SB), Milton (M), and Cille Pheadair (CP). Transects are numbered from the northern to southern end of each site.

Figure 6.7. Boxplot comparisons of A. EPR, and B. NSM, at Staoinebrig (SB), Milton (M), and Cille Pheadair (CP).

Figure 6.8. Changes in the position of the vegetation between 1948-2005. The 0 line represents the position of the vegetation line in 1948. Vertical axis indicates transect number (profile no. x 10 = distance (m) from northern end of site). A. Staoinebrig. B. Cille Pheadair. The red boxed area indicates the section of the site for which the 1948 imagery was unclear.

Figure 6.9. Temporal variations in EPR. A. Staoinebrig. B. Cille Pheadair.

Figure 6.10. EPR (1948-2005) at Staoinebrig (SB) and Cille Pheadair (CP). Transects are numbered from the northern to southern end of each site.

Figure 6.11. Boxplot comparisons of A. EPR, and B. NSM, at Staoinebrig (SB) and Cille Pheadair (CP).

Figure 7.1. Idealised semi-variogram with key features annotated.

Figure 7.2. Combined position and height data quality against datum number. Outliers (outlined in black) were removed prior to DTM creation. This dataset is from the beach survey of Cille Pheadair, conducted in October 2011.

Figure 7.3. Photographs from Stoneybridge., A. October, 2011. B. March 2012, C. June 2012, D. February 2013, E. March 2013, F. November 2013, G. March 2014. Photographs from the January 2013 surveys are omitted due to poor image quality caused by inclement weather conditions. Similarly, only two photos are included from the October 2011 visit due to heavy rain.

Figure 7.4. Planimetric change in the machair front and crest of the shingle ridge between 2005 and March 2014. Vertical axis indicates transect number, numbered from north-south of site (spaced at 10 m alongshore intervals). The grey box indicates likely greater error (up to ~ 2 m) due to break down of the shingle ridge.

Figure 7.5. Aerial photograph (left) and LiDAR derived DTM (right) of Staoinebrig in November 2005. Area corresponds to 450 m to 630 m from the northern end in Fig 7.4. Note the area of high elevation in the centre of the lower image which terminates abruptly.

Figure 7.6. Aerial photograph of Staoinebrig showing the position of MHWN (seaward black line) and MHWS (landward black line). Note the proximity of MHWS to the crest, and the proximity between MHWS and MHWN in the southern section of the beach.

Figure 7.7. Changes in beach face elevation at Staoinebrig between November 2005 and March 2014. Green areas initiate accretion and red areas indicate erosion. The grey section indicates intertidal rock outcrop.

Figure 7.8. show changes in elevation between each subsequent survey.

Figure 7.9. Photographs from Milton., A. October 2011, B. March 2012, C. June 2012, D. January 2013, E. February 2013, F. March 2013, G. March 2014. Due to technical problems with the RTK-dGPS there was insufficient daylight time to photograph Milton during the November 2013 field visit.

Figure 7.10 Position of the dune crest in March 2014 relative to the November 2005 position. Changes from transect 1-61 were less than the method error.

Figure 7.11. Position of the dune crest at the southern end of Milton in November 2005 and March 2013, superimposed on aerial photography of the site © SNH on behalf of the Western Isles Data Partnership.

Figure 7.12. Aerial photography of Milton showing the MHWN (seaward black line) and MHWS (landward black line).

Figure 7.13. Map of changes in beach face elevation at Milton between November 2005 and March 2014. Green areas initiate accretion and red areas indicate erosion.

Figure 7.14 Changes in elevation between each subsequent survey.

Figure 7.15. Photographs from Cille Pheadair., A. October 2011, B. March, 2012, C. June, 2012, D. January 2013, E. February 2013, F. March, 2013, G. November 2013, H. March 2014.

Figure 7.16. Planimetric change in the position of the vegetation line relative to the November 2005 position. The grey box indicates the position of the artificial bund.

Figure 7.17. Aerial photograph of Cille Pheadair showing the position of MHWN (seaward black line) and MHWS (landward black line). Note the proximity of MHWS to the crest at the headland, compared to the relative distance of MHWN at this point.

North of the headland the position of MHWS appears to have been affected by densely packed seaweed in the intertidal zone.

Figure 7.18. The beach north of the coastal defence ridge at Cille Pheadair showing accumulated seaweed across the majority of the sub aerial beach face. In places the seaweed is sufficiently densely packed that pools of water have formed on the surface. View to the north, October 2011.

Figure 7.19. Aerial photography of Cille Pheadair from November 2005. Note the large quantities of seaweed on the northern section of the beach.

Figure 7.20. a) LiDAR-derived DTM of Cille Pheadair from November 2005. Reflections apparently coinciding with the seaweed accumulations shown in Figure 5.36 are indicated by arrows. b) Cross-shore profile (location marked by line A-B on Figure 5.37a) with elevations which may be derived from reflections from seaweed circled in red.

Figure 7.21. Changes in beach face elevation at Cille Pheadair between November 2005 and March 2014. Green indicates accretion and red indicates erosion.

Figure 7.22. Changes in elevation between subsequent survey.

Figure 7.23. Boxplots comparing A) EPR, and B) NSM, between the three sites (November 2005-March 2014). Green crosses are positive outliers; red crosses are negative outliers.

Figure 7.24. Changes in beach volume above minimum elevation planes from November 2011 to March 2014.

Figure 7.25. Beach volume change at all three sites from November 2011 to March 2014.

Figure 7.26. Volume change as a percentage of net volume change above the lowest elevation planes for each site.

Figure 7.27. Changes in volume as a percentage of net volume change from November 2005 to March 2014. The sign (positive or negative) of the bars indicates whether change over each interim period was in the same direction (loss or gain of volume) as net change.

Figure 8.1. Aerial photographs of the three sites showing the sampled transects. A. Cille Pheadair. B. Milton. C. Tobha Mor. Black lines indicate the positions of sampled transects.

Figure 8.2. Rotary sieve after the design of Tisdall et al. 2012.

Figure 8.3. Mass (g) of air-dried soil passing through the rotary sieve over 300 s for samples from CP. Labels indicate the distance of the sample from the coast. Error bars indicate 2 x SE.

Figure 8.4. Regression of mean WAR values for each sample against distance from the coast for Cille Pheadair, Milton, and Tobha Mor. Note that the maximum possible value for WAR is 40.

Figure 8.5. M (g) of air-dried soil passing through the rotary sieve over 300 s for samples from M. Labels indicate the distance of the sample from the coast. Error bars indicate 2 x SE.

Figure 8.6. Mass (g) of air-dried soil passing through the rotary sieve over 300 s for samples from TB. Labels indicate the distance of the sample from the coast. Error bars indicate 2 x SE.

Figure 8.7. Box plot of Wind Abrasion Resistance data from CP, M, and TB showing mean, median and standard deviation.

Figure 8.8. Percentage of each 40 g sample that was erodible, potentially erodible, and non-erodible, with distance from the coast at CP.

Figure 8.9 Percentage of each 40 g sample that was erodible, potentially erodible, and non-erodible, with distance from the coast at M.

Figure 8.10. Percentage of each 40 g sample that was erodible, potentially erodible, and non-erodible, with distance from the coast at TB.

Fig. 8.11. Proportion (by mass) of sample material < 850 μm in diameter to the proportion (by mass) of sample material which passed through the rotary sieve with mesh size 850 μm. A. CP. B. M. C. TB.

Figure 8.12. Scatterplots of soil properties against WAR for soil properties with statistically significant positive relationships with WAR. a)Zinc, b) LOI, c) water content, d) As, e) Co, f) distance from the coast, g) PS (skewness).

Figure 8.13. Scatterplots of soil properties against WAR for soil properties with statistically significant negative relationship with WAR. a) PS, b) Sr, c) Ca, d) WDPT class, e) bulk density, f) Cr, g) Cu.

Figure 8.14. Scatterplots of soil properties against WAR for soil properties with no statistically significant relationship with WAR. a) PS (kurtosis), b) WDPT (mean time), c) water repellency, d) pH, e) K, f) Ti, g) Mn, h) Fe.

Figure 8.15. FTIR data showing a) spectra for the most coastal sample from each site, and b) spectra for the most inland sample from each site. The main carbonate stretch is

LIST OF TABLES

which hourly weather data are available); min. pressure data was available from 1957-2014; max. significant wave height data was available from 2009-2014.

Table 5.8. General summary of results. The generalised character indicates the nature of the measured variable relative to data from the rest of the time-series.

Table 5.9. Trends in storminess (as indicated by gale day frequency) over different temporal scales determined by linear regression.

Table 6.1. Details of all maps with spatial coverage of Staoinebrig, Milton, and/or Cille Pheadair. (EDM = Edina Digimap; NMLS = National Map Library of Scotland). N.B. Dates indicate year when surveying was conducted (as opposed to publication date).

Table 6.2. Details of all aerial photographs with spatial coverage of Staoinebrig, Milton, and/or Cille Pheadair. NCAP = National Collection of Aerial Photographs; CUCAP = Cambridge University Collection of Air Photos; SNH = Scottish Natural Heritage on behalf of the Western Isles Data Partnership.

Table 6.3. Details of all data sources selected to analysis coastal change.

Table 6.4. Estimations of maximum planimetric error in the position of linear features indicating the position of high-water levels from a range of authors.

Table 6.5. Number of GCPs and RMSE for each georectified photograph.

Table 6.6. Definitions and descriptions of shoreline change data generated using the DSAS extension (adapted from information provided in Himmelstoss, 2009).

Table 6.7. Comparison of mean NSM and EPR values for the northern and southern sections of the Staoinebrig site.

Table 6.8. Comparison of mean NSM and ESR values for the headland and the rest of the site at Cille Pheadair.

Table 6.9. Comparison of mean NSM and EPR values for the three sites.

Table 6.10. Comparison of mean NSM and EPR values for the northern and southern sections of the Staoinebrig site.

Table 6.11. Comparison of mean NSM and ESR values for the headland and the rest of the site at Cille Pheadair.

Table 6.12. Comparison of mean NSM and EPR values for the two sites.

Table 6.13. EPR values obtained from photographs and maps.

Table 6.14. Summary of relative EPR values and climate information. Data source of EPR value is indicated next to time period (m = map, p = photo). EPR indicators are as follows: S = stable (median EPR = -0.01-0.01), L = low (median EPR = ± 0.01-0.1), H

= high (median EPR = >/< ± 0.1). Plus and minus signs indicate EPR direction. Climate summary data is obtained from Table 9.1.

Table 7.1. Dates and aims of field surveys.

Table 7.2. Mean data quality (combined position and height) values and standard deviations for all surveys.

Table 7.3. Mean, maximum, and minimum differences between actual data and estimated values, and root-mean-square error, for each profile spacing tested. Maximum and minimum difference values indicate maximum and minimum error, and disregard the sign of the difference.

Table 7.4. Mean, maximum, and minimum differences between actual data and estimated values, and root-mean-square error, for each interpolation method. Maximum and minimum difference values indicate maximum and minimum error, and disregard the sign of the difference.

Table 7.5. Mean, maximum, and minimum differences between actual data and estimated values, and root-mean-square error for each model. Maximum and minimum difference values indicate maximum and minimum error, and disregard the sign of the difference.

Table 7.6. Maximum difference between the mean elevation values for all ten control points for any combination of two survey datasets.

Table 7.7. Table showing the area, δe, and δV values for each site.

Table 7.8. Comparison of EPR and NSM for the machair front and shingle ridge.

Table 7.9. Numerical summary of elevation changes occurring at Staoinebrig.

Table 7.10. Numerical summary of volumetric changes at Staoinebrig. Volumes are measured relative to a planar surface set at the minimum measured elevation (-3.5 m in February 2013). Percentage change is calculated relative to previous beach volume.

Table 7.11. Results of Student's T-test (two tailed, unequal variance) for each RTK-dGPS survey interval.

Table 7.12. Summary of elevation changes at Milton.

Table 7.13. Summary of volumetric changes at Milton. Volumes are relative to a planar surface set at the minimum measured elevation (-4.83 m in February 2013). Percentage change is calculated relative to previous beach volume.

Table 7.14. Results of Student's T-test (two tailed, unequal variance) for each RTK-dGPS survey interval.

Table 7.15. Mean NSM and EPR for the parts of Cille Pheadair located north and south of the artificial ridge.

Table 7.16. Numerical summary of elevation changes occurring at Cille Pheadair.

Table 7.17. Summary of volumetric changes at Cille Pheadair. Volumes are relative to a planar surface set at the minimum measured elevation (-2.18 m in March 2013). Percentage change is relative to previous beach volume.

Table 7.18. Results of Student's T-test (two tailed, unequal variance) for each RTK-dGPS survey interval.

Table 7.19. Climatic and coastal change data for the three winter seasons investigated. Mean Atm. P = mean atmospheric pressure; mean WS = mean wind-speed. Bold text indicates the value in each column indicative of highest storminess.

Table 7.20. Relationships (R^2) between climatic parameters and beach volumes. SB (Staoinebrig), M (Milton), and CP (Cille Pheadair) are relationships with data from each site. 'All' refers to relationships between climatic factors and data from all sites, normalised to prevent differences in the original size of the beach affecting the relationship. + indicates positive relationships; - indicates negative relationship. Significance of relationship is : *** ($p < 0.01$); ** ($p < 0.05$); * ($p < 0.01$).

Table 7.21. Mean EPR values obtained from analysis of change in the position of the vegetation line/crest over short (2005-2014) and long (1948-2005) timescales.

Table 8.1. WDPT classes and ratings for the severity of water repellency along with the associated penetration time classes. Modified from Doerr et al. (2006). t(s) indicates time in seconds.

Table 8.2 Wind abrasion resistance of each sample, and rankings for the samples in terms of distance from the coast (ranked closest to furthest) and abrasion resistance (ranked lowest to highest) at CP.

Table 8.3 Wind abrasion resistance of each sample, and rankings for the samples in terms of distance from the coast (ranked closest to furthest) and abrasion resistance (ranked lowest to highest) at M.

Table 8.4 Wind abrasion resistance of each sample, and rankings for the samples in terms of distance from the coast (ranked closest to furthest) and abrasion resistance (ranked lowest to highest) at M.

Table 8.5. R values for linear regressions of soil variables against WAR for samples from all sites. Statistical significance (2-tailed T-test) is indicated by asterisks ($p < 0.1$ = *, $p < 0.05$ = **, $p < 0.01$ = ***).

Table 9.1. Key factors from Figure 9.1that inform an index of machair coastal sensitivity, and description of each factor for each site. '% DC<WL' refers to the length of crest below current MHWOST (as investigated in Chapter 4). The number in brackets indicates the percentage of crest below water levels under the most extreme high water scenario investigated in Chapter 4. 'Sediment budget' is the net volume change between 2005-2014.

Table 9.2. Descriptive results from Table 9.1 assigned numerical values to provide an index of machair sensitivity. T indicates total for each site and provides a relative indication of the sites sensitivity. Higher values indicate higher sensitivity.

CHAPTER 1
INTRODUCTION

Synopsis:
This chapter describes the machair system, defines key terminology used in this thesis, and provides the rationale for investigating erosion in the machair landscape.

In January 2005 a severe storm caused widespread damage along the Atlantic coast of the southern Outer Hebrides. The effects of the storm drew attention to the sensitivity of the machair soils and landforms to erosion, and raised concerns that the machair coast is becoming increasingly susceptible to storms due to the cumulative effects of rising sea-level and a negative sediment budget. These conditions have prevailed since the mid-Holocene, but accelerated rates of sea-level rise since the Industrial Revolution, and changes in management of the machair since the 1940s, are thought to have exacerbated erosion (Gordon et al., 2014).

This thesis investigates erosion of machair soils and landforms at three sites in South Uist, the Scottish Outer Hebrides, with an emphasis on assessing change in the coastal zone. Spatial and temporal trends in the rate and volume of erosion of coastal landforms are evaluated. Spatial trends in soil erodibility and the relationship between erodibility and soil properties are also examined. Additionally, climatic variations and their association with erosion are explored.

1.1 Background

1.1.1 Definition of machair

'Machair is a Gaelic word, used by native speakers in western Ireland and the Scottish Highlands and Islands to describe low-lying coastal grasslands found immediately inland of the beach and dunes. The term may also refer to the full geomorphic system which extends from the offshore sediments to the 'blacklands' (a transition zone between the sandy machair soils and inland peats) and includes the beach, dunes, and grasslands (Fig. 1.1) (Ritchie, 1966; Angus, 1999; 2006).

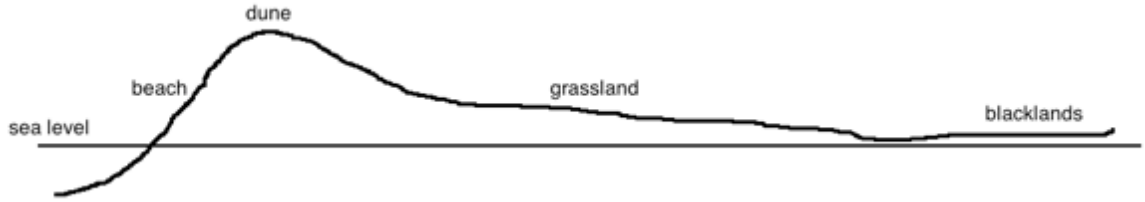

Figure 1.1. Cross-section of idealised machair system extending from the beach to the blacklands (after Angus, 2001).

Ritchie (1976; 1979) provided the first definition of the machair, which includes the following criteria:

- geomorphologically mature, low-gradient surface;
- soil with a substantial percentage of calcareous shell fragments, and a pH which is normally alkaline;
- an oceanic location with a cool, wet climate;
- sandy grassland type vegetation lacking long dune-grasses;
- evidence of biotic interference caused by grazing, trampling, cultivation, and sometimes artificial drainage in the recent historical period; and
- a tendency to flood or become marshy in the winter.

This is the most comprehensive published definition of the machair, and applies only to the grasslands.

For this thesis which focuses on the physical aspects of the machair, the distinction between the system as a whole and its components is important. To avoid confusion the full system will be referred to as 'machair'. Where a distinct component of the machair is discussed it will be added to the term, e.g. 'machair coast, 'machair grassland'.

1.1.2 Evolution of the machair

The machair was formed by the onshore movement of glacial and calcareous sediments due to Holocene relative sea level rise, and is approximately synchronous with the evolution of other dune systems in north-west Europe (Clarke and Rendell,

2009). Sediments were subsequently re-worked and re-deposited by further aeolian and wave action. These processes have continued to exert an important influence on the evolution of the machair throughout the Holocene. Interaction with local and regional factors (e.g. climate, coastal orientation, geology) has altered the effects of wind and wave erosion, leading to a complex stratigraphy.

The wide range of dates of earliest sand movement established by Ritchie and Whittington (1994), Gilbertson et al. (1999), and Ritchie et al. (2001) provide strong evidence for non-synchronous initiation of machair formation, initially suggested by Ritchie and Whittington in 1994, and supported by later work, which emphasise the importance of site-specific factors, e.g. coastal orientation and topography (Ritchie et al., 2001). The theory of non-synchronous machair formation is further reinforced by the lack of regional synchronicity in some later sand blow events (Gilbertson et al., 1996; Ritchie et al., 2001), and also in historical and contemporary records. These show that even regional events, such as storms, may cause sediment movement in one locality, and have negligible impacts on others.

The theory of machair formation and evolution has developed since the mid-1960s when Ritchie began to explore the origins of the system (e.g. Ritchie, 1967, 1979). His work was the first to identify the relationship between the coastal dunes and the machair grassland, establishing that the machair grassland was formed by the deposition of sand eroded from the dunes, and the grassland's reliance on new inputs of sand for its maintenance. Ritchie (1979) identified key periods of machair dune building due to the onshore movement of shelf sediments between ~7-4.5 kya. His work was further developed by Gilbertson who used emerging dating techniques to identify multiple sand-blow events and periods of both stability and instability throughout the evolution of the machair (e.g. Gilbertson et al., 1996, 1999). The detailed stratigraphic work carried out by Gilbertson et al. (1996, 1999) led to the discovery of machair stratification (the inter-layering of wind-blown sand and more organic rich soil horizons), and this raised the question of the role of humans in machair formation. During the 2000's Hansom and Angus have synthesised information on the machair to provide the currently accepted model of machair evolution (e.g. Angus, 2001; Hansom and Angus, 2001, 2005). Their work has established the importance of changes in the rate of relative sea-level (r.s.l.) rise and climate on machair formation, as well as raising concerns for the future of the machair. Most recently, Cooper et al.

(2012) suggested that the bedrock morphology of the Lewisian gneiss strandflat – which underlies much of the western side of the southern Outer Hebrides – has acted as a further control on the development of the characteristic machair morphology shown in Figure 1.1.

1.1.3 Distribution of the machair

The geographical extent of the machair is limited to parts of northern and western Scotland (Fig. 1.2), and some small sites in north-west Ireland. There is considerable uncertainty in the exact area of machair, due to the difficulty of identifying both the machair grassland and the wider machair system in the field (Angus, 2001; Angus, 2006). The total global extent of the machair is thought to be 30-40,000 ha, with machair grassland accounting for ~25,000 ha of this (Angus, 1994; Hansom and Angus, 2005; JNCC, 2007). More than half of Scotland's machair is in the Outer Hebrides, with the most extensive areas on South Uist.

Figure 1.2. Map of Scotland showing the machair habitat range (shaded grey), and the location of South Uist (ringed in black) (adapted from JNCC, 2007).

1.1.4 The 'Great Storm' of January 2005

On the 11th and 12th of January 2005 a severe storm highlighted the sensitivity of the western coast of South Uist to erosion. The storm was caused by a northwest tracking cyclone with a central pressure of 935 hPa (Dawson et al., 2007a). The extremely low pressure and high wind speeds (max velocity ~ 170 km/h) coincided with high spring tides, causing a storm surge of up to 2 m (Dawson et al., 2007a) in South Uist, with localised observations indicating even higher surges in North Uist and Benbecula (Angus and Rennie, 2014). The exposed Atlantic coastline of South Uist was particularly vulnerable as the predominant wind direction during the storm was from the south and west.

The morphological effects of the storm were varied, including: coastal retreat; erosion/breaching of the dune face and machair front (Angus and Rennie, 2014); widespread deposition of storm debris; and severe flooding (Moore et al., 2005; Dawson et al., 2007a). Local people described the storm as the "worst in living memory", and were adversely affected by widespread damage to infrastructure. Roads were damaged and covered with storm debris, and property destroyed (Richards and Phipps, 2007). In addition, agricultural land was lost to coastal retreat, and damaged by flooding and storm debris. In some areas, the coast retreated more than 10 m due to the storm, and the coastline remains vulnerable to over-wash and flooding. Tragically, the January 2005 storm also caused the loss of life when a family trying to escape the rising flood waters drowned.

Angus and Rennie (2008, 2014) surmised that although the geomorphological effects of the storm were dramatic for a single event, they were probably only slightly greater than during a standard winter, and within the bounds of expected coastal dynamism. This suggests that the machair system may be currently relatively-resilient to storm events. However, the loss of life, disruption to services, and widespread damage to infrastructure has raised concern among local people and authorities about future erosion.

1.2 Sensitivity, Resilience, and Resistance

Sensitivity is a concept used to consider the susceptibility of a system, or a system's components, to change. The concept of 'sensitivity' has been used in a range of disciplines, and has numerous interpretations. In this work Brunsden's (2001) definition of sensitivity in the context of landscape change is adopted, with sensitivity defined as 'the spatial variation in the ability of a landscape to change'. The ability of a landscape to change is a function of complex interactions between external and internal properties. The internal properties of the system may have varying degrees of resilience or resistance to change over temporal and spatial scales, and equally the magnitude and frequency of external forces capable of disturbing the system may also vary. When the strength of the external force is greater than the resilience and resistance of the system, a threshold will be crossed and the system will undergo a major change, and shift to a new equilibrium (Schumm, 1979). Such a shift in equilibrium may have major consequences for humans if it involves changes in the services the physical system provides, or its capacity to maintain pre-existing ecosystem services.

The resistance of a system can be thought of as the magnitude and/or frequency of external forces which it can withstand without undergoing a major change in function or form (Brunsden, 2001). The resilience of a system can be considered the ability of a system to recover following a disturbance, i.e. its ability to bounce back to conditions which are qualitatively (if not quantitatively) similar to the original system (Brunsden, 2001). When the resilience and resistance of the system is overcome by external forces, i.e. the system is unable to resist change, and is also unable to recover and return to its original form and function in the wake of a disturbance, a shift in the system's equilibrium will occur, with associated changes in form and function (Schumm, 1979). The new conditions are maintained until a further disturbance of sufficient magnitude and/or frequency overcomes the resilience and resistance of the system in its new equilibrium position. Resilience and resistance are likely to vary widely both between and within landscapes due to variations in the materials and landforms which influence resilience and resistance to change. This gives rise to the 'spatial variation in the ability of a landscape to change', identified by Brunsden (2001) as the sensitivity of a landscape.

Sudden and dramatic changes in a physical system, occurring when external forces exceed the system's capacity to withstand them and lead to critical thresholds being crossed, tend to attract the most attention due to their often high and undesirable impacts on human activities and infrastructure. However, these shifts in equilibrium are superimposed on a background of constant, gradual change, which is the norm in most physical systems. Continual, minor changes may pre-condition the system, gradually wearing down its capacity for resistance and resilience, and leading to a situation where internal thresholds for change can be approached without any significant external forces being recorded (Phillips, 2009). This pre-conditioning of the system can result in relatively minor changes in external forces causing seemingly large thresholds to be crossed to new equilibrium positions (Phillips, 2009), which may lead to dramatic changes in the function of the system.

With reference to the coastal machair system of the Outer Hebrides, the major internal properties likely to influence the system's sensitivity are variations in machair landforms and soil properties. The major external forces with the capacity to cause change in the machair system are climatic events (particularly storms, but also periods of reduced precipitation or enhanced wind speeds) and changes in relative sea-level. Anthropogenic activities, particularly certain agricultural practices, are also capable of influencing susceptibility to erosion.

1.3 Layout of the Thesis

This thesis contains 10 chapters, including the introduction:

- Chapter 2 (Literature Review) provides a review of machair erosion (including a summary of machair landforms and sediments, and the erosive forces acting on the machair system) and details the aims of this work;

- Chapter 3 (Field Sites) describes the three field sites used in this research, including their location, geomorphology, land use, and management;

Chapters 4-8 include results and their interpretations for each of the investigations undertaken as part of this research:

- Chapter 4 (Results and Analysis) provides an initial indication of the sensitivity of the three sites to flooding and erosion;

- Chapter 5 (Results and Analysis) details research investigating recent and historic storm climatology in the southern Outer Hebrides;

- Chapter 6 (Results and Analysis) details investigations of long-term coastal change;

- Chapter 7 (Results and Analysis) details investigations of short-medium term coastal change;

- Chapter 8 (Results and Analysis) details investigation of trends and variations in the wind abrasion resistance of machair soil;

- Chapter 9 (Discussion) discusses the implications of the findings with regards to the machair system and its management, considers the limitations of the thesis, and provides suggestions for further work;

- Chapter 10 (Conclusion) summarises the main findings of the research.

CHAPTER 2
LITERATURE REVIEW

Synopsis:
This chapter reviews erosion of the machair landscape of the southern Outer Hebrides, focusing on the sensitivity of machair soils and landforms to erosion, erosive forces acting on the machair, and a summary of the available qualitative and quantitative information on machair erosion.

2.1 Introduction

The fragile nature of the machair ecosystem and its sensitivity to changes in climate and land-use are widely acknowledged and the subject of numerous studies (e.g. Angus 1994; Owen et al., 2000; Angus and Dargie, 2002; Lewis et al., 2014). While the sensitivity of the physical components of the machair system has also been acknowledged (e.g. Seaton, 1968; Angus and Elliot, 1992; Angus and Rennie, 2008), particularly in the wake of the January 2005 storm, this aspect of the machair system has received less attention in the academic literature. A meta-analysis of papers published on the machair between 1950 and 2014 (Web of Knowledge) reveals that the majority of research is on biological and ecological topics, with geological and geographical themes receiving less attention (Fig. 2.1); 76% of all papers considered machair ecology (including biodiversity and conservation), 50% of papers considered machair biology (including animal behaviour, entomology, ornithology, parasitology, and zoology). This is in comparison to just 11% of papers which consider aspects of machair geography (including physical and human geography), and 12% of papers which considered purely physical aspects of the machair system (including geomorphology and geology). The advent of technologies since the 1990s (e.g. LiDAR, RTK-dGS, GIS) has made it possible to quantitatively investigate physical change in the machair system, with recent reductions in cost and improvements in productivity enhancing the range of investigations which can be undertaken (e.g. Dawson et al., 2007b, 2012).

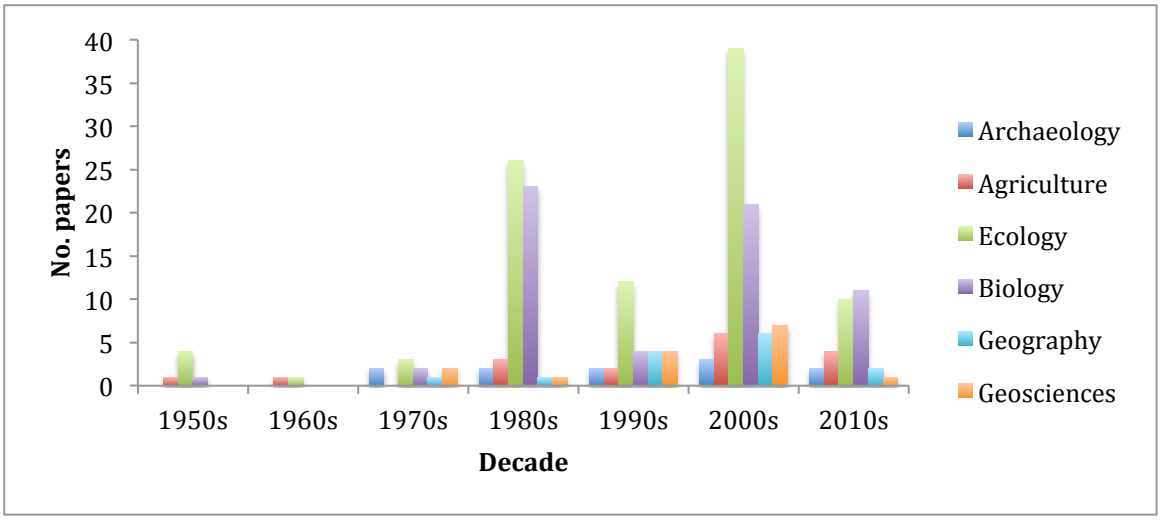

Figure 2.1. The number of published research articles on the machair on Web of Knowledge, broken down by discipline, as of February 2015. Multi-disciplinary papers were counted in all relevant categories. Number of papers = 124.

2.2 Machair Sediments and Geomorphology

The machair overlies a strandflat surface composed of Lewisian gneiss (Cooper et al., 2012), which extends offshore as a low gradient shelf. The machair coast developed during the early and mid-Holocene when large volumes of sand were brought onshore by rising sea-levels (Ritchie, 1979). These sediments were reworked by marine and aeolian processes to form an extensive dune complex. Periods of intense aeolian activity redistributed some of the sediments inland to form the low-lying machair grasslands, with the regional and local morphology dependent on variations in the bedrock surface (Cooper et al., 2012). It is also thought that the southern Outer Hebrides may be an example of an extensive barrier island system, with topographic expression controlled by the elevation of the strandflat surface (Cooper et al., 2012). Between periods of sand blow the windblown sands have been colonised by plants, leading to the development of thin soils. During episodes of climatic instability the soils are buried by sand, producing a soil profile characterised by alternating layers of sand and soil, known as machair stratification (Gilbertson et al., 1996).

Sandy, alkaline soils and a low-lying geomorphologically mature surface are two of the defining characteristics of the machair system. In general, machair soils have an organic matter content < 10% (Dickinson, 1975), and a carbonate shell sand content

up to 95% (Ritchie, 1974; Dickinson, 1975; Randall, 2004). The topography is generally low gradient and at a similar elevation to relative sea-level (r.s.l.). However, there is considerable variation both between and within machair systems; in particular there is a distinctive sequence of landforms and sediments on moving inland from the coastline. This sequence includes the beach, dunes, grasslands, and 'blacklands' (a transition zone between the machair and the inland peats).

2.2.1. Sediment source and supply

During the Devensian glaciation (110-12 kya), large quantities of glacial till were deposited across the continental shelf to the west of the Uists by the Scottish ice sheet (Hall, 1996). These siliceous glacial sands were moved onshore by the rise in relative sea-level during the Holocene, and are one of the main sediment sources for the machair system. The only other major sediment supply is from offshore calcareous sands, consisting of the shell detritus from past and present marine organisms (Mate, 1992; Gilbertson et al., 1999). As the Uists have no sea cliffs or major rivers, offshore shelf sediments represent the only significant sediment source for the machair.

The machair system was formed by the onshore movement of these sediments during the Holocene marine transgression. Once at the coast, sediments were reworked by marine and aeolian processes to form dunes, and further aeolian erosion redistributed some of this material inland to form the machair grasslands. A reduction in the rate of r.s.l. rise at ~7 kya may have been conducive to the development of an extensive dune system, but by ~6.5 kya the system is thought to have switched from sediment surplus to deficit, and erosion began to outpace accretion (Hansom and Angus, 2001). This is thought to be due to depletion of the finite glacial sediments available for onshore movement on the area of the shelf floor affected by the active wave base (Hansom and McGlashan, 2004). With reduced sediment input from the shelf, the existing sediments were recycled (Gilbertson et al., 1999).

Mate (1992) suggested that the similarity between living and dead faunal assemblages of marine organisms on the continental shelf implied a continuous source of carbonate sands. However, Gilbertson et al. (1999) showed a history of sediment re-working with limited new inputs. In addition, significant stretches of the Uists' western

coasts appear to be currently dominated by processes of erosion (Mather and Ritchie, 1977; Dawson et al., 2007b; Gomez et al., 2014).

This reduction in sediment supply is likely to reduce the resilience of the machair, with limited potential for recovery in areas which lose material. There is already some evidence for a loss of resilience, as on many parts of the machair coast the dunes have been completely eroded (Mather and Ritchie, 1977; Moore et al., 2005). Very few locations have any evidence of embryo dunes, which would indicate areas of accretion and stabilisation.

2.2.2. Beach sediments and geomorphology

Beaches function as a natural buffer to wave energy. The beaches of the Uists are typically wide and dissipative in character, with poorly defined berms. Most are sandy, although a sandy lower beach coupled with a shingle upper beach is not uncommon. In general, sediment eroded from beaches during winter storms is deposited in offshore bars, and subsequently brought back to the coast during the summer recovery period (Angus and Rennie, 2008). There is concern among the local population and some scientists (Crawford, 1997) that in severe storm events some of this sediment is removed from the system, either being channelled through the fords (the channels separating the islands of the southern Outer Hebrides) into the Minch, or being transported beyond the limits of the active wave base under normal conditions on the continental shelf.

In addition to the ability of sand to absorb wave energy, the beaches of South Uist are further protected by the seasonal deposition of kelp from offshore beds. This can form a layer up to ~1 m thick, which is considered to perform a critical role in absorbing wave energy during storms (Angus and Rennie, 2014). Many of the beaches are also protected by a shingle ridge, which provides a similar function. However, on some parts of the coast the visible shingle is not a current depositional coastal feature, but is instead a pre-existing sub-sand structure which has been exposed due to coastal erosion (Ritchie, 1971).

There is an on-going exchange of sediment between the beaches and dunes, with aeolian erosion moving sediment inland, and marine erosion during storms or extreme high tidal conditions removing sediment from the dune toe. This is one of the

mechanisms allowing coastal zones to adapt rapidly to changing environmental conditions. However, the erosion of the dune cordon along many parts of the coast, and reports of beach lowering in some areas, such as Staoinebrig (David Muir, personal communication), suggest that sediment depletion may be reducing the coast's capacity to recover following storms.

2.2.3. Dune sediments and geomorphology

Dunes are a key element in the development and maintenance of the machair system. They provide a source of sediments for redistribution inland to form the alkaline grasslands, and also act as a barrier to flooding and marine erosion, as much of the machair grasslands are very low-lying. While much of the machair coast is fringed by linear dunes of moderate height (2-8 m), in some areas there are more extensive dune systems, such as at Askernish (NF727241) and north of Cille Pheadair (NF732200).

Once vegetated, the dunes are relatively stable, with localised blowouts attributed to various causes, including over-grazing, rabbit damage, and poor agricultural management (Seaton, 1968; Ritchie 1971). Blowouts can be problematic, often depositing sand on agricultural land, or providing a route for seawater to travel inland during storms. Some degree of dune erosion is essential to resupply the machair grasslands with sediment, as these are exposed to continual deflation. The current lack of a dune cordon along ~38% of the southern Hebridean coast (Mather and Ritchie, 1977) is further evidence for a depleted sediment supply, and a major concern. Without a dune cordon, the machair grasslands are directly exposed to marine erosion and flooding during storms, and are also deprived of their primary sediment source. Archaeological remains found in the dunes also provide evidence of coastal retreat and on-going dune erosion (Moore et al., 2005).

2.2.4. Grassland sediments and geomorphology

The machair grasslands are low-lying, geomorphologically mature surfaces which extend from the dunes to the blacklands. Most of the grasslands are used for agriculture, with cereal cultivation in narrow strips running perpendicular to the coast, and common grazing of livestock. The grasslands are protected from marine erosion by

the beach and dunes, but in extreme storm events may be damaged by the deposition of storm debris, flooding, and severe coastal erosion, particularly in areas where the dunes have been eroded.

The grasslands are also susceptible to aeolian erosion, due to their topographic simplicity and sandy soils. Vegetation provides a degree of protection to the soils, but the soils are exposed by cultivation, rabbit burrowing, vehicle erosion, and sometimes overgrazing. The water table is the base level for aeolian erosion (Ritchie, 1979), and this shows considerable seasonal variation, with areas of the machair waterlogged during the winter months.

The soils of the machair are highly influenced by the nature of the beach and dune sand, and this influence can be seen in the physical and chemical structure of the soil. The main components of the machair soils are the glacial and shell sands, with most soils having an organic matter content of less than 5%, and very little clay or silt sized material. This may contribute to the sensitivity of machair sands to wind erosion, as soil aggregates stabilised by inorganic minerals tend to be stronger than those stabilised by organic matter (Oades and Waters, 1991). The proportion of shell sand may vary between 0-95 % with measurements indicating considerable variation between systems (Ritchie, 1974; Dickinson, 1975; Randall, 2004; Cooper et al., 2005), and within systems (Angus, 2006). The mean shell sand composition was found to be 53%, and this high value (relative to other UK links systems) contributes to alkaline pH values ranging from 7.0-8.9 (Ritchie, 1976; Cooper et al., 2005). The soils are thin, with organic matter concentrated in the top 10-15 cm of soil (Knox, 1974). In addition, the grassland soils have low aggregate stability and capacity for water retention (Knox, 1974; Ritchie, 1971). The combination of low organic matter, high sand content, low aggregate stability and low water retention make the machair soils very susceptible to erosion. Additionally, the large size and low density of calcium carbonate sand fragments compared to siliceous sand fragments is thought to further increase susceptibility to erosion (Randall, 2004).

Soil properties are not uniform across the machair, and several trends have been identified moving inland from the coast. These include decreasing pH and particle size, and increasing water content, organic matter and conductance (Randall, 2004), although these results are from the Monach Isles, and may not be representative of current conditions on the typical Uist machairs. These changes are attributed to the decreasing

influence of wind-blown sand, and increasing influence of water logging on moving inland, as well as proximity to acidic peat lands at the inland margins of the grasslands.

While the generalisation that machair sediments and landforms are susceptible to erosion is valid, there is clearly considerable variation in geomorphology and soil characteristics across the machair landscape, and these variations may enhance or reduce sensitivity to erosion within the system. The most obvious example of this is the presence or absence of a dune cordon; the absence of a dune cordon is generally attributed to on-going erosion (Mather and Ritchie, 1977) and indicates an area that is particularly sensitive to further erosion during storms or as a consequence of sea-level rise, due to lower crest height and width. Less is known about the effects of variations in soil properties. Any trends identified have been considered descriptively rather than analytically (e.g. Dickinson, 1975; Angus, 2006), although there is speculation that some characteristics of machair soil may influence susceptibility to aeolian erosion (e.g. Randall, 2004).

2.3. Machair erosion

Marine and aeolian processes have both played an important role in the formation and maintenance of the machair system. Marine erosion of the soft coastline allows the machair coast to adapt naturally to any changes in external conditions, e.g. storminess, sea-level. Aeolian erosion led to the formation of an extensive dune system (now eroded in many places), and the redistribution of sand to the machair plains, which are themselves continually deflated by wind erosion. While the importance of these processes to the continued existence of the machair system is acknowledged, there are also concerns that erosion may now pose a threat to the machair system due to a reduced offshore sediment supply.

2.3.1. Causes of erosion

The main causes of machair erosion are: i) marine erosion of the beach, resulting in longshore or offshore transport of sand and in some areas, beach lowering; ii) marine erosion of the dunes or machair front, resulting in slumping, undercutting, and coastal

retreat; iii) aeolian erosion of the dunes, resulting in blowouts; and iv) aeolian erosion of the grasslands, resulting in deflation. The rate of erosion is influenced by the erodibility of the sediments, and the erosivity of the marine and aeolian forces acting on the machair is influenced by weather conditions, trends in climate (particularly storminess), and relative sea-level change. Additionally, human activities have the potential to mitigate or exacerbate erosion.

2.3.1.1 Weather and climate

The southern Outer Hebrides have a temperate maritime climate, with mild summers and cool winters. Rainfall is high, although late spring and early summer are often characterised by limited precipitation. Frost and snow are rare due to the influence of the Gulf Stream. High wind speeds are perhaps the most distinctive characteristic of Hebridean weather, with the area being exposed to the highest mean wind speeds in the UK. The mean annual wind speed for South Uist is ~ 14.5 knots (Met Office data, 2005-2010).

Sand transport by saltation is initiated at wind speeds of 4.5 ms^{-1} (8.7 knots) (Boorman, 1977), and is proportional to wind speed above this velocity, although other factors such as sorting and wetness influence this (Bagnold, 1948; Belly, 1964). The mean annual wind speed of 14.5 knots in South Uist is well in excess of the 8.7 knots threshold (Fig. 2.1). The high wind speeds represent an erosion hazard, especially on parts of the coast with minimal sediment accretion or areas where bare soil is exposed by agriculture, over-grazing (by livestock or rabbits), or public access. Machair stratification, a distinctive sequence of layers of sand and soil found in cores taken on the machair, provides evidence for periods of greater and lesser sand blow throughout the development of the machair (Gilbertson et al., 1996). During more stable periods a layer of thin soil forms as the land is cultivated and vegetation develops. In periods of greater instability sand is deposited on top of the soil layer, burying it. There is evidence that this process has repeated numerous times during the mid- and late-Holocene (Gilbertson et al., 1999). The machair is currently thought to be in a relatively stable period that started at the beginning of the 20th C. However, wind erosion has still caused more localised problems (e.g. Seaton, 1968), and is generally linked to poor agricultural management (Ritchie, 1971; Angus, 2001).

The prevailing wind direction also influences erosion. In the southern Outer Hebrides, this is from ~ 180-270 °, or from the south and west. This makes the machair coast, running along the western side of South Uist particularly exposed to marine erosion, as high energy waves are driven onshore during periods of high wind speed. Additionally, the prevailing wind direction has led to the movement of sand from the beach, to the dunes, to the machair grasslands, and has contributed to their north-south orientation. Most storms track from the south (Dawson et al., 2007a), which means that stretches of coast facing in this direction (e.g. on sandy headlands) are particularly exposed to marine erosion.

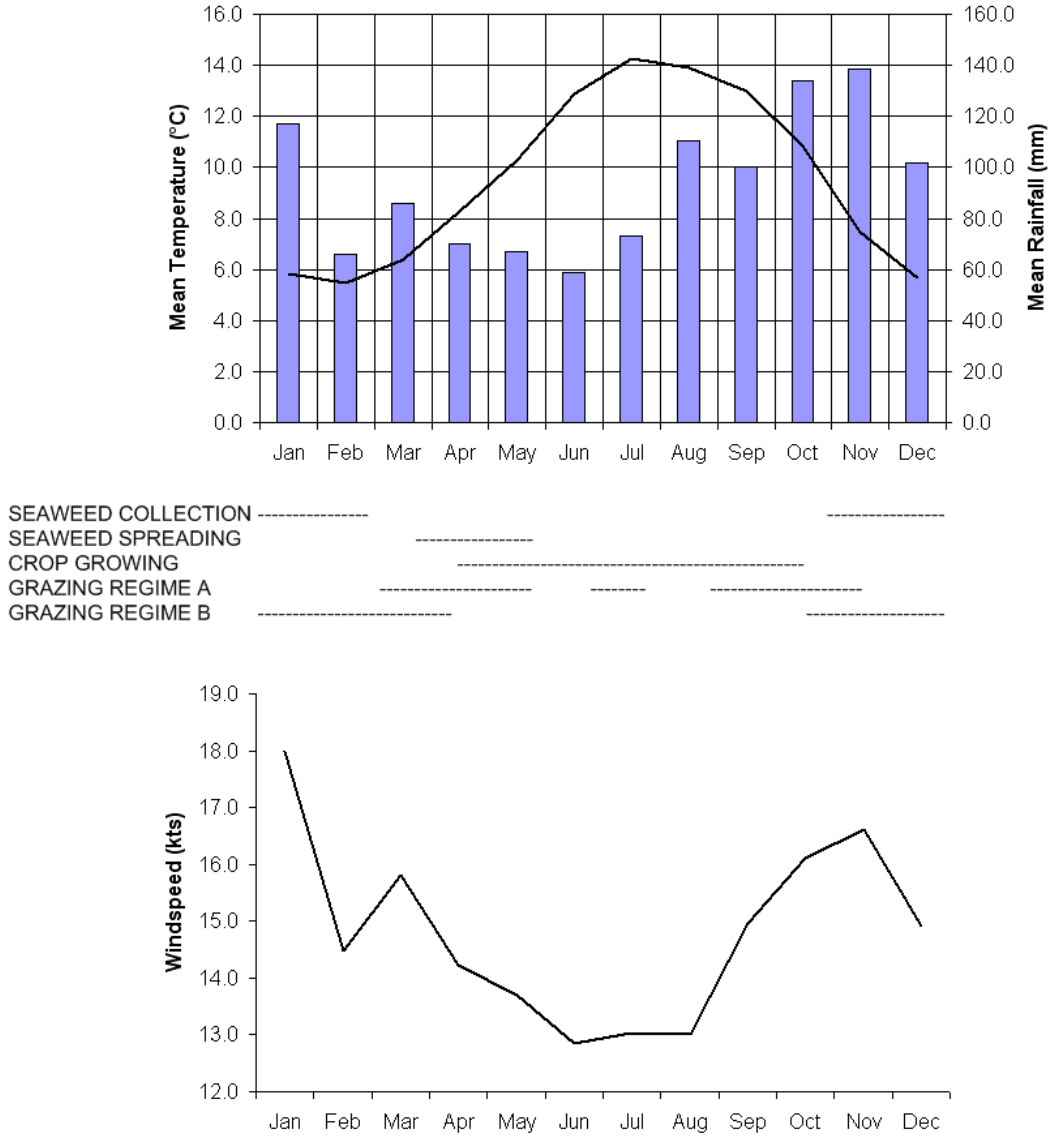

Figure 2.2. Seasonal mean rainfall, temperature and wind speed for South Uist from 2005-2010, and typical timings for agricultural activities. Climatic data sourced from the Met Office.

As is typical of the west of Scotland, the Outer Hebrides have relatively high annual rainfall totals, with particularly high precipitation during the winter months (Fig. 2.2). This often leads to seasonal water logging of the lowest lying parts of the machair grassland. As the water table represents the base at which aeolian erosion ceases to act, this water logging provides some degree of protection against soil erosion. It should be noted, however, that excessive water logging poses a problem for crofters, delaying cultivation. The current perception among local people is that the extent and duration of standing water is increasing. In contrast, from April to June there is often reduced precipitation. The lower late spring water table increases the volume of soil susceptible to wind erosion. This coincides with the period when fields are bare, and agricultural soil is most exposed to wind erosion (Fig. 2.2). The seasonal variation in rainfall is expected to increase in magnitude with projected climatic changes (UK CIP, 2009). Additionally, temperatures are expected to rise (UK CIP, 2009). Lower precipitation and higher temperatures are likely to intensify the 'dry period' (Hansom and Angus, 2001), which may increase wind erosion rates, particularly on soil exposed by cultivation.

Although the western coast of South Uist is exposed to high energy waves from the north Atlantic, the shallow continental shelf extending ~ 100 km offshore to the west provides some protection to the coastline due to the shoaling effect. Large kelp beds offshore also absorb some energy before waves reach the shore. Despite this, the mean significant wave height is ~ 3 m, ~ 50 km offshore (data from Wavenet, 2009-2012), and the region is considered to have one of the highest energy wave climates in the world (Mørk et al., 2010).

High wind speeds and a high energy wave climate, along with an exposed location, sandy sediments, and a largely soft coastline, have contributed to the evolution of the unique machair landscape. However, the marine and aeolian forces which formed the machair are now thought to pose a threat to the machair in its current form. With the system operating under a sediment deficit there is limited new material, and areas of erosion outbalance areas of accretion. Projected changes in climate for this region may exacerbate the issue, with drier summers and increased storminess concerning crofters.

2.3.1.1.1 Storminess

Prior to the 'Great Storm' of January 2005 the local population believed sea-level to be the greatest threat to the machair coastline. However, the dramatic and rapid coastal changes that occurred during this event shifted attention to the threat of future storms. While the effects of the January 2005 storm were particularly severe, they are common to any storm event. On areas where a dune cordon is present, the base of the dunes may be eroded, and sediment exchanged between the dunes, beach face, and offshore bars. In areas where the machair front is exposed this is generally undercut during storm events, leading to slumping and coastal retreat. Additionally, in areas where crest elevation is low, sand and shingle may be deposited inland in sediment fans and plumes (e.g. Dawson et al., 2007a), and overtopping and/or breaches may occur leading to flooding. As mentioned in section 1.4, it has been suggested the severe storm of January 2005 did not cause significantly more damage that would normally occur during a typical winter (Angus and Rennie, 2008). This suggestion has implications for how the storm threat should be perceived and managed relative to gradual, on-going relative sea-level rise. However, this cannot be confirmed without knowledge of seasonal erosion and recovery rates, and long-term rates of coastal erosion in this area.

Currently, there is a perception that storminess in the Outer Hebrides is increasing. This is a major concern as marine undercutting is thought to be one of the greatest threats to machair stability. However, there is limited historical evidence to support this. Dawson et al. (2007a) found that there had not been a sustained increase in storminess in the Outer Hebrides over the preceding 40 years. This is in agreement with the findings of Wolf and Woolf (2006), who found no increase in storminess or maximum wave heights in the north-east Atlantic over this period. Some authors suggest that anthropogenic climate change may lead to increased storminess over the next century by influencing atmospheric circulation so that a more positive North Atlantic Oscillation (NAO) regime is favoured (e.g. Wang et al., 2004). There is also the possibility that storm frequency will decrease, but storm intensity will increase (e.g. Tsimplis et al., 2005; Lambert and Fyfe, 2006; Woolf and Coll, 2008).

There is considerable uncertainty as to how climate change will affect the frequency and severity of storms in the Outer Hebrides. However, even if the *status quo* is maintained it is possible that the adverse effects of storms will increase due to

reduced resilience in the coastal zone. This may occur due to on-going: i) erosion of the dunes; ii) lowering/narrowing of the dune crest or machair front, increasing the probability of over wash/breaching during storms; and iii) rising sea-levels, leading to a reduced shoaling effect and subsequently higher energy, larger waves, and higher water levels, which would also increase the probability of over wash, breaching, and flooding during storms.

2.3.1.2 Sea-level

Until recently, much of Scotland has been experiencing isostatic uplift, with maximum rates round the Western Highlands where ice cover was greatest. However, rates of uplift appear to be decreasing, and it is thought that the rate of sea-level rise is likely to outpace even the highest uplift rates by 2050 (Dawson et al., 2001). The rate of relative sea-level rise will be greater for parts of Scotland which were at the peripheries of the major ice sheets, including the Outer Hebrides. In 2001, the rate of sea-level rise in the Uists was thought to be > 1mm/yr, and this was predicted to increase to > 3.4 mm/yr by 2050, leading to best estimates of relative sea level rise of ~35-70 cm by 2100 (Dawson et al., 2001; Angus and Hansom, 2004). Significantly higher estimates of the rate of relative sea-level rise have been predicted from short-term tide gauge records (Rennie and Hansom, 2011). However, the reliability of these predictions is questionable due to the many issues associated with using short-term records to estimate longer term trends in relative sea-level change (Dawson et al., 2013). The Coastal Flooding in Scotland Report (Dawson and Powell, 2012), which provides advice for coastal practitioners, assumes a current rate of relative sea-level rise of ~ 2 mm/yr in Scotland.

Rises in sea-level are likely to exacerbate coastal erosion in a number of ways, e.g. through a decrease of the shoaling effect, decreased protection from the offshore kelp beds (Angus and Rennie, 2014), and decreased recurrence interval of extreme storm events (Emery and Aubrey, 1991), etc.

2.3.1.3 Anthropogenic causes

Throughout the Holocene, human actions have had the potential to both exacerbate and mitigate rates of coastal and aeolian erosion through a variety of

activities. Two areas where human influence is both widespread, and of current concern, are coastal zone management and agriculture.

In the aftermath of the January 2005 storm coastal defences were constructed at several locations in South Uist, including Cille Pheadair and Staoinebrig. Coastal defence sites cause major disruption to sediment dynamics, in their immediate vicinity, and throughout the coastal cell within which they are situated (de la Vega-Leinert and Nicholls, 2008). This is a major concern in the Uists given the dependence of the machair system on a continuous sediment supply from the beach. As well as changing the distribution of sediment along the coast, defences may provide a physical barrier to sediment movement. Prior to the January 2005 storm, several researchers had expressed their belief that coastal defences were inappropriate for the Outer Hebridean coast, due to the complex sediment dynamics and their importance in maintaining the larger machair system, and the perception that defences tend to transfer the erosion problem to another part of the coast rather than solving it (Ritchie, 1971; Angus, 1999; Hansom and McGlashan, 2004).

Agriculture has been practiced on the machair of the Uists for at least 5 kya. Traditional agriculture is encouraged on the islands by conservationists and in the form of EU subsidies provided to farmers who engage in certain management practices. There is no set definition of traditional management, or a particular time which the encouraged practices are derived from. However, encouraged management practices often include: cultivation in narrow strips perpendicular to the coast; use of kelp as fertiliser; stocking with cattle rather than sheep; and shallow ploughing to a depth of 10 cm. Hebridean crofters were encouraged to use more modern agricultural methods from the 1950s to the 1980s, and the recent shift to policies favouring more traditional agricultural methods can often be more expensive and inconvenient.

Most conservationists expect that erosion will be exacerbated by modern agricultural practices, and reduced by traditional agriculture (Angus, 1996; Owen et al., 2000), but little research exists on the machair system to support this view. For example, Thorsen et al. (2010) found that soil aggregate stability and microbial biomass were not improved by the application of kelp compared to artificial fertilisers over one growing season. Evidence for deflation of the machair grasslands in some areas of northern South Uist has been tentatively attributed to agricultural activity (Dawson et al., 2012). It is also evident from the historical record that prior to modern agricultural

techniques, injudicious use of historic management practices (e.g. shallow ploughing, use of seaweed fertiliser, etc.) is likely to have contributed to machair erosion (e.g. Brayshay and Edwards, 1996).

2.3.2 A brief history of machair erosion

Throughout the history of the machair there have been considerable variations in the rate and frequency of erosive events, due in turn to variations in the erosive factors acting on the machair (summarised in section 2.2.1), and the availability and abundance of sediments. Periods of widespread erosion throughout the Holocene have been identified using soil cores, and the historic record identifies episodes of sand blow from ~ 300 years ago to the present. More recently, historic maps and photographs have been used to quantify rates of erosion over the last ~ 100 years. This section provides a summary of machair erosion events throughout the Holocene to provide a context for investigating current erosion.

The earliest episodes of sand blow identified from sediment cores are dated to 9-4.4 ky (Ritchie and Whittington, 1994; Gilbertson et al., 1999; Ritchie et al., 2001), varying with location, and are associated with the aeolian erosion of sand from the dunes to form the machair grasslands. Between 7-4.5 ky a major period of dune building occurred (Ritchie, 1979), which has been attributed to a reduction in the rate of r.s.l. rise and a subsequent reduction in the rate and intensity of marine erosion (Ritchie et al., 2001). This is concurrent with dune building episodes elsewhere in Scotland (e.g. Firth et al., 1995; Wilson, 2002). From ~6.5 ky onwards it is thought that, in general, rates of erosion began to outpace accretion (Hansom and Angus, 2001, 2005; Hansom and McGlashan, 2004) due to a reduction in the volume of sediment available for onshore movement on the area of the continental shelf affected by the active wave base (Hansom and McGlashan, 2004). Within this general trend, several periods of accelerated sand movement have been identified (Bennet et al., 1990; Gilbertson et al., 1996; Grattan et al., 1996; Dawson et al., 2004) (Fig. 2.3). A relationship between reduced stability and colder temperatures has been established, both in the Outer Hebrides (Jordan et al., 2004; Dawson et al., 2007a), and elsewhere in western Europe (Clarke and Rendell, 2009). This is thought to be due to higher temperature gradients in

the North Atlantic during colder periods increasing atmospheric circulation, which in turn contributes to higher wind speeds in the region (Jordan et al., 2004).

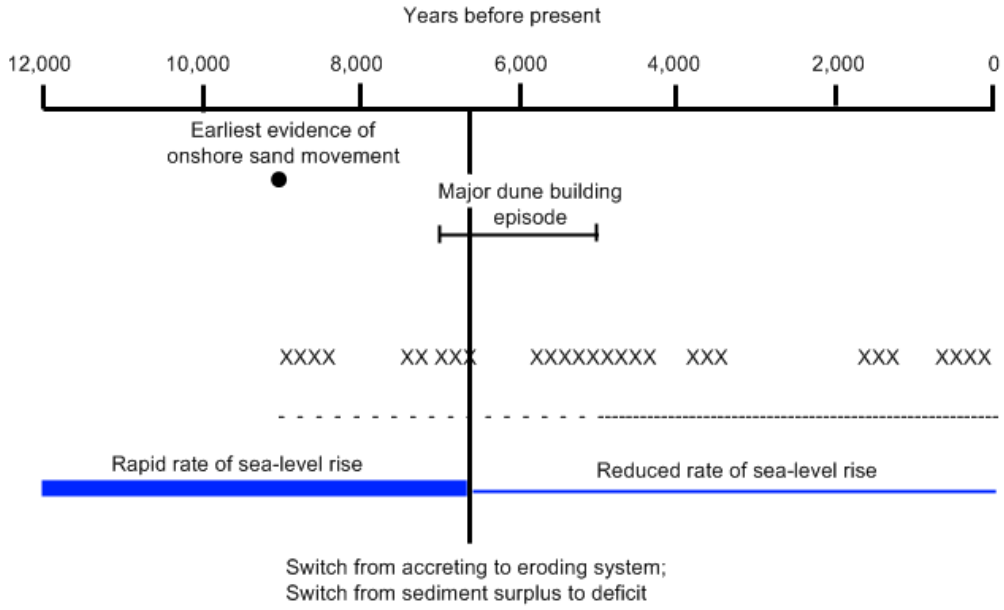

Figure 2.3. Holocene time-line of events in the formation and evolution of the machair. Periods of increased sediment movement are indicated by the symbol 'x'. The presence of humans on the Uists is indicated by the symbol '-'. Closely spaced dashes indicate conclusive evidence for a human presence; widely spaced dashes indicate circumstantial or contested evidence for a human presence exists for the indicated period.

The most recent period of elevated storm frequency and machair destabilisation lasted from ~ 1400-1900 (Dawson et al., 2004; Dawson et al., 2007a). The machair is thought to have entered a relatively stable phase ~ 1900, which continues today (Hansom and Angus, 2005). A number of severe storms have occurred since 1900, but with less frequency than the 500 years prior to this. The 'Great Storm' of January 2005 was the most recent severe storm, with up to 10 m coastal retreat at vulnerable locations (Dawson et al., 2007a; Angus and Rennie, 2008).

In 2007, SNH published a report aimed at providing and testing a methodology for quantitatively assessing rates of coastal erosion (and accretion) for Scotland (Dawson et al., 2007b). The northern half of South Uist, between 1984 and 2005, was one of the sites chosen to test the methodologies proposed. In this area, maximum shoreline movement is ~ 50 m and maximum loss of elevation is ~ 11 m between 1984 and 2005, with volume losses on the order of tens to hundreds of thousands of cubic

metres of sediment along some parts of the coast, although rates were highly variable, with localised areas of accretion (Dawson et al., 2007b). Dawson et al. (2012) conducted a second quantitative analysis of long-term coastal change in the southern Outer Hebrides, this time focused on the South Ford area between the islands of South Uist and Benbecula. Due to the nature of the coastal geomorphology this area has experienced particularly high rates of coastal erosion, with the erosion of a spit, and dramatic changes in the position of the barrier island feature studied between 1825 and 2005, including a loss of almost 130,000 m^3 of sediment (between 1984-2005) from the central section of the island. Gomez et al. (2014) investigated change in the position of linear coastal features, and the relative abundance of different coastal surfaces (e.g. water, vegetation, sand, etc.) along the coastline of South Uist using Landsat imagery from 1989-2011. Their findings indicated mean rates of erosion of 0.3 m/yr (considered to be very low), with localised areas experiencing much higher rates of up to 2.5 m/yr and very high temporal variability (Gomez et al., 2014). These studies represent the only quantitative investigations of coastal change in South Uist. The only other sources of information about rates of change are through historical sources (e.g. reports of a township to the west of Baleshare, a small island off the coast of North Uist, that existed in the 1500s but is now offshore), and snapshot assessments of coastal retreat and erosion in the wake of a severe storm (e.g. the January 2005 storm).

Evident from the above discussion of machair sediments and landforms, the machair is particularly susceptible to erosion for reasons including, the low aggregate stability, low organic matter content, and sandy texture of the soils, the sediment deficit, and the exposed position and topography of the landforms. It is also evident that the susceptibility of the machair to erosion is further increased by exposure to high wind speeds, severe North Atlantic storms, sea-level rise, and human actions. There are also considerable spatial and temporal variations in both the sediments and landforms which make up the machair landscape, and the intensity of the erosive forces acting on them, but limited quantitative research into how these variations effect the erodibility of soils and landforms, or rates of erosion.

2.4. Research Aims

This thesis seeks to quantitatively investigate variations in the sensitivity of the machair landscape to erosion, with particular emphasis on the dunes, as this landform has a crucial role as both a sediment bank and a topographic barrier against flooding (Angus and Rennie, 2014). The machair is considered to be a 'fragile' system with high susceptibility to erosion, and the aim of this thesis was to determine whether there were variations, spatially and/or temporally, in the rates of erosion and erodibility of the machair soils and landforms. The three field sites described in Chapter 3 were used for this investigation, which incorporated the collection and analysis of field samples, remote sensing data, and archive data.

The objectives of the thesis were:

i) to quantify long term trends in planimetric coastal evolution using historic maps (from the National Library of Scotland and the Ordnance Survey) and aerial photography (from the Royal Commission on the Ancient and Historic Monuments of Scotland);

ii) to quantify short-medium term trends in planimetric and volumetric coastal evolution using RTK-dGPS measurements collected between 2011 and 2014, and a 2005 LiDAR dataset (provided by Scottish Natural Heritage (SNH) on behalf of the Western Isles Data Partnership);

iii) to use the data gathered from the completion of aims i) and ii) on coastal change at multiple nested temporal scales (tidal cycle, seasonal, annual, decadal, centennial) to provide a context for interpreting the significance of erosion during storm events relative to gradual, on-going coastal erosion;

iv) to investigate whether storminess has increased in the southern Outer Hebrides over the last ~150 years using Met Office archive data (from Saughton House, Edinburgh) and MIDAS data, and to consider the implications of these findings for coastal change over this period;

v) to determine if there are spatial trends in the susceptibility of machair soils to aeolian deflation - using wind abrasion resistance as a proxy for sensitivity to wind erosion - particularly with relation to distance from the coast and cultivation of land on the back dune area, and to establish which, if any, soil properties can be correlated with wind abrasion resistance.

CHAPTER 3
FIELD SITES

Synopsis:
This chapter describes the three field sites investigated.

The South Uist machair was selected as: i) it is one of the largest areas of continuous machair habitat; ii) the machair is considered to be "best developed on the Uists, Tiree, and on Barra" (SNH, 2012); and, iii) in the 'Great Storm' of January 2005 the most severe and widespread coastal damage occurred along the coastlines of South Uist and Benbecula (Dawson et al., 2007a). However, it is acknowledged that other machair settings exist (e.g. Harris, Coll and Tiree, Orkney, etc.), and results obtained from investigating the machair of South Uist may not be applicable to other areas due to differences in geomorphology, management, and offshore conditions. Three field sites located on the Atlantic coast of South Uist were selected (Fig. 3.1).

A

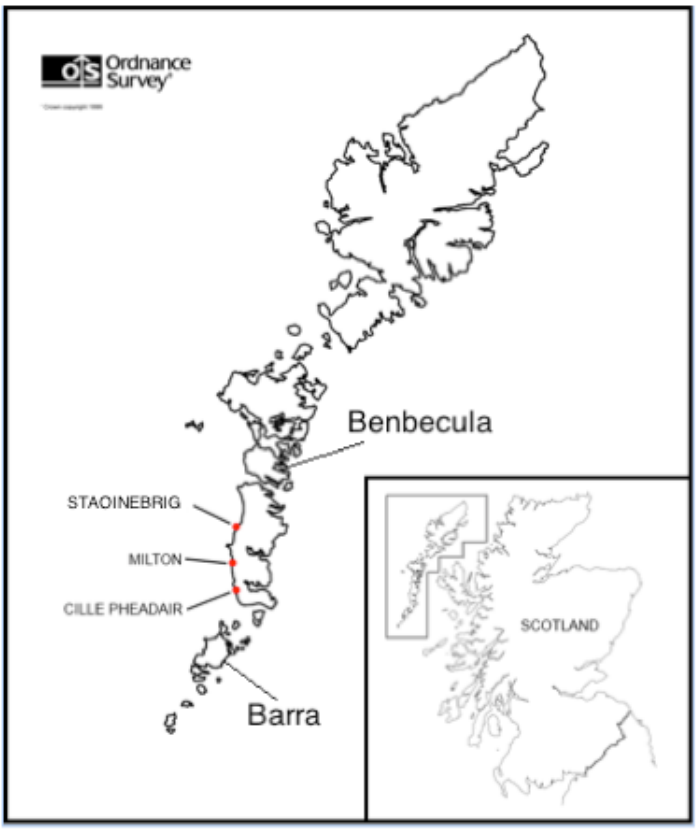

B

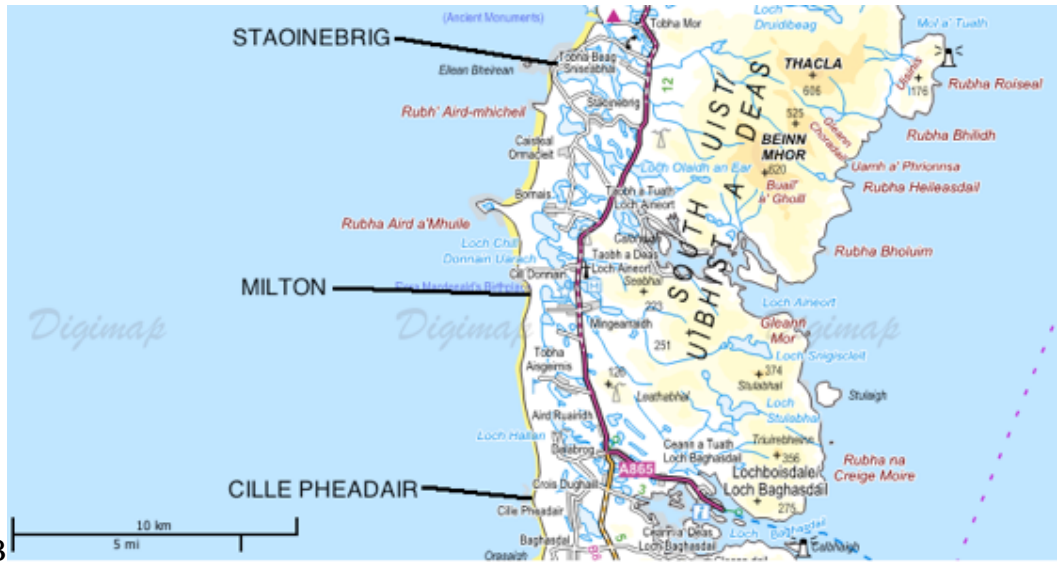

Figure 3.1. a) Map of Scotland showing the location of the Outer Hebrides (inset), and map of the Outer Hebrides showing the location of the three field sites used in this research within the island of South Uist, and other islands mentioned in the text. Map of Scotland adapted from Ordnance Survey map data by permission of Ordnance Survey © Crown copyright 2013. b) 1:50,000 Ordnance Survey maps of the three field sites (circled). © Crown Copyright/database right 2014. An Ordnance Survey/EDINA supplied service.

The main criteria used to select field sites were linked to perceived sensitivity to change, and lanforms/geomorphology. It was determined that two sites should be selected which had experienced dramatic changes in the January 2005 storm, as research into such sites would be valuable in terms of management. To act as a 'control' and provide a context for interpreting results from highly sensitive sites, it was decided that one site should be selected based on its perceived resilience to coastal change. In terms of geomorphology and landforms, sites were selected to ensure that the majority of coastal and machair landforms (bays, linear beaches, shingle ridges, eroding machair front scarps, high dunes, hummocky machair, etc.) occuring in South Uist should be represented.

Two sites, Cille Pheadair and Staoinebrig, were selected due to their perceived sensitivity to erosion, and/or overwash during storms (Richards and Phipps, 2007). At these sites there are active attempts to manage and defend the coastline. The third site, Milton, was selected as it was not identified as sensitive to coastal change following the January 2005 storm; no changes were reported for this site in any of the literature published in the wake of the storm (e.g. Dawson et al., 2007; Richards and Phipps, 2007; Angus and Rennie, 2008). Additionally, the selected sites cover three of the main coastal morphologies found on the western coast of South Uist: Cille Pheadair is a sandy headland; Staoinebrig is a mixed sand and shingle bay; and Milton is part of a sandy, linear beach extending for almost 20 km. Hard rock headlands are also found on the Atlantic coastline, however these are generally less susceptible to erosion (although displacement of gneiss bedrock was reported in Ardivachar, north of Staoinebrig, following the January 2005 storm (Dawson et al., 2007)), and are predominantly found in the northern third of the island where the machair is less widespread. It should be noted that Cille Pheadair and Milton are more typical examples of machair coastline while Stoneybridge is less so, possessing a shingle ridge which plays a major part in responses to waves and storms. Stoneybridge also lacks a dune cordon, and true machair grasslands inland from the coast – agricultural land at Stoneybridge is used for grazing but does not presently show any evidence of recent cultivation (one criteria for identifying a system as machair).

The use of three sites made it possible to investigate two sites where coastal change is considered to present a threat to society and/or infrastructure, and one where coastal change was not perceived to be a problem, and to compare differences and

similarities between these sites. Additionally, given the frequency of field visits, three sites was considered to be an appropriate number to survey during each field visit in terms of length of field visit and cost.

3.1 Staoinebrig and Tobha Mor

Staoinebrig is the northernmost site, situated approximately in the middle of the western coastline of South Uist. The site is an ~ 800 m long linear beach, orientated NNW-SSE. The beach is bounded to the south by a rocky headland and to the north by a sandy headland and a tidal tombolo joining the mainland to a small rocky island (Figs. 3.2-3.3). The lower beach is sandy, with a shingle upper beach and ridge, and one outcrop of intertidal bedrock about 300 m from the southern end of the beach. There is no dune cordon at Staoinebrig, and the eroding machair-front marks the transition between beach and grasslands. Although the site has a history of cultivation, at present the land is used only for sheep grazing. The machair grasslands extend ~ 200 m inland to Loch Altabrug, and is marshy towards the south of the site. The only infrastructure is a single track road 25 m inland from the machair front.

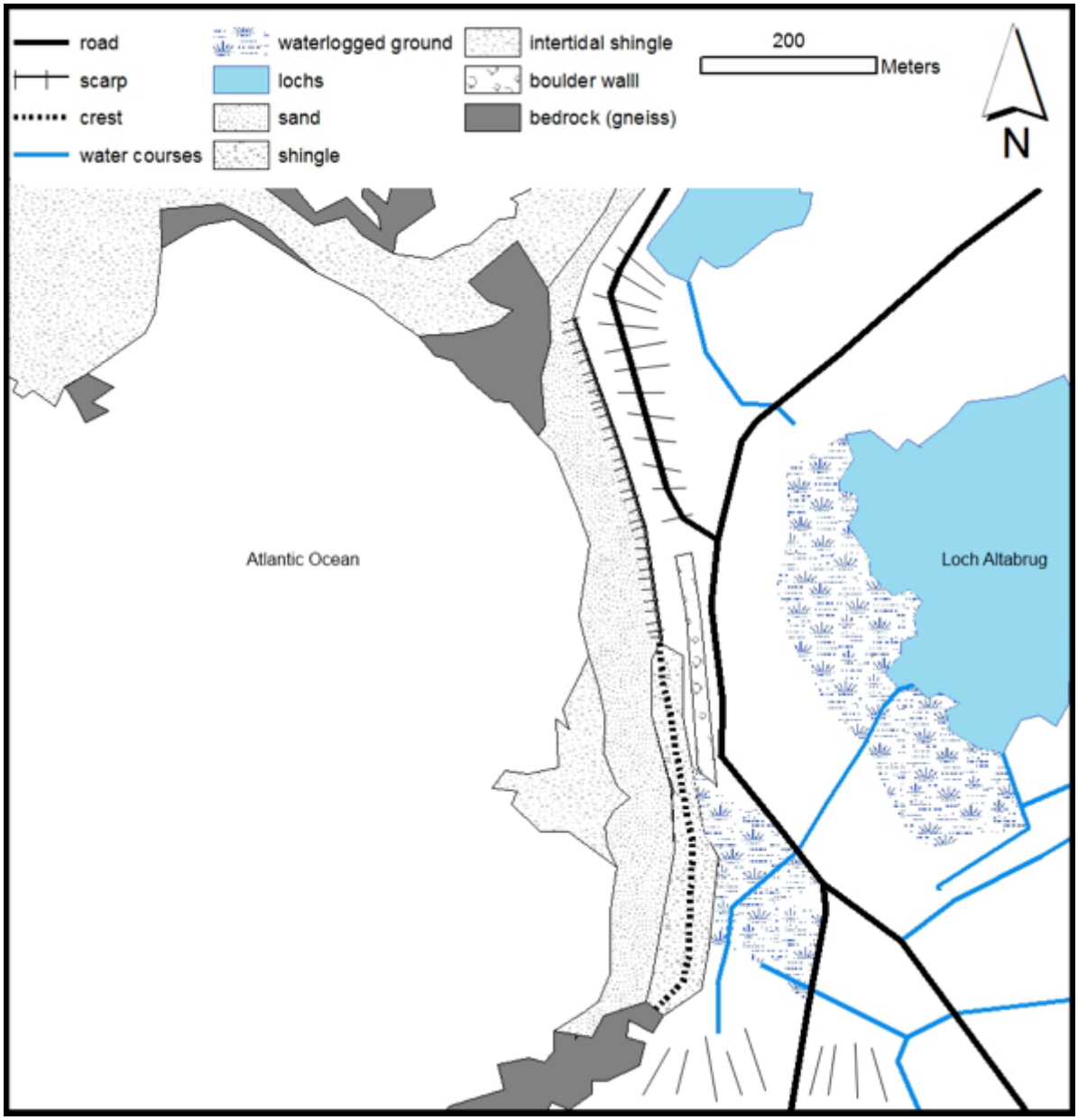

Figure 3.2. Geomorphological map of Staoinebrig.

Figure 3.3. Aerial photograph of Staoinebrig. Overwash plumes from the January 2005 storm are circled in black. Aerial imagery © SNH on behalf of Western Isles Data Partnership.

In the 'Great Storm' of January 2005 the main problems at this site were the widespread deposition of storm debris and over washing of the shingle ridge, introducing marine water to the terrestrial ecosystem (Angus and Rennie, 2008). Shingle and sand were deposited across the machair up to a thickness of ~ 35 cm (Dawson et al., 2007a), and made the road impassable. Although the January 2005 storm had the most dramatic effects, storm debris has been a recurring problem at this site. The ridge is considered an important landform as "…it protects a particularly low-lying machair and a network of important lochs." (Angus and Rennie, 2008, p. 62). Additionally, the south of the site has a history of beach lowering (David Muir, personal communication). Following the January 2005 storm the local council, Comhairle nan Eilean Siar (CnES), manually rebuilt the shingle ridge, and in 2011 erected a boulder wall inland of the ridge at the south of the site where the road is closest to the coast.

Tobha Mor is an area of cultivated machair grassland slightly to the north of Staoinebrig. The coastal soils consist of calcareous regosols and brown calcareous soils (units 261F and 259) from the Fraserburgh Series, which transition to eutrophic flushed peat and peaty gleys (unit 263 of the Fraserburgh Series) ~ 650 m inland from the coast (Soil Survey of Scotland, 1985). Land management is typical of machair habitats, with cultivation of cereal crops in narrow strips on a 2-3 year rotation, with seasonal grazing by sheep and cattle. This area was used as an alternative to Staoinebrig for soil sampling (see Chapter 8) for two reasons: i) the land at Tobha Mor is in regular cultivation, so results of soil analysis will be relevant to land management; ii) the area of machair grassland between the coast and Loch Altabrug at Staoinebrig is very limited (extending only ~ 200 m inland), and much of it is submerged or marshy for parts of the year, providing limited scope for analysis of trends in soil properties.

3.2 Milton

Milton is ~ 8 km south of Staoinebrig. The site is an ~ 900 m long stretch of beach, bounded to the north by a rocky headland, and the south by a rock outcrop on the beach (Figs. 3.4-3.5). This beach is orientated N-S and is part of a continuous 13 km long sandy beach, broken only by sandy headlands, extending from Milton in the north to the southern end of South Uist. The beach is wide and sandy with no visible shingle. A high dune cordon exists at Milton. Although much of the dune face is erosional with

evidence for slumping and blowouts along the length of the site, there is some embryo dune formation, and much of the dune face is fixed by marram grass. An access track runs along the dune crest, and in places this has been re-routed due to erosion. The dune crest and top of the backdune has been fenced off to prevent grazing, and is well vegetated with the only bare sand found on the access track. Elevation decreases on moving inland from the dune crest. The machair grasslands terminate in the marshy blacklands transition zone ~ 350 m inland. The land at Milton is cultivated for cereal crops in comparatively wide strips (~ 40-100 m wide), with seasonal cattle grazing. The sequence of soil units repeats the pattern found at Tobha Mor, with calcareous regosols and brown calcareous soils being succeeded by eutrophic flushed peat and peaty gleys ~ 400 m inland (Soil Survey of Scotland, 1985).

No significant change was recorded at Milton following the January 2005 storm.

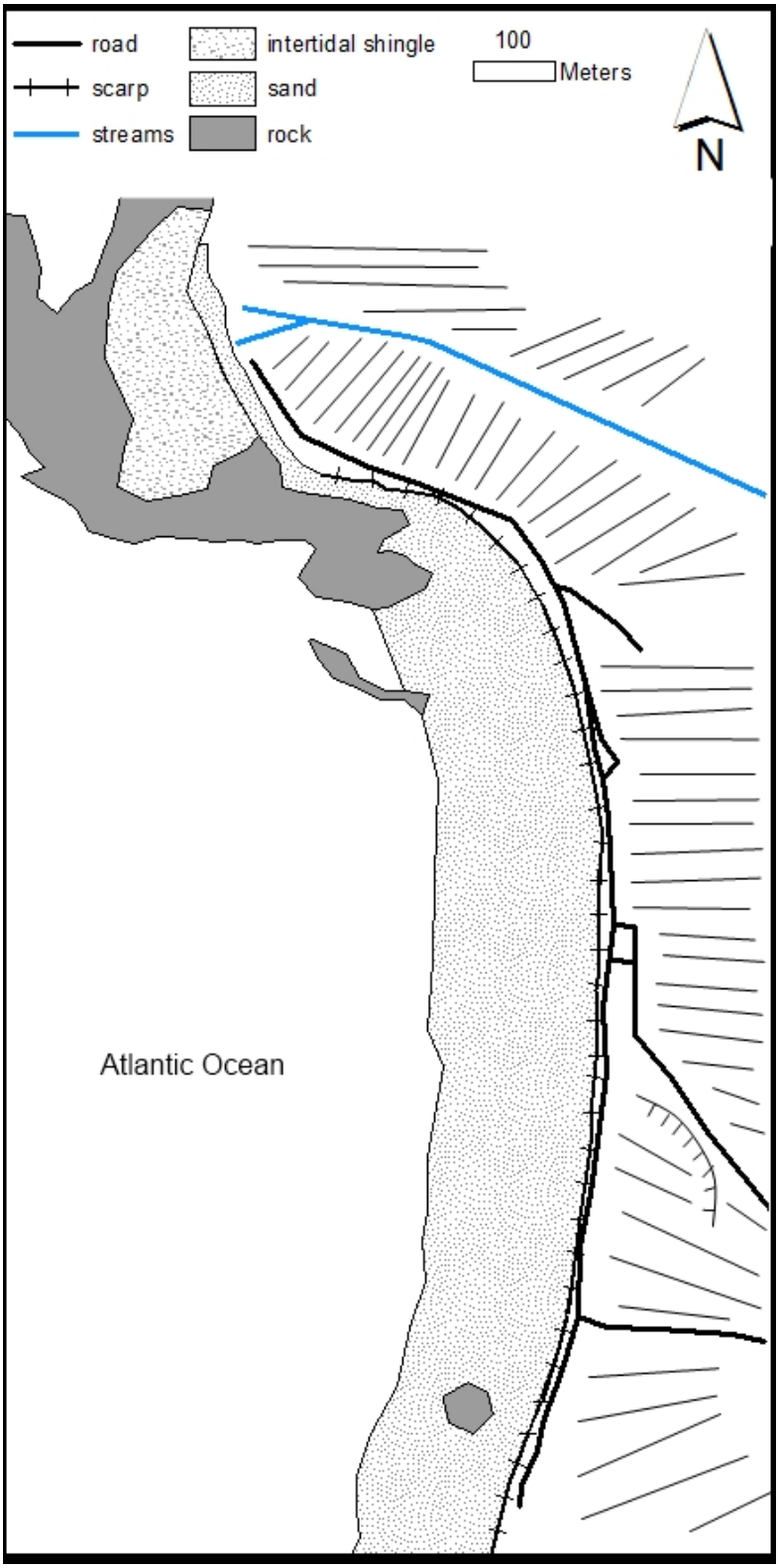

Figure 3.4. Geomorphological map of Milton.

Figure 3.5. Aerial photograph of Milton. Aerial imagery © SNH on behalf of Western Isles Data Partnership.

3.3 Cille Pheadair

Cille Pheadair is the most southerly site, located ~ 7.5 km south of Milton, and ~ 5 km north from the southern end of South Uist. The site is part of the continuous ~13 km stretch of beach of which Milton marks the north. Cille Pheadair is characterised by a soft, sandy headland projecting WSW into the Atlantic Ocean (Figs. 3.6-3.7). High dunes (≤ 10 m O.D.), similar to those found at Milton are found north of the headland. However they are more erosional in character, with less vegetation cover, no embryo dunes, and evidence for slumping. South of the headland the machair is hummocky and slopes down gradually to the coastline. There is a very narrow band of dune vegetation. The beach is sandy, with an intertidal rock outcrop immediately in front of the headland. For ~150 m along the centre of the headland there is no dune cordon and the machair front is very low lying (~ 4 m O.D.). The machair grasslands extend for ~ 350 m on a negative gradient to a marshy and seasonally waterlogged area. Much of the grasslands are at or below the level of MHWOST (mean high water at ordinary spring tide) at Cille Pheadair. The land is cultivated for cereals in the traditional narrow strips (~ 20-40 m wide) running perpendicular to the coast. At Cille Pheadair these often terminate < 10 m from the dune crest. The areas is grazed by sheep and cattle. The only infrastructure is an unsurfaced access track for farm vehicles which runs along the edge of the headland. As at Tobha Mor and Milton, calcareous regosols and brown calcareous soils are found in the coastal zone, with eutrophic flushed peats and peaty gleys occurring further inland (Soil Survey of Scotland, 1985).

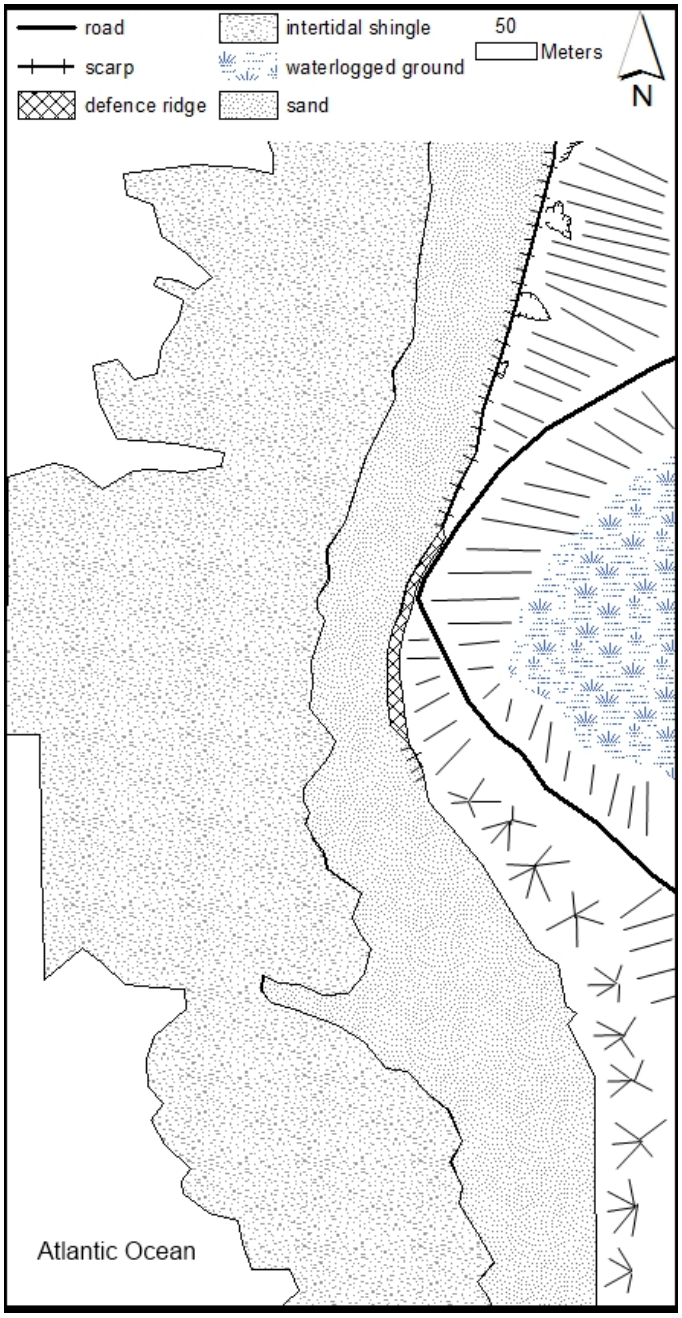

Figure 3.6. Geomorphological map of Cille Pheadair.

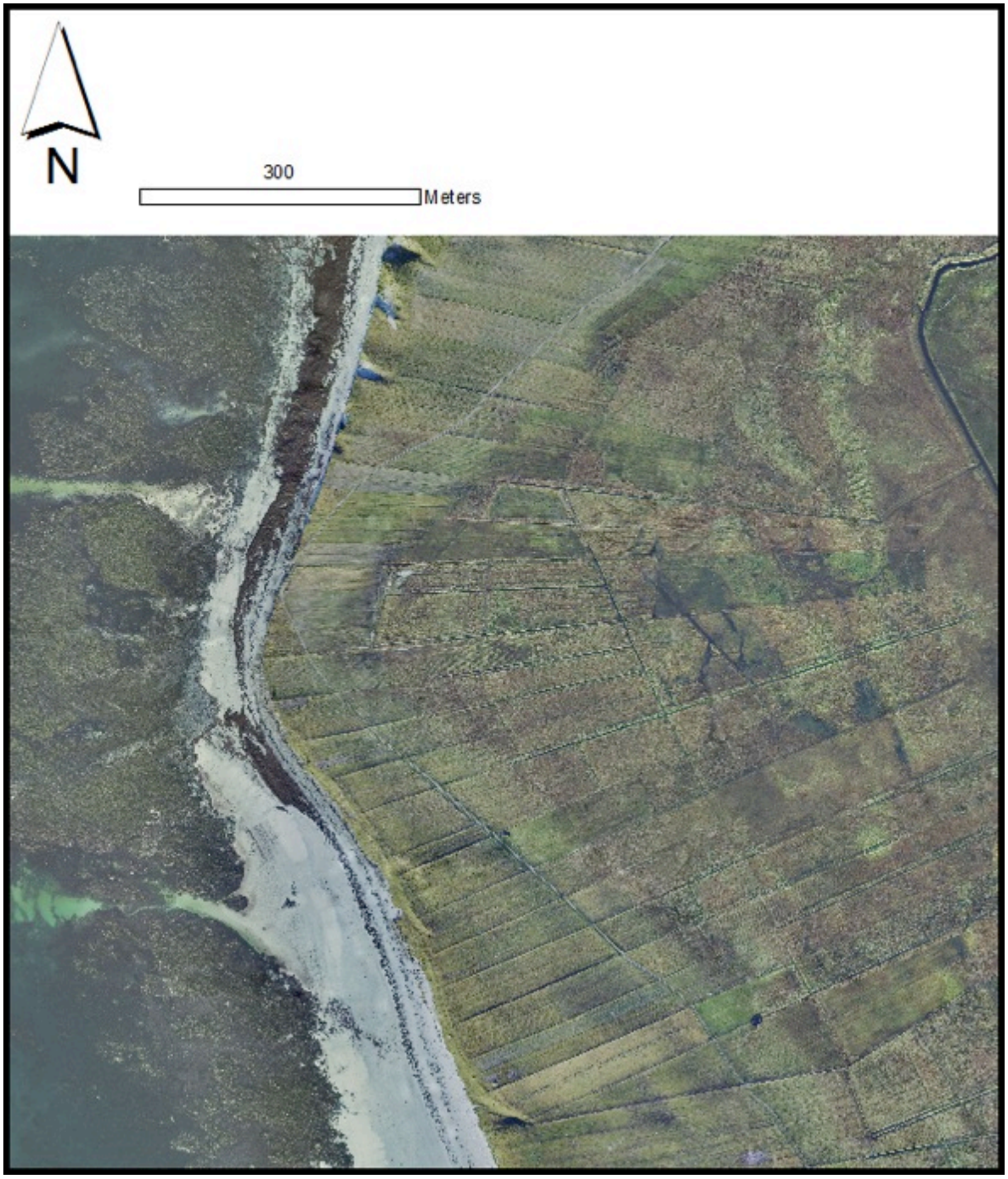

Figure 3.7. Aerial photograph of Cille Pheadair. Aerial imagery © SNH on behalf of Western Isles Data Partnership.

This site experienced > 5 m of coastal retreat along the ~ 150 m stretch lacking a dune cordon during the 'Great Storm' of January 2005. This was a major concern to local people, who worried about the possibility of overwash or breach of the low lying machair front and possible flooding of the machair grasslands. In the wake of the January 2005 storm Cille Pheadair was identified as sensitive to further storm damage

(Richard and Phipps, 2007). Following a period of consultation between local residents, CnES, Oxfam Scotland, coastal geomorphologists, and the landowners (Stòras Uibhist), an artificial sand, shingle, and crushed rock ridge was erected along the existing ~ 150 m of machair front lacking a dune cordon (Fig. 3.8). The ridge raises the elevation of the machair front by 2 m, and is ~ 15 m wide at the base. To improve the stability of the ridge it was fixed using fishing nets and seaweed, and fenced to prevent livestock access. The action taken at this site was against the advice of coastal geomorphologists who advised that managed retreat would be the preferred option, with a second choice of an artificial dune several metres inland and at a shallower gradient than the existing headland (David Muir, personal communication). However, their advice was not taken as land managers felt it would not be acceptable to local people and crofters who would not accept the loss of land in an area where land suitable for agriculture is generally limited in extent and/or of poor quality.

Figure 3.8. The artificial ridge at Cille Pheadair. Crushed rock was covered with sand and fishing nets, and fenced off to prevent damage by livestock. View is to the north. April 2013.

CHAPTER 4
MACHAIR SENSITIVITY TO FLOODING: SITUATION AND SCENARIOS

Synopsis:
This chapter provides an evaluation of the susceptibility of each of the three sites investigated to breaching, over-wash, and flooding by comparing the elevation of coastal morphologies at each site to current and predicted future water levels under normal and storm conditions.

4.1 Introduction

4.1.1 Background

Scotland has experienced isostatic uplift since the melting of the last major ice sheets ~ 10,000 years ago, with maximum rates occurring in the Western Highlands where ice cover was greatest (Trewin, 2002). Rates of uplift are lower for parts of Scotland which were at the peripheries of the last Scottish ice sheet, including the Outer Hebrides. Shennan et al. (2012) provide a rate of relative land-level change of 0.2 mm a^{-1} over the last 1 ky for the Outer Hebrides, which is comparable to current estimates of relative sea-level change for Scotland (Dawson and Powell, 2012). Dawson et al. (2001) suggested that the rate of sea-level rise may outpace vertical land level uplift rates by 2050, largely due to an increase in the projected rate of relative sea-level rise from > 1 mm a^{-1} in 2001 to > 3.4 mm a^{-1} by 2050. Best estimates of relative sea-level rise by 2100 are 14.3-62 cm for Stornoway (Dawson and Powell, 2012).

In addition to the threat of relative sea-level rise, there is a perception that storminess in the Outer Hebrides is increasing. This opinion has been supported in the scientific literature, e.g. in the IPCC 2007 and 2013 reports, although the predictions are regional rather than localised to the Outer Hebrides. This is a major concern as marine undercutting is thought to be one of the greatest threats to machair stability, and the western coastline of South Uist is acknowledged to be at risk from overtopping (McClatchey et al., 2014). However, there is limited historical evidence to support this for the Outer Hebrides area. Dawson et al. (2007a) found that there had not been a

sustained increase in storminess in the Outer Hebrides over the last 40 years. Similarly, Wolf and Woolf (2006) found no increase in storminess or maximum wave heights in the north-east Atlantic over this period. However, even if the *status quo* is maintained it is possible that the adverse effects of storms will increase due to on-going: i) erosion of the dunes, ii) lowering/narrowing of the dune crest or machair front, increasing the probability of over-wash/breaching during storms, and iii) rising sea-levels, leading to a reduced shoaling effect and subsequently greater energy, larger waves, and higher water levels, which would also increase the probability of over-wash, breaching, and flooding during storms.

The people of South Uist perceive sea-level rise and storms – and associated loss of land and life – to be the main risks for their community (Muir et al., 2014). Prior to the 'Great Storm' of January 2005 sea-level rise, as a result of melting Antarctic and Greenland ice sheets, was considered by local people to be the more pressing threat to the low-lying coastline of the Outer Hebrides, with concerns that it would lead to flooding of large areas of machair. However, the rapid and dramatic changes associated with the January 2005 storm shifted community focus to the threat of flooding associated with a breach of the machair front during another extreme storm event. A comparison of the figures involved supports this opinion: current best predictions suggest a relative sea-level rise of less than a metre, occurring gradually over the next 85 years, while the January 2005 storm surge led to an instantaneous rise in sea level, albeit temporary, of the order of 2 m along the South Uist coastline. An analysis of recent climatology by Dawson et al. (2005) shows that maximum gust speeds similar to those recorded in January 2005 were also recorded in January 2000 and February 1989, suggesting that this magnitude of storm might be a 1 in 5-10 yr event. However, locals referred to the January 2005 storm as 'the worst in living memory' (David Muir, personal communication). The exceptionally long duration of the storm (> 36 hours), and the coincidence with two high tides may suggest a less frequent recurrence interval for this magnitude of storm, of the order of 50-100 yrs (see Chapter 5 for detailed analysis of historical climatology data).

4.1.2 Aims

This chapter:

i) provides an initial indication of the sensitivity of the three field sites to flooding, over-wash, or breaching of the dune cordon/machair front under current sea-level conditions, storm surge conditions, extreme astronomical high tides, and predicted future rises in sea-level. The crest height of the dune cordon is a key indicator of coastal vulnerability during storm events as: when peak water levels during storms are higher than the dune crest elevation over-wash and dune erosion occur, with deposition of sediment inland as debris plumes and fans; and when mean water levels during a storm exceed the dune crest height the area inland of the dune is exposed to flooding (Stockdon et al., 2009);

ii) identifies the most 'at risk' parts of the dune cordon and/or machair front within each site, with relevance to the investigation of rates of coastal erosion in later chapters.

4.2 Methods

A digital terrain model (DTM) derived from a 2005 LiDAR (light detection and ranging) dataset, provided by SNH on behalf of the Western Isles Data Partnership, covering the western coastline of South Uist and Benbecula was used as the basis for this investigation. The DTM is a 3D model of the ground surface with all surface feature, e.g. buildings, removed, and is referenced to the British National Grid (OSGB36 datum), and was created using airborne LiDAR data collected in November 2005. Data are horizontally accurate to 10 cm and vertically accurate to 15 cm, and have been processed at a cell size of 1 m. This DTM is compared with a series of planar surfaces - generated using information on current sea-level, storm surges, predicted astronomical tides, and predicted future increases in sea-level – with respect to i) elevation difference between crest height and water level; and ii) length of crest below water level. The crest was identified as a linear feature extending along the highest points of the dune cordon and/or eroded machair front, and was easily identified on the DTM and extracted as a linear feature due to the idealised nature of the dunes at the sites studied (single ridges rather than dune fields, or multiple dune ridges).

4.2.1 Planar Surfaces

A series of planar surfaces at the elevation values specified in sections 4.2.1.1-4.2.1.4 were created using ArcGIS version 10. Planar surfaces indicate mean water levels for the scenarios listed, and do not account for transitory increases in water level associated with individual waves.

4.2.1.1 Current sea-level

Current sea-level was established using tide tables for the year 2012 from Balivanich (Lat. 57°29'N, Long. 7°23'W), the nearest port to the field sites. The level for mean high water at ordinary spring tide (MHWOST) in 2012 was selected to represent current water levels. At Balivanich, this is 4.1 m above the local chart datum. The local chart datum-ordnance datum conversion of -2.59 m (from Dawson et al., 2007b) was used to give a water level of 1.51 m O.D.

4.2.1.2 Storm surge levels

Three surfaces for storm surge levels were created: i) for a relatively minor storm surge of 0.5 m; ii) for a storm surge of 1 m; iii) for an extreme storm surge of 2 m (the estimated maximum surge associated with the January 2005 storm along the South Uist coast (Dawson et al., 2007a)). These values were added to the value of 1.51 m O.D. for MHWOST in 2012 (section 3.2.1.), to indicate the greatest height water which might occur under the combination of storm conditions and high tide. It should be noted that observations from North Uist and Benbecula indicated localised surges of up to 3 m (4.6-4.7 m O.D.) in the January 2005 storm (Angus and Rennie, 2014); it is probable that storm surge levels were highly variable due to localised coastal configuration.

4.2.1.3 Highest astronomical tides

The highest astronomical tide predicted between 2005 and 2025 is 0.69 m higher than MHWOST at Stornoway, the nearest port to the field site for which predictions are

available, and is predicted to occur on 19.09.24 (Dawson et al., 2007b). Two planar surfaces were created to indicate water levels under the highest predicted astronomical tide conditions: i) one at 2.22 m O.D. for normal conditions (1.51 (MHWOST) + 0.69 (max. predicted increase in water level due to astronomical conditions) + 0.02 (2 cm sea-level rise by 2024 assuming rate of s.l.r. of 0.2 mm/yr)); ii) and one at 4.42 m O.D. for extreme storm surge conditions (2.22 + 2 (estimated storm surge associated with January 2005 storm)).

4.2.1.4 Sea-level rise

Dawson et al. (2001) predicted that relative sea-levels in the Outer Hebrides would rise by 0.35-0.7 m by 2100 in the southern Outer Hebrides. More recently, Dawson and Powell (2012) have provided a current rate of relative sea-level rise of 2 mm a^{-1} for Scotland, which would equate to a rise in relative sea-level of 0.18 m by 2100. However this rate is expected to increase throughout the 21st Century, leading to localised predictions of sea-level rise of 14.3-62 cm by 2100 (Dawson and Powell, 2012). The IPCC 2013 report suggest the likely range of global relative sea-level rise by 2100 will be ~ 0.3-1.0 m.

Two surfaces were created to represent increased water levels associated with 0.7 m of sea-level rise, indicating the 'worst case' for sea-level rise specific to the Outer Hebrides: i) one surface for normal conditions at 2.21 m O.D. (1.51 (MHWOST for Balivanich, 2012) + 0.7 (max. predicted s.l.r.)); ii) and one surface for extreme storm conditions at 4.9 m O.D. (2.21 + 0.69 (max. predicted increase in water levels due to astronomical conditions) + 2 (estimated storm surge associated with the January 2005 storm)).

The planar surfaces created are summarised in Table 4.1. As surfaces S-LR_n and HAT_n (see caption for Table 4.1) have very similar elevations, one surface was created to represent both of these scenarios.

Table 4.1. Summary of elevation levels for each planar surface created. Surfaces are listed by increasing elevation.

Surface	Level	Level (m O.D.)
CS-L	Current sea-level	1.51
$SS_{0.5}$	Storm surge of 0.5 m	2.01
$S\text{-}LR_n$	Sea-level rise of 0.7 m (normal conditions)	2.21
HAT_n	Highest astronomical tide (normal conditions)	2.22
SS_1	Storm surge of 1 m	2.51
SS_2	Storm surge of 2 m	3.51
HAT_s	Highest astronomical tide (storm conditions)	4.22
$S\text{-}LR_s$	Sea-level rise of 0.7 m (storm conditions)	4.90

4.2.2 Crest height identification and sensitivity analysis

The dune crest was identified as a linear feature joining points of maximum seaward elevation along the dune cordon, or machair front in areas where the dune cordon has eroded. At all three sites the dune cordon/machair front is a single linear feature, which facilitates easy identification of the feature on the DTMs. A polyline shapefile tracing the dune crest at each site was created using the 3DEditor tool in ArcScene. The interpolate line function was used to help identify the highest point of the dune crest where this was not immediately clear from the DTM. A profile graph showing elevation along the length of the dune crest shapefile was generated using the 3D Analyst toolbar.

Parts of the coast with high sensitivity to overtopping and inundation were identified where water levels exceed dune crest elevation, after Stockdon et al. (2009), i.e. :

Equation 4.1.

$$DC - WL \leq 0$$

where DC = the elevation of the dune crest in metres, and WL = water level in metres. Values < 0 indicate that WL exceeds DC elevation, and values > 0 indicate that WL does not exceed DC elevation.

4.3 Results

Table 4.2 shows the analysis for the seven scenarios listed in section 4.2.1. At all three sites, the first five scenarios (in order of ascending water level) produce DC – WL_{min} values > 0, indicating that during these conditions the full length of the dune crest is above the simulated water levels. At Milton, DC-WL_{min} values are > 0 for the two scenarios associated with the highest water levels, HAT_s and SL-R_s (Fig. 4.1a), indicating that Milton is unlikely to experience over-wash, breaching, or inundation, even under the 'worst case' scenario, combining sea-level rise with extreme high tide levels and an extreme storm surge. At Staoinebrig, DC-WL_{min} is ≈ 0 for the HAT_s scenario, and -0.67 for the S-LR_s scenario (Fig. 4.1b), with 12.22% of the machair front below WL. The parts of the dune crest below the water surface occur at either end of the site. These values indicate that Staoinebrig is susceptible to over-wash and breaching during the HAT_s scenario (witnessed during site visits following severe storms in winter 2013), and potentially susceptible to inundation under the S-LR_s scenario. At Cille Pheadair, DC-WL_{min} values are similar to those calculated for Staoinebrig, with DC-WL_{min} ≈ 0 for the HAT_s scenario, and DC-WL_{min} = -0.69 for the S-LR_s scenario (Fig. 4.1c), with a slightly higher percentage of the crest height at this site being below water levels (16.84%). At Cille Pheadair the lowest-lying section of the dune crest occurs at the centre of the site. DC-WL_{max} values show that max. dune crest elevations are approximately 2 m higher at Milton than at Cille Pheadair, and approximately 2.5 m higher than at Staoinebrig.

Table 4.2. Maximum and minimum elevation differences between crest height and water level, and length of crest below water level, at each site for each scenario. Scenarios where water levels exceed crest height are highlighted by bold, underlined text. CP = Cille Pheadair; M = Milton; SB = Staoinebrig.

Scenario	Site	DC-WL_{max} (m)	DC-WL_{min} (m)	Length DC below WL (%)
CS-L	CP	7.78	2.70	0
	M	10.00	5.11	0
	SB	7.44	2.72	0
$SS_{0.5}$	CP	7.28	2.20	0
	M	9.50	4.61	0
	SB	6.94	2.22	0
S-LR_N/HAT_n	CP	7.07	2.00	0
	M	9.30	4.40	0
	SB	6.74	2.01	0
SS_1	CP	6.78	1.70	0
	M	9.00	4.11	0
	SB	6.44	1.71	0
SS_2	CP	5.78	0.70	0
	M	8.00	3.11	0
	SB	5.44	0.72	0
HAT_S	CP	5.07	-0.01	**0.12**
	M	7.29	2.4	0
	SB	4.73	0.01	0
S-LR_s	CP	4.39	-0.69	**16.84**
	M	6.61	1.72	0
	SB	4.05	- 0.67	**12.22**

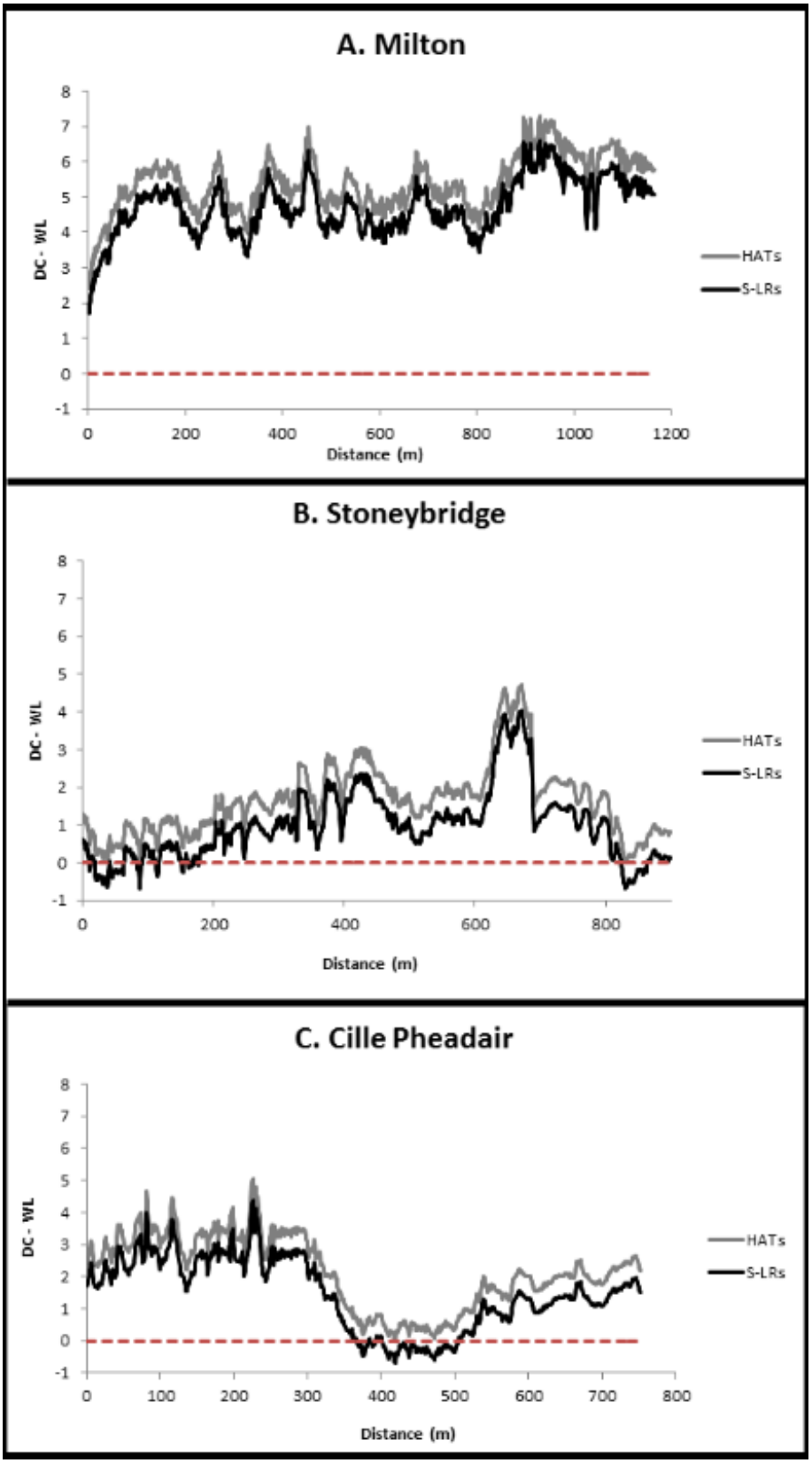

Figure 4.1. The DC-WL (dune crest elevation minus water level (m)) values for the HAT_s and $S\text{-}LR_s$ scenarios at A. Milton, B. Staoinebrig, and C. Cille Pheadair. The horizontal dashed line indicates the value for DC-WL below which water level exceeds dune crest elevation. The x-axis indicates distance from the northern end of each site.

Water levels for three of the scenarios (CS-L, S-LR_N, and S-LR_S) are shown in Figures 4.2-4.4. Comparison of Figures 4.2 (current sea-level) and 4.3 (maximum expected sea-level rise by 2100) shows very little change in the area below the simulated water level for Milton and Staoinebrig At these sites inland areas below the planar surface are predominantly pre-existing machair lochs, or the marshy areas surrounding drainage channels (see Figures 1.4, 1.7, and 1.9). At Cille Pheadair the area under the water surface in Figure 4.2c is low-lying machair grassland with a narrow (~ 1 m wide) drainage channel. The area of machair grassland below the water surface increases substantially from Figure 4.2c to 4.3c, despite the water level rising by only 0.7 m. At all three sites the dune crest remains above water level, and a wide stretch of elevated land in the back dune area provides a barrier between the sea and the lowest-lying machair grasslands found at the eastern side of each site.

The differences between Figures 4.2 and 4.4 are far more obvious than those between Figures 4.2 and 4.3, with the majority of the machair grasslands below the simulated water level at Milton and Staoinebrig. At Cille Pheadair only the dunes to the north and hummocky machair to the south of the headland are above the water surface. At Staoinebrig and Cille Pheadair sections of the dune crest/machair front are below the water level, most notably at the centre of the headland at Cille Pheadair (Fig. 4.4c). Additionally, the width of the dune crest above the water surface has decreased substantially at all three sites: at Milton the width of dune and back dune above water is considerably narrower than in Figures 4.2 and 4.3, but remains ≈100 m wide at its narrowest; at Staoinebrig the width of the dune crest is < 15 m at all points along the site; and at Cille Pheadair the width of the dune crest above the water surface is < 10 m at the centre of the headland, although it is considerably wider to the north and south.

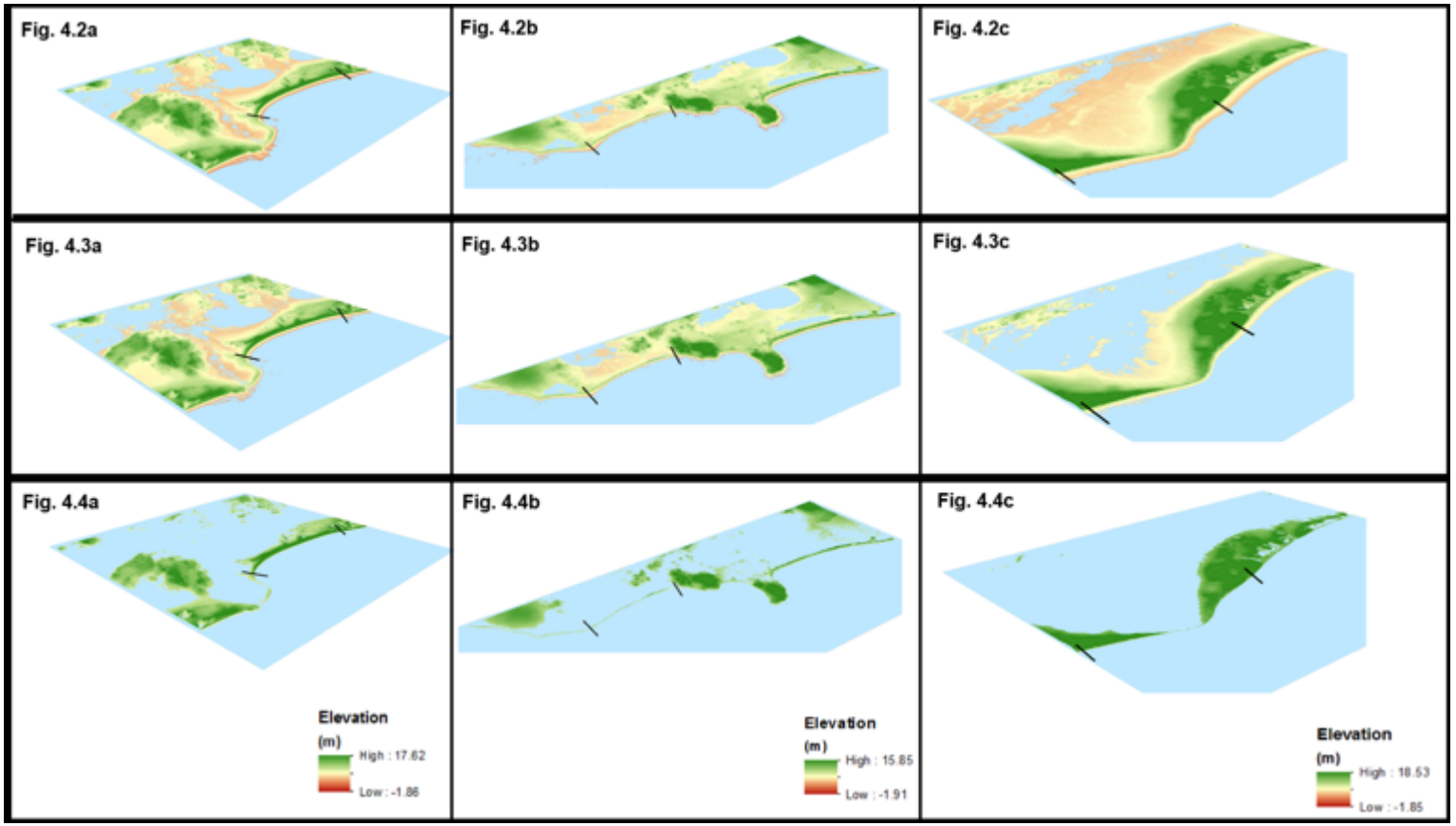

Figures 4.2-4. DTMS of the three sites (a. Milton, b. Stoneybridge, c. Cille Pheadair) with blue surfaces indicating water levels for i) the CS-L scenario (Fig. 4.2); ii) the S-LR_N scenario (Fig. 4.3); iii) the S-LR_S scenario (Fig. 4.4). Black lines indicate the limits of the field sites investigated as discussed in Chapter 3, and the stretch of coast for which the

4.4 Interpretations

This analysis showed intra- and inter-site variation in dune crest elevation between the three sites investigated. Cille Pheadair and Staoinebrig showed greater susceptibility to over-wash, breaching, and inundation of the dune crest during severe storms than Milton due to areas of lower dune crest elevation. Additionally, Cille Pheadair is particularly sensitive to flooding (whether temporary, due to storm water, or permanent, due to sea-level rise), due to the low elevation of the machair grasslands inland of the low-lying headland. As described in section 1.5, Cille Pheadair and Staoinebrig both experienced coastal retreat, over-wash and deposition of storm debris during the January 2005 storm, while no significant change occurred at Milton. Following this event, coastal defences were erected at both sites to increase crest height at the most sensitive parts of the coast (Richards and Phipps, 2007), which were investigated further in Chapters 6-7. Additionally, the headland at Cille Pheadair has been identified as being among the most at risk from inundation in the Outer Hebrides (CoastAdapt, 2011).

At Milton, dune crest elevation was higher than water levels for all seven scenarios. However, at Cille Pheadair and Staoinebrig - sites identified as at risk from breaching, over-wash, and inundation (e.g. Richards and Phipps, 2007; Angus and Rennie, 2008) - water levels only equalled or exceeded minimum dune crest elevation for the two scenarios associated with a combination of extreme high tide and extreme storm surge conditions – conditions which coincide relatively rarely; Dawson et al. (2011) found seven storms of similar magnitude to the January 2005 storm in the 19th C, and one in the 20th C, with durations long enough to ensure they coincided with high tide. Under these conditions, minimum dune crest elevation at Cille Pheadair and Staoinebrig was equalled by water levels for current sea-levels, and exceeded by water levels associated with a 0.7 m rise in sea-level, suggesting that storms, rather than sea-level rise, represent the greatest risk for over-wash, breaching, and inundation. This suggests that periods of temporary flooding and inundation associated with storms are a more probable threat than permanent marine transgression. While flooding and deposition of debris which occur during storm conditions cause considerable damage to infrastructure, and danger and inconvenience to the local population, the machair

ecosystem appears to be relatively resilient to the short-term incursion of saline water associated with storms (Angus and Rennie, 2008).

While the maximum anticipated sea-level rise by 2100 will not lead to water levels exceeding or equalling minimum dune crest elevation under normal conditions, it will increase sensitivity to storm events; the frequency of events with an impact similar to the January 2005 storm may be increased as smaller, more frequent, storm surges of 1-1.5 m will elevate the water to levels currently experienced only during extreme events. Similarly, water levels associated with extreme storm surges of 2 m will have the potential to cause breaching, flooding, and erosion for longer stretches of the coast. A sea-level rise of 0.7 m will increase the sensitivity of Cille Pheadair and Staoinebrig to storm events without requiring any increase in the frequency, intensity, or duration of storms.

The parts of Staoinebrig and Cille Pheadair identified as most at risk from flooding, breaching, or inundation, have similar morphologies; both exist as an eroding scarp at a direct transition between the machair front and the beach. These parts of the site lack both a dune cordon and a shingle ridge, two key coastal landforms which provide protection for the coastal zone during storm events. The identification of these parts of the sites as most at risk under the storm/sea-level rise scenarios is of concern given that Mather and Ritchie (1977) established that 38% of beaches in the Outer Hebrides lacked a dune cordon between the beach and inland areas. The percentage of beaches which have a shingle ridge present has not been identified, nor has any change in the percentage of beaches lacking a dune cordon, but could usefully be investigated as the presence or absence of these features is likely to be tied to risk during storms.

Note that the water levels used in the scenarios associated with this analysis represent mean water levels for the events they represent, and do not take into consideration transitory increases in water-level at the land-sea boundary which will occur due to wave run-up (Walton, 1992), specific values for which are dependent on beach and wave parameters. For this reason, the water-levels used represent a good indication of whether inundation of the dune crest will occur during any of the given scenarios, but breaching and over-wash are likely to occur for mean water levels lower than the dune crest elevation, as these effects may be associated with individual waves that exceed the mean water level. This is demonstrated by the evidence for over-wash, breaching, and widespread deposition of debris plumes and fans at Cille Pheadair and

Staoinebrig during the January 2005 storm (Dawson et al., 2007a; Angus and Rennie, 2008), despite mean water levels for this event being estimated as slightly lower than the minimum dune crest elevation at both sites.

It should also be stressed that this investigation has used dune crest elevation to indicate sensitivity to flooding, over-wash, and breaching, and not to indicate sensitivity to erosion, for which dune crest elevation has been found to be a poor indicator when used in isolation (Judge et al., 2003). However, the areas of lowest dune crest elevation identified at either end of the field site at Staoinebrig, and at the centre of the site at Cille Pheadair merit monitoring after storm events; while these parts of the dune cordon may not be any more sensitive to erosion than the rest of the dune cordon, any further reduction of crest height in these areas will increase the sensitivity of these sites to over-wash, breaching, and inundation during storms.

4.5 Key Findings

4.5.1 Staoinebrig

- Minimum dune crest elevation is similar to predicted water levels for a severe storm coinciding with an extremely high astronomical tide;
- Minimum dune crest elevation is lower than predicted water levels for a severe storm in combination with projected sea-level rise;
- The northern and southern sections of this site may be vulnerable to the effects of overtopping during the above mentioned scenarios.

4.5.2 Milton

- Minimum dune crest height is higher than all predicted water levels;
- Over-washing, breaching, and/or flooding are unlikely to occur at Milton.

4.5.3 Cille Pheadair

- Minimum dune crest elevation is similar to predicted water levels for a severe storm coinciding with an extremely high astronomical tide;
- Minimum dune crest elevation is lower than predicted water levels for a severe storm in combination with projected sea-level rise;

- The central section of this site may be vulnerable to the effects of overtopping during the above mentioned scenarios.
- The machair grasslands at this site are particularly low-lying, and likely to be more susceptible to flooding should the dune cordon/machair front be breached.

4.5.4 General

- At all sites predicted water levels are lower than the minimum crest height for the first five scenarios investigated;
- At all sites large areas of machair grassland are at or below the water level associated with a severe storm surge in combination with projected sea-level rise.

CHAPTER 5
RECENT (2005-2014) AND HISTORIC (1867-2014) STORM CLIMATOLOGY OF THE SOUTHERN OUTER HEBRIDES

Synopsis:

This chapter analyses atmospheric and oceanic conditions over which short, medium and long term coastal changes were quantified (1878-2014), as well as investigating historic climatology during the 20th C. The aims of this chapter are i) to provide a context for interpreting measured changes in the coastal zone, ii) to establish the frequency with which storms of a similar magnitude to the 'Great Storm' of January 2005 have occurred, iii) to quantify temporal variations in storminess and other climatic variables which may affect coastal change; and to, iv) investigate relationships between climatic variables and the NAO index.

5.1 Introduction

Morphological effects of the 'Great Storm' of January 2005 illustrate the dramatic changes severe storms can cause in the coastal zone. A public perception has existed since the mid-1990s that the frequency and intensity of storms has increased in the North Atlantic region (Matulla et al., 2008), although the evidence for such a trend is limited. In addition to changes in storminess (generally indicated by variation in the frequency or intensity of gales), other climatic factors may influence coastal evolution. For example, Wolf and Woolf (2006) found that increased North Atlantic wave heights could be generated by an increase in mean wind speeds as well as increases in storminess. Thomas et al. (2011a) showed that changes in the prevailing wind direction also have the potential to influence coastal evolution, without requiring any change in wind speeds or storminess. Morphological variability at the coast may be caused by a range of factors including: increased frequency and/or severity of storms, changes in the prevailing wind direction, increased mean and maximum wave heights, changes in wave direction, and changes in atmospheric pressure (through influencing wind speeds and water levels) (Phillips et al., 2013). As these aspects of climatology represent key drivers of coastal evolution it is important to understand how the climate has changed over the period for which coastal change is investigated. In addition, understanding

how the climate has changed provides a context for interpreting extreme events such as the January 2005 storms and a background for consideration of predictions of future anthropogenic climate change.

Trends in storminess in the North Atlantic region vary considerably with temporal scale. For example, an increase in storminess over the latter half of the 20th C has been reported by Matulla et al. (2008), and Phillips et al. (2013) found that the frequency of storms had increased across the southern UK over the same period. McClatchey et al. (2014) suggest that at the end of the 1990s an increasing trend in severe windstorms could be observed, with no clear trend evident in the following decades. However, gale day frequencies from Stornoway (Lewis, Outer Hebrides) over the last 100 years suggest that storminess decreased from the 1940s to the 2000s (Dawson et al., 2007a). Trouet et al. (2012) found an inverse relationship between the frequency and intensity of storms, further complicating the observed trends. Additionally, Phillips et al. (2013) and Allan et al. (2008) observed some differences in the trends in storminess for October-December and January-March.

Several researchers have investigated the links between the North Atlantic Oscillation (NAO) and storminess in the North Atlantic region. NAO index values indicate the pressure differences between the Azores High and Icelandic Low pressure systems; changes in the value influence atmospheric circulation, particularly the position of the North Atlantic storm track. The relationship between the NAO and storminess is complicated, with the strength and nature of any relationship varying temporally and spatially (Matulla et al., 2008), and dependent on the storm period studied (e.g. October-December vs. January-March, winter vs. all year) (Allan et al., 2008). Generally, more positive NAO values are linked to stormier European winters (e.g. Dawson et al., 2004; Matulla et al., 2008), higher waves (Wolf and Woolf, 2006; Thomas et al., 2011b), and beach lowering and/or increased coastal erosion (Thomas et al., 2010; Thomas et al., 2011a; Thomas et al., 2011b). Phillips et al. (2013) found that a more positive NAO regime was linked to more westerly winds around the Bristol Channel. Some authors have suggested that the magnitude of the NAO index (irrespective of sign) may be correlated with tidal range (Thomas et al., 2011a), wave heights (Wolf and Woolf, 2006; Thomas et al., 2011b) and storminess (Dawson et al., 2010), further highlighting the complexity of the NAO's influence. Additionally, Dawson et al. (2010) and Wolf and Woolf (2006) suggest that some of the variance in

the strength of the relationship between the NAO and storminess may be explained by the extent of winter sea ice, which influences wind speeds and wave heights by limiting fetch. The relationship between the NAO index and storminess appears to be particularly strong around the Scottish coastline (McClatchey et al., 2014).

This chapter aims to investigate changes in the historic climatology of South Uist over the period for which coastal change was investigated, thereby providing a context for interpreting the results of Chapters 6 and 7.

5.2 Methods

5.2.1. Short-medium term climatology (2005-2014)

Information on atmospheric conditions during the study (January 2005 to March 2014) were collected from the Met Office Integrated Data Archive System (MIDAS) via the Centre for Environmental Data Archive (CEDA). Hourly wind direction, wind speed, and altimeter pressure data were obtained from the Benbecula weather station (Table 5.1), located approximately 20 km north of Staoinebrig (the most northerly field site), and approximately 35 km north of Cille Pheadair (the most southerly field site). Atmospheric data were sorted to identify: i) gale and storm events; and ii) severe atmospheric depressions of $\leq$ 970 hPa (the typical maximum pressure associated with an 'intense' storm event (Lambert and Fyffe, 2006)), and $\leq$ 960 hPa. Gales are identified as any event where mean wind speeds $\geq$ 34 kts are recorded, while storms are identified as any events where mean wind speeds $\geq$ 48 kts are recorded. Gale or storm force recordings which are maintained over several readings are considered to be part of the same event unless separated by a reading less than 30 kts. The windspeeds selected for identification of storm and gale events are those agreed by national and international meteorological agencies to define these events (e.g. UK Met Office, U.S. National Weather Service, the modernised Beaufort Scale, etc.). These definitions of strong wind events are commonly used within the academic literature (e.g. Bowditch, 2005; Von Ahn et al., 2006; Brennan et al., 2009; Burningham & French, 2013, etc.) and follow navigation and forecasting convention for North Atlantic high windspeed events (e.g. as used by the National Oceanic and Atmospheric Administration, the UK

Meteorological Office, etc.). However, other systems are used (particularly when considering historical datasets which predate accurate wind speed recording devices).

Table 5.1. Station location information.

Station	Network	Data	Latitude	Longitude	Elevation (m)
Benbecula 18909	MIDAS	weather	57.4636	-7.37303	6
Benbecula Airport 84	MIDAS	weather	57.4754	-7.36976	6
West of Hebrides	WaveNet	wave	57.29833	-7.916389	-

Half-hourly information on wave conditions during the study was obtained from WaveNet through the Centre for Environment, Fisheries, and Aquaculture Science (CEFAS). Half-hourly information on wave direction, and significant wave height (Hs) throughout the study was collected from the West of Hebrides WaveNet WaveRider buoy (Table 5.1), located ~60 km offshore to the west of Staoinebrig. Quarter-hourly tide gauge data were obtained from the British Oceanographic Data Centre for the Stornoway tide gauge.

The West of Hebrides WaveNet site was not operational until 23rd February 2009, and therefore it is not possible to make direct comparisons between wave conditions experienced during the January 2005 storm and conditions during the study period, or to determine wave conditions associated with all events listed in Table 5.3 (see below). Furthermore, all WaveNet buoys located off the north-west coast of Britain were deployed from January 2006 onwards so it is not possible to extrapolate data from these. Wolf (2007) modelled maximum wave heights of 12-14 m during the January 2005 storm in the vicinity of the location where the West of Hebrides wave buoy was later deployed.

5.2.2 Long term climatology (1867-2014)

Long-term climate data were sourced from a range of locations. Information on atmospheric conditions was obtained from MIDAS via CEDA. Hourly information on wind speed and atmospheric pressure was collected from Benbecula site 18909 (Table 5.1) from 1997-2014. Hourly data were collected from Benbecula Airport site 84 (Table 5.1) from 1971-1996. Three hourly data were collected from the same site for

the period 1957-1971. Site 18909 replaced site 84, and is located ~1 km to the south of site 84.

Earlier data were obtained from climate returns held at the Meteorological Office Archives in Edinburgh. Monthly mean pressure values and gale force events were obtained from the returns. From 1946-1956 atmospheric data was obtained from Benbecula (the island immediately north of South Uist) where they were recorded at six hourly intervals. From 1928-1946 data were obtained from the Skallery, Benbecula, site, for which no atmospheric pressure data were available, and only one measurement of wind conditions was made per day. Data from 1921-1927 were obtained from the Castlebay, Barra site (an island to the south of South Uist) where data were recorded four times a day at 7 am, 1 pm, 6 pm, and 9 pm. Earlier data from 1867-1921 were provided by Alastair Dawson, having been previously obtained and catalogued from the Met Office Archives by himself and Mark Ritchie. For this period data were obtained from the Monach Isles, consisting of twice daily pressure readings and recordings of gale and storm events.

Tide gauge data were obtained from 1976-2014 from the British Oceanographic Data Centre for Stornoway, with hourly information on significant wave height and wave direction available from 1976-1992, and quarter-hourly data from 1993-2014. Monthly NAO data from 1950-2014 were obtained from the CPC. Earlier NAO data from 1867-1949 were obtained from the University of East Anglia Climate Research Unit (CRU) (Hurrell, 1995; Jones et al., 1997). It should be noted that slightly different sites are used to calculate the two NAO indexes, resulting in some differences in values when overlapping times were examined.

From 1949-2014 wind speed data were provided in knots (kts), for which a gale force day was determined to be a 24 hour period where wind speeds $\geq$ 34 kts were measured, and a storm force day was a 24 hour period where wind speeds $\geq$ 48 kts were measured. From 1905-1948 wind speed data were recorded in the Beaufort scale, for which a gale force day was determined to be a 24 hour period where wind speeds $\geq$ 8 were recorded, and a storm force day was a 24 hour period when wind speeds $\geq$ 10 were recorded. From 1867-1904 a six-point scale was using to classify wind speed, with 5 indicating a gale and 6 indicating a storm. The implications of the different temporal resolutions of the various records used in this research are discussed in section 5.2.2.1.

5.2.2.1 Implications of variability of temporal resolution in data-sets

The implications of the variability of the temporal resolutions of the various data-sets used on results was investigated by re-sampling data from the stormiest and least stormy years in the period for which hourly meteorological data were available (1971-2014); 1990, and 2001, respectively. Data from these years were resampled at 3-hourly, 6-hourly, 12-hourly, and 24-hourly resolutions to determine how changing the temporal resolution affected i) the number of storm and gale events detected; ii) annual mean wind speed; and iii) annual mean atmospheric pressure. The results from this analysis are summarised in Table 5.2.

Table 5.2. Comparison of meteorological parameters for 1990 and 2001 derived from different temporal resolutions of data.

Year	Resolution	No. gale/storm days	Mean wind speed (kts)	Mean atm. pres. (hPa)
1990	1-hourly	32	14.64	1008.87
	3-hourly	23	14.62	1008.86
	6-hourly	19	14.59	1008.86
	12-hourly	11	14.71	1009.05
	24-hourly	8	13.77	1009.17
2001	1-hourly	1	11.31	1011.61
	3-hourly	1	11.43	1011.47
	6-hourly	1	11.46	1011.55
	12-hourly	1	11.75	1011.54
	24-hourly	0	11.75	1011.54

From Table 5.2 it is evident that variations in the temporal resolution of different datasets are unlikely to cause significant deviations in the accuracy of determinations of mean annual meteorological parameters. Even re-sampling at the coarsest temporal resolution produced mean annual wind speeds and atmospheric pressures that are similar to those achieved using 1-hourly measurements. However, reducing the sampling frequency appears to reduce the number of gales and storms detected. The relationship between sampling frequency and the number of storms/gales identified for 1990 indicates a logarithmic relationship ($y = 7.76^{\ln(x)} + 7.21$; $p < 0.05$; $R^2 = 0.84$) between the number of storm and gale days detected and the measurements taken per 24

hours. This relationship may impact on results with temporal resolution of data needing to be carefully considered when making interpretations.

5.2.3 Statistical analysis

Regression analysis was performed on all time-series, and between meteorological variables and monthly/annual NAO index values. Generally, a linear regression was fitted to data unless another model was clearly more appropriate. A two-tailed Student's T-test was used to determine the significance of differences between and/or within datasets.

5.3 Results

5.3.1 Climatology 2005-2014

5.3.1.1 Storminess

Table 5.3 summarises storm force events during the study period. Figure 5.1 shows the number of gale days each month between 2005-2014, while Figure 5.2 shows the maximum monthly wind speed recorded over the same period. The stormiest months (months with the highest number of gale days) are summarised in Table 5.4.

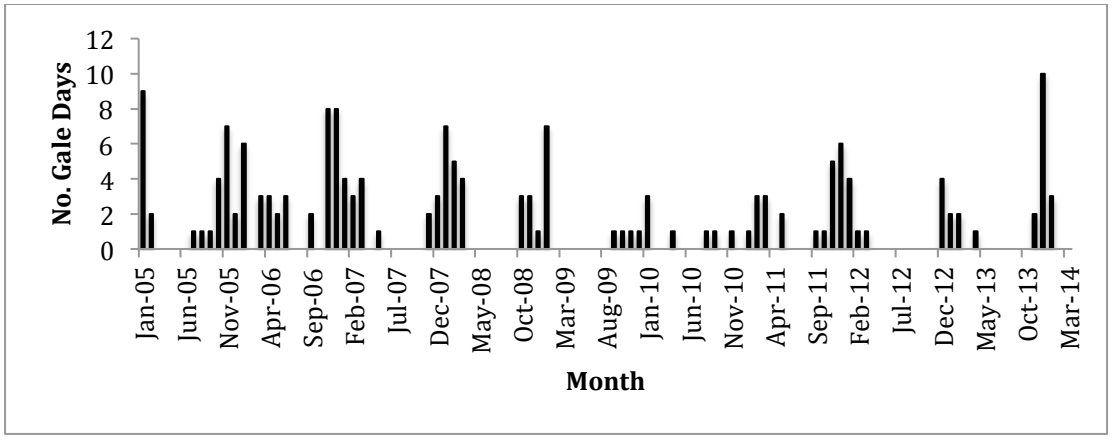

Figure 5.1. The number of gale days occurring each month between 2005-2014. Gale days are defined as periods of 24 hours during which the wind speed exceeded 34 knots for at least one hourly measurement. N = 175.

Table 5.3. Weather data for extreme events during the period from 2005-2014. An event was identified as extreme if i) wind speed was ≥ 48 kts for at least one hour; and/or, ii) atmospheric pressure was ≤ 960 hPa for at least one hour; and/or, iii) significant wave height was ≥ 12.5 m for at least half an hour. Max. WS = maximum wind speed; $t_{WS>GF}$ = duration of gale force winds; $t_{WS>SF}$ = duration of storm force winds; W. direction = wind direction(s); Min. P = minimum atmospheric pressure; $t_{\leq 970\ hPa}$ = duration of atmospheric pressure ≤970 hPa; $t_{\leq 960\ hPa}$ = duration of atmospheric pressure ≤960 hPa; Max. Hs = maximum significant wave height; HT = indicates whether the storm lasted for at least one full tidal cycle (12 hours). Bold text indicates the most severe values (in terms of storminess) for each column.

Date	Max. WS (kts)	$t_{WS>GF}$ (hrs)	$t_{WS>SF}$ (hrs)	W. Direction	Min. P (hPa)	$t_{\leq 970\ hPa}$ (hrs)	$t_{\leq 960\ hPa}$ (hrs)	Max. Hs (m)	TC
11-12 jan 05	61	**19**	**9**	170-280	959/944/934*	15	5	12-14**	yes
08 nov 05	**62**	4	1	230-250	973	3	0	-	
11 nov 05	55	15	5	190-290	972	5	0	-	yes
03 dec 06	38	6	0	150-260	957	10	9	-	
17 mar 07	55	16	1	260-310	989	0	0	-	yes
17 jan 09	54	18	4	140-240	952	**123**	**69**	-	yes
25 nov 09	42	6	0	260	959	29	7	9.08	yes
03 feb 11	42	1	0	190	982	0	0	13.39	
10 mar 11	53	8	1	260-280	986	0	0	10.59	yes
03 dec 11	50	6	1	270-290	983	0	0	12.65	yes
08 dec 11	47	4	0	220-320	962	7	0	12.85	
13 dec 11	31	0	0	200	**944**	34	16	8.89	
28 dec 11	49	13	2	240-310	983	0	0	14.48	yes
04 feb 13	39	10	0	270-290	989	0	0	**16.39**	yes
05 dec 13	33	0	0	340	1001	0	0	12.62	
19 dec 13	52	5	1	240-260	951	11	6	-	
26 jan 14	42	10	0	140-210	961	0	0	15.87	yes

*First pressure value is from the Benbecula station sourced through MIDAS for Benbecula weather station. The second value is quoted in Woolf (2006). The third value is quoted in Dawson et al. (2007b).

**This value is modelled rather than measured, and obtained from Woolf (2007).

Table 5.4. Weather data for the five stormiest months from January 2005 to March 2014. Gales are days with at least 1 hour with windspeeds > 34 kts. Storms are days with at least 1 hour with windspeeds > 48 kts. Bold values indicate the most severe values (in terms of storminess) in each column.

Month	Mean wind speed (kts)	Highest wind speed (kts)	No. gale days	No. storm days	Mean air pressure (hPa)	NAO index
January 2005	19.1	61	9	**2**	1008.1	**+ 1.26**
November 2005	16.4	**62**	7	**2**	1009.5	- 0.46
November 2006	18.9	47	8	0	1002.0	+ 0.33
December 2006	16.0	42	8	0	1006.4	+ 1.15
December 2013	**19.5**	52	**10**	1	**995.9**	+ 0.79

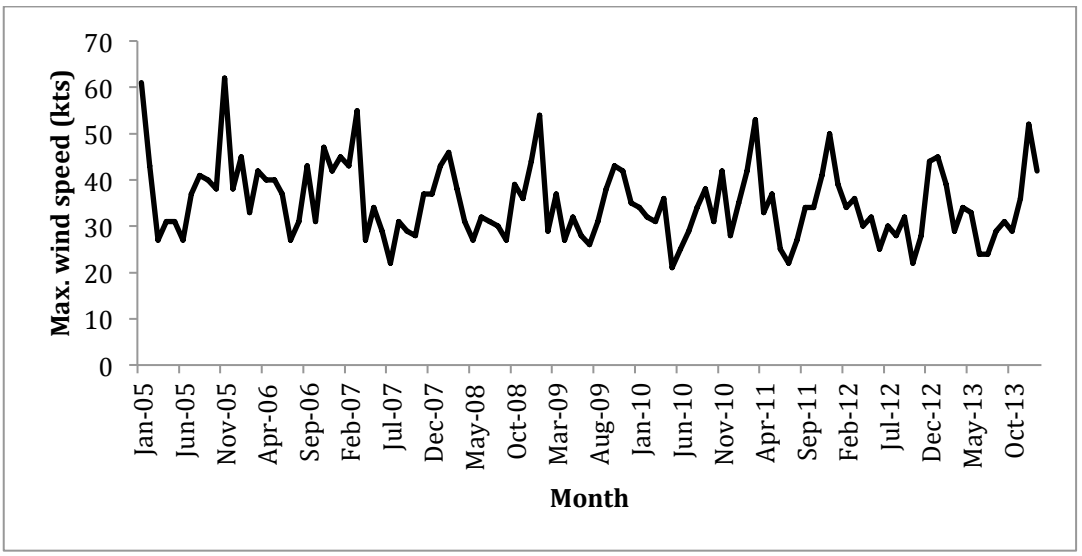

Figure 5.2. Maximum wind speed recorded for each month January 2005 to March 2014. N = 112.

The maximum wind speed recorded over this period was 62 kts on 8th November 2005. This speed was 1 kt higher than the maximum wind speed during the 'Great Storm' of January 2005, but storm force wind speeds were maintained for only 1 hour (gale force conditions for 4 hours), while storm force winds lasted for 9 hours (gale force conditions for 19 hours) during the January 2005 storm, and coincided with high tide (Table 5.3). The maximum duration of gale force winds and storm force winds both occurred during the January 2005 storm (19 hours and 9 hours, respectively). A storm on 17th January 2009 recorded a similar duration of gale force conditions (18 hours), although the duration of storm force winds was only 5 hours. This event had the second longest duration of storm force conditions – lasting slightly over half the time storm force conditions occurred for during the January 2005 storm.

Figures 5.1 and 5.2 both show negative trends in storminess, as considered both in terms of the number of gale days and maximum recorded wind speeds. Both relationships are significant at the $p < 0.05$ level.

Table 5.2 shows that four of the five of the stormiest months occurred during the first two years of the period studied, and include January 2005. However, the highest mean wind speed, highest number of gale days, and lowest mean atmospheric pressure were all recorded for the more recent month of December 2012.

The temporal resolution shown in Figure 5.2 is too short to draw meaningful conclusions about trends in storminess (discussed further in section 9.1.2). Note that no

events of similar wind speed to the January 2005 storm have occurred during the site survey period (October 2011 – March 2014), and the number of gales occurring annually appears to be lower in recent years (particularly 2009, 2010, and 2012, and with the exception of 2013) than in the years immediately following the January 2005 storm. This contrasts with local opinion, that suggests that the years following the January 2005 storm were characterised by relatively calm conditions, with 'normal' conditions returning more recently (David Muir, personal communication (2012)).

5.3.1.2 Wind speed and direction

As with indicators of storminess, the mean monthly wind speed has decreased during the period studied ($p < 0.05$) (Fig. 5.3). However, there is a clear peak in mean wind speeds during the survey period in December 2013, which has the highest monthly mean wind speed between 2005-2014 (19.5 kts).

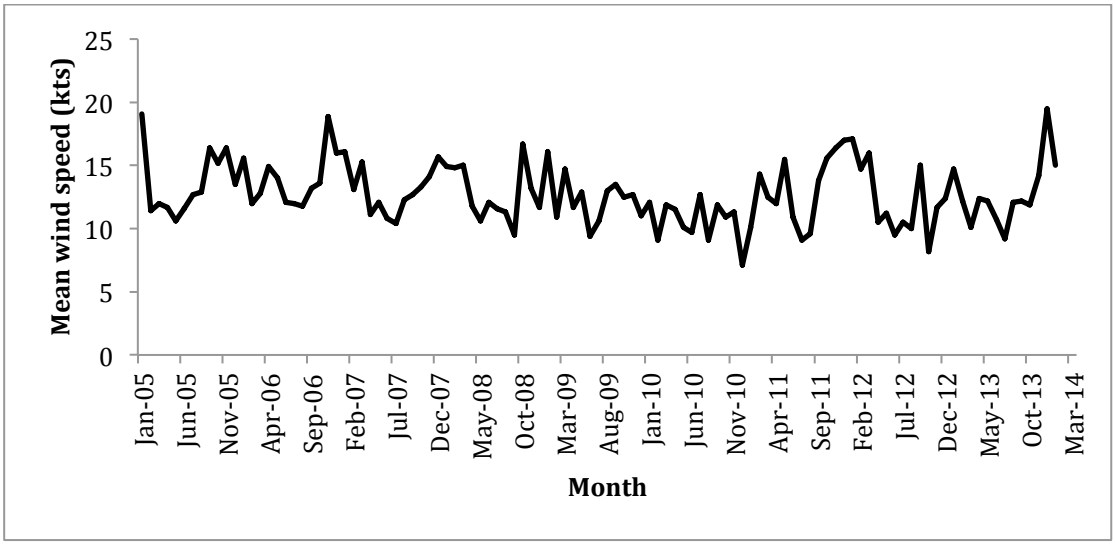

Figure 5.3. Mean monthly wind speed from January 2005 to March 2014. N = 112.

Prevailing winds are generally from the south and southwest (although winds from all bearings are not uncommon) (Fig. 5.4a). Gale force (and above) strength winds are also predominantly from the south and west, although with more westerly components (Fig. 5.4b). No gale force winds are recorded from the northeast.

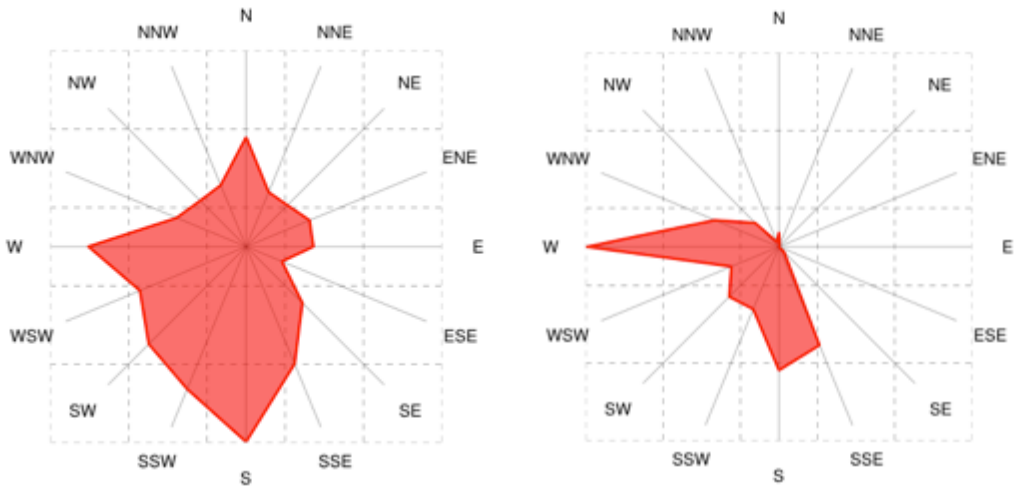

Figure 5.4. Wind roses showing wind direction during A) all conditions (n=88,155), B) gale and storm conditions (n=719), from 2005-2014. Wind roses generated using WindRose Pro (Enviroware).

5.3.1.3 Atmospheric pressure

Table 5.3 shows events associated with severe atmospheric depressions (minima ≤ 970 hPa). Figure 5.5 shows monthly mean values of atmospheric pressure.

Minimum atmospheric pressure recorded between 2005 and 2014 was 944 hPa. This was 15 hPa lower than the atmospheric pressure minima recorded at Benbecula weather station during the January 2005 storm. However, this event was not associated with storm, or even gale force wind speeds (max wind-speed of 31 kts). Four other events registered atmospheric pressures equal to or lower than the January 2005 storm (Table 5.3). Two of these events recorded maximum wind speeds less than storm force. The other two had maximum wind speeds considerably lower than those recorded in the January 2005 event (52 and 54 kts). Additionally, the event of 17th January 2009 is exceptional for the duration of extremely low pressures (~ 5 days at or below 970 hPa and ~ 3 days at or below 960 hPa). Evident from Table 5.3 is that several events with lower or similar atmospheric pressure minima to that recorded during the January 2005 storm have occurred between 2005 and 2013, although the depth of the depression does not appear to be strongly correlated with maximum wind speeds during the event.

Figure 5.5 shows a slight trend to lower monthly mean atmospheric pressures during the study. However, this relationship is not statistically significant. December 2009 has the highest mean atmospheric pressure (1033.2 hPa, 1 gale day) which is noteworthy as generally higher pressures would be expected during the summer months.

The lowest mean atmospheric pressure occurred in January 2014 (988.7 hPa, 3 gale days).

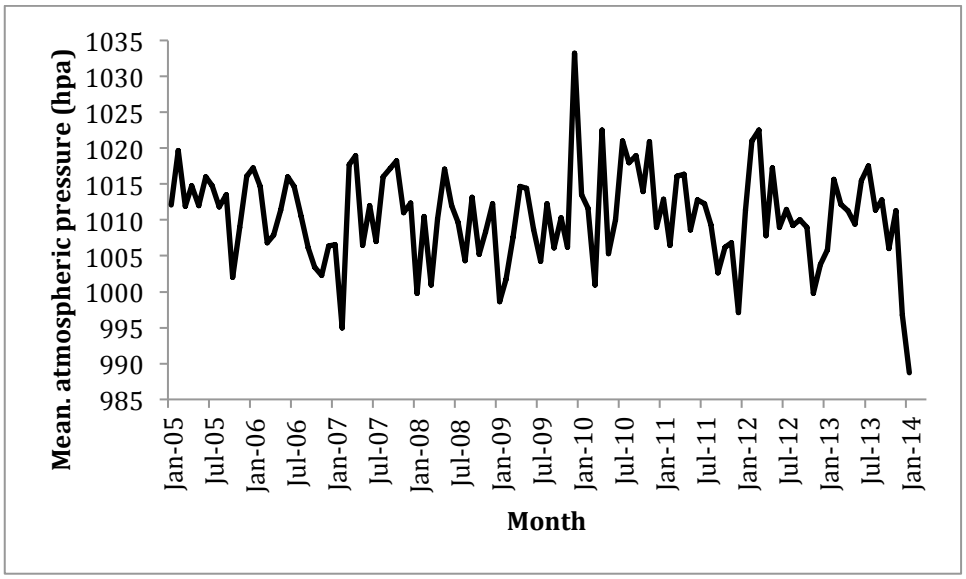

Figure 5.5. Monthly mean values of atmospheric pressure from January 2005 to March 2014. N = 109.

5.3.1.4 Ocean conditions

Maximum significant wave heights during storm events are summarised in Table 5.3. It is evident from Table 5.3 that the modelled wave heights for the January 2005 storm (12-14 m) were met and exceeded three times within the 3 year period for which records exist. The maximum significant wave height recorded during the study was 16.39 m on 4th February 2013 (2.39-4.39 m higher than the modelled wave height for the January 2005 storm). This event was associated with gale force winds (max. wind speed = 39 kts), and a relatively high atmospheric pressure minima (989 hPa). Comparison with the data in Table 5.2 suggests that the wave heights modelled for the January 2005 storm are not unusual, with significant wave heights > 12 m occurring 8 times, and significant wave heights > 14 m occurring 3 times in the 4 year period for which data are available. 2010 had no storm events. It should be noted that wave data is obtained from an offshore wave buoy – while this is the closest available source of information on sea conditions, it is recognised that wave height will be significantly lower at the coast due to the shoaling effect of the shallow continental shelf, and loss of wave energy on moving towards the coast (e.g. while passing through kelp beds).

Figure 5.6 shows monthly mean tide gauge levels from Stornoway. There is very little evidence for any increase in water levels over this time, and while some months show very low tidal levels (identifiable as troughs in Figure 5.6), there are no particularly high peaks in monthly mean value.

Change in monthly mean significant wave height between March 2009 and March 2014 is shown in Figure 5.7, which indicates an increase in wave heights ($p < 0.10$, $n = 59$). Peaks occur in February and December 2011, and December 2013.

The prevailing wave direction during all conditions is from the west (Fig. 5.8a), while for higher significant wave heights (> 10 m) the prevailing wave direction is from WSW to WNW. All waves approach from the western half of the compass due to the orientation of the coast.

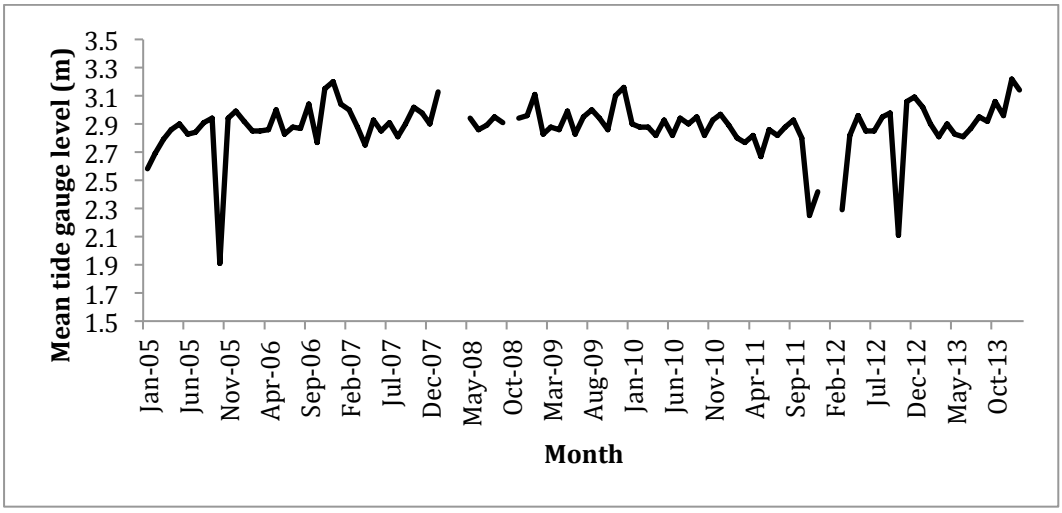

Figure 5.6. Monthly mean tide gauge levels from January 2005 to March 2014. N = 109.

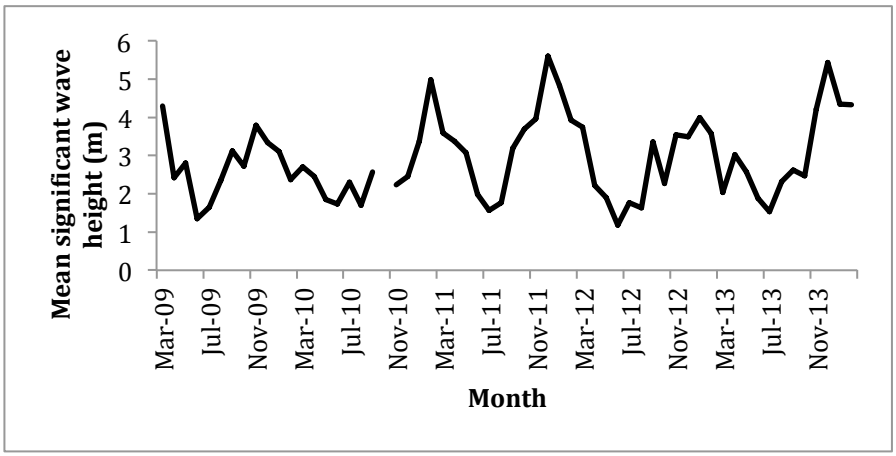

Figure 5.7. Change in monthly mean significant wave height from March 2009 to March 2014. N = 109.

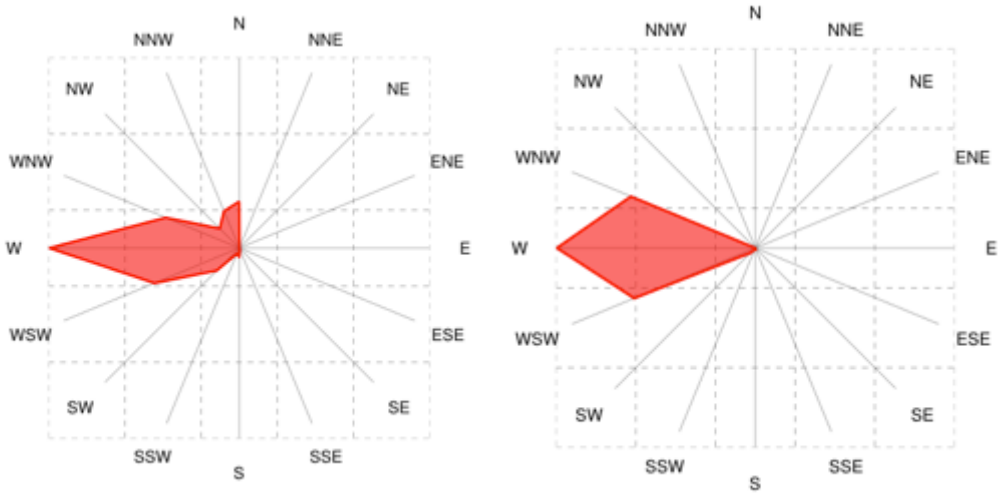

Figure 5.8. Wave rose showing wave direction during A) all conditions (n=85,038), B) high wave conditions (significant wave heights > 10 m) (n=277), from 2005-2014. Wave roses generated using WindRose Pro (Enviroware).

5.3.1.5 NAO

The NAO index has not changed significantly over the study.

Relationships between NAO and atmospheric and oceanic variables are summarised in Table 5.5. Four of six variables are very strongly correlated with NAO index values ($p < 0.01$). Monthly values for monthly maximum wind speed, mean wind speed, number of gale days, and mean significant wave height all positively and significantly ($p < 0.01$) correlate with NAO index values. Two variables, atmospheric pressure and tide gauge level have no relationship with NAO index values.

Table 5.5. r- and p-values for relationships between NAO and atmospheric and oceanic variables.

Variable	r-value	p-value	n
maximum monthly wind speed	- 0.33	< 0.01	109
mean monthly wind speed	- 0.55	< 0.01	109
monthly no. gale days	- 0.36	< 0.01	109
mean monthly atmospheric pressure	0.00	-	109
mean monthly tide gauge level	+ 0.25	-	109
mean monthly significant wave height	+ 0.74	< 0.01	59

5.3.2. Climatology 1867-2014

5.3.2.1 Storminess

Figure 5.9a and b show the annual and decadal number of gale and storm days from 1869-2014, respectively. Storminess has varied considerably over this period, with extremely high numbers of gale days (≤ 78 gales/yr) during the 19th C (particularly between 1867-1880, and 1890-1905), then a dramatic decline in the number of gale days during the early 20th C. Storminess remained very low until the late 1940s, when the number of gale days increased. However, late-20th C levels of storminess have not been recorded during any part of the 21st C. A second lull in storminess appears between 1995-2005, with storminess since 2005 being generally close to or slightly above the average of 15.6 gale days/yr. While the number of storm days appears to follow the same broad pattern as the number of gale days, there are some differences. For example, the highest frequency of gale days occurs during the 1860s and 1870s, while the highest frequency of storm days occurs in the early 1900s. Over the last decade, the number of storms has been similar to, or slightly below, the average of 1.4 storms/yr, with the exceptions of 2005 and 2011, which had 4 and 3 storm days, respectively. The decadal totals shown in Figure 5.9b provide a more simplistic view of the data, and confirm the results from Fig. 5.9a, that the highest frequency of gale days was during the 1860s and 1870s, a lull in gale activity occurred from 1910-1930, and then there was an increase in storminess until the 1950s. The decadal totals also suggest a slight decrease in the number of gales from the 1970s (197 gales) to the 2000s (115 gales).

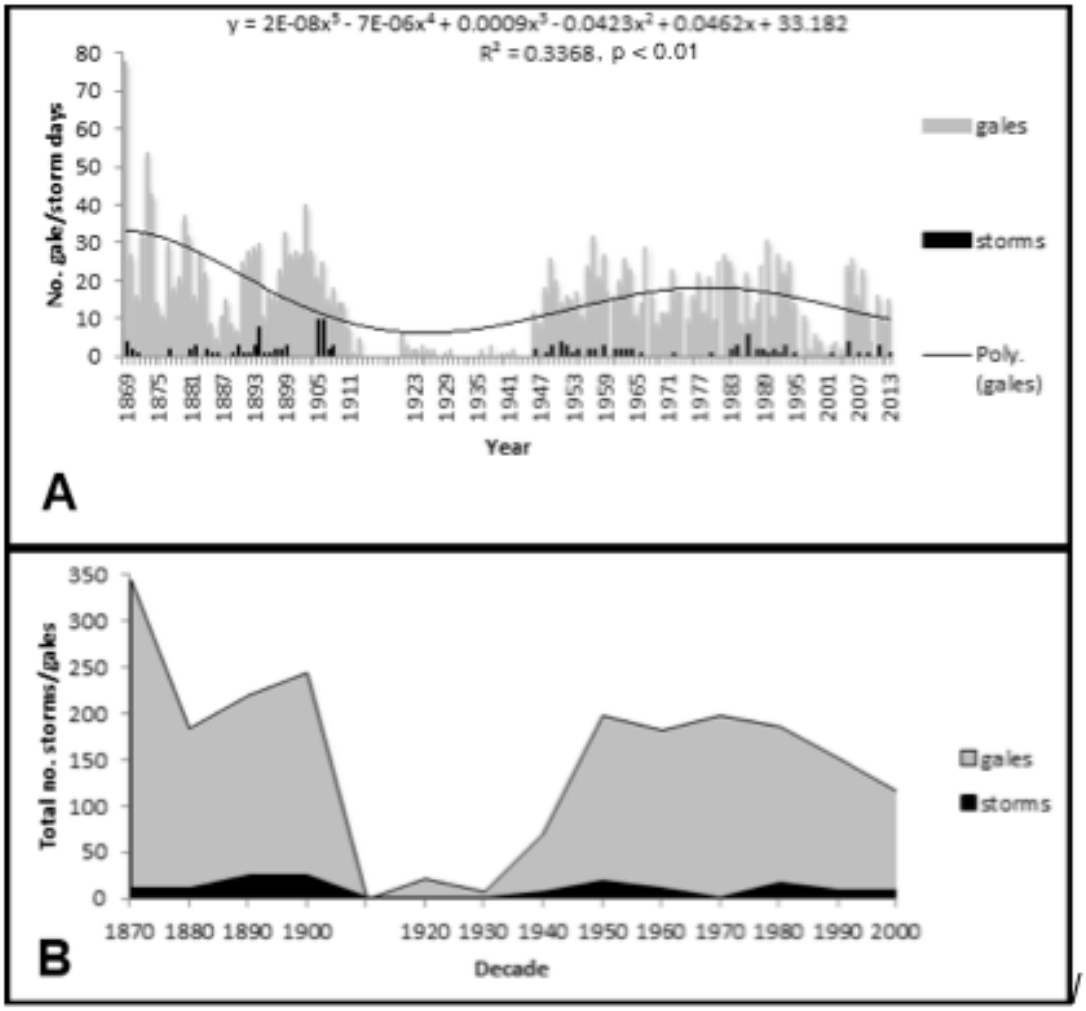

Figure 5.9. Storm and gale day frequencies from 1867-2014. A) annual totals, B) decadal totals. A 5th order polynomial trend line is fitted to the annual total number of gales.

Figure 5.10 shows the frequency distribution of wind directions for storm and gale force winds from 1867-2014. The wind rose indicates that the majority of storms track from the west, with relatively high numbers also tracking from the south and west-north-west. Compared to the prevailing wind direction during all conditions which are generally southerly (see Fig. 5.14), wind directions during storms appear to contain noticeably more westerly components, and less northerly components.

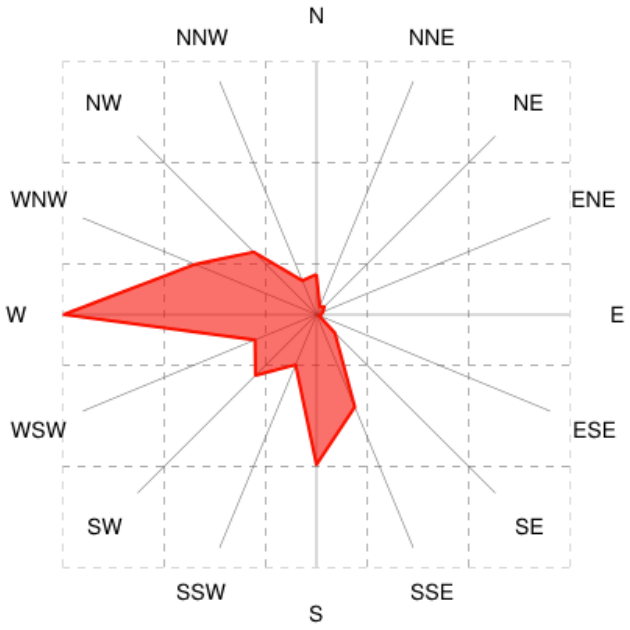

Figure 5.10. Wind rose showing wind direction gale and storm events (events where wind speed ≥ 34 kts) (n=5,933). Wind rose generated using WindRose Pro (Enviroware).

5.3.2.1.1 Frequency vs. intensity of storms

A strong positive relationship between the frequency and intensity of storms was found (Fig. 5.11) (n=138; r = + 0.42; p < 0.01); there was no indication of an inverse relationship between the frequency and intensity of events.

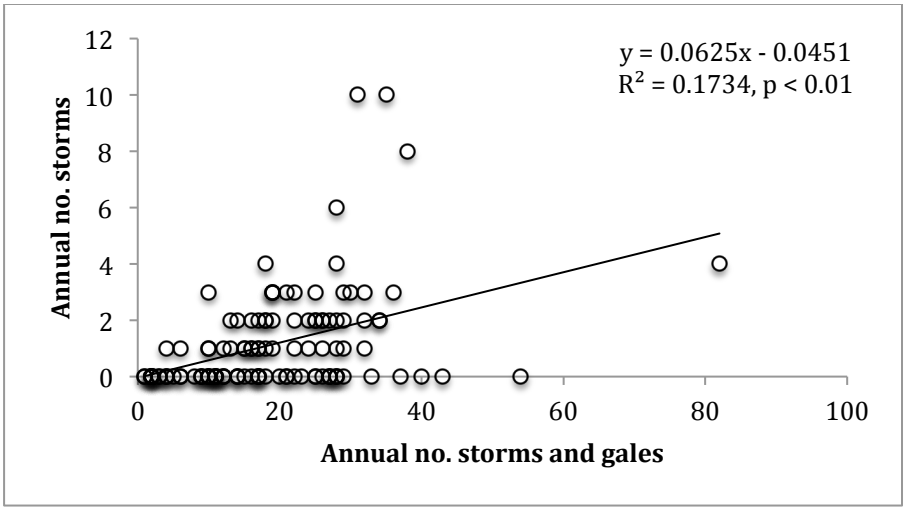

Figure 5.11. The annual no. of storms plotted against the annual total number of storm and gale events for the period from 1867-2014. N = 138.

5.3.2.2 Wind speed and direction

Figures 5.12a and 5.12b show changes in mean annual wind speed between 1929-1945 (Beaufort scale), and 1957-2014 (knots), respectively. Both graphs show speeds decreasing with time. This trend is not significant for the earlier period. However, for the latter period, the decrease in mean annual wind speed is significant at the $p < 0.01$ level ($n = 57$; $r = -0.45$).

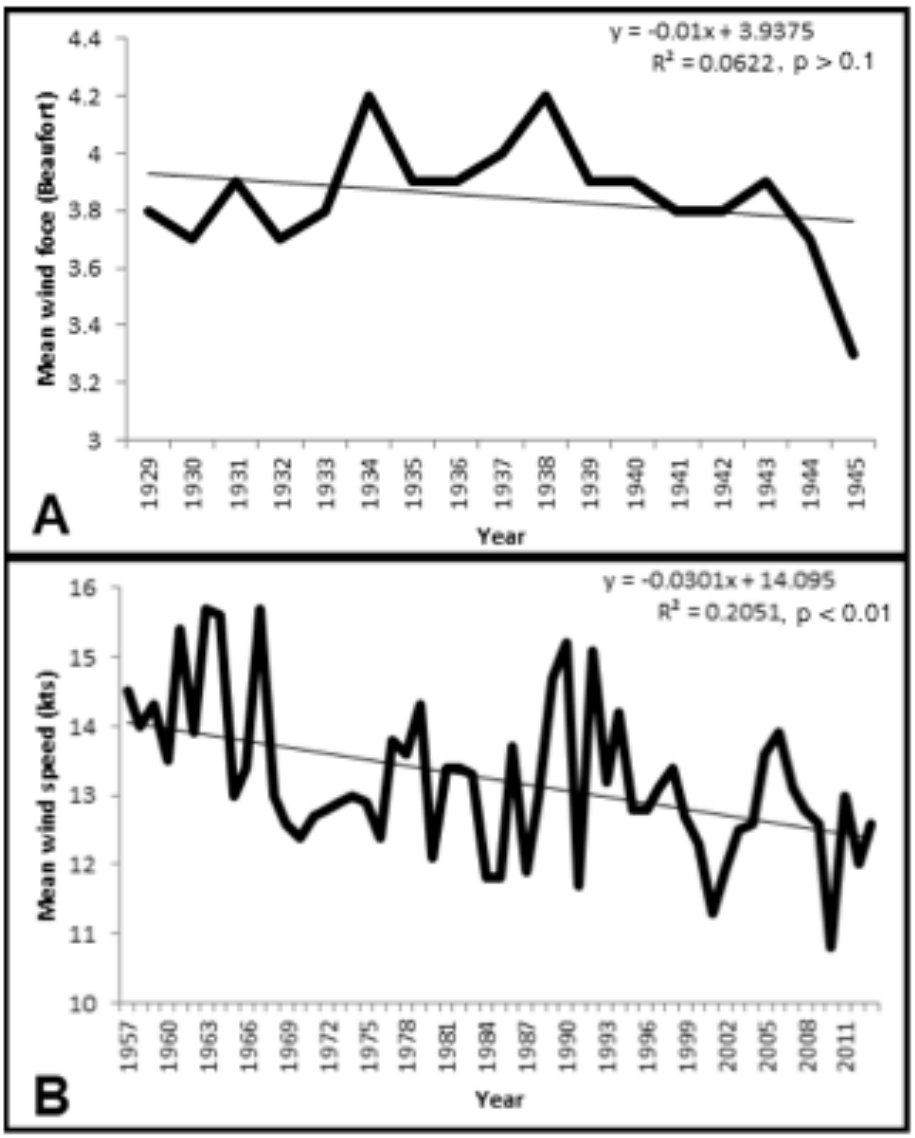

Figure 5.12. Mean annual wind speed from A) 1929-1945, B) 1957-2014. N = 57.

Highest monthly gust speeds are shown in Figure 5.13 for the periods for which these data were recorded; 1997-2014, and 1950-1956. Although the lack of data for the

majority of the study makes conclusions difficult, it appears from Fig. 5.13 that max. gust speeds were generally slightly higher in the 1950s than in the 1990s and 2000s. Mean highest gust speed from 1950-1956 was 64.48 kts; from 1997-2014 mean highest gust speed was 49.47 kts ($p < 0.01$). While the January 2005 storm stands out in the more recent run of data, the maximum gust speed recorded during this storm was exceeded three times in the 6 year period from 1950-1956.

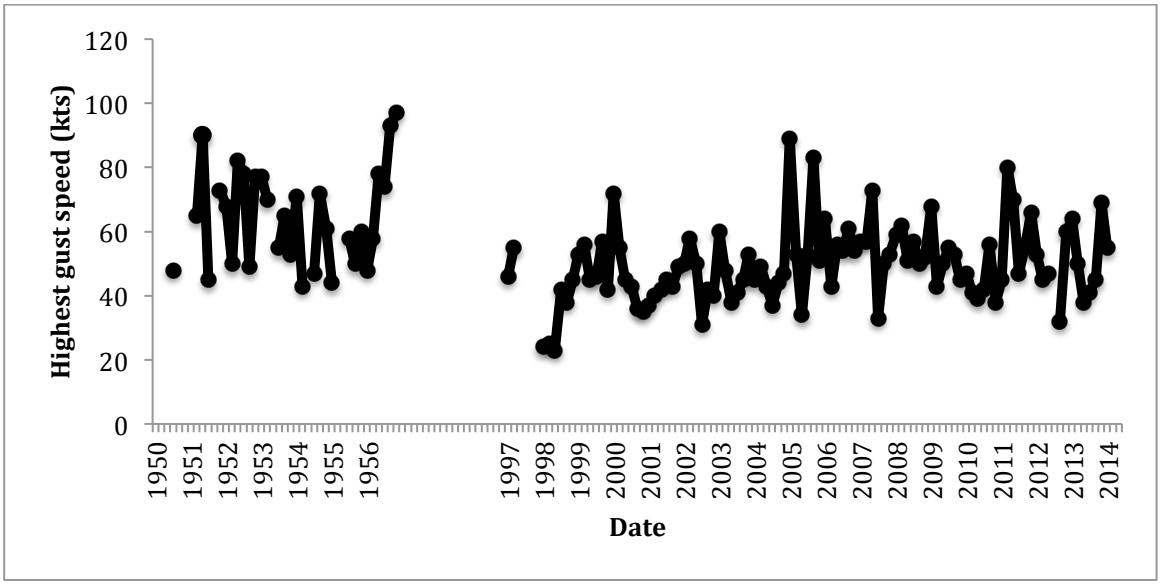

Figure 5.13. Highest monthly gust speeds (October-March). N = 129.

Visual analysis of cardinal wind direction data from 1928 to 1950 revealed a rapid shift in the prevailing wind direction from north-westerly to south-westerly c. 1940, and visual analysis of degree wind direction data from 1957 to 2014 indicated a gradual shift to more westerly components. Based on these findings, wind roses were generated for the full period for which wind direction data were available (1928-2014), and also for smaller timer periods to investigate the apparent changes. Figures 5.14 b and c confirm the initial visual inspection of the data, showing noticeably more southerly winds from 1940-1950 relative to 1928-1939. However, Figures 5.14 d and e representing summed wind directions from 1957-1985 and from 1986-2014 respectively, are very similar. There is an increase in the frequency of winds from the SW but this appears to be very slight. There is evidently a dramatic difference in the distribution of wind directions from 1928-1950 and 1957-2014.

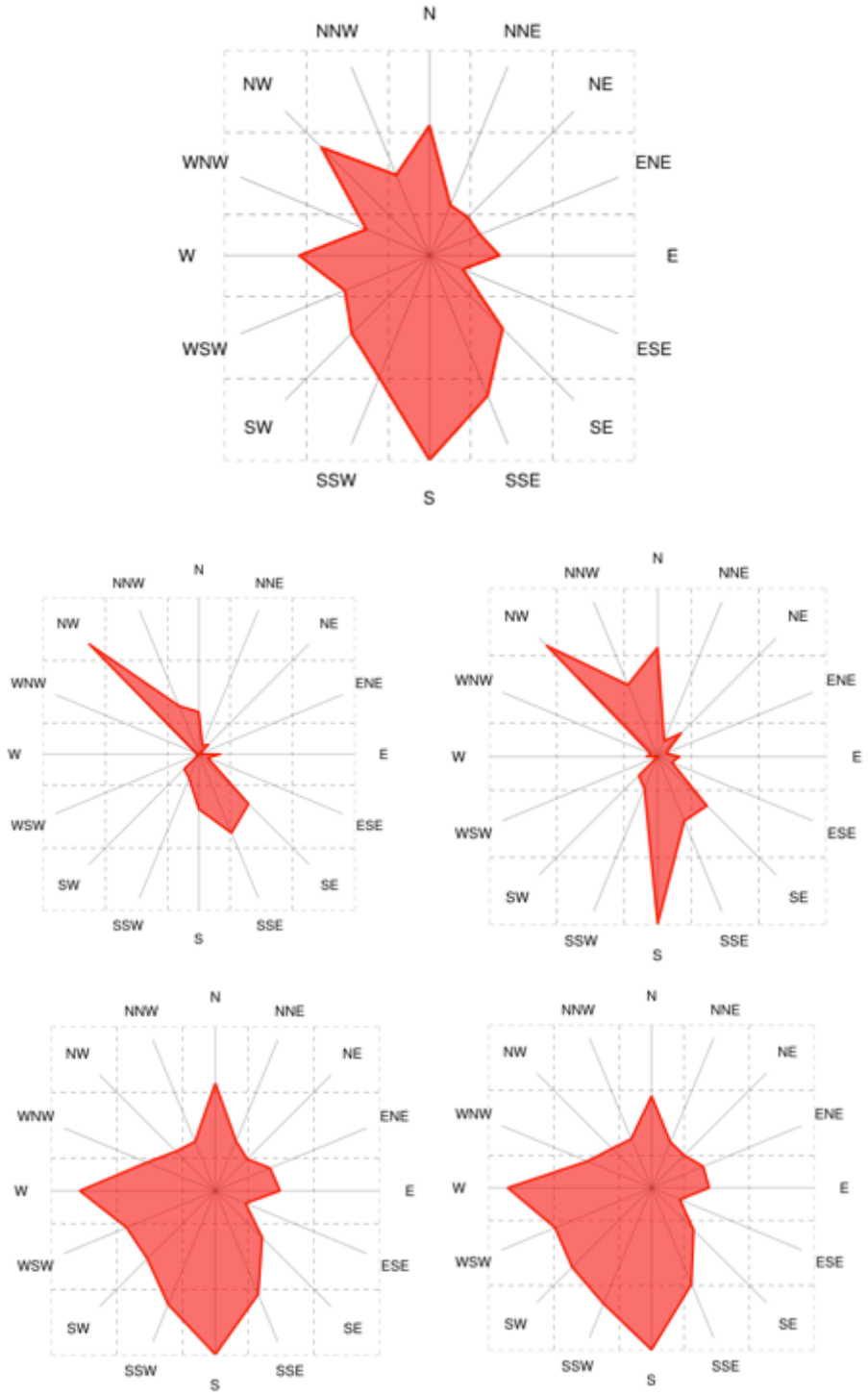

Figure 5.14. Wind roses for A) 1928-2014; B) 1928-1939; C)1940-1950; D)1957-1985; E) 1986-2014. Note that for A) the frequency counts for each wind direction from 1957-2014 were divided by 40 so that the number of readings per year was comparable in order of magnitude to the earlier period when measurements were less frequent.

5.3.2.3 Atmospheric pressure

Figure 5.15 shows annual mean atmospheric pressure from 1867-2013. An increase in annual pressure is indicated for this period, with the greatest change appearing in the late 19th C and early 20th C – there is no clear trend in atmospheric pressure from the 1950s to the present. The overall relationship between atmospheric pressure and time is statistically significant at the $p < 0.01$ level. Due to slight pressure differences between the two stations used – on average values from the Monach Isles are 0.3 hPa higher than those from Benbecula when compared over the period for which data from the two sites overlaps – this trend may represent a slight underestimate of the increase in mean annual atmospheric pressure.

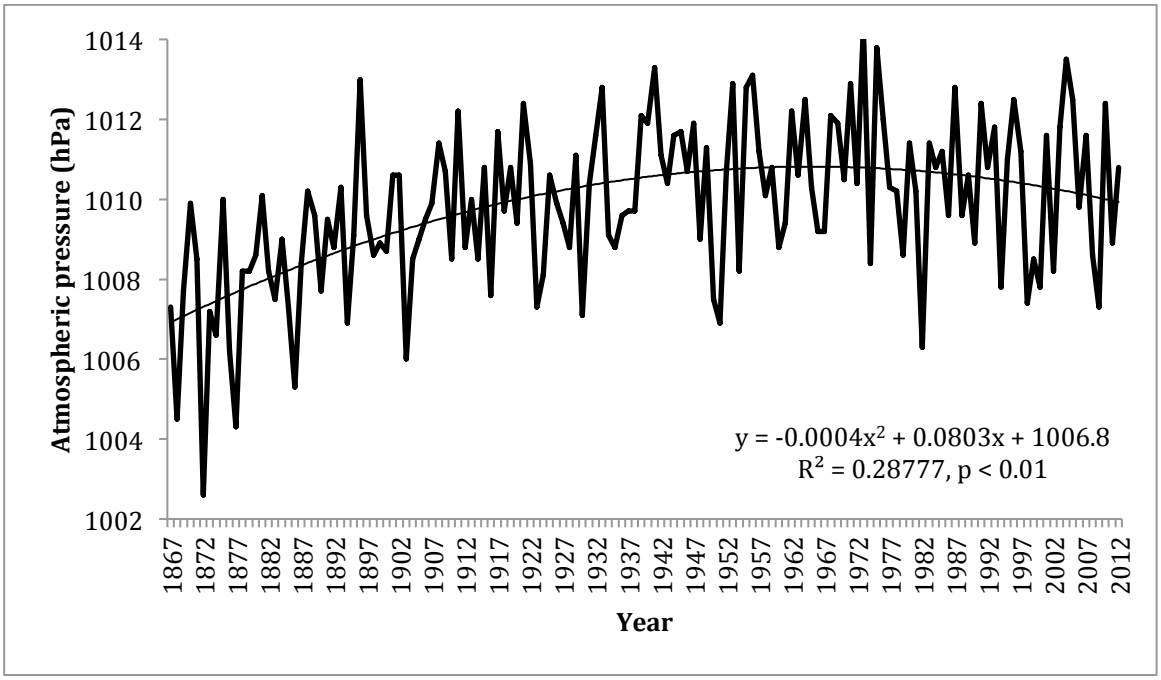

Figure 5.15. Annual mean atmospheric pressure (hPa). Data from 1867-1956 is from the Monach Isles; data from 1957-2013 is from Benbecula. On average, annual mean air pressure values from the Monach Isles were found to be 0.3 hPa higher than those from Benbecula. N = 147.

5.3.2.4 Tide gauge levels

Mean annual tide gauge levels for Stornoway from 1976-2014 are shown in Figure 5.16. There is a strong positive relationship between year and tide gauge levels, equivalent to an increase of ~ 2 mm/yr. The relationship is significant at the $p < 0.01$ level ($R = 0.63$, $n = 36$).

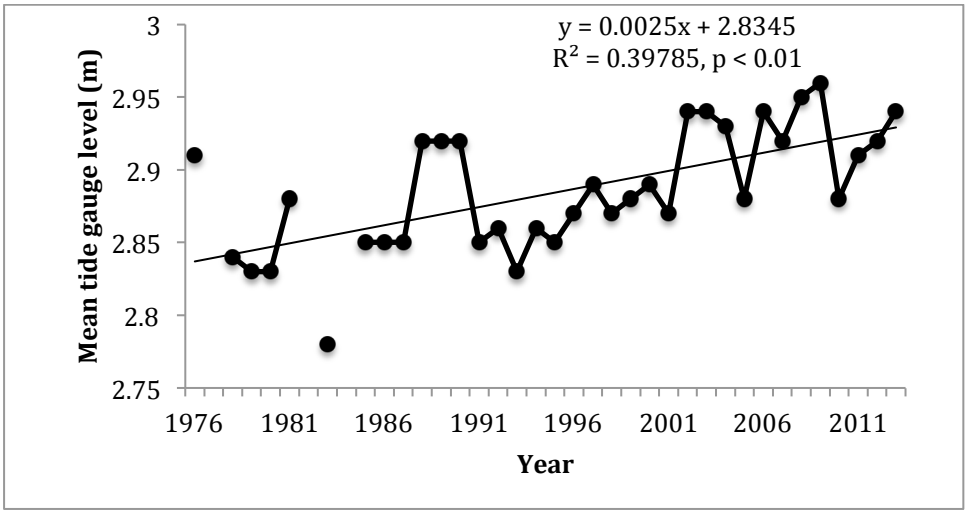

Figure 5.16. Mean annual tide gauge levels from Stornoway, 1976-2013. N = 37.

5.3.2.5 NAO

Annual NAO index values from 1867-2013 are shown in Figure 5.17. These indicate considerable variability throughout the study period, with an overall trend of a slight decrease in the NAO index ($p < 0.05$). Also evident are periods when the NAO index remains in a predominantly positive or negative phase, e.g. from 1880-1940 the NAO is generally positive, while from 1950-1970 it is generally more negative.

Relationships between the NAO index and climatic variables are shown in Table 5.6. Generally, significant relationships between the NAO index and other variables appear when the variable considered has been recorded over the entire period 1867-2013, or from the 1950s onwards; there are no statistically significant relationships between NAO index and climate variables when only pre-1950 data are considered. This difference in relationships may be due to the different sources for which NAO data was obtained pre- and post- 1950. Significant positive relationships between NAO index are indicated for the total number of gale days and atmospheric pressure.

Table 5.6. r-values and p-values for relationships between annual NAO and atmospheric variables. Relationships which are significant at the $p < 0.01$ level are in bold text.

Variable	r-value	p-value	n
No. gale days	- 0.18	< 0.05	146
No. gale days 1867-1949	- 0.04	-	82
No. gale days 1950-2013	**- 0.31**	**< 0.01**	**63**
Wind speed 1929-1950	- 0.25	-	21
Wind speed 1957-2013	- 0.45	< 0.05	56
Atmospheric pressure	**+ 0.20**	**< 0.01**	146

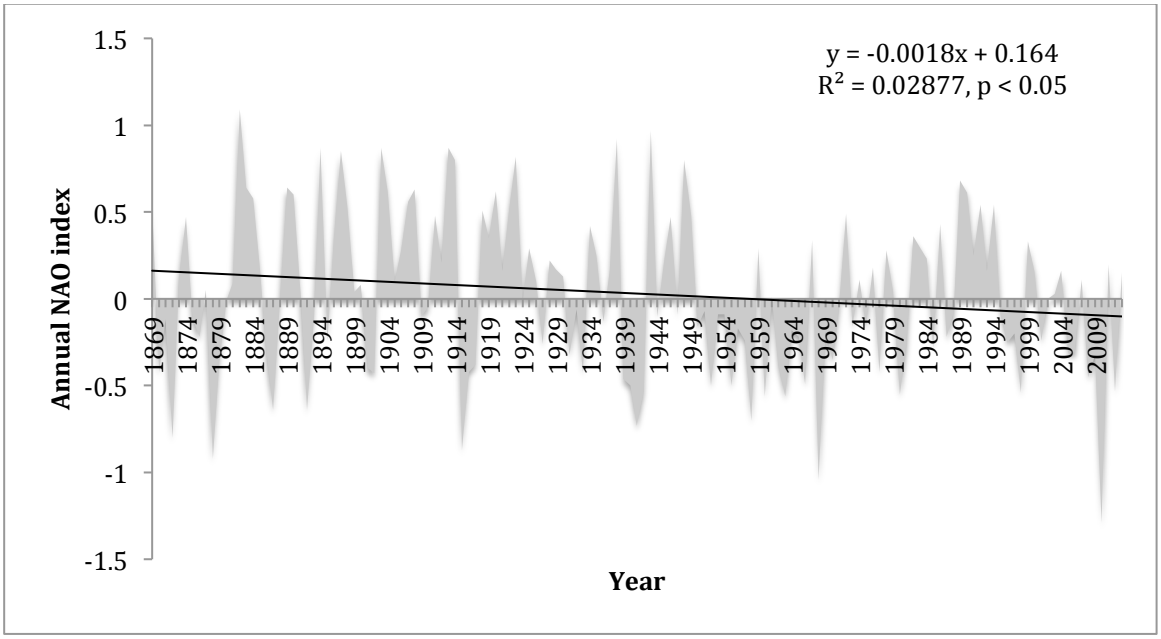

Figure 5.17. Annual NAO index values from 1867-2013. 1867-1949 values are from the Climate Research Unit; 1950-2013 values are from the Climate Prediction Centre. N = 146.

5.3.2.6 Comparison of October-December and January-March trends with full winter seasons

There was no statistically significant difference between the number of storm and gales days occurring in January-March (JFM) vs. October-December (OND) i.e. in each half of the winter season (Fig. 5.18). The only periods over which there is a noticeable difference between OND and JFM storminess are the 1920s, when storminess was very low and the storms appear predominantly in the JFM period, and in the late 1980s to mid 1990s when JFM storminess appears considerably higher than

OND storminess (Fig. 5.17). Comparison of these results with NAO values for the same periods each winter indicates that a stronger relationship is found between the monthly NAO index values and JFM storminess ($p < 0.01$), than with OND storminess ($p < 0.1$).

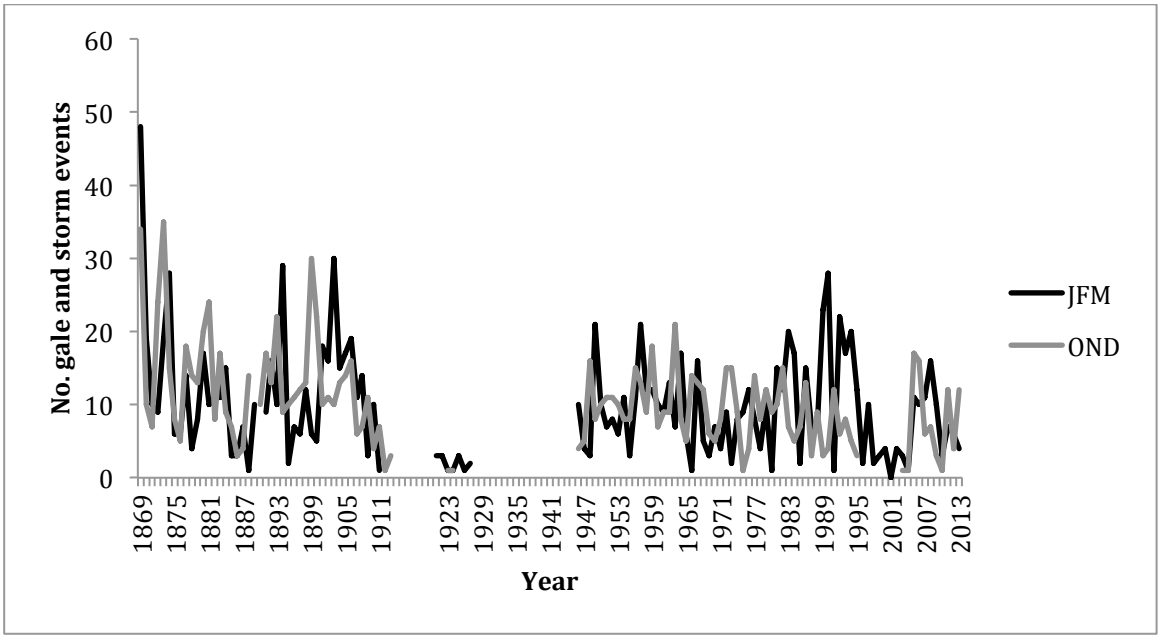

Figure 5.18. JFM and OND storminess from 1867-2013. N = 115.

5.3.3 The meteorological significance of the January 2005 storm

The key meteorological characteristics of the January 2005 storm were a maximum wind speed of 61 kts, a minimum atmospheric pressure of 959 hPa, gale force winds for 19 hours, and storm force winds for 9 hours. Additionally, maximum significant wave heights are modelled at a maximum of 14 m at the site of the Waverider buoy deployed in 2009 (Wolf, 2007). Table 5.7 shows recurrence data that indicate individual values measured during the January 2005 storm are not extreme within the context of the last ~65 years. For example, the minimum pressure recorded during the January 2005 storm (959 hPa), is commonly surpassed, with pressure readings in the 930 and 940 hPa ranges recorded during previous events. A pressure of 959 hPa also has a recurrence interval of 1.5 years, i.e. pressures equal to or lower than 959 hPa are recorded every 1.5 years. The lowest recurrence interval is the time that winds remain above storm force; in the January 2005 storm winds equal to or greater than storm force lasted for 9 hours. Meteorological data suggest that similar durations

of storm force conditions can be expected once every 15 years. These results contrast with the public opinion that the January 2005 storm was the 'greatest storm in living memory' (Richards and Phipps, 2007). It is also probable that the geomorphological severity of the storm is a product of the combination of relatively low pressure, severe swell conditions, very high peak wind-speeds and long duration of storm and gale force winds. For example, Dawson et al. (2007a) considered the storm to be a 1-in-80-year event after assessing its climatological and geomorphological significance.

events of similar wind speed to the January 2005 storm have occurred during the site survey period (October 2011 – March 2014), and the number of gales occurring annually appears to be lower in recent years (particularly 2009, 2010, and 2012, and with the exception of 2013) than in the years immediately following the January 2005 storm. This contrasts with local opinion, that suggests that the years following the January 2005 storm were characterised by relatively calm conditions, with 'normal' conditions returning more recently (David Muir, personal communication (2012)).

5.3.1.2 Wind speed and direction

As with indicators of storminess, the mean monthly wind speed has decreased during the period studied ($p < 0.05$) (Fig. 5.3). However, there is a clear peak in mean wind speeds during the survey period in December 2013, which has the highest monthly mean wind speed between 2005-2014 (19.5 kts).

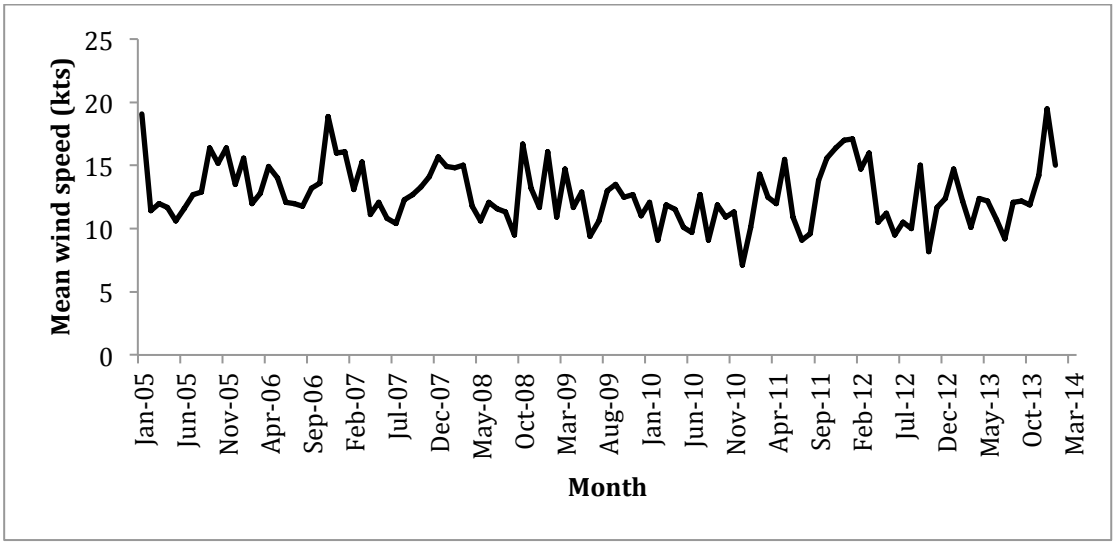

Figure 5.3. Mean monthly wind speed from January 2005 to March 2014. N = 112.

Prevailing winds are generally from the south and southwest (although winds from all bearings are not uncommon) (Fig. 5.4a). Gale force (and above) strength winds are also predominantly from the south and west, although with more westerly components (Fig. 5.4b). No gale force winds are recorded from the northeast.

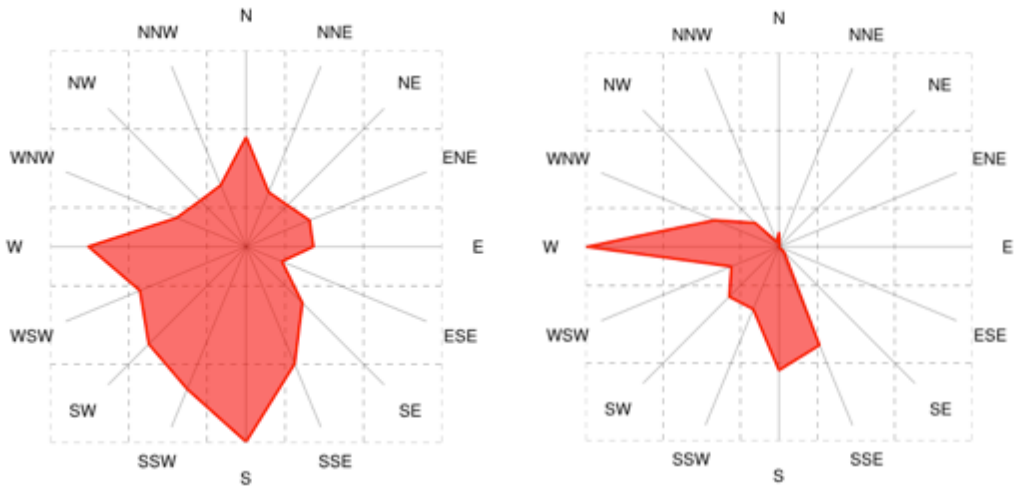

Figure 5.4. Wind roses showing wind direction during A) all conditions (n=88,155), B) gale and storm conditions (n=719), from 2005-2014. Wind roses generated using WindRose Pro (Enviroware).

5.3.1.3 Atmospheric pressure

Table 5.3 shows events associated with severe atmospheric depressions (minima ≤ 970 hPa). Figure 5.5 shows monthly mean values of atmospheric pressure.

Minimum atmospheric pressure recorded between 2005 and 2014 was 944 hPa. This was 15 hPa lower than the atmospheric pressure minima recorded at Benbecula weather station during the January 2005 storm. However, this event was not associated with storm, or even gale force wind speeds (max wind-speed of 31 kts). Four other events registered atmospheric pressures equal to or lower than the January 2005 storm (Table 5.3). Two of these events recorded maximum wind speeds less than storm force. The other two had maximum wind speeds considerably lower than those recorded in the January 2005 event (52 and 54 kts). Additionally, the event of 17th January 2009 is exceptional for the duration of extremely low pressures (~ 5 days at or below 970 hPa and ~ 3 days at or below 960 hPa). Evident from Table 5.3 is that several events with lower or similar atmospheric pressure minima to that recorded during the January 2005 storm have occurred between 2005 and 2013, although the depth of the depression does not appear to be strongly correlated with maximum wind speeds during the event.

Figure 5.5 shows a slight trend to lower monthly mean atmospheric pressures during the study. However, this relationship is not statistically significant. December 2009 has the highest mean atmospheric pressure (1033.2 hPa, 1 gale day) which is noteworthy as generally higher pressures would be expected during the summer months.

The lowest mean atmospheric pressure occurred in January 2014 (988.7 hPa, 3 gale days).

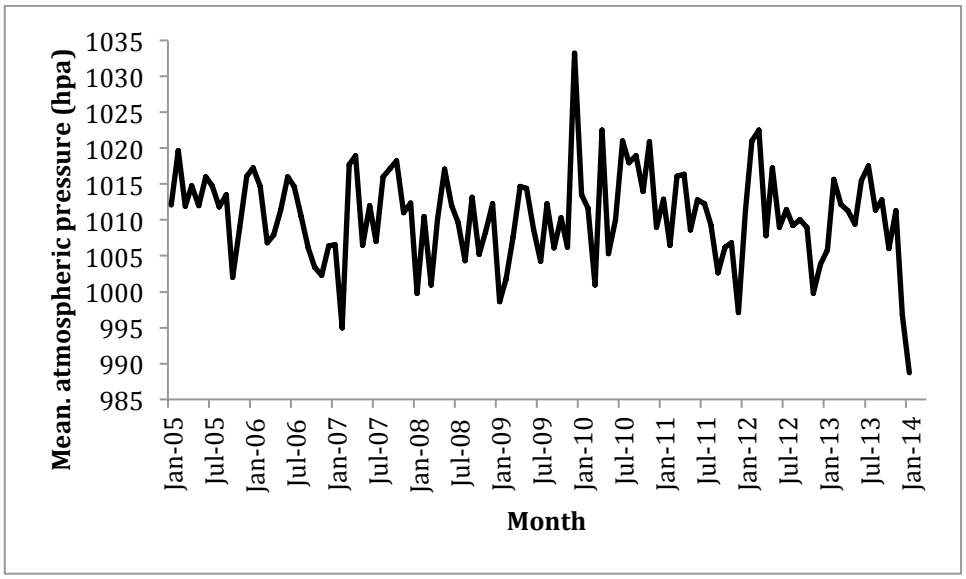

Figure 5.5. Monthly mean values of atmospheric pressure from January 2005 to March 2014. N = 109.

5.3.1.4 Ocean conditions

Maximum significant wave heights during storm events are summarised in Table 5.3. It is evident from Table 5.3 that the modelled wave heights for the January 2005 storm (12-14 m) were met and exceeded three times within the 3 year period for which records exist. The maximum significant wave height recorded during the study was 16.39 m on 4th February 2013 (2.39-4.39 m higher than the modelled wave height for the January 2005 storm). This event was associated with gale force winds (max. wind speed = 39 kts), and a relatively high atmospheric pressure minima (989 hPa). Comparison with the data in Table 5.2 suggests that the wave heights modelled for the January 2005 storm are not unusual, with significant wave heights > 12 m occurring 8 times, and significant wave heights > 14 m occurring 3 times in the 4 year period for which data are available. 2010 had no storm events. It should be noted that wave data is obtained from an offshore wave buoy – while this is the closest available source of information on sea conditions, it is recognised that wave height will be significantly lower at the coast due to the shoaling effect of the shallow continental shelf, and loss of wave energy on moving towards the coast (e.g. while passing through kelp beds).

Figure 5.6 shows monthly mean tide gauge levels from Stornoway. There is very little evidence for any increase in water levels over this time, and while some months show very low tidal levels (identifiable as troughs in Figure 5.6), there are no particularly high peaks in monthly mean value.

Change in monthly mean significant wave height between March 2009 and March 2014 is shown in Figure 5.7, which indicates an increase in wave heights ($p < 0.10$, $n = 59$). Peaks occur in February and December 2011, and December 2013.

The prevailing wave direction during all conditions is from the west (Fig. 5.8a), while for higher significant wave heights (> 10 m) the prevailing wave direction is from WSW to WNW. All waves approach from the western half of the compass due to the orientation of the coast.

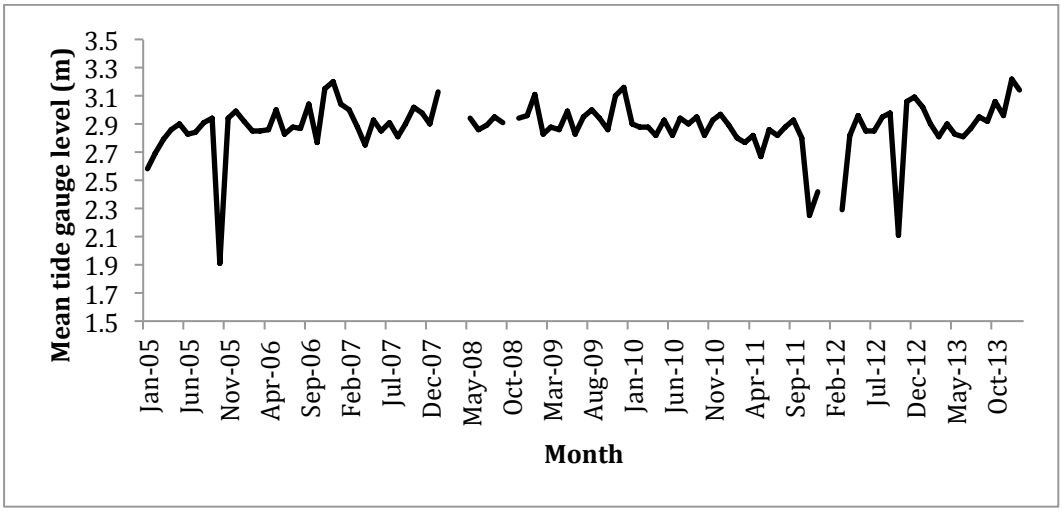

Figure 5.6. Monthly mean tide gauge levels from January 2005 to March 2014. N = 109.

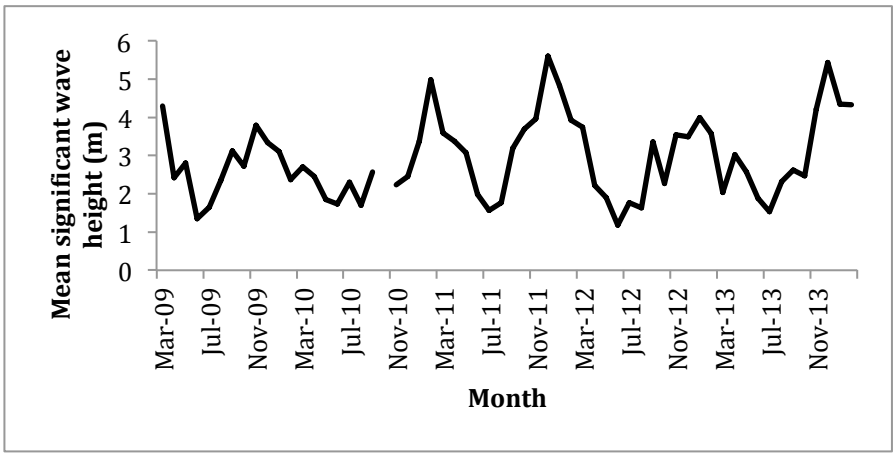

Figure 5.7. Change in monthly mean significant wave height from March 2009 to March 2014. N = 109.

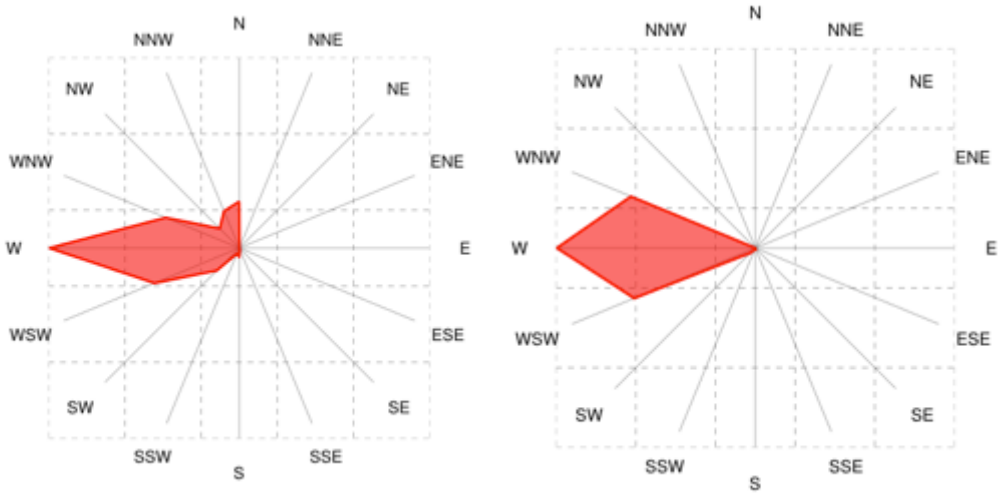

Figure 5.8. Wave rose showing wave direction during A) all conditions (n=85,038), B) high wave conditions (significant wave heights > 10 m) (n=277), from 2005-2014. Wave roses generated using WindRose Pro (Enviroware).

5.3.1.5 NAO

The NAO index has not changed significantly over the study.

Relationships between NAO and atmospheric and oceanic variables are summarised in Table 5.5. Four of six variables are very strongly correlated with NAO index values ($p < 0.01$). Monthly values for monthly maximum wind speed, mean wind speed, number of gale days, and mean significant wave height all positively and significantly ($p < 0.01$) correlate with NAO index values. Two variables, atmospheric pressure and tide gauge level have no relationship with NAO index values.

Table 5.5. r- and p-values for relationships between NAO and atmospheric and oceanic variables.

Variable	r-value	p-value	n
maximum monthly wind speed	- 0.33	< 0.01	109
mean monthly wind speed	- 0.55	< 0.01	109
monthly no. gale days	- 0.36	< 0.01	109
mean monthly atmospheric pressure	0.00	-	109
mean monthly tide gauge level	+ 0.25	-	109
mean monthly significant wave height	+ 0.74	< 0.01	59

5.3.2. Climatology 1867-2014

5.3.2.1 Storminess

Figure 5.9a and b show the annual and decadal number of gale and storm days from 1869-2014, respectively. Storminess has varied considerably over this period, with extremely high numbers of gale days (≤ 78 gales/yr) during the 19th C (particularly between 1867-1880, and 1890-1905), then a dramatic decline in the number of gale days during the early 20th C. Storminess remained very low until the late 1940s, when the number of gale days increased. However, late-20th C levels of storminess have not been recorded during any part of the 21st C. A second lull in storminess appears between 1995-2005, with storminess since 2005 being generally close to or slightly above the average of 15.6 gale days/yr. While the number of storm days appears to follow the same broad pattern as the number of gale days, there are some differences. For example, the highest frequency of gale days occurs during the 1860s and 1870s, while the highest frequency of storm days occurs in the early 1900s. Over the last decade, the number of storms has been similar to, or slightly below, the average of 1.4 storms/yr, with the exceptions of 2005 and 2011, which had 4 and 3 storm days, respectively. The decadal totals shown in Figure 5.9b provide a more simplistic view of the data, and confirm the results from Fig. 5.9a, that the highest frequency of gale days was during the 1860s and 1870s, a lull in gale activity occurred from 1910-1930, and then there was an increase in storminess until the 1950s. The decadal totals also suggest a slight decrease in the number of gales from the 1970s (197 gales) to the 2000s (115 gales).

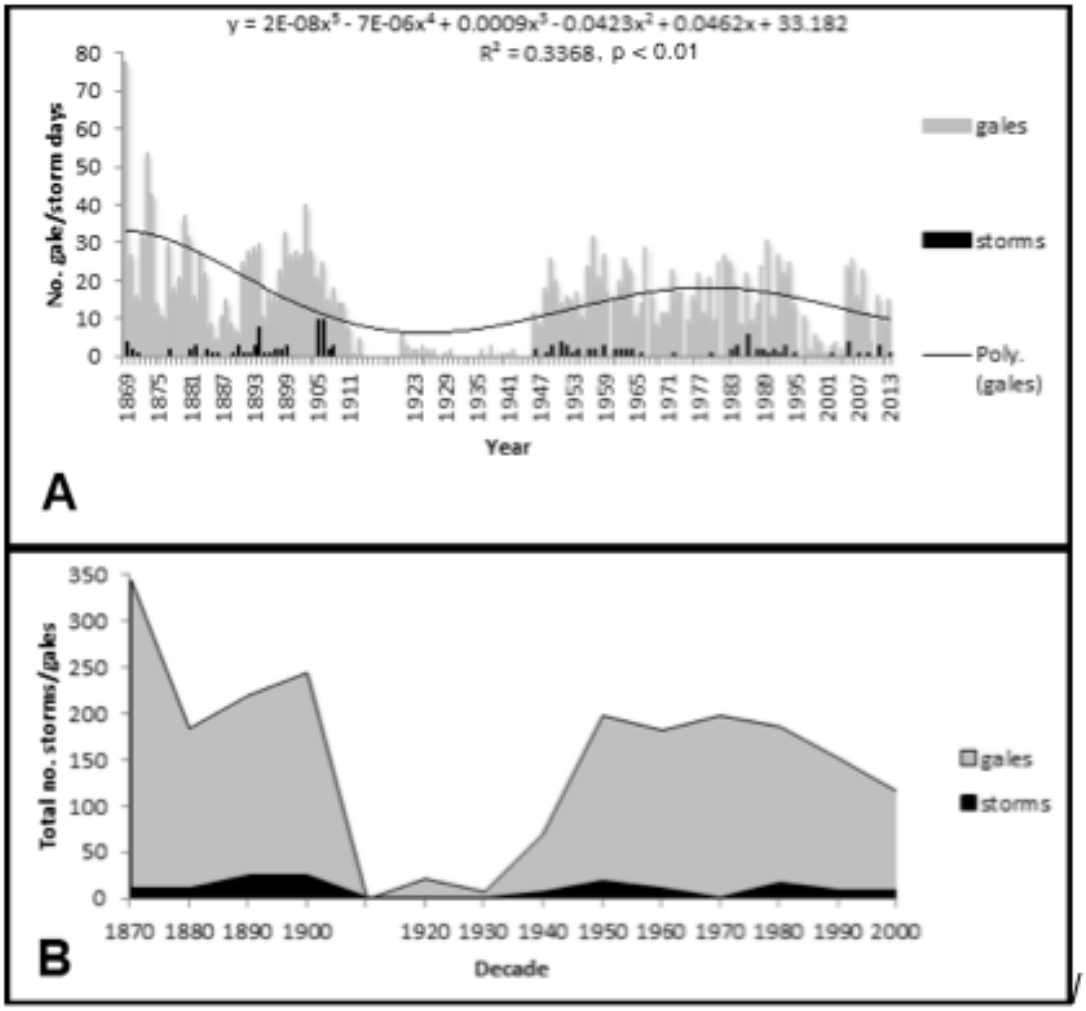

Figure 5.9. Storm and gale day frequencies from 1867-2014. A) annual totals, B) decadal totals. A 5th order polynomial trend line is fitted to the annual total number of gales.

Figure 5.10 shows the frequency distribution of wind directions for storm and gale force winds from 1867-2014. The wind rose indicates that the majority of storms track from the west, with relatively high numbers also tracking from the south and west-north-west. Compared to the prevailing wind direction during all conditions which are generally southerly (see Fig. 5.14), wind directions during storms appear to contain noticeably more westerly components, and less northerly components.

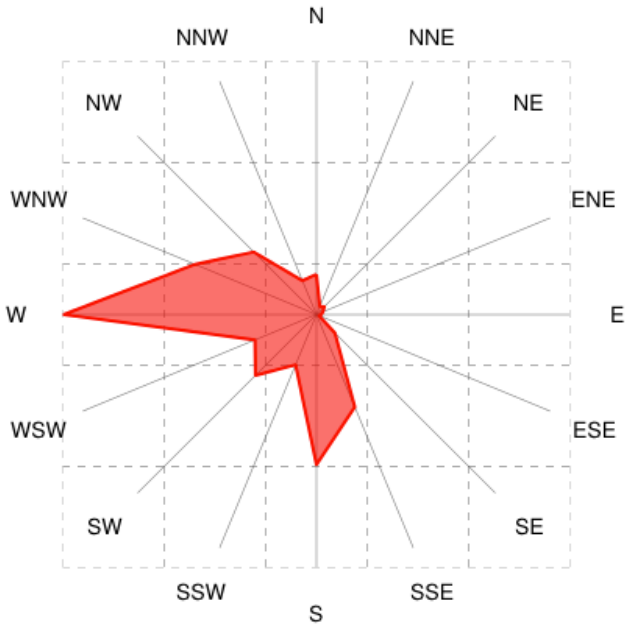

Figure 5.10. Wind rose showing wind direction gale and storm events (events where wind speed ≥ 34 kts) (n=5,933). Wind rose generated using WindRose Pro (Enviroware).

5.3.2.1.1 Frequency vs. intensity of storms

A strong positive relationship between the frequency and intensity of storms was found (Fig. 5.11) (n=138; r = + 0.42; p < 0.01); there was no indication of an inverse relationship between the frequency and intensity of events.

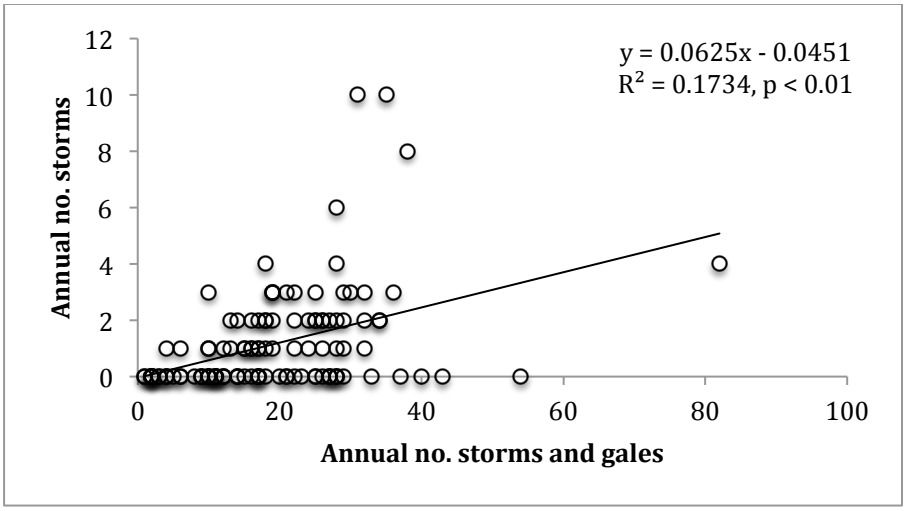

Figure 5.11. The annual no. of storms plotted against the annual total number of storm and gale events for the period from 1867-2014. N = 138.

5.3.2.2 Wind speed and direction

Figures 5.12a and 5.12b show changes in mean annual wind speed between 1929-1945 (Beaufort scale), and 1957-2014 (knots), respectively. Both graphs show speeds decreasing with time. This trend is not significant for the earlier period. However, for the latter period, the decrease in mean annual wind speed is significant at the $p < 0.01$ level ($n = 57$; $r = -0.45$).

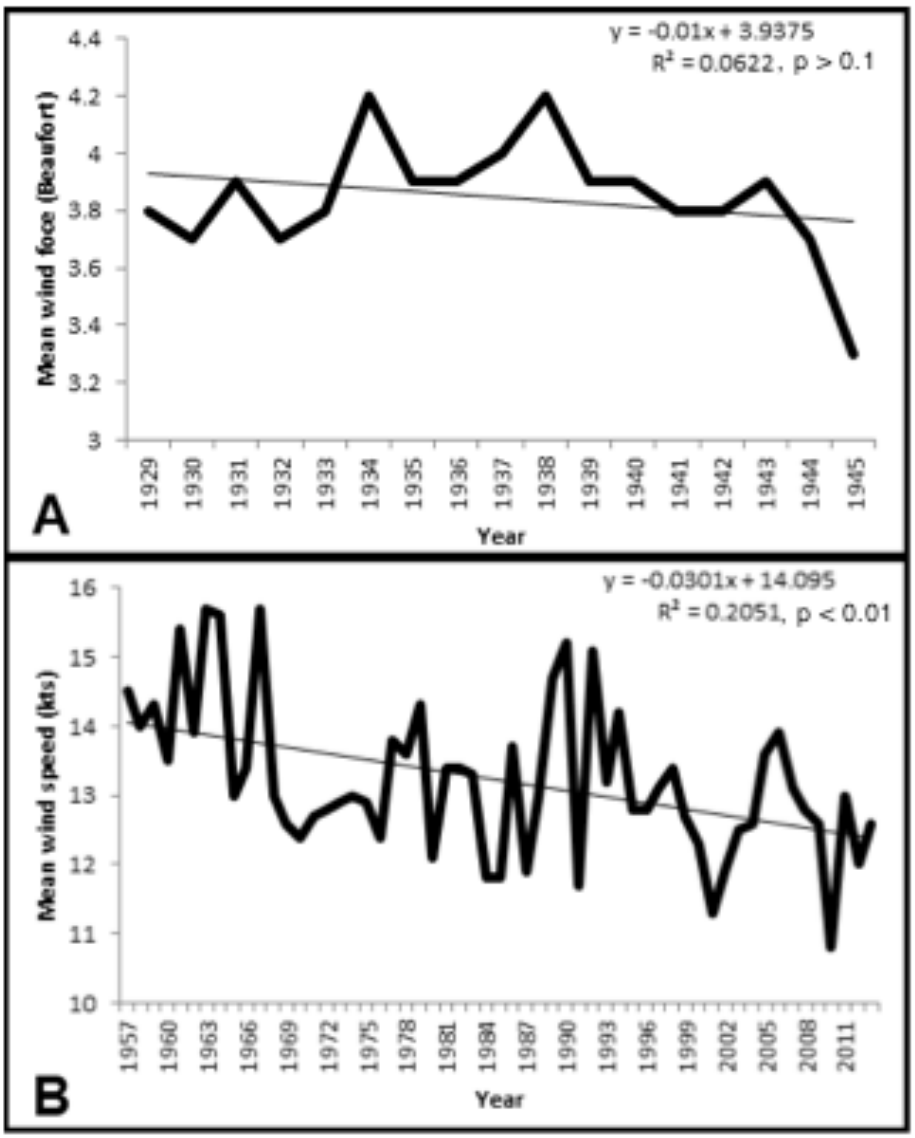

Figure 5.12. Mean annual wind speed from A) 1929-1945, B) 1957-2014. N = 57.

Highest monthly gust speeds are shown in Figure 5.13 for the periods for which these data were recorded; 1997-2014, and 1950-1956. Although the lack of data for the

majority of the study makes conclusions difficult, it appears from Fig. 5.13 that max. gust speeds were generally slightly higher in the 1950s than in the 1990s and 2000s. Mean highest gust speed from 1950-1956 was 64.48 kts; from 1997-2014 mean highest gust speed was 49.47 kts ($p < 0.01$). While the January 2005 storm stands out in the more recent run of data, the maximum gust speed recorded during this storm was exceeded three times in the 6 year period from 1950-1956.

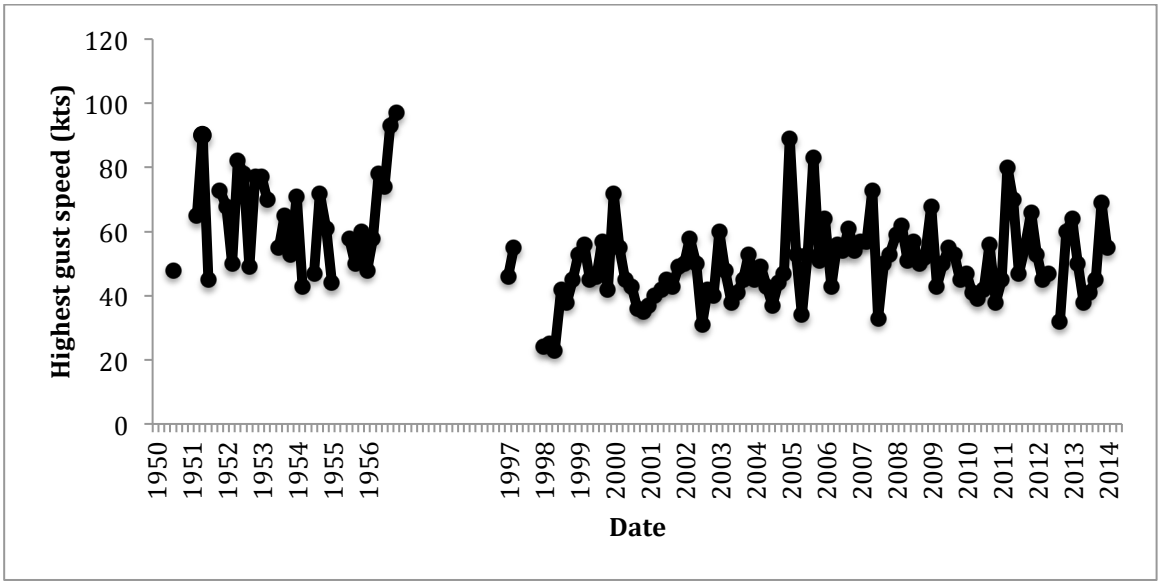

Figure 5.13. Highest monthly gust speeds (October-March). N = 129.

Visual analysis of cardinal wind direction data from 1928 to 1950 revealed a rapid shift in the prevailing wind direction from north-westerly to south-westerly c. 1940, and visual analysis of degree wind direction data from 1957 to 2014 indicated a gradual shift to more westerly components. Based on these findings, wind roses were generated for the full period for which wind direction data were available (1928-2014), and also for smaller timer periods to investigate the apparent changes. Figures 5.14 b and c confirm the initial visual inspection of the data, showing noticeably more southerly winds from 1940-1950 relative to 1928-1939. However, Figures 5.14 d and e representing summed wind directions from 1957-1985 and from 1986-2014 respectively, are very similar. There is an increase in the frequency of winds from the SW but this appears to be very slight. There is evidently a dramatic difference in the distribution of wind directions from 1928-1950 and 1957-2014.

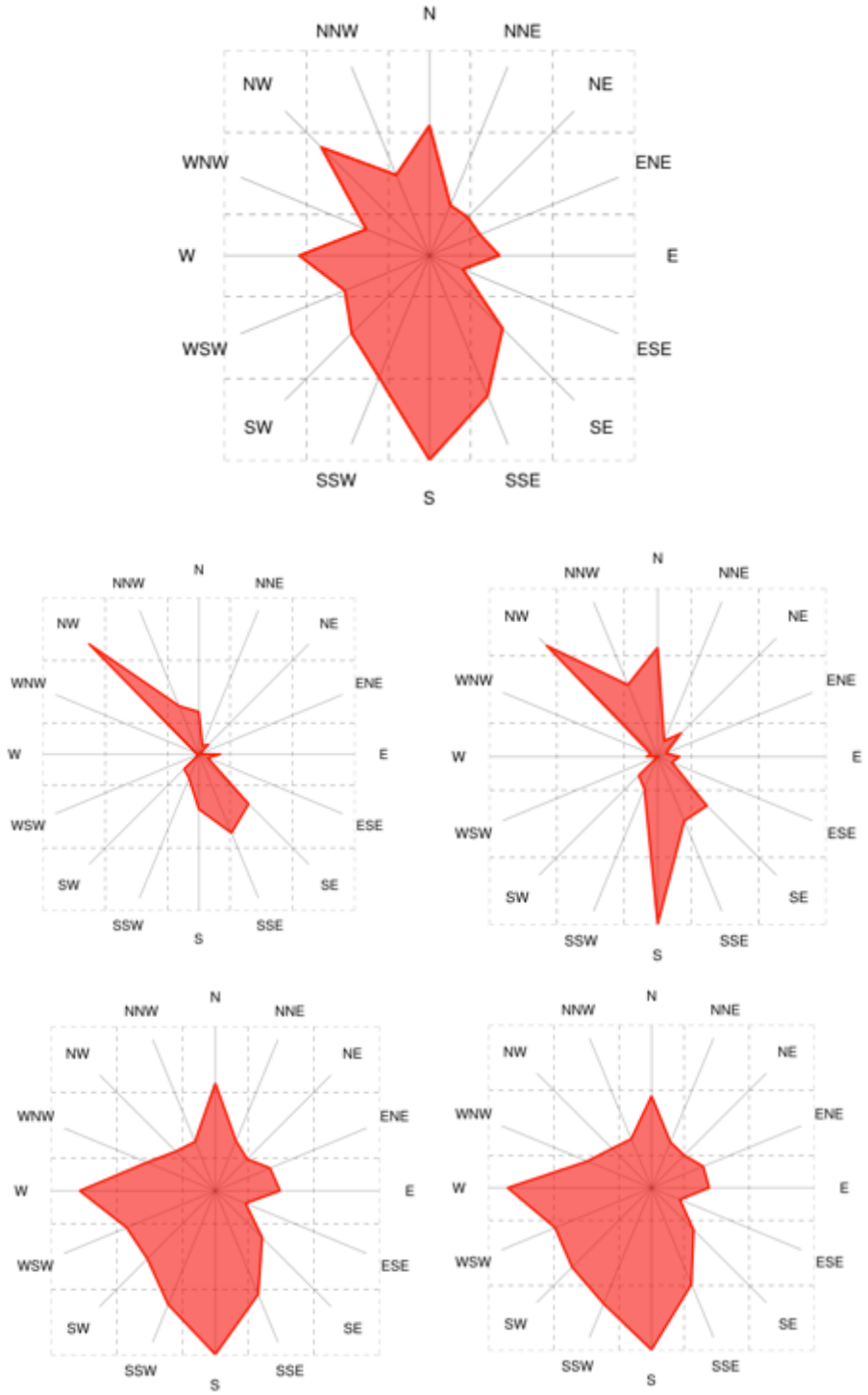

Figure 5.14. Wind roses for A) 1928-2014; B) 1928-1939; C)1940-1950; D)1957-1985; E) 1986-2014. Note that for A) the frequency counts for each wind direction from 1957-2014 were divided by 40 so that the number of readings per year was comparable in order of magnitude to the earlier period when measurements were less frequent.

5.3.2.3 Atmospheric pressure

Figure 5.15 shows annual mean atmospheric pressure from 1867-2013. An increase in annual pressure is indicated for this period, with the greatest change appearing in the late 19th C and early 20th C – there is no clear trend in atmospheric pressure from the 1950s to the present. The overall relationship between atmospheric pressure and time is statistically significant at the $p < 0.01$ level. Due to slight pressure differences between the two stations used – on average values from the Monach Isles are 0.3 hPa higher than those from Benbecula when compared over the period for which data from the two sites overlaps – this trend may represent a slight underestimate of the increase in mean annual atmospheric pressure.

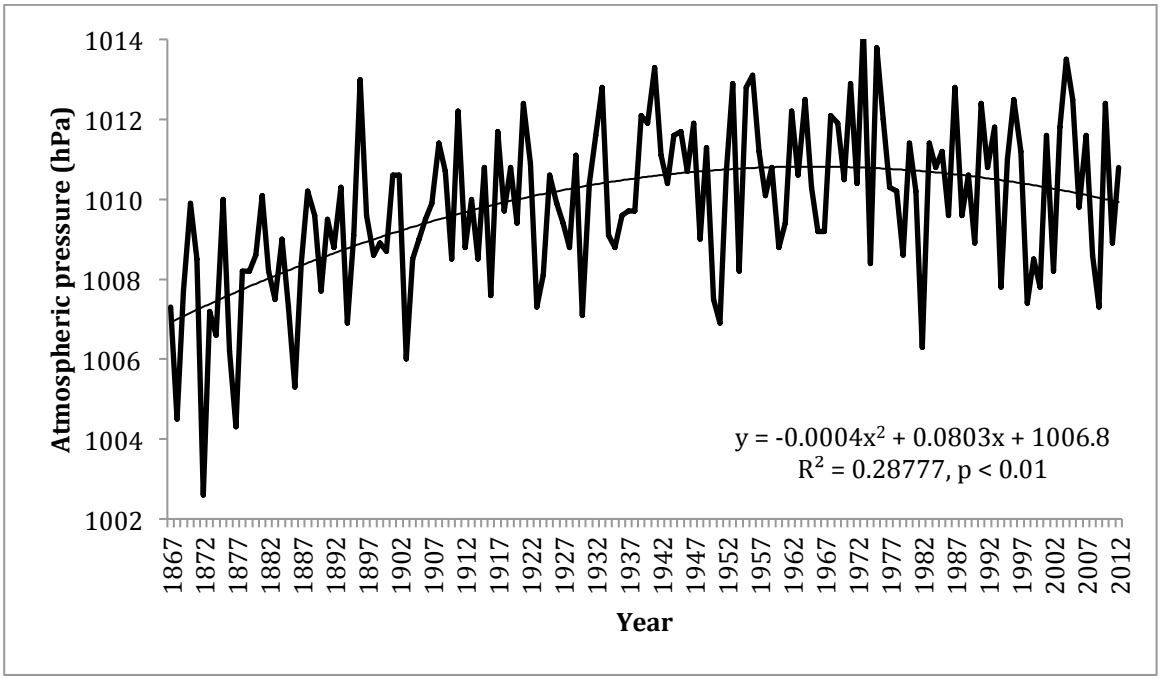

Figure 5.15. Annual mean atmospheric pressure (hPa). Data from 1867-1956 is from the Monach Isles; data from 1957-2013 is from Benbecula. On average, annual mean air pressure values from the Monach Isles were found to be 0.3 hPa higher than those from Benbecula. N = 147.

5.3.2.4 Tide gauge levels

Mean annual tide gauge levels for Stornoway from 1976-2014 are shown in Figure 5.16. There is a strong positive relationship between year and tide gauge levels, equivalent to an increase of ~ 2 mm/yr. The relationship is significant at the $p < 0.01$ level ($R = 0.63$, $n = 36$).

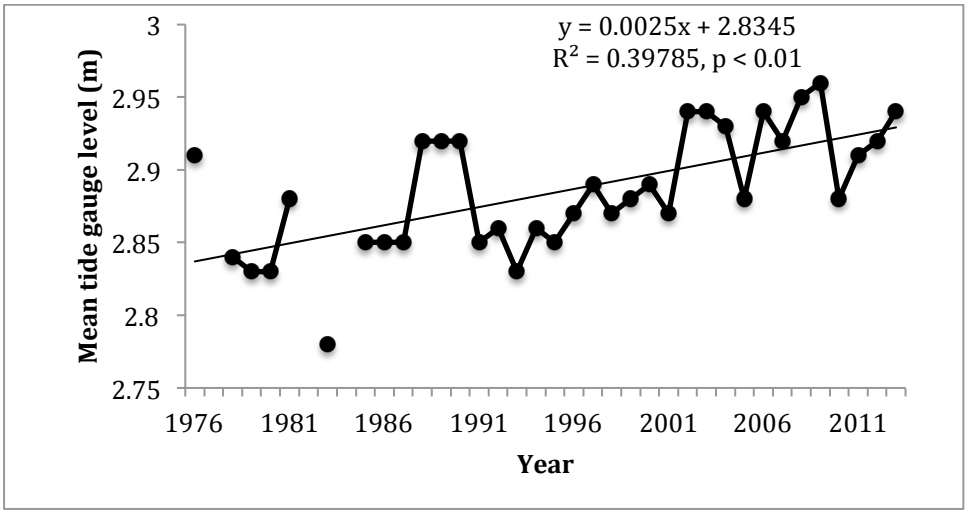

Figure 5.16. Mean annual tide gauge levels from Stornoway, 1976-2013. N = 37.

5.3.2.5 NAO

Annual NAO index values from 1867-2013 are shown in Figure 5.17. These indicate considerable variability throughout the study period, with an overall trend of a slight decrease in the NAO index ($p < 0.05$). Also evident are periods when the NAO index remains in a predominantly positive or negative phase, e.g. from 1880-1940 the NAO is generally positive, while from 1950-1970 it is generally more negative.

Relationships between the NAO index and climatic variables are shown in Table 5.6. Generally, significant relationships between the NAO index and other variables appear when the variable considered has been recorded over the entire period 1867-2013, or from the 1950s onwards; there are no statistically significant relationships between NAO index and climate variables when only pre-1950 data are considered. This difference in relationships may be due to the different sources for which NAO data was obtained pre- and post- 1950. Significant positive relationships between NAO index are indicated for the total number of gale days and atmospheric pressure.

Table 5.6. r-values and p-values for relationships between annual NAO and atmospheric variables. Relationships which are significant at the $p < 0.01$ level are in bold text.

Variable	r-value	p-value	n
No. gale days	- 0.18	< 0.05	146
No. gale days 1867-1949	- 0.04	-	82
No. gale days 1950-2013	**- 0.31**	**< 0.01**	**63**
Wind speed 1929-1950	- 0.25	-	21
Wind speed 1957-2013	- 0.45	< 0.05	56
Atmospheric pressure	**+ 0.20**	**< 0.01**	146

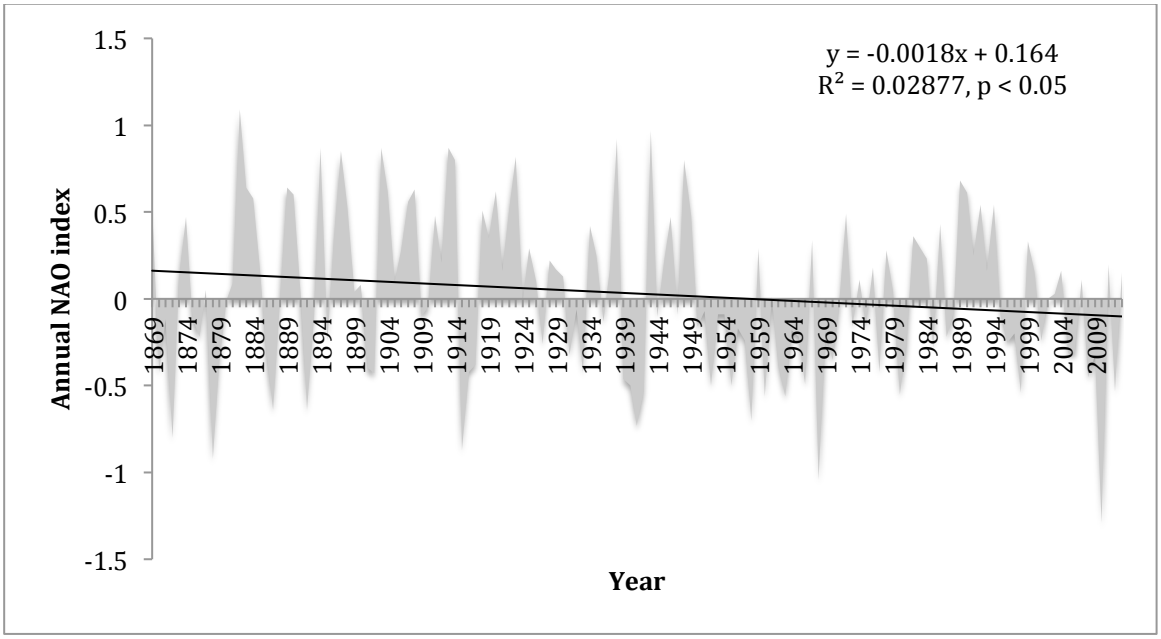

Figure 5.17. Annual NAO index values from 1867-2013. 1867-1949 values are from the Climate Research Unit; 1950-2013 values are from the Climate Prediction Centre. N = 146.

5.3.2.6 Comparison of October-December and January-March trends with full winter seasons

There was no statistically significant difference between the number of storm and gales days occurring in January-March (JFM) vs. October-December (OND) i.e. in each half of the winter season (Fig. 5.18). The only periods over which there is a noticeable difference between OND and JFM storminess are the 1920s, when storminess was very low and the storms appear predominantly in the JFM period, and in the late 1980s to mid 1990s when JFM storminess appears considerably higher than

OND storminess (Fig. 5.17). Comparison of these results with NAO values for the same periods each winter indicates that a stronger relationship is found between the monthly NAO index values and JFM storminess ($p < 0.01$), than with OND storminess ($p < 0.1$).

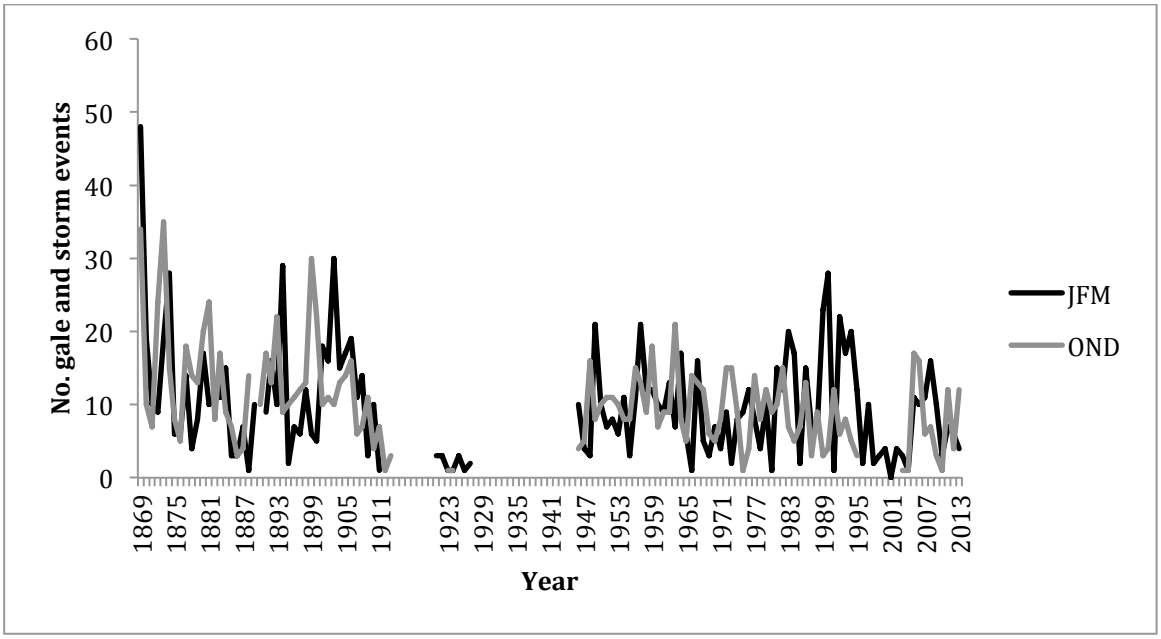

Figure 5.18. JFM and OND storminess from 1867-2013. N = 115.

5.3.3 The meteorological significance of the January 2005 storm

The key meteorological characteristics of the January 2005 storm were a maximum wind speed of 61 kts, a minimum atmospheric pressure of 959 hPa, gale force winds for 19 hours, and storm force winds for 9 hours. Additionally, maximum significant wave heights are modelled at a maximum of 14 m at the site of the Waverider buoy deployed in 2009 (Wolf, 2007). Table 5.7 shows recurrence data that indicate individual values measured during the January 2005 storm are not extreme within the context of the last ~65 years. For example, the minimum pressure recorded during the January 2005 storm (959 hPa), is commonly surpassed, with pressure readings in the 930 and 940 hPa ranges recorded during previous events. A pressure of 959 hPa also has a recurrence interval of 1.5 years, i.e. pressures equal to or lower than 959 hPa are recorded every 1.5 years. The lowest recurrence interval is the time that winds remain above storm force; in the January 2005 storm winds equal to or greater than storm force lasted for 9 hours. Meteorological data suggest that similar durations

of storm force conditions can be expected once every 15 years. These results contrast with the public opinion that the January 2005 storm was the 'greatest storm in living memory' (Richards and Phipps, 2007). It is also probable that the geomorphological severity of the storm is a product of the combination of relatively low pressure, severe swell conditions, very high peak wind-speeds and long duration of storm and gale force winds. For example, Dawson et al. (2007a) considered the storm to be a 1-in-80-year event after assessing its climatological and geomorphological significance.

Table 5.7. Data showing the frequency of events equalling or exceeding the January 2005 storm, recurrence intervals, and probability of exceedence for selected meteorological parameters. Continuous: max. windspeed data in knots was available form 1949-2014; time > gale/storm force is available from 1971-2014 (the period for which hourly weather data are available); min. pressure data was available from 1957-2014; max. significant wave height data was available from 2009-2014.

Variable	January 2005 value	Times exceeded	Recurrence (yrs)	Probability of exceedence/annum
Max windspeed (kts)	61	6	11	9
Time > gale force (hrs)	19	14	3	33
Time > storm force (hrs)	9	3	15	7
Min. pressure (hPa)	959	40	1.5	67
Max. Hs. (m)	14	3	2	50

5.4 Interpretations

Section 5.3 qualitatively and quantitatively describes climatic and oceanic parameters which have the potential to influence coastal change, identifying changes occurring over different temporal scales. The frequency with which storms with a similar severity to the January 2005 event occur was also investigated, and the relationship between the North Atlantic Oscillation (NAO) and climate variables was explored. From the literature review, it was expected that the January 2005 storm would be an 'extreme' weather event, with a long recurrence interval (Richards and Phipps, 2007; Angus and Rennie, 2008). It was unclear whether storminess would be expected to have increased over the last decade or not; published results conflicted with each other (e.g. Dawson et al., 2007; Allan et al., 2008; Matulla et al., 2008; Phillips et al., 2013) – possibly due to the consideration of different timescales – and explanatory mechanisms exist to explain both increases and decreases in storminess with projected changes in the NAO (e.g. Wang et al., 2004; Tsimplis et al., 2005).

5.4.1 Expected influence of climate on coastal change

Weather data corresponding to the period for which RTK-dGPS and LiDAR data were considered (2005-2014) indicate that prevailing wind and wave direction were generally from the south and west, which would be expected to lead to longshore transport of beach sediments from the southern to northern ends of each site. No events with a similar impact to the January 2005 storm were experienced during this period. However, several events with greater significant wave heights than the modelled wave height for the January 2005 storm (12-14 m, (Wolf, 2007)) occurred, with the highest being 16.39 m on 4th February, 2013. Winter 2013-2014 experienced more storms than the previous two winters; therefore, coastal change would be expected to be greater over this period.

Long term analysis of climate data (1869-2014) showed that current storminess (as indicated by storm and gale day frequencies) is lower than in the period from 1869-1910, and higher than in the period from 1910-1950 (Table 5.8). Storminess has been comparatively unchanged from 1950-2014, with the exception of a decade of decreased storminess from 1995-2005 (see Figure 5.12). The shift from low storminess to

moderate storminess occurring c. 1950 appears to be synchronous with a shift in modal wind direction from predominantly north-westerly to predominantly south-westerly, after which it remained fairly stable, with a slight trend to more westerly components. From this information it would be expected that rates of coastal erosion would be highest from 1869-1910, lowest from 1910-1950, and intermediate from 1950-2014. The shift in prevailing wind direction c. 1950 might be expected to influence sediment transport dynamics, with implications for coastal change, e.g. by leading to morphological realignment (Thomas et al., 2010; Thomas et al., 2011b; Phillips et al., 2013), or altering the areas which are sheltered/exposed by antecedent geology and geomorphology (Thomas et al., 2011b). The other parameters investigated which are linked to coastal change indicate: a decrease in mean wind-speed from 1957-2014; lower max. gust speeds from 1990-2014 than in the 1950s; an increase in mean atmospheric pressure from 1867-2014; and a slight increase in westerly wind direction components from the 1950s to the present. These changes would generally be expected to contribute to a trend of decreasing coastal erosion rates.

Tide gauge data from 1976-2014 show a ~ 2 mm/yr rise in sea-level. This would correspond to a landwards shift in the position of MHWOST of ~ 1-2 m over the period from 1976-2014, assuming a cross-shore gradient of ~ +0.05 m/m (determined from Staoinebrig DTM).

The effect of changes in the NAO index on coastal change is less certain. However, results from the North Atlantic region suggest that a more positive NAO index may be linked to stronger winds (Tsimplis et al., 2005; Wolf and Woolf, 2006), more storms (Dawson et al., 2004; Wolf and Woolf, 2006; Matulla et al., 2008), and a more westerly prevailing wind direction (Phillips et al., 2013). Recent studies within the North Atlantic region indicate that these effects on climate have been linked to beach rotation (Thomas et al., 2011b), erosion at the southern end of beaches in Wales (Thomas et al., 2011b), a lowering of beach level and volume (Thomas et al., 2010; Thomas et al., 2011a), larger tidal ranges, and larger waves (Tsimplis et al., 2005; Wolf and Woolf, 2006). Correspondingly, Thomas et al. (2010, 2011b) found that more negative NAO values and periods of transition between positive and negative NAO regimes were characterised by dune building and lower wave heights, with the latter finding also supported by the work of Tsimplis et al. (2005). From this information it would be expected that the period from 1880-1925, and to a lesser extent from 1985-

1995, would be characterised by the greatest rates of coastal retreat, while dune building and accretion might be expected to occur from 1925-1975, and from 2005 to the present. Over the more recent period examined using beach surveys, only three years were characterised by positive NAO values: 2007, 2011, and 2013. It might therefore be expected that retreat of linear features would be highest, and beach volumes lowest during these years (see Chapter 8 for combined analysis of short-term climatological and geomorphological data). Furthermore, it may also be expected that there will be differences in coastal behaviour between periods characterised by different prevailing NAO conditions (Table 5.8) due to the expected influences on wind and wave direction, wind strength, and wave height, which may influence sediment transport dynamics.

Table 5.8. General summary of results. The generalised character indicates the nature of the measured variable relative to data from the rest of the time-series.

Climate variable	Period	Generalised character
Storminess	1870-1910	high
	1910-1950	very low
	1950-1995	moderate
	1995-2005	low
	2005-2014	moderate
Wind speed	1920-1945	moderate, decreasing to low
	1950-2014	high, decreasing to moderate
Max. gust speed	1950-1960	high
	1995-2014	low
Wind direction	1930-1940	north-westerly
	1940-1950	transitional, highly variable
	1960-2014	southsouthwesterly, gradually changing to south-westerly
Atmospheric pressure	1870-1900	low
	1900-2014	high
Tide gauge level	1975-2014	gradual increase
NAO	1870-1880	variable
	1880-1925	strongly positive
	1925-1950	transitional
	1950-1970	negative
	1970-2000	positive
	2000-2014	negative to strongly negative

5.4.2 Storminess

Matulla et al. (2008) reported that the public perception was that storminess was increasing in the early 1990s. Authors have also shown that storm frequency (Phillips et al., 2013; McClatchey et al., 2014) and severity (Matulla et al., 2008) have increased from 1950-1960 to the mid-1990s in the North Atlantic region. When looking at storminess over longer timescales Dawson et al. (2007a) found that storminess during the late 20th C was lower than in the late 19th C, and that storminess had generally declined since the 1940s. Consideration of the results presented in Chapter 5 indicates that over 145 years, storminess has declined (Table 5.9). However, when the period examined is limited to the 20th C, a trend of increasing storminess is shown. If the time is then reduced to the mid-19th C to the present, the relationship changes again. From Table 5.9, it is evident that the observed trend varies dramatically when the time period considered is altered. Of particular note is the alteration in trend obtainable by reducing/increasing the dataset by as little as one decade at both ends of the range (e.g. compare the difference in trend observed in data from 1900-2014 relative to 1910-2000). This highlights the importance of interpreting climatic trends with caution, e.g. the predominant 'trend' of increasing storminess observed over the last 20 years becomes a fluctuation when viewed as part of a 145 year time-series.

Table 5.9. Trends in storminess (as indicated by gale day frequency) over different temporal scales determined by linear regression.

Time period	r-value	Nature of change
1869-2014	- 0.30	decrease
1900-2014	- 0.10	decrease
1910-2000	+ 0.36	increase
1940-2014	- 0.28	decrease
1950-2014	- 0.31	decrease
1950-1995	0.00	-
1970-1995	+ 0.33	increase
1995-2014	+ 0.41	increase

To provide context to interpret coastal change, a more general division of the storminess time-series into three periods with different levels of storminess (1867-1910 (high), 1910-1940 (low), 1940-2014 (moderate)) is probably more useful than

indicating whether storminess has increased or decreased over a given period, and is in general agreement with previous findings (e.g. Dawson et al., 2007a). The data from Barra extending back to the 1920s confirm that 1920-1945 was characterised by exceptionally low storminess in the Outer Hebrides, as identified from Stornoway meteorological data by Dawson et al. (2007). The number of gale days appears to have increased between 1965 and the mid-1990s, with more storms occurring between 1985-1995 than in the preceding decade, providing evidence to support the public perception that storminess was increasing in the mid 1990s (Matulla et al., 2008). However, this increase was short-lived, with very low gale and storm day numbers from 1995-2005, before a return to conditions similar to those from 1950-1995 after 2005.

The data presented in section 5.3 suggest that the change in storminess in the Outer Hebrides may be better characterised as a fairly rapid shift from a period of low storminess (1910-1940) to moderate storminess (1950-the present), with the increase in storminess occurring over one decade (the 1940s). This finding does not contradict previous results indicating an increase in storminess from the mid-20th C to the present (e.g. Matulla et al., 2008; Phillips et al., 2013), but temporally refines the increase to the 1940s, rather than indicating a gradual increase in storminess from the 1940s to the 2010s. The difference in interpretation may be due to the slightly different temporal scales considered (discussed above), or to real differences between the sites studied within the North Atlantic region. For example Phillips et al. (2013) present data from the Bristol Channel, ~ 655 km south of the Barra weather station. Regional differences in storminess would be expected from the results of Matulla et al. (2008) who determined that the same overall trend in storminess had been experienced in different parts of Europe, but the timing and nature of the increase in storminess had varied within the region. Further evidence of spatial variability in storminess trends is provided by the differences between results presented here and the findings of Phillips et al. (2013) relating to differences in OND and JFM storminess. The results of Phillips et al. (2013) from the Bristol Channel indicate that the highest frequency of JFM storms occurred in the 1990s, while OND storminess was highest during the 1920s and 1960s. Results from the Outer Hebrides indicate that while JFM storminess was higher than OND storminess in the 1990s, both winter periods (and JFM) storminess was very low during the 1920s.

The lack of clarity in terms of trends in storminess may also result from the use of different meteorological parameters to indicate storminess. For example, while Woolf and Coll (2013) found that the frequency of higher wave heights and stronger winds had increased around the UK since the 1960s, they did not find any clear trend in the number of gale days over the same period. However, the results presented in section 5.3 indicate that all investigated variables linked to coastal change showing a slight negative trend since the 1960s.

The results from the southern Outer Hebrides showed no statistical evidence to support the results presented by Trouet et al. (2012) which indicated the possibility of an inverse relationship between storm frequency and severity. Data analysed in Chapter 5 instead showed a strong positive relationship between the severity and frequency of storms. While the January 2005 storm occurred during a period of low storminess, this appears to be the exception when considering the full 145 year time-series.

5.4.3 NAO

The NAO showed statistically significant relationships with all climate variables identified as likely to influence coastal change (wind speed and direction, no. of gale days, and atmospheric pressure) over short (2005-2014) and long (1869-2014) timescales. This potentially indicates that the NAO index is influencing both long term trends and shorter term fluctuations in weather in the Outer Hebrides, as well as acting more widely as a regional scale variable. The statistical significance of the relationship between NAO index and the number of gale days was stronger ($p < 0.01$) for the period from January to March (JFM) than for the period from October to December (OND) ($p < 0.10$). Results from the analysis of relationships between the NAO index and climate variables are in agreement with existing literature (e.g. Dawson et al., 2002; Wakelin et al., 2003; Burningham & French, 2013), and provide further evidence from a newly analysed weather station dataset to highlight the NAO's significance in influencing climatic variability.

From comparison of changes in the NAO index to the three periods of different storminess levels identified above the relationship between the NAO index and these periods of differing storminess is not immediately clear. The NAO index is characterised by high positive values from 1880-1950, negative values from 1950-1970,

moderate to high positive values from 1970-1995, and generally low to very low negative values from 1995 to the present. Despite the statistically significant relationship between the NAO index and storminess these changes appear to be somewhat out of phase with the shifts in storminess occurring c. 1910, 1940, and to a lesser extent 1995, e.g. while the high storminess experienced from 1869-1910 corresponds to a strongly positive NAO regime, positive NAO values remain dominant until 1925, and appear intermittently until 1950, a period characterised by very low storminess. This may be explained to some degree by the suggestion in Dawson et al. (2010) that the relationship between the NAO index and storminess had changed from the end of the 19th C to the end of the 20th C due to the additional influence on climate of changes in Northern Hemisphere sea ice extent. For example, periods of transition between positive and negative NAO index values in the latter half of the 20th C appear to be more strongly correlated with the number of storms (as opposed to gales); periods of low storminess in the 1970s and from 1995-2005 both correspond to transitions in the NAO regime.

However, earlier in the 19th C the shift from a generally positive dominated NAO regime to a negative dominated NAO regime occurring c. 1935-1955 appears to correspond to the shift in prevailing wind direction observed 1945-1950 (see Figure 5.17). This provides support for the suggestion by Phillips et al. (2013) that changes in wind regimes in the North Atlantic region are influenced by the NAO index. However, some aspects of the results do not completely correspond to previous findings. For example, a more positive NAO regime has generally been linked to more (and stronger) westerly components in wind direction (Tsimplis et al., 2005; Wolf and Woolfe, 2006; Phillips et al., 2013). The shift in wind direction to more westerly components shown in results from Chapter 5 appears to precede the shift to more positive NAO values by 10-15 years; this lag has implications for the determination of cause and effect.

The greater significance of the relationship between JFM-storminess and the NAO index relative to OND-storminess is in agreement with the findings of Allan et al. (2008). However, the relationship between OND-storminess was significant at the 90% confidence level for the results presented in Chapter 5, while Allan et al. (2008) found no relationship between OND storminess and the NAO index. Instead, they found that early winter storminess was linked to El Nino oscillations, and suggested that different oceanic-atmospheric mechanisms were responsible for driving storminess between

OND and JFM. The evidence presented in Chapter 5 suggests that storminess in the Outer Hebrides is related to the NAO index throughout the winter. However, the weaker relationship in OND may indicate that other processes are involved.

5.4.4 The climatological significance of the January 2005 storm

The results presented in section 5.3.3 indicate that the climatological significance of the individual meteorological parameters associated with the January 2005 storm is limited, despite the dramatic geomorphological consequences of the event. Within the 9 year period for which short-medium term coastal change was investigated, many of the individual weather conditions were equalled or exceeded. For example: the highest wind-speed of 62 kts was recorded on 8th November, 2008; the continuous duration of winds above gale force experienced during the January 2005 storm (19 hours) was almost equalled on 17th March 2007 (16 hours) and 17th January 2009 (18 hours); storms and gales with minimum pressures equal to or lower than the January 2005 minima (959 hPa) occurred 5 times; the duration of air pressures lower than 970 hPa was exceeded three times; the duration of air pressures lower than 960 hPa was exceeded 4 times; and maximum significant wave heights greater than the modelled height for the January 2005 storm (12-14 m (Wolf, 2007)) occurred three times. In fact, the only indicator of the storms severity which was not matched or exceeded in this nine year period was the duration of winds equal to or above storm force (9 hours).

In contrast with the local perception of the storm as the 'worst in living memory' recurrence intervals for the climate parameters recorded during the storm range from 1.5-15 years (see Table 5.5). Supporting the analysis of shorter term climate data, the calculated recurrence intervals indicate that the most extreme aspect of the storm was the duration of winds equal to or exceeding storm force, which has a recurrence interval of 15 years, based on data from 1971-2014.

The findings from Barra and Benbecula weather stations agree with those from Stornoway shown in Dawson et al. (2007a), who drew attention to two other events with similar max. gust velocities to the January 2005 storm occurring within a 25 year period, and four other months with similar mean wind velocities in the same period. This suggests that some climatological aspects of the January 2005 storm had been equalled or exceeded within living memory. Furthermore, Wolf (2007) suggested that

the wave heights associated with the January 2005 may have a recurrence interval of 10 years, with a more extreme event with a recurrence interval of 50 years being expected to have wave heights approaching 17 m. This would suggest that the storm on 4th February 2013 with a maximum wave significant wave height of 16.39 m was a considerably rarer and more severe event than the January 2005 storm in terms of oceanic conditions. Note that as the West of Hebrides Waverider buoy (February 2009) was only recently deployed, results related to the January 2005 storm are from wave models validated using datasets from neighbouring buoys (Wolf, 2007).

Evidently the results from Chapter 5 contrast with the perception that the storm was the 'worst in living memory' held by the local population (Richards and Phipps, 2009), in terms of meteorological chapters 6 and 7, but there are several factors likely to have influenced the public perception of the event. For example, the severity of the storm may lie in the combination of meteorological factors rather than the individual meteorological parameters investigated. However, when the storminess parameters listed in Table 5.3 are ranked and summed, the January 2005 storm's cumulative rank places it as second to the event of 17th January 2009. Admittedly, it is probable that some of the factors listed have a greater influence on the morphological effects of a storm than others. There is also the possibility that decreased resilience in the coastal dune (due to on-going erosion) leads to each subsequent storm of any given magnitude having increased morphological effects, i.e. a system threshold is crossed due to preconditioning (see Chapter 9 for further consideration of this topic). This would explain the perception of a storm that does not appear to be particularly extreme from a climatic perspective as 'the worst in living memory' if the geomorphological consequences were more widespread and of a greater magnitude. While Angus and Rennie (2008) indicated that the physical changes occurring along the machair coastline were generally not significantly different from those associated with a typical winter season, the deposition of a sediment plume at Stoneybridge has not been repeated at Stoneybridge since January 2005, suggesting that this storm did have a notably greater geomorphic impact than typical winter erosion. A final factor which may have understandably influenced local perceptions of the storm is likely to be the tragic loss of life during the event.

5.4.5 Critique

The major limitations of this chapter stem from the use of data sourced from different weather stations, with different temporal resolutions, and the use of different recording approaches/equipment. These are widely acknowledged pitfalls of using historic climate data (Matulla et al., 2009). Due to the historic nature of the data investigated there is generally little that can be done to resolve these issues. The similarity of the trends observed with data from Stornoway (Dawson et al., 2007a), and the similarity in the pattern observed between Benbecula and Stornoway data (Dawson et al., 2007a), indicate that the distances between the different stations used in this region may be small enough that the shift from data from Barra to Benbecula in the mid-19th Century may not significantly impact results. Furthermore, some confidence may be given to the results based on the observation that key shifts in storminess and other weather parameters do not appear to coincide with the temporal boundaries between different stations/changes in temporal resolution of data, e.g. key shifts in storminess occur at 1910 and ~1945-50, and a key shift in wind direction occurs during the 1940s, while the major changes in data source/resolution occur at 1921, 1928, 1957, and 1997. Additionally, increasing temporal resolution of data with time would lead to more storms being detected as time continued. As results indicate that storminess is highest in the period for which temporal resolution is lowest (1867-1910), it appears that this has not adversely influenced results. Further evidence for this is that after the period of low storminess from 1910-1945, storminess begins to increase in 1947, ten years before a shift to increased data resolution, and a switch from Barra data to Benbecula data. While it is certainly probable that a uniform temporal resolution would impact the details of the results, the above factors indicate that the general trends in storminess and weather may be accepted with some confidence.

Another consideration when investigating climate data for the purposes of understanding its influence on coastal change is whether the climate parameters selected provided a reliable and valid indication of climatic conditions during storms or over time. For example, Matulla et al. (2008) criticised the use of wind speed data to identify storm days due to the limited availability of records of sufficient length, and errors introduced by changes in instrumentation and recording scale, instead preferring the use of atmospheric pressure to identify storms. However, data from Barra and Benbecula

indicated that several occurrences of low pressures were not associated with high wind speeds, and were therefore unlikely to be linked to increased coastal erosion, e.g. the lowest atmospheric pressure recorded between 2005 and 2014 was 944 hPa on 13th December 2011, but this event wasn't associated with storm or gale force winds, despite continuous pressures lower than 970 hPa for 34 hours, and pressures lower than 960 hPa for 16 hours. This indicates that for the purposes of investigating coastal change in the Outer Hebrides, using factors related to wind-speed or oceanic conditions may be more appropriate that consideration of atmospheric pressure. The relationships between various indicators of storminess (no. gale days, no. storm days, max. gust speed, max. wind speed, significant wave height, etc.) and coastal change are discussed in chapters 6 and 7, where measured changes in the coastal zone are interpreted in relation to the climatological forcing agents. The impacts of the January 2005 storm – when compared with the climatological data – certainly suggest that the combination of climatological parameters is critical in determining the severity of the event.

5.5 Key Findings

5.5.1 Recent climatology 2005-2014

- Prevailing winds are from the south and southwest, but gales and storms are from a westerly direction;
- Waves during storm and gale events also tend to come from a more northerly direction than during normal conditions.

5.5.2 Historic climatology 1867-2014

- Storminess was greatest in the late 18th and early 19th C, and lowest in the period from 1910-1945;
- The current frequency of storms is not particularly high or low, and there appears to have been a slight decrease in storminess since the 1970s;
- Mean annual wind speeds have decreased since the 1950s, while winds have become increasingly westerly;

- The period of low storminess in the 1920s coincides with a period of different prevailing wind directions (consistently north-westerly) than those experienced during periods of higher storminess (generally south-westerly);
- There has been an increase in annual mean atmospheric pressure since 1869, with the majority of the increase occurring by the mid 20th C;
- A ~ 2 mm/yr rise in sea-level has occurred since 1976;
- The NAO index is positively correlated with wind speed, storminess, wind direction, and wave heights, with relationships being generally stronger from 1950 onwards;
- The NAO index is more strongly correlated with JFM storminess than OND storminess.

5.5.3 The significance of the January 2005 storm

- A higher max. wind speed and higher significant wave height than those experienced during the January 2005 storm have been recorded in the 9 years since the storm;
- The climatological significance of the January 2005 storm appears to be relatively low – an evaluation of the individual meteorological parameters suggests that the recurrence intervals of similar conditions are between 1.5-15 years. However, from a combined geomorphological and climatological analysis of the January 2005 storm (Dawson et al., 2007a) it appears that it is the combination of climatological parameters that may be key in determining the physical and hydrological impact of a storm. This has implications for the application of historical climatological analyses which consider only a single – or a limited range – of meteorological parameters to interpret past storminess levels.

CHAPTER 6
ANALYSIS OF VARIATIONS AND TRENDS IN MEDIUM-LONG TERM COASTAL CHANGE

Synopsis:
This chapter presents the methodology and results for analysing medium-long term coastal change using historic maps and aerial photography, and the Digital Shoreline Analysis System (Thieler et al., 2009).

6.1 Introduction

6.1.1. Background

Understanding how the coastal zone has changed over medium-long temporal scales (decadal to centennial) is crucial for coastal management; the way any coastline has previously responded can provide an indication of its potential sensitivity to future changes, and change over medium temporal scales is often the most useful for coastal management (Montreuil and Bullard, 2012). The purposes of investigating coastal change include: research into sea-level change; designing coastal defences; planning development; and identifying areas and people at risk from storms and shoreline change (Boak and Turner, 2005). Changes in the coastal zone occur over different timescales due to tides, storms, land-use, seasonal changes in weather, and longer term changes in climate and sediment supply. The significance of severe and rapid changes (as during the January 2005 storm) can be understood when quantitatively compared to longer term trends in coastal geomorphology; the severity of an event is often a function of the timescale over which it is considered (Cambers, 1976). Additionally, spatial variations in coastal change may be 'evened out' over longer timescales – areas which appear sensitive to change over a short timescale (days, months, years), may appear to be less so over longer timescales (decades, centuries) (Cambers, 1976). However, the most extreme events are often preserved in the coastal stratigraphy (e.g. Bondevik et al., 2005).

Shoreline retreat, loss of machair grassland, and depleted sediment supplies are all major concerns for the western coast of South Uist (Angus, 2001). Dawson et al. (2012) investigated changes in shoreline position from 1805-2005, and volume change from 1984-2005, at South Ford (the body of water between South Uist and Benbecula), and changes in shoreline position, cross-shore profiles, and sediment volume were quantified between 1984-2005 for the coast along the northern half of South Uist (Dawson et al., 2007b). However, no long-term quantitative analysis of change has been undertaken for the southern Atlantic coastline of the island (including Milton and Cille Pheadair), and no analysis of change pre-1984 has been conducted for the majority of the northern Atlantic coastline (including Staoinebrig).

Quantification and analysis of change in the coastal zone is limited by the availability of suitable data. Aerial photographs of sufficient quality to quantify changes are generally available in the UK from the 1940s onwards, and Ordnance Survey maps (which were the most rigorously surveyed topographic maps) can extend the historic record of shoreline position to 100-150 years. Other sources (e.g. estate maps, written records, oblique ground photographs) may provide further information, but are generally of insufficient quality for quantitative analyses. Surveyed profiles, and DTMs may be available after 1990 for some sites. Additionally, it may be necessary to integrate different proxies for change, e.g. tide lines are generally the only shoreline indicators extractable from maps, while a range of shoreline indicators can be extracted from photographs (e.g. wet/dry lines, cliff tops, vegetation lines, etc.) (Boak and Turner, 2005; Montreuil and Bullard, 2012). Thus for any investigation it is important to quantify all sources of error and their magnitude to determine whether changes are within the error threshold (James et al., 2012).

6.1.2 Aims

The aims of this chapter are:

i) to document changes in the coastal zone at the three study sites over the period from 1654-2005 (qualitatively) and from 1876-2005 (quantitatively);

ii) to quantify spatial and temporal variations in the pattern and rate of change in shoreline position;

iii) to use a comparison of long, medium, and short-term coastal changes to evaluate shoreline stability over different timescales.

6.2 Methods

6.2.1 Data sources

The two types of data used for analysis of medium to long term coastal change were maps and aerial photographs. Maps were from two organisations: Edina Digimap and the National Map Library of Scotland, Edinburgh. Aerial photographs were from Scottish Natural Heritage (on behalf of the Western Isles Data Partnership), and the National Collection of Aerial Photography, part of the Royal Commission on the Ancient and Historical Monuments of Scotland, Edinburgh.

6.2.2 Data selection

Initially, all maps and aerial photographs covering at least one of the three field sites were catalogued (Tables 6.1 and 6.2). This provided 26 maps spanning 430 years from 1583 to the present, and 9 sets of aerial photographs spanning 60 years from 1945 to 2005.

Table 6.1. Details of all maps with spatial coverage of Staoinebrig, Milton, and/or Cille Pheadair. (EDM = Edina Digimap; NMLS = National Map Library of Scotland). N.B. Dates indicate year when surveying was conducted (as opposed to publication date).

Source	Item	Scale	Year	Site(s)
NMLS	Map of South Uist (Timothy Pont)	-	1583-1614	M, CP
NMLS	Vistus Insula (Timothy Pont)	-	1614-1650	all
NMLS	Blaeu Atlas of Scotland	-	1654	all
NMLS	A map of the north west part of the Western Isles (Herman Moll)	-	1745	all
NMLS	A general chart of the west coast and western islands of Scotland from Cantire to Cape Wrath and Butt of Lewis	-	1775	all

(continued overleaf)

NMLS	The south part of Long Island from Bara Head to Benbecula I.	-	1776	all
NMLS	A new chart of the west coast of Scotland from the point of Ardnamurchan to Cape Wrath (Joseph Huddart)	-	1794	all
NMLS	Carte particuliere de le cote occidentale d'Ecosse, depuis le Cape Wrath jusqu'a la Pointe d'Ardnamurchan	-	1804	all
NMLS	Plan of the island of South Uist (William Bald)	-	1805	all
NMLS	Western Isles (John Thomson)	-	1820	all
EDM	County Series 1st edition	1:2500	1854-1901	all
NMLS	Hydrographic Chart. Hebrides or Western Isles from Barra Head to Scarpa Id.	-	1865	all
NMLS	Ordnance Survey	1 inch	1876	all
NMLS	Ordnance Survey	6 inch	1876	all
NMLS	Ordnance Survey	25 inch	1878	all
EDM	County Series 1st revision	1:2500	1893-1915	SB, CP
NMLS	Ordnance Survey	1 inch	1895	all
NMLS	Ordnance Survey	6 inch	1903-4	all
NMLS	Ordnance Survey	25 inch	1903-4	SB
NMLS	Ordnance Survey popular	1 inch	1909	all
NMLS	North and South Uist (John Bartholomew)	-	1912	all
NMLS	Ordnance Survey popular	1 inch	1928	all
EDM	National Survey	1:2500	1943-1995	all
NMLS	Ordnance Survey popular (National Grid)	1 inch	1947	all
NMLS	Ordnance Survey 7th series	1 inch	1956	all
EDM	Ordnance Survey National Grid	1:2500	current	all

Table 6.2. Details of all aerial photographs with spatial coverage of Staoinebrig, Milton, and/or Cille Pheadair. NCAP = National Collection of Aerial Photographs; CUCAP = Cambridge University Collection of Air Photos; SNH = Scottish Natural Heritage on behalf of the Western Isles Data Partnership.

Source	Year	Site(s)
NCAP	1945	CP
NCAP	1946	all
NCAP	1948	all
NCAP	1963	SB
NCAP	1965	SB, CP
NCAP	1971	CP
CUCAP	1984	all
NCAP	1987	all
SNH	2005	all

Each source was investigated further to determine its suitability for analysis of historic coastal change. Many of the maps pre-dating the Ordnance Survey are very large scale, are unlikely to represent rigorous survey procedures, and lack usable control points. Hence many early maps are not suitable for quantitative assessment of coastal change. However, James et al. (2012) note that interesting qualitative information may still be obtained from maps when the time period investigated exceeds 100 years. The Blaeu (1654) map of South Uist is the clearest of the older maps and provided visual indication of the general character of the South Uist coastline in the 17th Century. Additionally, the Bald (1805) map was judged to be of sufficient quality and detail to provide qualitative information. For quantitative analysis of coastal change all Ordnance Survey maps were selected as these represent the results of a rigorous survey procedure.

For aerial photographs, ideally survey quality photos should be used for quantitative analysis of change. Survey quality images have the detailed information on flight and camera parameters required for softcopy photogrammetric methods. This information was lacking for the majority of photos, and the photos for which this information was available had additional issues (inappropriate spatial scale, damage to film, large areas of water, lack of sufficient ground control points). However, as reasonable quantifications of change have been made by the simpler georectification procedure where detailed flight and camera information is not available, the best quality

(smallest scale, least cloud cover, highest resolution) images from each decade were selected to quantify planimetric changes.

This selection identified 6 maps and 4 sets of aerial photographs, spanning the period 1654 to 2005, to be used in analysis of long-term coastal change (Table 6.3). Due to funding constraints it was only possible to access photos for two field sites. Due to the perceived higher sensitivity of Staoinebrig and Cille Pheadair (compared to Milton), photos for these sites were selected.

Table 6.3. Details of all data sources selected to analyse coastal change.

Type	Source	Year	Use
map	NMLS	1654	qualitative
map	NMLS	1805	qualitative
map	OS	1876	quantitative (planimetric)
map	OS	1903/4	quantitative (planimetric)
photo	NCAP	1948	quantitative (planimetric)
photo	NCAP	1965	quantitative (planimetric)
map	OS	1965	quantitative (planimetric)
photo	NCAP	1987	quantitative (planimetric)
map	OS	2002	quantitative (planimetric)
photo	SNH	2005	quantitative (volumetric)

6.2.3 Analysing historic change using maps

For qualitative analysis of change, maps are reoriented and clipped to facilitate visual comparisons of the same areas. For quantitative analysis of shoreline change using historic maps all maps must be displayed to scale using the same projection. Digital images of all maps were imported to ArcGIS (version 10, ESRI). Maps sourced from Digimap (i.e. the Ordnance Survey maps) are already georectified to the British National Grid and needed no further processing.

A common map feature must be identified to indicate shoreline change. For the maps used, the positions of mean high water at ordinary spring tide (MHWOST) and mean low water at ordinary spring tide (MLWOST) were the available options.

MHWOST was preferred to MLWOST as a shoreline indicator for ease of location in the field as it is generally associated with a physically identifiable feature (Oliver, 1993; Baily, 2009). Additionally, the process for tideline mapping was formalised by the Ordnance Survey in 1968 (Baily, 2009), with the mapping procedure for high tide lines more rigorous than for low tide lines due to greater accessibility and visibility. Unlike England and Wales, the same tidal features have been mapped continuously on Ordnance Survey maps in Scotland since the mid-19th Century (Oliver, 1993), making comparisons of change simpler. The position of MHWOST was digitised to create a polyline feature for each year a map was available for (1876, 1903, 1965, 1971, and 2002), using the Editor toolbar in ArcMap (ArcGIS version 10, ESRI).

6.2.3.1 Error identification and quantification

Historic maps are valuable for analysing coastal change as they enable timescales to be extended from decadal to centennial, which is important to distinguish between long-term trends in coastal evolution and shorter term fluctuations. However, several limitations apply; notably, the irregular temporal spacing of data sources (Brooks, 2010); the need to interpolate rates over periods of time where information is not available (James et al., 2012); lack of information on survey date (which may differ from the publication date by several years) (Brooks, 2010); and partial revisions (Carr, 1962). In general, Boak and Turner (2005) suggest that maps from the 19th Century on are suitable for the analysis of shoreline change, and James et al. (2012) considered that for centennial scale studies even maps capable only of providing qualitative information could be considered useful for the detection of geomorphic change.

The use of historical maps to assess geomorphic change is inaccurate due to a range of inherent and operational errors. Inherent errors are those arising from the maps themselves, either due to the surveying, or alterations to the maps over time. Several authors attempt to quantify planimetric errors in the position of MHWOST (or a similar indicator of high tide water levels) arising from inherent errors in historic maps, producing varying results ranging from ≤ 4 m to ≤ 20 m (Table 6.4). Inherent errors may arise from: map shrinkage, distortion, or damage over time; seasonal and tidal changes in the position of MHWOST; interpretation of MHWOST by the surveyor; and

annotation (i.e. the width of the line on the map may cover several metres) (Moore, 2000).

Table 6.4. Estimations of maximum planimetric error in the position of linear features indicating the position of high-water levels from a range of authors.

Max. planimetric error (m)	Source	Notes
4	Pye and Blott, 2006	For georeferenced, digitised maps at a scale of 1:10,560 or smaller
5	Valentin, 1954	
10	Shalowitz, 1964	
20	Morton and Speed, 1998	due to seasonal variations over a 12 month period
10 (20)	Moore, 2000	20 pre-1941

As the maps used were from the same source (Ordnance Survey), and would therefore have been surveyed using the same procedures, and as the maps are generally small scale (see Table 6.1), the inherent errors in most of the maps might be expected to be close to the lower end of the range shown in Table 6.4. Operational errors arise during the analysis of historic maps, e.g. comparisons between different maps. Using georectified images minimises the error associated with comparisons between maps (James et al., 2012).

6.2.4 Analysing historic change using aerial photographs

The aerial photographs selected had a dpi (dots per inch) of 1200 and scales which ranged from 1:10,500 (1948 and 1965 photos) to 1:26,500 (1987 photos). The former exceeds the minimum dpi recommended for quantitative analysis of change (725 dpi) (Moore, 2000); the scales for the earlier photos exceed the minimum recommendations for quantitative analysis of change using aerial photographs (1:20,000) (Moore, 2000), while the 1987 photos are slightly poorer than recommended scale.

Aerial photographs were imported into ArcGIS and georectified using the Georeferencing toolbar (ArcGIS version 10, ESRI). As the number of ground control points (GCP) used is inversely correlated with error (Hughes et al., 2006), as many GCPs as possible were used to georeference each image (see section 6.2.4.1). To

minimise error where possible, man-made structures were used as GCPs in preference to natural features as this approach generally minimises error (Hughes et al., 2006). GCPs were distributed as widely and evenly as possible across the images to maximise accuracy (James et al., 2012). Georectification allows the user to spatially 'match up' the same features in different images. The image being georectified is altered using a first order polynomial transformation which minimises root-mean-square error (RMSE) between all of the GCPs used. The 2005 aerial imagery was used as the base photograph, with older photographs georeferenced to this.

The vegetation line was manually identified and digitised on the georectified images as a shoreline proxy for the aerial photographs because it was consistently visible at all sites and on all photos as a clear tonal difference. Other commonly used shoreline indicators for aerial photographs (e.g. dune toe, cliff top) were inappropriate here due to the different morphologies at each site. Also, Boak and Turner (2005) considered the vegetation line to be a good shoreline indicator for identifying erosion, and erosion was expected to be the predominant coastal change at all sites. In their review of shoreline detection, Boak and Turner (2005) note that the vegetation line as a shoreline proxy also shows accretion, however with a lag due to the time taken for vegetation to recolonise. As the times between photographs are relatively long (17-22 yrs) it was decided that the vegetation line was an appropriate indicator of both accretion and erosion. Digitisation was completed manually using the same method described for digitisation of MHWOST in section 6.2.3 (e.g., as used in Miller and Fletcher, 2003; Milne et al., 2012).

6.2.4.1 Error identification and quantification

Many of the limitations listed in section 6.2.3.1 for historic maps are applicable to historic photographs (e.g. sampling interval determined by data availability, errors arising due to paper warping, damage to images, etc.). A further source of error with historical photographs is distortions in the original photograph. Such errors can be corrected for during photogrammetric orthorectification, provided the camera parameters are known. However, this was not possible as the camera and survey details were not known for the available images. During georectification (used when camera and flight information is not available (Rogers et al., 2010)), the photograph is matched

up to a georeferenced base (either a map or a photograph) using GCPs. Errors are minimised by the transformation process, and indicated by the resultant RMSE – indicating the residual differences in position between the GCPs on the two images.

The number of ground control points used to georeference each photograph and the RMSE for each georectified image is shown in Table 6.5. In all cases the minimum recommendation of 10 GCPs per photograph (Rogers et al., 2010) was exceeded. The RMSE of the georectification ranged from 3.81-8.80 m. This compares with estimates of the accuracy of this technique of 5 m (Hughes et al., 2006), and 6-17 m (Rogers et al., 2010).

Table 6.5. Number of Ground Control Points and Root Mean Square Error for each georectified photograph.

Site	Year	No. GCPs	RMSE
CP	1948	27	4.86
CP	1965	39	6.89
CP	1987	71	3.81
SB	1948	20	8.80
SB	1965	32	6.78
SB	1987	34	6.69

A further error is inaccuracy in mapping the selected shoreline indicator during digitisation. This has been estimated as 1-2 m (Brown et al., 2003).

The RMSE's of ~4-9 m in Table 6.5 for the photographs may be slightly higher for the digitised vegetation line due to the non-uniform distribution of control points across the images; no GCPs can be on the part of the image taken up by sea and beach, and the number of GCPs on land tends to increase with distance from the coast. This is because the man-made features which make the most accurate GCPs (road intersection, corners of buildings, etc.) are mostly found towards the inland end of the machair. Uneven distribution of control points may reduce the accuracy of the transformation on parts of the image for which fewer GCPs are available. At both sites, sections of the 1948 vegetation line were hard to identify due to a lack of contrast between the beach and machair grassland. These sections are identified in section 6.3, and could only be identified to within ~ 20 m.

6.2.5 The Digital Shoreline Analysis System (DSAS)

The DSAS was developed by the U.S. Geological Survey (USGS) to calculate numerical and statistical data on changes in shoreline position (Thieler et al., 2009). It can be used either by uploading digitised shorelines to an online platform, or downloaded and installed as an extension to the ArcGIS software. For this study, the DSAS version 4.3.4730 for ArcGIS 10 was used (Thieler et al., 2009).

For use with the DSAS extension for ArcGIS the shoreline indicator positions were appended to a single feature class for each site. A baseline feature was digitised ~ 45 m offshore from the seaward-most shoreline indicator position running parallel to the this feature. Transects were generated by the DSAS extension along the length of the digitised shoreline indicator feature class with a 10 m along shore spacing (Fig. 6.1). A smoothed baseline cast produced a more uniform transect orientation along curved sections of the coast than would have been achievable using a simple baseline cast. An uncertainty of 4 m was assigned to shoreline indicator positions generated from the pre-rectified OS maps and photographs (see section 6.2.3.2 for justification). Numerical and statistical data on change in the position of this feature was then calculated using the DSAS extension and a MATLAB component runtime utility. The data generated are summarised in Table 6.6.

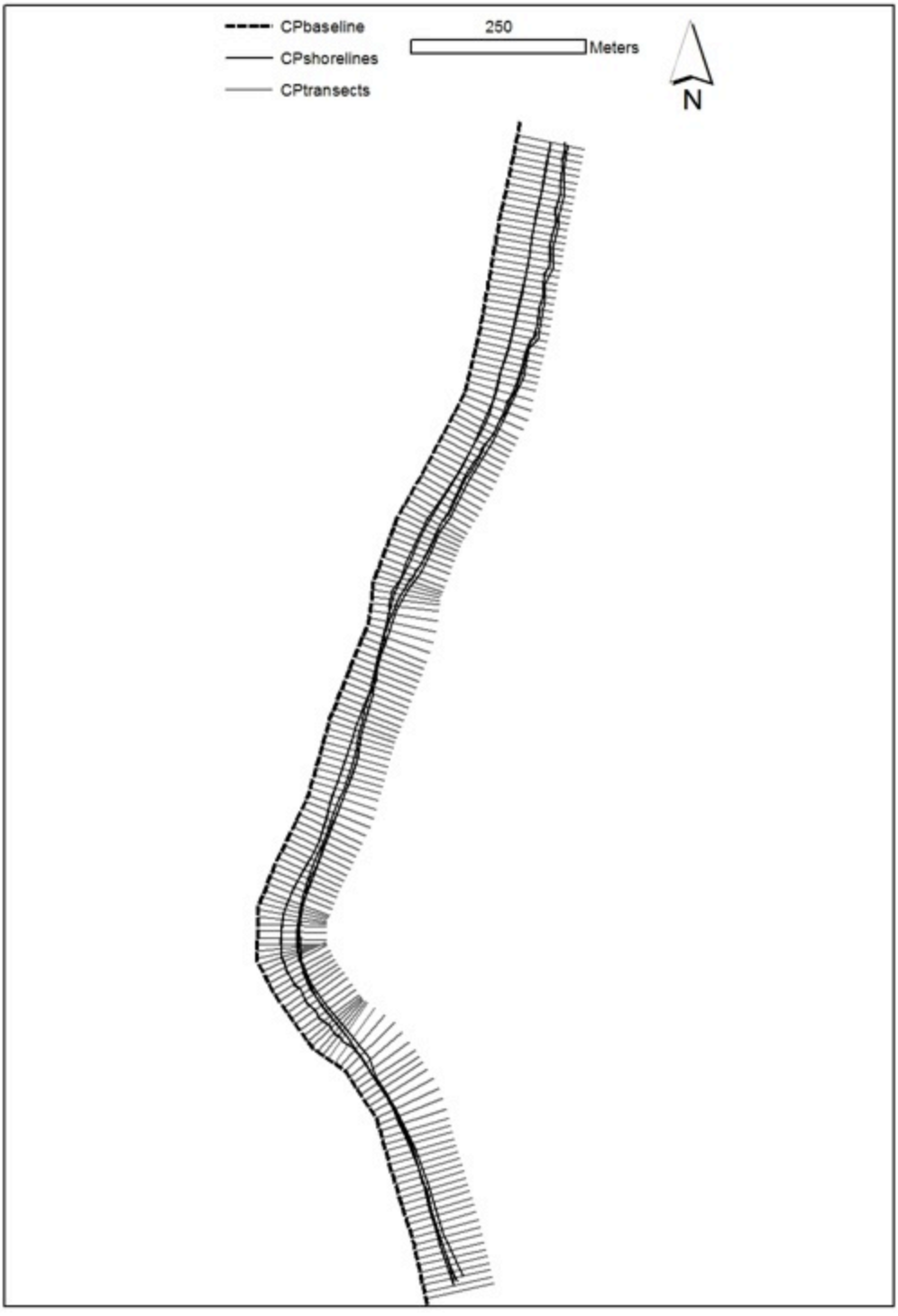

Figure 6.1. Map of transect positions and polylines digitised from the position of MHWOST on OS maps at Cille Pheadair.

Table 6.6. Definitions and descriptions of shoreline change data generated using the DSAS extension (adapted from information provided in Himmelstoss, 2009).

Data/Statistic	Definition	Description
Distance (m)	-	Distance between the baseline and each MHWOST position for each transect
NSM	net shoreline change movement	Distance between the oldest and youngest positions of MHWOST
EPR	end point rate	NSM divided by the number of years between the oldest and youngest shorelines

6.2.6 Comparing rates of change from different sources

Analysing historic shoreline change best practice is to compare results based on two or more different shoreline indicators, e.g. to obtain different temporal or spatial resolutions. However, using multiple sources can introduce additional errors (Boak and Turner, 2005).

Change in position of the MHWOST with the position of the vegetation line is not a 'like-for-like' comparison. MHWOST is a tidal datum. Its position depends on the shape of the beach profile (which in turn is controlled by sediment availability, waves, tides, and storms). The vegetation line is a visually identifiable feature, and reliant on the morphology of the dunes and machair front, as well as water levels (i.e. frequency of inundation), and anthropogenic impacts. Its position may be concealed on aerial imagery by sand blows that temporarily bury permanent vegetation on the machair coast. Therefore, although changes in the position of MHWOST and the vegetation line are broadly similar over the same temporal intervals, their responses to changes in the coastal environment are unlikely to be identical. MHWOST is generally a more dynamic feature than the vegetation line, due to seasonal and tidal variations in beach profile, as well as any changes in profile due to storms (Montreuil and Bullard, 2012). In contrast the vegetation line responds very rapidly to erosion, but there may be a lag in the response to accretion to allow time for recolonisation.

For these reasons, the shorelines obtained from the historical maps and photographs are not compared directly. Instead, the results are analysed and statistically assessed separately, with discussion of the combined results in Chapter 9.

6.3 Results

6.3.1 Qualitative analysis of historic maps

Figure 6.2 shows side-by-side maps of South Uist from 1654, 1805, and 2010. While the Blau map of 1654 pre-dates reliable surveying techniques, is large scale, and generally lacks detail, and the Bald map of 1805 is also of a large scale and does not indicate the specific coastal feature mapped as the dividing line between sea and land, these maps provide an overview of coastal change on the western coast of South Uist over 350 years.

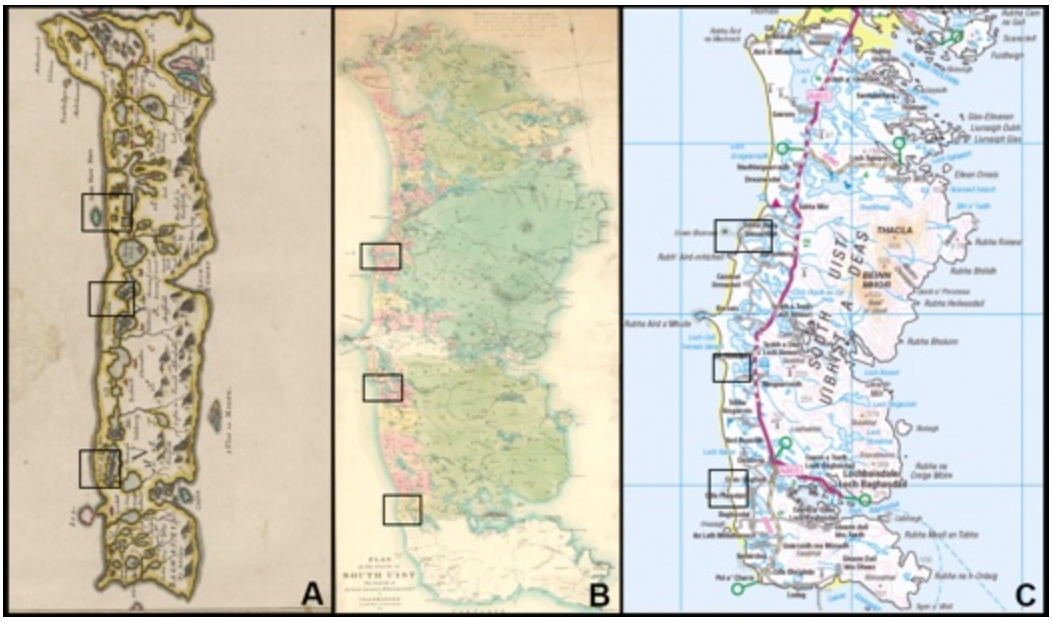

Figure 6.2. Maps of the island of South Uist with location of field sites marked by black boxes (locations approximate on map A). A) Blau 1654 map; B) Bald 1805 estate map; C) Ordnance Survey 2010 map. Maps A and B reproduced by courtesy of the National Map Library of Scotland. Map C contains Ordnance Survey data. (c) Crown copyright and database right 2010. Data provided by Digimap OpenStream, an EDINA, University of Edinburgh Service.

There are several clear and generalised differences between the 1654 Blau map and the later Bald and Ordnance Survey maps of the southern Outer Hebrides (e.g. as used to demonstrate barrier island evolution at Gualan Island between South Uist and Benbecula by Dawson et al. (2012)). The coastline of South Uist appears more linear in the earlier map, particularly around Staoinebrig (the most northerly field site); the headland to the south of this site and the long curved embayment to the north are both

missing from the Blau map. However, the reverse is true of the southern portion of the map, where the headlands south of Cille Pheadair (the most southerly field site) are markedly more pronounced in the 1654 map. The machair lochs are larger and with more inter-connections, particularly at the far south of the island where several lochs appear in the 1654 map but are later absent. The offshore islands are larger in the 1654 map than in the 1805 and 2010 maps. The field site at Cille Pheadair is a much less prominent headland in the 1654 map; the headland north of Milton is absent in the 1654 map; and the coastline around Staoinebrig is almost completely linear in the 1654 map compared to a more indented coastline in the later maps.

There are very few differences between the Bald 1805 and the 2010 Ordnance Survey maps, suggesting that the 1805 map is a more accurate reflection of the coastline than previous maps. Figure 6.3 enlarges each site from the 1805 and 2010 maps, showing only slight differences in the coastline. At Staoinebrig there are minimal changes – the most apparent being the inland drainage patterns. At Milton the rerouting of the Roe Glass burn (the drainage channel at the northern end of the beach) is notable. This is likely anthropogenic rather than a natural change, and was probably part of the extensive alterations and additions to drainage in the South Uist machair during the 19th Century. At Cille Pheadair changes are also minimal. Aside from a possible slight change in the shape of the headland the most noticeable changes are those related to drainage of the lochs.

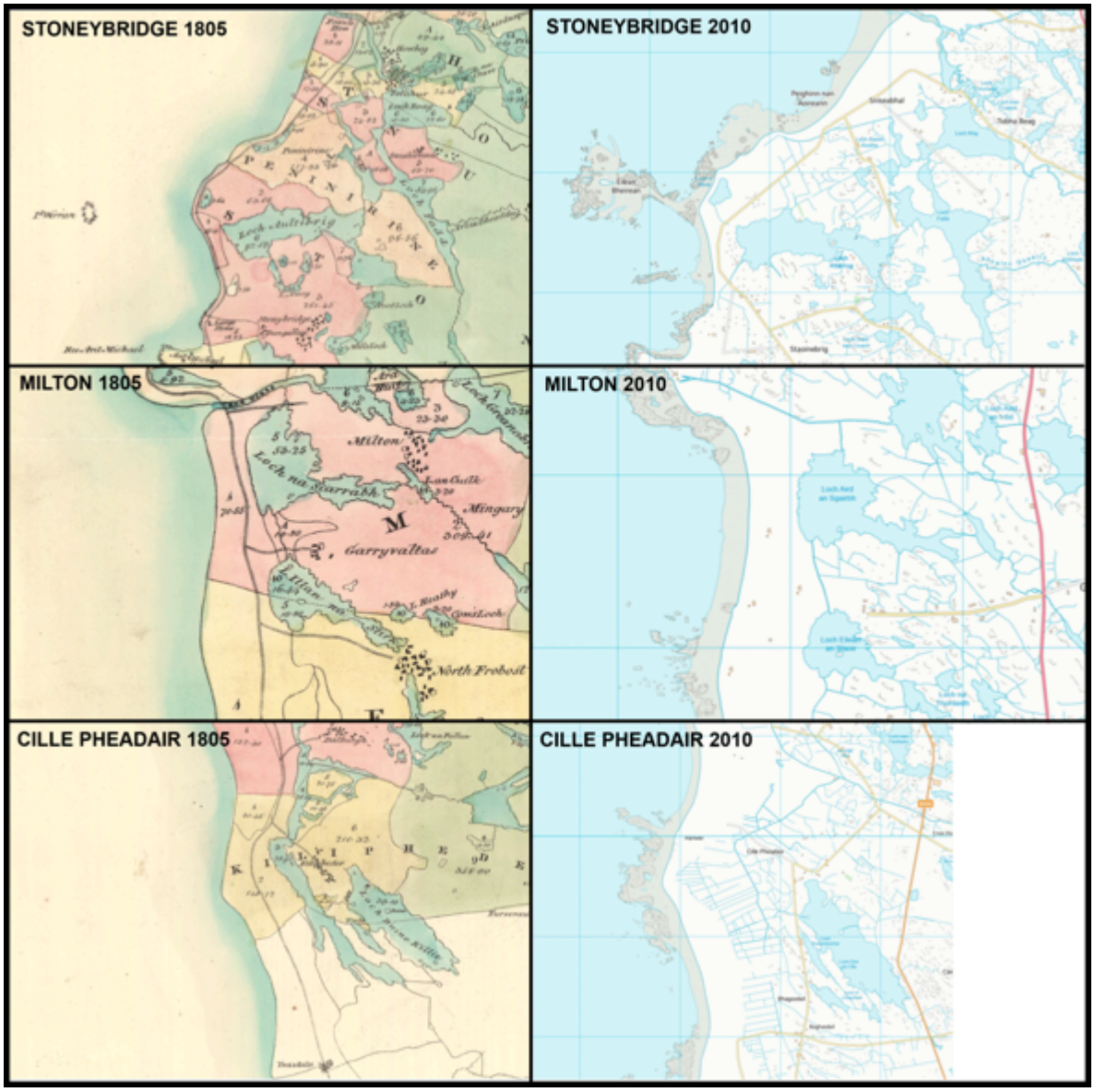

Figure 6.3. Maps of each of the three field sites in 1805 (Bald) and 2010 (Ordnance Survey). The 1805 Bald map is reproduced by courtesy of the National Map Library of Scotland. The 2010 map contains Ordnance Survey data. (c) Crown copyright and database right 2010. Data provided by Digimap OpenStream, an EDINA, University of Edinburgh Service.

6.3.2 Quantitative analysis of historic maps

6.3.2.1 Staoinebrig

Figure 6.4a shows MHWOST from 1878-2002. There are clear intra-site variations, however, the majority of the shoreline at Staoinebrig has retreated with the northern and central sections (transects 0-40 and 50-70) most severe. In contrast there has been a slight net seawards movement of the position of MHWOST over a small stretch of shoreline at the centre of the site (transects 40-50), and the rocky southern end of the site (transects 75-100) has experienced minimal change over the 124-year period. There are also temporal variations in change in MHWOST position. The period from 1878-1905 is characterised by a slight seawards movement of the shoreline along the majority of the site. The largest changes occurred between 1905-1965, and there appear to have been minimal changes between 1965-2002 – generally slight and discontinuous (< 3 m) seawards movements of MHWOST position. Mean NSM is retreat of 6.02 m. The maximum seawards shoreline movement (progression) is 3.93 m at transect 44, and the maximum landwards shoreline movement (retreat) is 17.3 m at transect 21. At Staoinebrig the mean EPR was -0.05 m/yr, but EPR ranged from + 0.03 m/yr at transects 42-44 at the centre of the site to – 0.14 m/yr at transect 21.

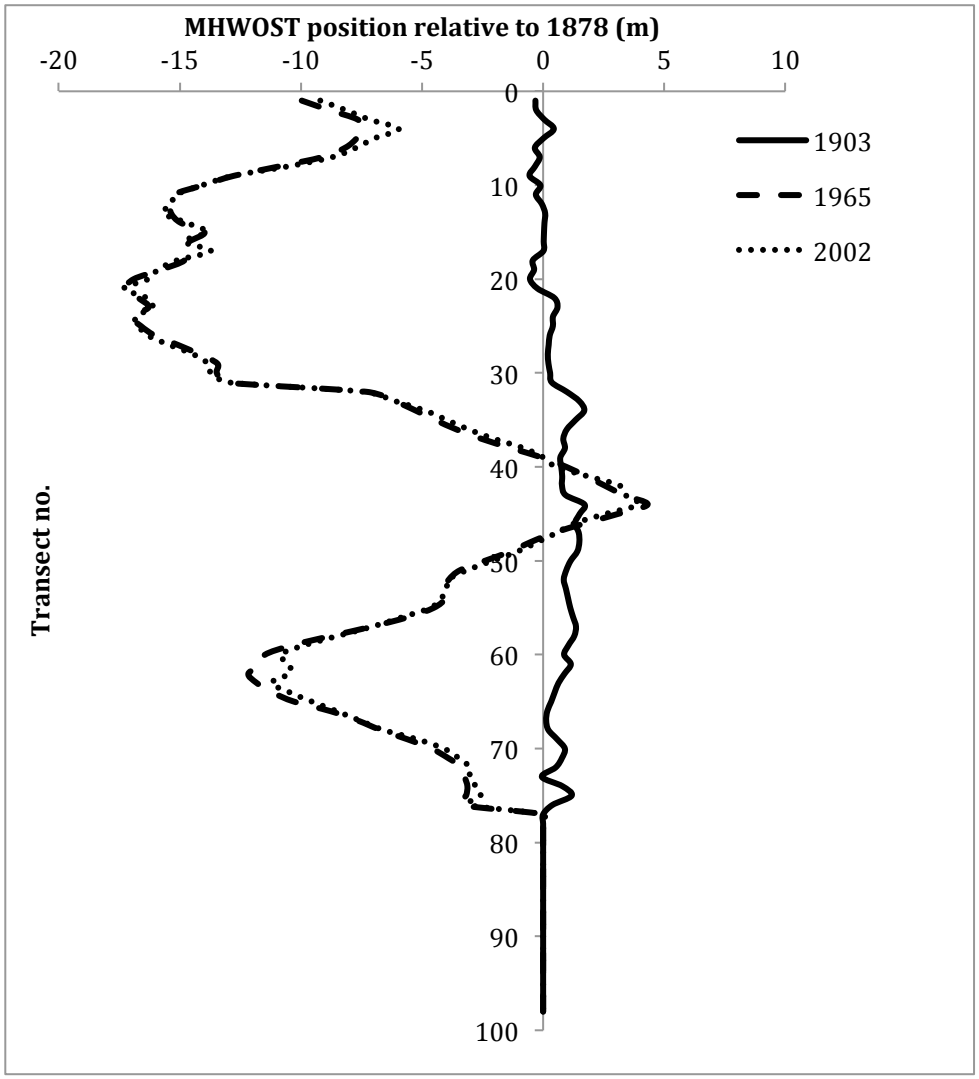

A.

Figure 6.4a. Changes in the position of MHWOST between 1878-2002 at Staoinebrig. The 0 line represents the position of MHWOST in 1878. Vertical axis indicates transect number (profile no. x 10 = distance (m) from northern end of site).

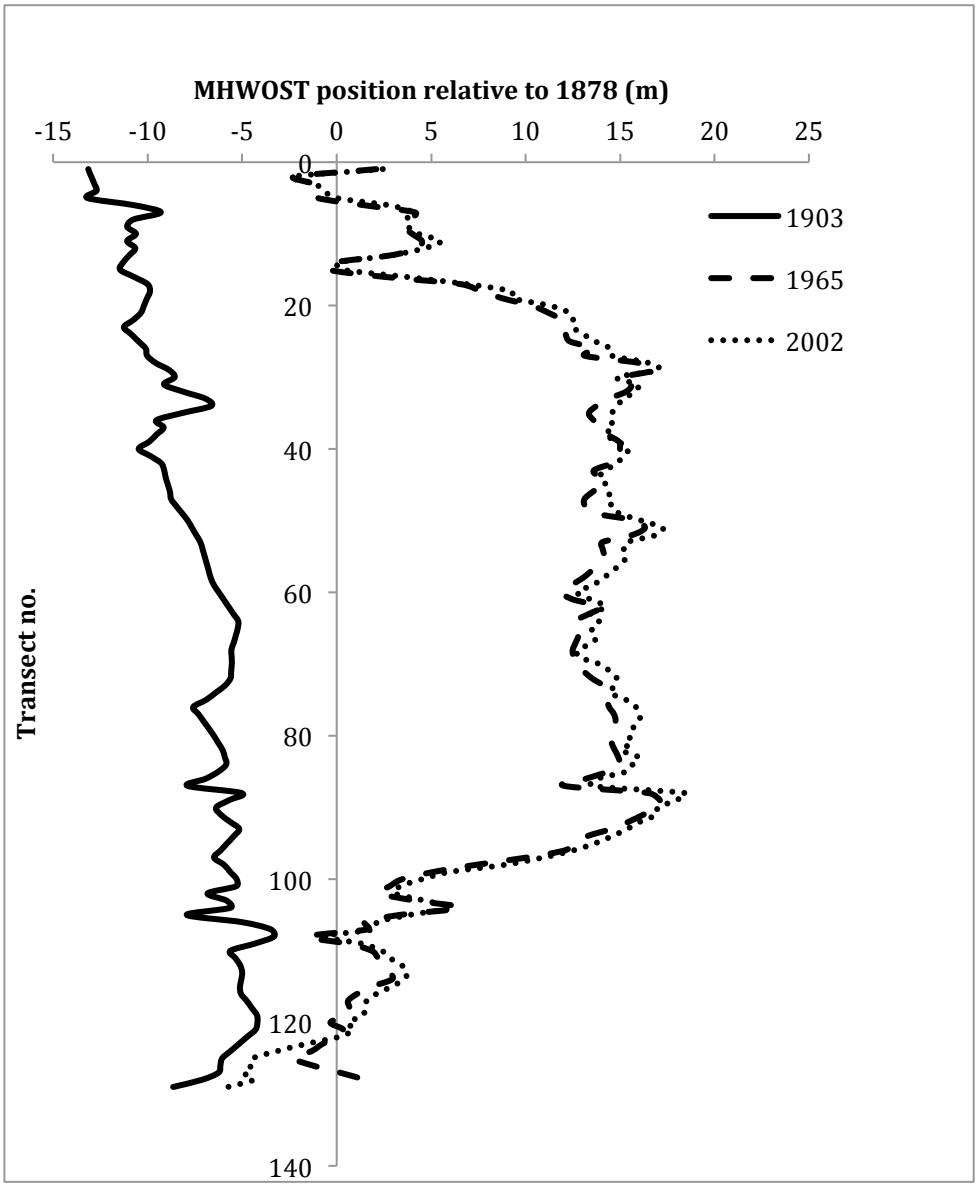

B.

Figure 6.4b. Changes in the position of MHWOST between 1878-2002 at Milton. The 0 line represents the position of MHWOST in 1878. Vertical axis indicates transect number (profile no. x 10 = distance (m) from northern end of site).

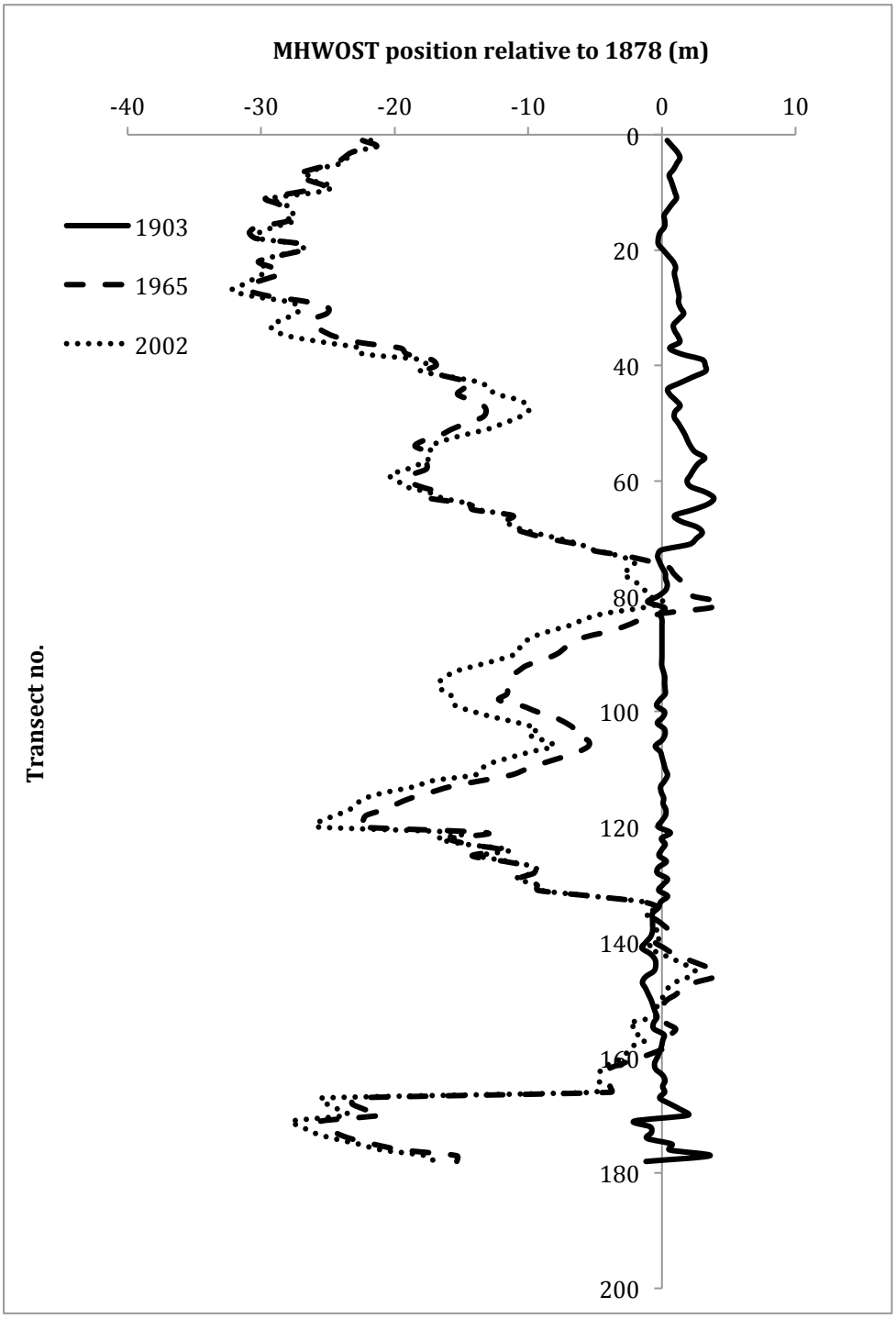

C.

Figure 6.4c. Changes in the position of MHWOST between 1878-2002 at Cille Pheadair. The 0 line represents the position of MHWOST in 1878. Vertical axis indicates transect number (profile no. x 10 = distance (m) from northern end of site).

Figure 6.5a shows temporal variations in EPR at Staoinebrig. Median EPR is similar for the earliest and latest periods; from 1873-1905 median EPR is + 0.01 m a^{-1} and from 1965-2002 median EPR is 0.00 m a^{-1}. During these periods the shoreline

appears almost stable with mainly low to slightly positive EPR values. Additionally, the range of EPRs is relatively low (compared to the 1905-1965 period), indicating that EPR was relatively consistent throughout the site. However, the median EPR from 1905-1965 is – 0.07 m a^{-1}, and the majority of EPR values are negative for this period, indicating that Staoinebrig experienced shoreline retreat throughout this period. The range of EPRs is also higher than for the earliest and latest periods, which supports evidence from Figure 6.5a which shows how intra-site variability in shoreline changed over this period. The median EPR of 0.00 m a^{-1} for the most recent period indicates that the position of MHWOST has been more stable recently than it has been for the earlier 20th Century.

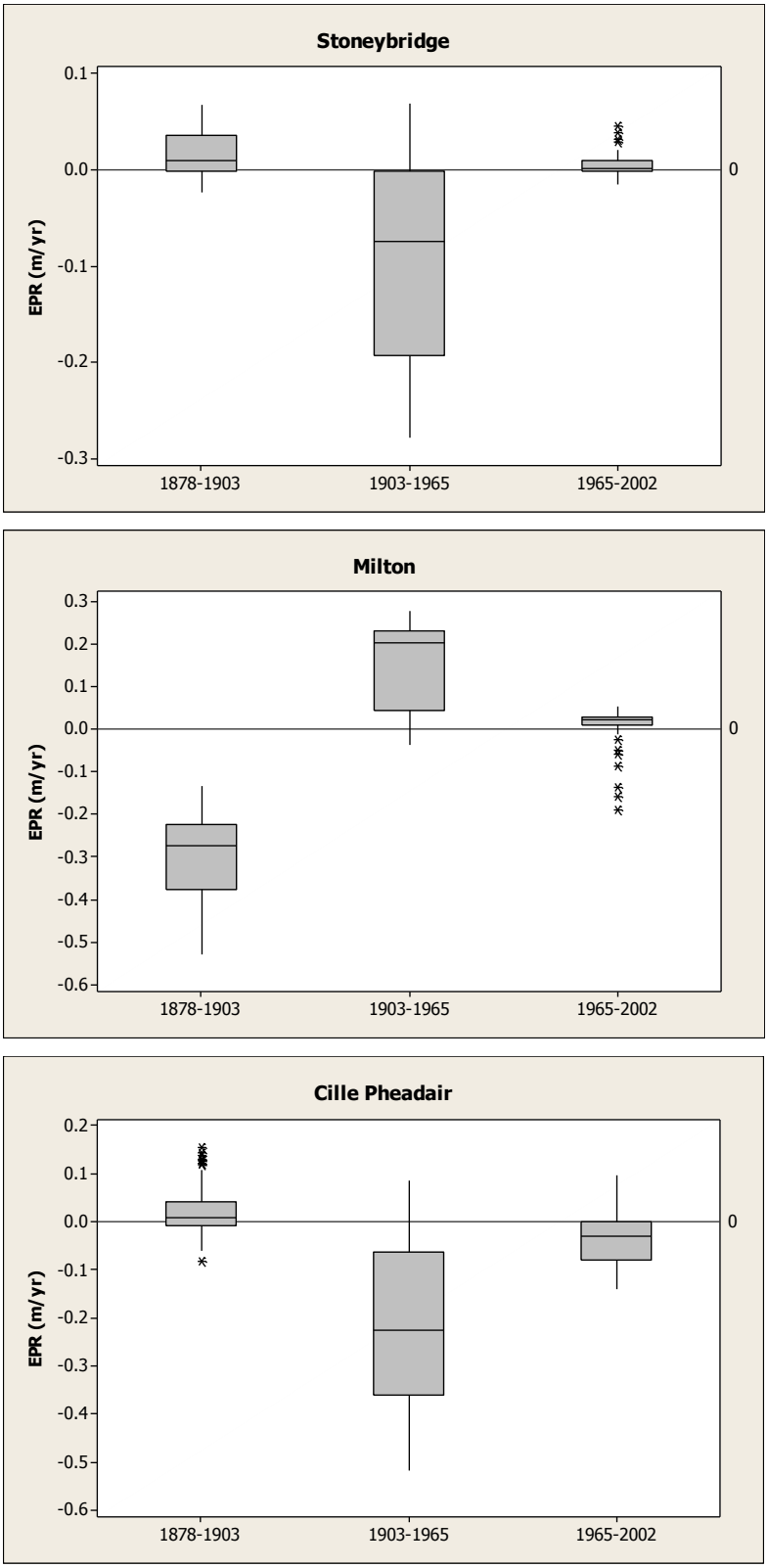

Figure 6.5. Temporal variations in EPR. A. Staoinebrig. B. Milton. C. Cille Pheadair.

As the northern and southern sections of the site have different geomorphologies (see section 3.1), a comparison of mean NSM and mean EPR are shown in Table 6.7 for

the two parts of the site. These show that northern end of the site (currently characterised by an eroding scarp) has experienced significantly ($p < 0.01$) more negative NSM and EPR than the southern end of the site (currently characterised by a banked shingle ridge) between 1878-2002.

Table 6.7. Comparison of mean NSM and EPR values for the northern and southern sections of the Staoinebrig site.

Section	Transect nos.	Mean NSM (m)	Mean EPR (m a^{-1})
north	1-37	-10.99	-0.08
south	38-98	-2.54	-0.02

6.3.2.2 Milton

Figure 6.4b shows changes in the position of MHWOST from 1878-2002. As with Staoinebrig, there are clear intra-site variations in the amount of change, however, the majority of the shoreline at Milton has experienced net seawards movement in the shoreline indicator on the order of 10-15 m. The central section has experienced the most seaward movement of MHWOST (transects 15-100), while transects at the extreme northern and southern ends of the site have experienced less change or slight retreat. In contrast to Staoinebrig, the period from 1878 to 1903 is characterised by shoreline retreat which is greater towards the northern end of the site and lesser towards the southern end. From 1903-1965 the shoreline indicator showed a large seawards movement along most of the shoreline, and the most recent period from 1965-2002 shows evidence for further slight seawards progression of MHWOST, apart from at the far southern end of the site (transects 120-130), which shows shoreline retreat of 0-5 m. Mean NSM is seawards movement in the position of MHWOST by 9.28 m, and the range of NSM is from – 8.68 m (transect 132) to + 18.43 m (transect 88). Mean EPR is + 0.07 m a^{-1}, and the range of EPR is from -0.23 to + 0.15 m a^{-1}.

Figure 6.5b shows temporal variations in EPR at Milton. Median EPR is clearly lowest (and negative) from 1878-1905 (-0.27 m a^{-1}), and most strongly positive from 1905-1965 (+ 0.20 m a^{-1}). EPR in the most recent period indicates that the shoreline has been comparatively stable from 1965-2002 with a median EPR value of + 0.02 m a^{-1} and a small range of values. However, there are some outlying values which show that at some transects retreat of ≤ - 0.25 m a^{-1} occurred during this period. The results from

Milton contrast with those of Staoinebrig; at Milton the period from 1878-1905 was characterised by shoreline retreat, while at Staoinebrig this was the period of most rapid seawards progression of the shoreline indicator. While from 1905-1965, Milton was characterised by shoreline progression and Stoneybridge by retreat. However, similar rates were experienced at both sites from 1965-2002.

6.3.2.3 Cille Pheadair

Changes in the position of MHWOST at Cille Pheadair appear to have followed the same general trends as those found at Staoinebrig (Fig. 6.4c). From 1878-1903 the majority of the site was characterised by very little change, with some slight seawards movements (< 5 m) in the position of the shoreline indicator at some transects, particularly those located north of the central headland (transects 0-70). Between 1905-1965 the majority of the site experienced retreat of 0-30 m, although two small areas located to either side of the headland (transects 70-82 and 133-160) appear to have experienced a slight seawards movement (< 5 m) in the position of MHWOST over this period. The most recent period is characterised by further slight retreat (≤ 5 m) along most of the coastline, with the greatest retreat occurring along the central headland (transects 80-130), although at some transects (e.g. transects 42-51) some seawards movement in the position of the shoreline indicator has occurred. Mean NSM is retreat of 14.28 m, and the range is from -32.18 m (transect 27) to + 2.49 m (transect 157).

Temporal variations in EPR are shown in Figure 6.5c. The pattern is similar to that seen at Staoinebrig, but with generally slightly more negative rates. Median EPR was 0.01 m a^{-1} and the range of values is relatively low from 1878-1905, indicating that the position of MHWOST was comparatively stable over this time period. From 1903-1965 the median EPR was lower (- 0.22 m a^{-1}) with some transects experiencing a retreat rate of up to 0.52 m a^{-1}. Cille Pheadair is the only site at which the most recent period is characterised by a negative median EPR (- 0.03 m a^{-1}), and is also the only site for which the majority of transects experienced retreat between 1965-2002.

As the headland at Cille Pheadair is most exposed to wave action, comparisons of mean NSM and ESR values for the headland with the rest of the site are shown in Table 6.8. The headland was found to have significantly more negative NSM and EPR

values when compared with the remaining transects ($p < 0.01$), which suggests that this is the most susceptible part of the site to shoreline retreat.

Table 6.8. Comparison of mean NSM and ESR values for the headland and the rest of the site at Cille Pheadair.

Section	Transect nos.	Mean NSM (m)	Mean EPR (m a^{-1})
Headland	75-135	- 16.5	- 0.13
Rest of the site	0-74, 136-178	- 13.5	- 0.11

6.3.2.4 Comparisons between the three sites

It is clear from the results shown in sections 6.3.1-3 that the position of MHWOST has followed similar trends at Staoinebrig and Cille Pheadair, while the pattern of change at Milton contrasts with the other two sites. Figure 6.6 shows spatial variations in EPR at all three sites, while Figures 6.7a and b show boxplots of EPR and NSM values, respectively. Milton is the only site which has experienced a positive EPR at the majority of measured transects, however it also has the largest range of EPR values, with very negative values occurring at the southern end of the site. Cille Pheadair and Milton are both characterised by mostly negative EPR rates, although rates at Cille Pheadair are noticeably more negative. Staoinebrig shows the least spatial variability in EPR (Fig. 6.7a). NSM and EPR values shown in Table 6.9 show that Cille Pheadair has experienced significantly more shoreline retreat than the other two sites ($p < 0.01$), and Staoinebrig has experienced significantly more retreat than at Milton ($p < 0.01$). All sites show evidence for both regression and seawards movement of the position of MHWOST at some transects.

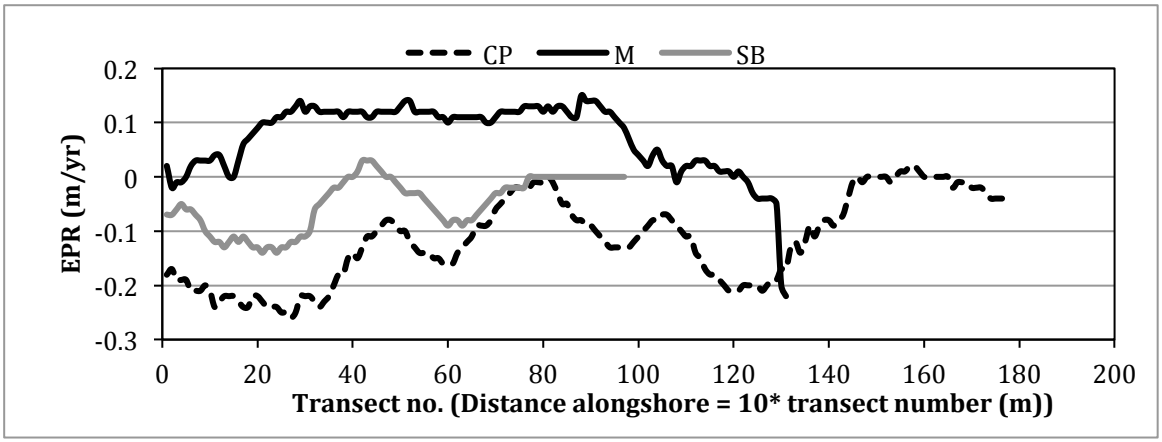

Figure 6.6. EPR (1878-2002) at Staoinebrig (SB), Milton (M), and Cille Pheadair (CP). Transects are numbered from the northern to southern end of each site.

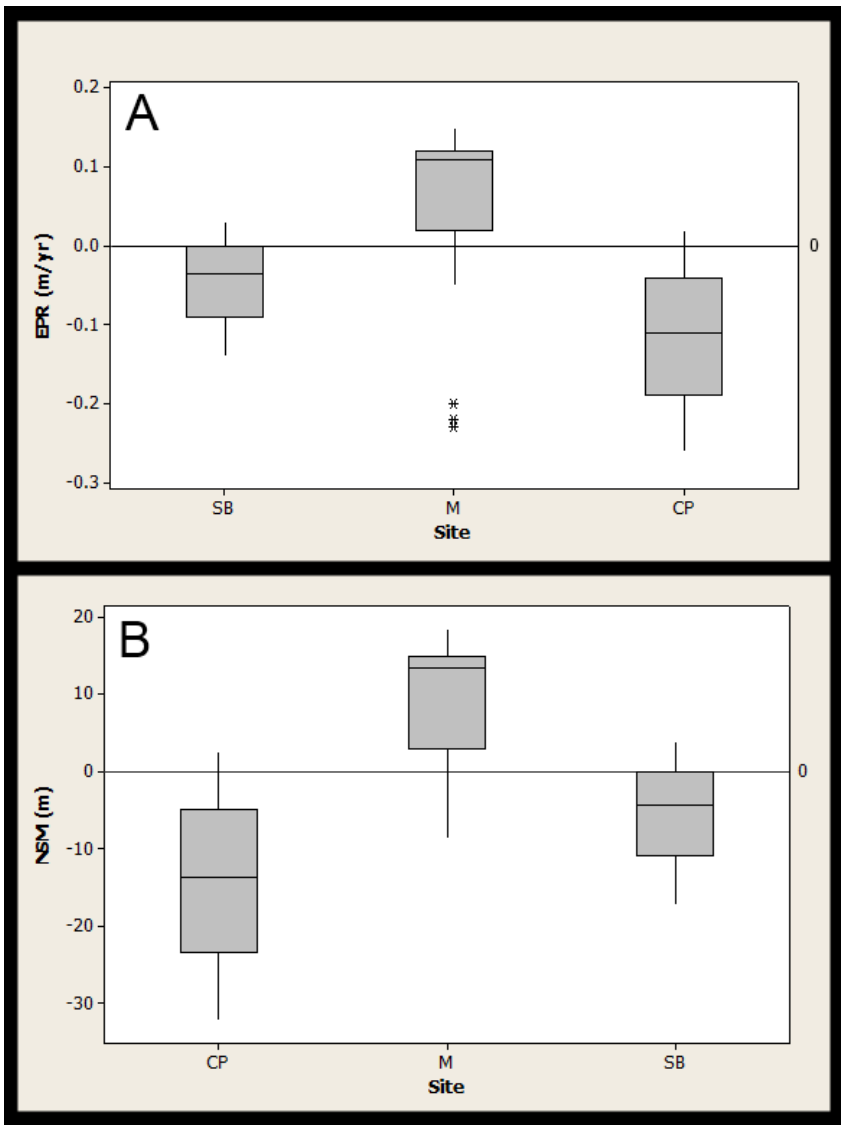

Figure 6.7. Boxplot comparisons of A. EPR, and B. NSM, at Staoinebrig (SB), Milton (M), and Cille Pheadair (CP).

Table 6.9. Comparison of mean NSM and EPR values for the three sites.

Site	Mean EPR (m a^{-1})	Mean NSM (m)
Staoinebrig	- 0.06	- 6.02
Milton	+ 0.07	+ 9.28
Cille Pheadair	- 0.11	- 14.23

6.3.3 Quantitative analysis of historic photographs

6.3.3.1 Staoinebrig

Figure 6.8a shows changes in the position of the vegetation line from 1948-2005. The majority of the site has experienced seawards movement of the shoreline indicator by ≤ 10 m over this period, although there are several sections distributed across the length of the site were retreat has occurred. The greatest period of seawards movement appears to have occurred between 1948-1965, when the majority of the site experienced progression of the vegetation line of ≤ 20 m. After this initial period of seawards movement, the vegetation line appears to have retreated towards the 1948 position between 1965-2005. The far southern end of the site (transects 85-100) shows the least changes, while the central section shows the largest changes of up to 40 m between 1948-2005. However, it should be noted that for this part of the site it was difficult to accurately determine the position of the vegetation line in the 1948 imagery. The mean NSM between 1948-2005 is + 3.33 m. Maximum and minimum changes are +20.04 m (transect 57) and – 12.04 m (transect 78), respectively. The mean EPR is + 0.06 m/yr, with maximum and minimum values of + 0.35 m/yr and – 0.21 m/y.

A.

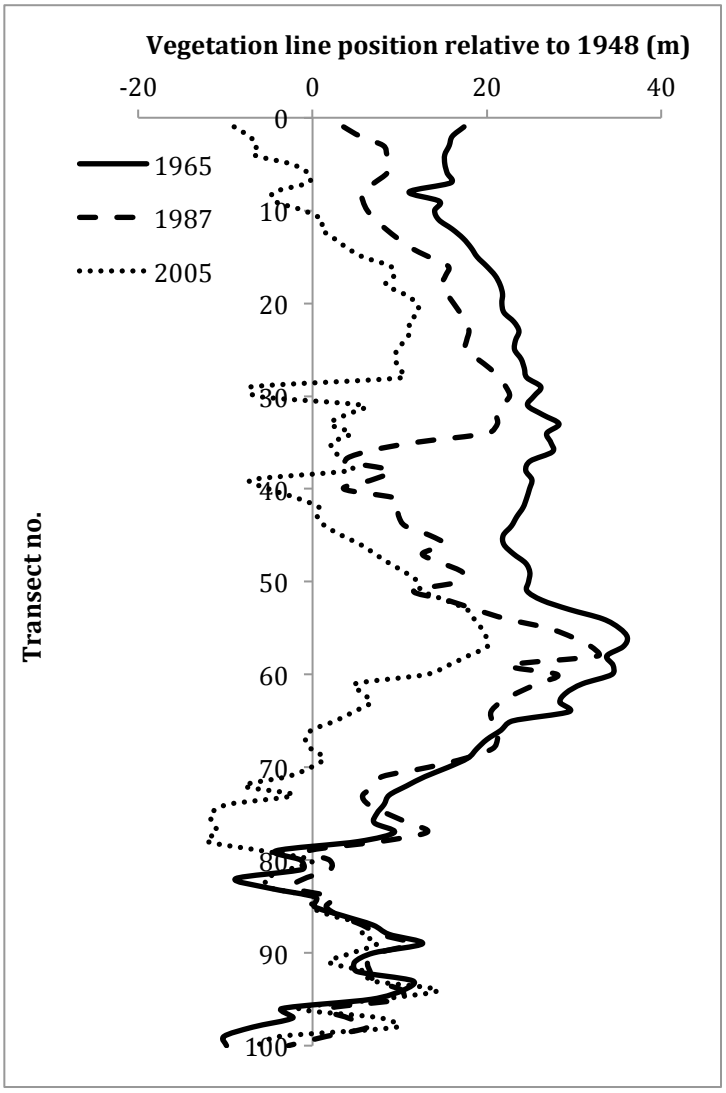

Figure 6.8a. Changes in the position of the vegetation between 1948-2005 at Stoneybridge. The 0 line represents the position of the vegetation line in 1948. Vertical axis indicates transect number (profile no. x 10 = distance (m) from northern end of site).

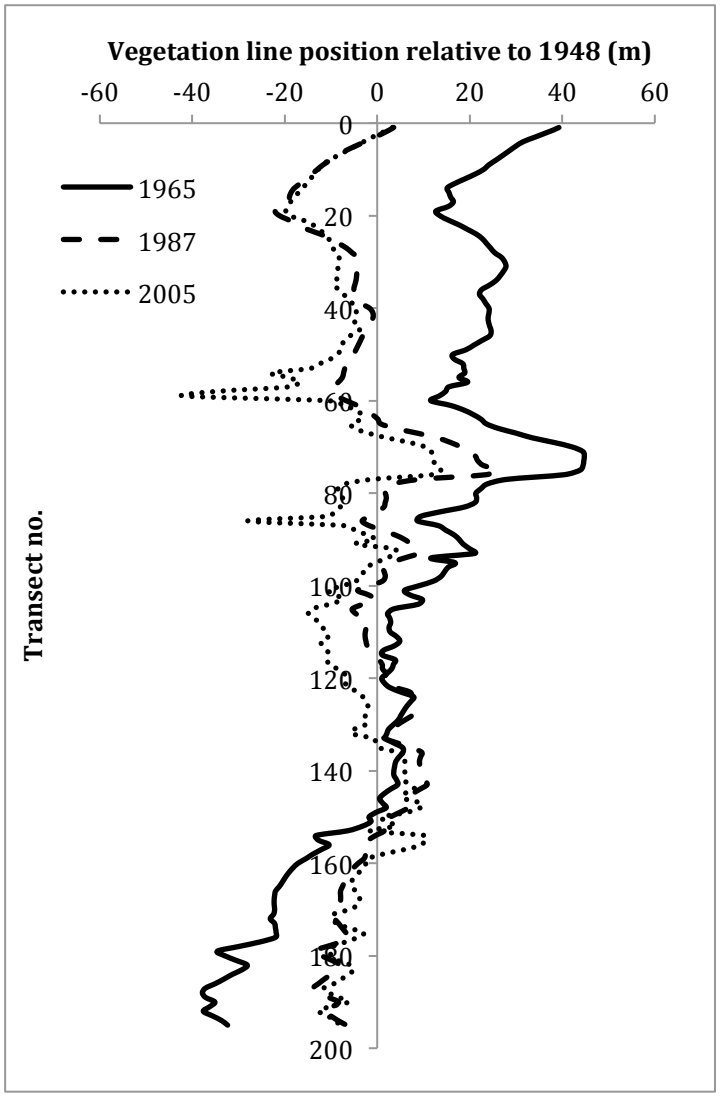

B.

Figure 6.8b. Changes in the position of the vegetation between 1948-2005 at Cille Pheadair. The 0 line represents the position of the vegetation line in 1948. Vertical axis indicates transect number (profile no. x 10 = distance (m) from northern end of site).

Temporal variations in EPR at Staoinebrig are shown in Figure 6.9a, which shows a clear trend of reducing median and maximum EPR over the period investigated; median EPR values are +1.20 m/yr (1948-1965), + 0.51 m/yr (1965-1987), and + 0.16 m/yr (1987-2005). In all periods median EPR is positive, although the results also show that during all periods some transects experienced a negative EPR. The range of EPR values is noticeably higher for the earliest period than the two later periods; this may be due to the lower accuracy of the results for some sections of the 1948 vegetation line.

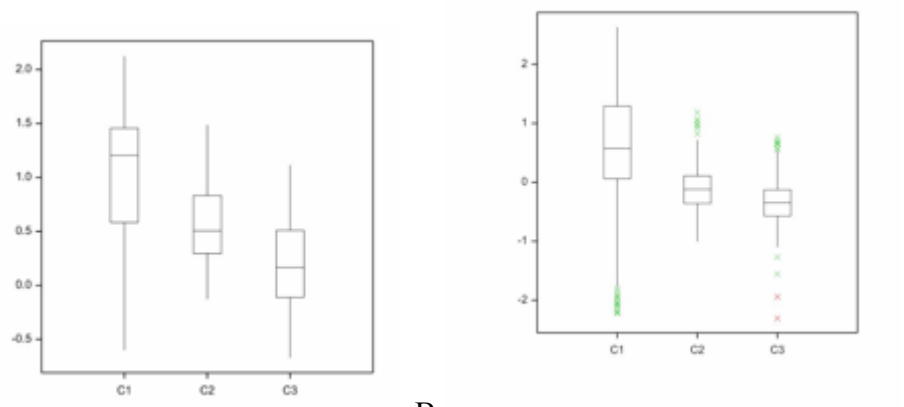

A. B.

Figure 6.9. Temporal variations in EPR. A. Staoinebrig. B. Cille Pheadair. C1 = 1948-1965; C2 = 1965-1987; C3 = 1987-2005.

As the northern and southern sections of the site have different geomorphologies (see section 3.1), a comparison of mean NSM and mean EPR are shown in Table 6.10 for the two parts of the site. These show that northern end of the site has experienced slightly lower NSM and EPR than the southern section of the site. The difference is not statistically significant.

Table 6.10. Comparison of mean NSM and EPR values for the northern and southern sections of the Staoinebrig site.

Section	Transect nos.	Mean NSM (m)	Mean EPR (m a^{-1})
north	1-37	+ 3.14	+ 0.05
south	38-98	+ 3.44	+ 0.06

6.3.3.2 Cille Pheadair

Changes in the position of the vegetation line at Cille Pheadair are shown in Figure 6.8b. The net change (1948-2005) is generally small, in comparison to changes occurring during the other time intervals studied. The majority of the site experienced a net retreat in the position of the vegetation line of < 15 m, although some parts of the site (particularly immediately to the south of the headland (transects 135-155)) show evidence for slight seaward movement of the shoreline indicator. There are two notable 'spikes' at transects 59 and 86 where exceptionally high values of retreat are recorded. Visual inspection of the photographs indicates that these may be due to blown sand

covering vegetation. The temporal pattern of change appears to be relatively similar to that described for Staoinebrig, with most parts of the site experiencing seawards movement of the vegetation line between 1948-1965, and retreat of the vegetation line in the following periods to close to the original 1948 position. However, at Cille Pheadair, there appears to have been relatively little change between 1987-2005, suggesting that the vegetation line had returned to a similar position to the 1948 line by 1987. The mean NSM between 1948-2005 is – 5.73 m. Maximum and minimum changes are + 13.76 m (transect 75) and – 41.48 m (transect 59), respectively. The mean EPR is – 0.10 m/yr, with maximum and minimum values of + 0.24 m/yr and – 0.73 m/y.

Temporal variations in EPR are summarised in Figure 6.9b. The earliest period (1948-1965) has both the highest positive EPR rate and the largest range of values. Results from 1965-1987 and 1987-2005 indicate that during both these periods EPR was generally negative. Median values and the range of values are very similar for the periods 1965-1987 and 1987-2005, although the latter has slightly lower values. Median EPR values are + 0.58 m/yr (1948-1965), - 0.12 m/yr (1965-1987), - 0.35 m/yr (1987-2005).

Due to the greater exposure to wave activity at the headland at Cille Pheadair, EPR and NSM values for this part of the site are compared to the rest of the site in Table 6.11. The NSM value for the headland is slightly more negative than the NSM value for the rest of the site, but the difference is not statistically significant. Mean EPR values are identical.

Table 6.11. Comparison of mean NSM and ESR values for the headland and the rest of the site at Cille Pheadair.

Section	Transect nos.	Mean NSM (m)	Mean EPR (m a^{-1})
Headland	75-135	- 5.93	- 0.10
Rest of the site	0-74, 136-178	- 5.64	- 0.10

6.3.3.3 Comparisons between the two sites

Cille Pheadair and Staoinebrig appear to have experienced broadly similar temporal patterns of change; both sites experienced seawards movement of the vegetation line between 1948-1965, and retreat of the shoreline indicator to close to its

original 1948 position in the following two periods. Figure 6.10 provides a direct comparison of EPR at the two sites. Both sites show similar spatial variability in EPR, with some parts of each site experiencing both positive and negative EPR values. EPR values at SB are generally higher than at CP; most of Staoinebrig is characterised by EPR values between – 0.2 and + 0.3, while most of Cille Pheadair is characterised by EPR values between – 0.4 and 0.2. This is confirmed by Figure 6.11 which shows comparisons of EPR and NSM between the two sites, indicating that Staoinebrig has higher maximum, median, and minimum EPR and NSM values than Cille Pheadair. Mean NSM and EPR values are provided in Table 6.12. The differences between EPR and NSM are both statistically significant ($p < 0.01$).

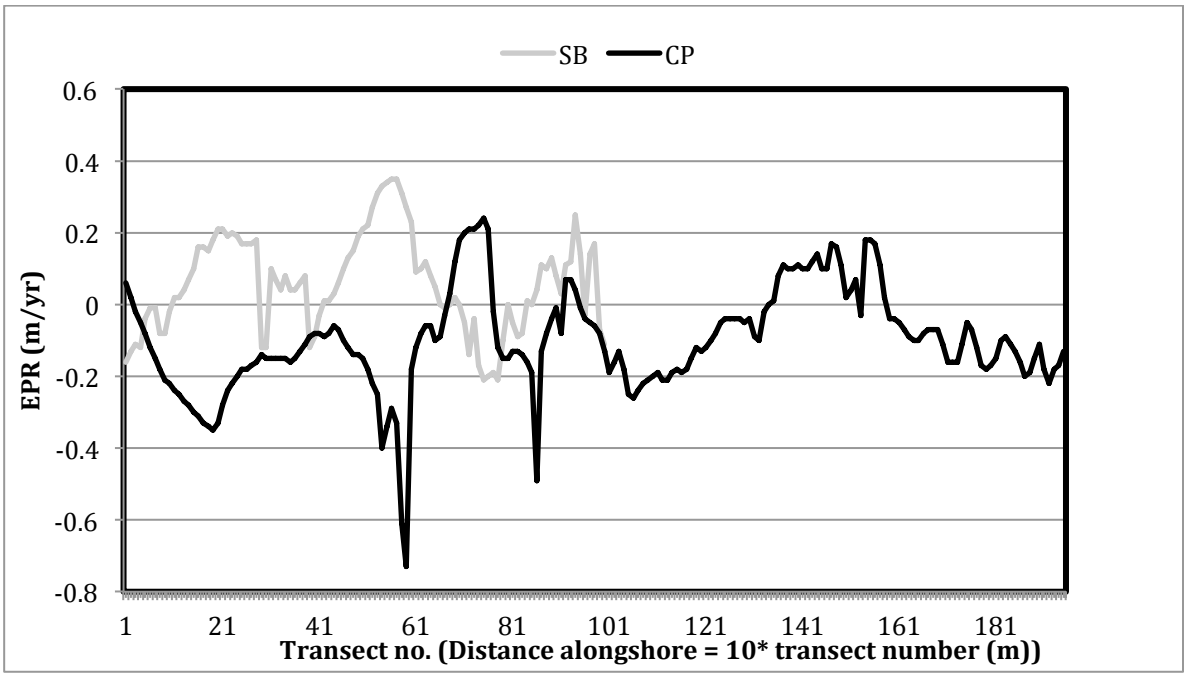

Figure 6.10. EPR (1948-2005) at Staoinebrig (SB) and Cille Pheadair (CP). Transects are numbered from the north to south for each site.

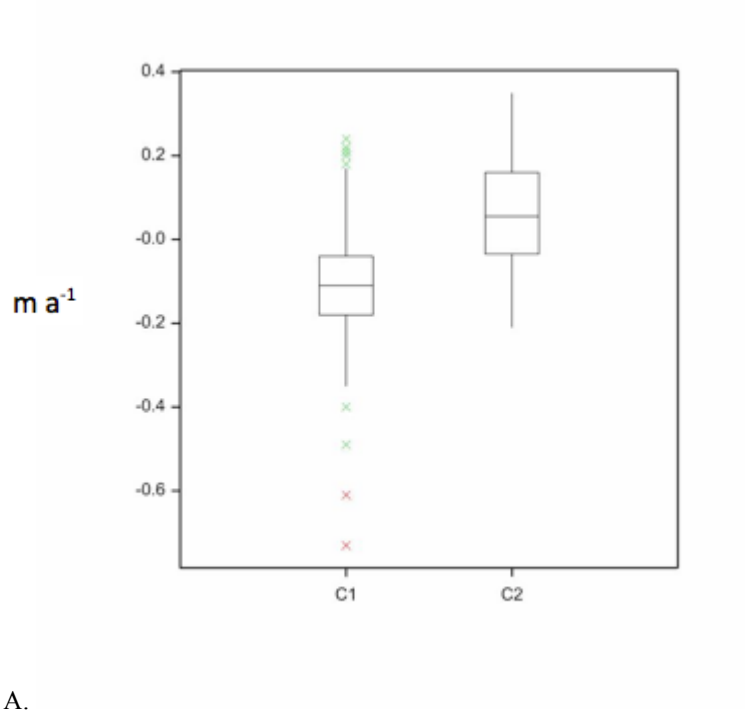

A.

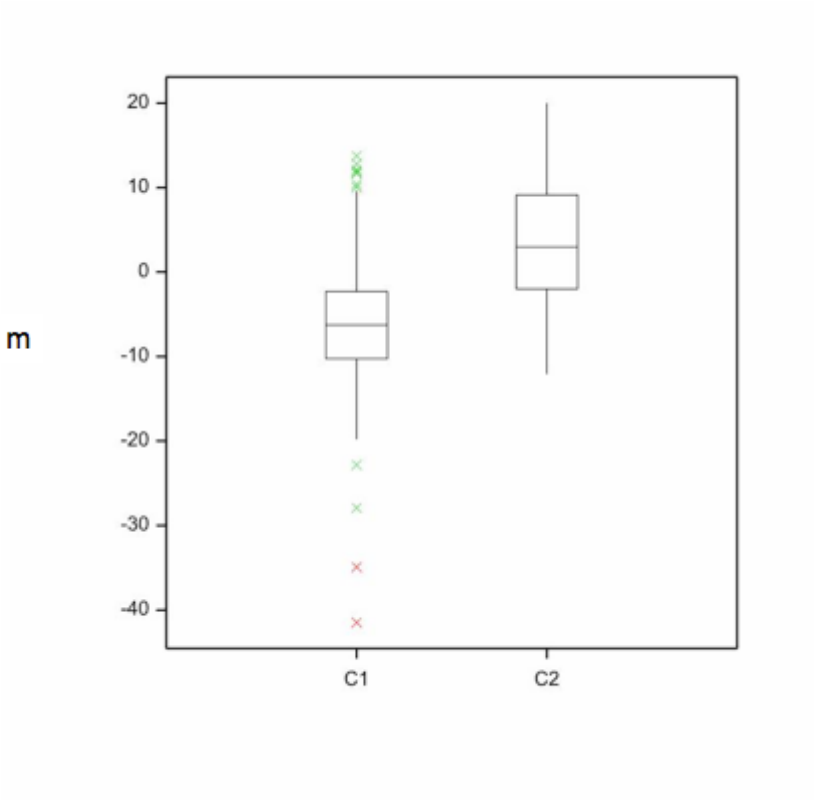

B.

Figure 6.11. Boxplot comparisons of A. EPR, and B. NSM, at Staoinebrig (C1) and Cille Pheadair (C2). Green crosses indicate outliers; red crosses indicate far outliers.

Table 6.12. Comparison of mean NSM and EPR values for the two sites.

Site	Mean EPR (m a^{-1})	Mean NSM (m)
Staoinebrig	+ 0.06	+ 3.33
Cille Pheadair	- 0.10	- 5.73

6.4 Interpretations

Chapter 6 sought to document changes in the coastline at Milton, Cille Pheadair, and Staoinebrig from the 17th Century to the present, and to quantify spatial and temporal variations in the pattern and rate of measured shoreline change, using the position of mean high water at ordinary spring tide (MHWOST) and the vegetation line as proxies for the shoreline. Additionally, along with Chapter 7 concerning short-medium term changes in the coastal zones at these sites, the data from Chapter 6 was intended to provide a means of evaluating shoreline stability over different timescales (discussed in Chapter 9). It was expected that all sites would show evidence for coastal retreat, and that rates of retreat would be higher at Staoinebrig and Cille Pheadair than at Milton. It was also anticipated that the centre of the headland at Cille Pheadair and the northern end of Staoinebrig - characterised by eroding machair front - would experience higher rates of retreat than the rest of the respective sites.

The results showed a similar pattern of shoreline change (in respect of direction and rate of change) for Staoinebrig and Cille Pheadair, while the pattern of change at Milton was different. As expected, Staoinebrig and Cille Pheadair both experienced net landwards movement of the shoreline indicators, while in contrast, Milton experienced a slight net seawards movement of the shoreline indicators. Comparison of rates of change indicated that the most recent periods considered were among the most stable. For comparisons of rates of change within sites, the results from analysis of the position of MHWOST indicate that the areas identified as sensitive to change showed higher rates of retreat, while analysis of the position of the vegetation line showed no significant differences when compared to the rest of the site. Variation between rates of change as identified by examining different time periods was high.

6.4.1 Spatial and temporal variation in coastal change and rates of change

The greater rates of retreat and net retreat measured at Cille Pheadair and Staoinebrig compared to Milton were as expected due to the site geomorphology; the higher dunes, greater fixation by vegetation, and un-grazed area immediately along the dune crest at Milton were expected to reduce sensitivity to coastal erosion. Field visits also indicated less visible signs of erosion at Milton compared to the other two sites. However, the variation in the patterns of change was not expected. For example, when considering data from historic maps, the period from 1903-1965 recorded the highest rates of retreat (most negative EPR values) for Cille Pheadair and Staoinebrig, while at Milton the EPR was most positive for this period. Similar inter-site variability in sensitivity to coastal change was found by Gomez et al. (2014), who observed high temporal variability in rates and patterns of change along the South Uist coastline from 1989-2011. For example, consideration of their results indicates that Staoinebrig was more sensitive to change from 1989-1995 compared to 1995-2011, while sensitivity to change at Milton increased over the same period. Results from both maps and photographs show that at Cille Pheadair and Staoinebrig, while the exact EPR values were different for the two sites for each time period, the relative changes from time period to time period were the same for both sites, e.g. 1878-1903 had the highest EPR values, 1903-1965 had the lowest EPR values, and 1965-2002 had intermediate EPR values with regards to the results from historic maps. In contrast, at Milton, the pattern of change in EPR was unrelated to that found at the other two sites. This indicates that the coastline at Milton is responding differently to external drivers relative to the other two sites.

The EPR's showed high temporal variability. This has implications for the interpretation of the results, similar to those discussed in section 5.4.2. For example, the net EPR at Cille Pheadair is – 0.11 m/yr from 1878-2003, but this value would be considerably altered if only data from 1903 onwards had been considered, etc.. Using only this value to indicate EPR also masks the temporal variations in EPR within this time period. It is evidently important to extend historical analysis of coastal change as far back as possible, and also to utilise as many intermediate data sets as possible, to separate longer term trends in coastal change from shorter term fluctuations.

Unfortunately, the limits to this type of analysis are set arbitrarily based on the availability of data (Brooks, 2010).

While it is often necessary to integrate different shoreline proxies for long-term analysis of coastal change due to the limited availability of data sources (Boak and Turner, 2005; Montreuil and Bullard, 2012), the results from Chapter 6 have highlighted the difficulties associated with doing so. For example, EPR values obtained using the vegetation line had a much larger range (~ -2 to + 2m/yr) than EPR values obtained using maps (~ -0.5 to +0.3 m/yr). Although this was expected due to the more dynamic nature of the vegetation line as a shoreline proxy (Montreuil and Bullard, 2012), it indicates that the rates obtained using the two proxies are not directly comparable. Additionally, the areas identified as especially sensitive to coastal change (the centre of the headland at Cille Pheadair and the northern end of Staoinebrig) showed higher EPR values than the other parts of the sites when data from historic maps are considered, but similar EPR values when data from historic photographs are considered. This is unexpected, as the vegetation line (used a shoreline proxy from historic photographs) is generally considered to be a dynamic feature (Montreuil and Bullard, 2012), and thus might have been anticipated to show higher sensitivity to change and faster rates of retreat. One possible explanation for this is that the position of MHWOST is more sensitive to change than the vegetation line for these parts of the site. The headland at Cille Pheadair might experience greater changes in beach profile than surrounding areas due to greater wave exposure, and the northern end of Staoinebrig may also be more exposed to waves than the southern end of the site, due to the presence of a rocky headland providing some protection for the southern half of the site. The lack of differences in EPR between sensitive and non-sensitive areas as identified by changes in the position of the vegetation line may be due to the fact that the vegetation along the machair coastline appears to rapidly recolonise eroded areas during the summer independent of geomorphology; even though the position of the crest may be retreating more rapidly at the more sensitive areas, vegetation recolonises eroded areas and is not always restricted to the crest line due to the lack of typical dunes at Staoinebrig and parts of Cille Pheadair. All of the photographs used were taken between April and November, periods when vegetation might be expected to be at a maximum, which may support this explanation.

Despite the differences discussed in the previous paragraph, the mean net EPR rates obtained from photographs and maps are almost identical for Cille Pheadair, and are the same order of magnitude for Staoinebrig (Table 6.13). This indicates that while the range of values obtained using the two different proxies are not directly comparable, the overall trends in terms of long term coastal change appear to be similar and may be usefully compared. Dawson et al. (2007b) found amounts of retreat varying from close to 0 to 40 m from 1984-2005 (equivalent to an EPR range of 0-2 m/yr) along the Atlantic coast of the north half of South Uist using 0 elevation contour lines derived from DTMs. Their area of study overlaps with Staoinebrig, but not the other two sites studied in this thesis. Dawson et al. (2007b) found very little change in the position of 0 elevation contour line at Staoinebrig; the findings in Chapter 6 are in agreement with this, showing EPR rates close to 0 for Staoinebrig over the most recent time periods studied. At Gualan, a highly dynamic barrier island located in the South Ford between South Uist and Benbecula, Dawson et al. (2012) measured EPRs of 0.5-1 m/yr between 1825-2005 using the position of MHWOST as a shoreline proxy. Gomez et al. (2014) found an average retreat rate of 0.3 m/yr along the coastline of South Uist, with higher localised values up to 2.5 m/yr between 1989-2011. Evidently, EPR values measured at the three sites investigated are relatively low compared to the most dynamic parts of the South Uist coastline (investigated in Dawson et al., 2007b, 2012; Gomez et al., 2014), and similar to the low rates of changes measured for the majority of the coastline (Dawson et al., 2007b; Gomez et al., 2014).

Table 6.13. EPR values obtained from photographs and maps.

Site	Net EPR (m/yr)	
	from maps	from photographs
CP	- 0.11	- 0.10
SB	- 0.06	+ 0.06
M	+ 0.07	-

The similarities in the net EPR rates (both between sites and between data sources) despite excursions of noticeably higher and lower EPR values over shorter temporal scales may be an example of the form of dynamic equilibrium observed by Cambers (1976), who proposed that a coastal system in retreat could still be classed as in equilibrium if the retreat rate was constant. The ‘dynamic’ aspect of the equilibrium

accounts for the high variability to either side of the mean rate. This is discussed further in section 9.1.4 where the results from short-medium term analysis of change are also considered.

The temporal variations in EPR values provide an indication of how dynamic the three sites are with relation to each other. The ranges for the three sites are all of the same order of magnitude (e.g. mean EPR has a range of ~ 0.1 for Staoinebrig, ~ 0.5 for Milton, and ~ 0.25 for Cille Pheadair), but indicate that the site which appears to be most resistant to coastal change is the most dynamic in terms of the position of shoreline indicators, while Staoinebrig is the least dynamic and appears to be the most sensitive to change over the short term (see Chapter 7).

6.4.2 Comparison of measured change and climate data

A comparison between measured rates of shoreline change and climatic factors is shown in Table 6.14. Comparison of climate data with MHWOST results from Milton shows that Milton experienced high retreat in the position of MHWOST during the period of greatest storminess, characterised by a positive NAO regime, switching to high progression of this feature when storminess and NAO values became transitional. More recently, rates of progression have decreased, coincident with moderate-low storminess and positive NAO regime. In contrast, the position of MHWOST at Cille Pheadair and Staoinebrig has responded differently, being stable during the period of high storminess from 1878-1903, showing retreat during the period of transitional storminess and NAO conditions from 1903-1965, and then being characterised by stable or slight retreat in the current conditions of low storminess. Evidently, the coastline at Milton is responding to external forces in a different manner to that at Cille Pheadair and Staoinebrig. Comparison of climate data and changes in the position of the vegetation line indicate that at Staoinebrig the rate of progression of this feature has decreased recently, while at Cille Pheadair the EPR of the vegetation line has shifted from slightly positive to stable to slightly negative. Over the same period, storminess has remained relatively stable, so there is no obvious climatic cause for these changes.

Table 6.14. Summary of relative EPR values and climate information. Data source of EPR value is indicated next to time period (m = map, p = photo). EPR indicators are as follows: S = stable (median EPR = -0.01-0.01), L = low (median EPR = ± 0.01-0.1), H = high (median EPR = >/< ± 0.1). Plus and minus signs indicate EPR direction. Climate summary data is obtained from Table 9.1.

Period	relative EPR			Climate Summary		
	SB	M	CP	storminess	wind direction	NAO
1878-1903(m)	S	H(-)	S	high		strongly positive
1903-1965(m)	L(-)	H(+)	H(-)	variable	NW	strongly positive → transitional → negative
1948-1965(p)	H(+)		L(+)	moderate	transitional	transitional → negative
1965-1987(p)	H(+)		S	moderate	SW	negative → positive
1965-2002(m)	S	L(+)	L(-)	moderate → low	SW	positive
1987-2005(p)	L(+)		L(-)	moderate → low	SW	positive → negative

It is evident from Table 6.14 that the period of highest storminess has been associated with retreat in the position of MHWOST at only one of the three sites investigated, and at the site with the lowest perceived sensitivity to coastal change. The results are somewhat unexpected as Cille Pheadair and Staoinebrig are perceived to be more susceptible to coastal change, and therefore would have been expected to show greater shoreline retreat in a period of elevated storminess. The lack of an obvious relationship between the shoreline proxies and changes in storminess and other climatic factors may be related to a number of factors.

With regards to the position of MHWOST, a possible explanation for the unexpected responses may be that the nature of the coastline has changed significantly at these sites over the last ~135 years. However, this seems unlikely due to the local perception that Cille Pheadair has been sensitive to coastal change for a long time (David Muir, personal communication). An alternative explanation may be related to the nature of the shoreline proxy being used. The position of MHWOST is not related to any identifiable geomorphological feature, instead being a product of the beach profile and water levels. While generally beach profiles after storms would result in the position of MHWOST moving landwards, extreme storm activity (as appears to have occurred from 1878-1910) might cause erosion and/or destabilisation and collapse of parts of the dunes and machair front and subsequent deposition of this material on the upper beach, resulting in no net movement in the position of MHWOST. The slumping and collapse of machair front onto the beach has been observed at Staoinebrig (see Chapter 7) and slumping and erosion of the dunes has been observed at Cille Pheadair (see Chapter 7). These effects have not been observed at Milton, due to storm water levels failing to reach the dunes at this site. Additionally, the unexpected results may highlight the issues associated with using historic 'snapshots' to investigate coastal change.

In the case of the vegetation line as a shoreline proxy, the variability in this feature may be influenced by a range of other factors in addition to storminess and climate. For example, changes in agricultural management, and recreational use may have caused changes in the pattern of vegetation. Additionally, there is generally a slight lag in vegetation progression following winter storms (Boak and Turner, 2005). The same is true for the position of MHWOST, which may also have been altered

artificially via *ad hoc* coastal management (e.g. re-shaping the ridge at Staoinebrig), or by sand and gravel extraction from the foreshore.

The case is further complicated by the limitations associated with the temporal availability of data (Boak and Turner, 2005; Montreuil and Bullard, 2012). For example, the results from Chapter 7 illustrate the highly mobile nature of the vegetation line along some parts of the coast – any aerial imagery represents antecedent conditions at one point in time, and is unlikely to represent an average of the shoreline position over the interval studied. The position of the shoreline as extracted from individual photographs or maps may be representative of the immediately preceding conditions, rather than climatic conditions averaged over a long period of time. A further limitation of the data sources available is that the time periods spanned between subsequent photographs and maps do not necessarily match up with time periods characterised by certain weather regimes, e.g. the interval between Ordnance Survey maps from 1903 to 1965 spans a period when the NAO regime was strongly positive, transitional, and negative. It is difficult to ascertain whether the measured changes in the position of shoreline proxies are attributable to the most recent storm or high tide event, for example, or indicative of the cumulative effects of climatic changes, or some combination of the two. This concept is also discussed further in chapter 7, where the results from analysis of short-term change are used to consider these issues.

In addition to climatic change, tidal levels from 1976-2014 indicate a rise of ~ 2 mm/yr. If this rate of change is assumed to have been similar for the previous decade, the change in the position of MHWOST between the Ordnance Survey maps from 1965 and 2002 attributable to sea-level rise can be estimated. Translation of sea-level rise to planimetric change of a datum is dependent on beach profile gradient which is highly variable at the three sites investigated in this thesis (see change in beach face DTMs in Chapter 7). Beach gradient ranges from ~ 0.04-0.1 m/m (calculated using raw data from beach surveys) for the three sites. A sea level rise of 2 mm/yr from 1965 to 2002 equates to a net rise of 74 mm, which translates to NSM of the position of MHWOST of 0.74-1.85 m over this period (EPR = 0.02-0.05 m/yr). Over this period, EPR was ~ 0 mm/yr for Staoinebrig, + 0.02 m/yr for Milton and -0.03 m/yr at Cille Pheadair. The similarity of the measured EPR at Cille Pheadair and EPR expected due to sea-level rise suggests that it is unnecessary to invoke other climatic factors to explain movement of the position of MHWOST. Comparison of results from Milton and Staoinebrig

indicates that these sites may have some resilience to coastal change – possibly in the form of a positive sediment budget as the position of MHWOST has remained stable or positive despite the expected negative effect of sea-level rise.

6.4.3 Critique

Given the difficulties inherent in using historic data to assess coastal change it is necessary to consider the results carefully in relation to potential sources of error. Improved mapping techniques and digitisation mean that more recent maps are generally more accurate than older maps. The results from Cille Pheadair and Staoinebrig show that the position of the 1878 and 1903 MHWOST positions are relatively similar, and all three sites show that the positions of MHWOST in 1965 and 2002 are also more similar to each other than either of the earlier positions. This suggests that some of the measured change may be due to changes in mapping procedures between 1903 and 1965 rather than real coastal change. However, the position of MHWOST at Milton shows considerable differences between 1878 and 1903, although it is difficult to explain why this site would have changed much more than Cille Pheadair or Staoinebrig. An alternative explanation could be that storminess has been relatively stable between 1965 and 2002, while the number of gale and storm days fluctuated significantly between 1878 and 1965. The noted similarity between the two earlier MHWOST positions and the two later positions indicates that the changes between 1903 and 1965 should be interpreted with caution.

While widely used to investigate coastal change (e.g. Dawson et al., 2007b, 2012; Milne et al., 2012; Montreuil and Bullard, 2012), the use of the position of MHWOST as a shoreline proxy has been criticised due to its dynamic nature. For example, estimated and measured errors in its use range from 4-20 m (Valentin, 1954; Shalowitz, 1964; Morton and Speed, 1998; Moore, 2000; Pye and Blott, 2006). The position of the vegetation line is also highly mobile, has a seasonal factor, and can introduce lag when progression occurs (Boak and Turner, 2005). The mobility of both the position of MHWOST and the vegetation line appear to be site specific. As these features were investigated as part of the analysis of short-medium term coastal change (see Chapter 7), the mobility of these features – and the implications of this with regards to interpreting longer term coastal change – are discussed in section 7.5.3.

When interpreting the results it is very important to consider the nature of the shoreline proxy being used. Although the similarities between net EPR rates obtained using the two proxies indicate that the position of the vegetation line and MHWOST are likely to be related to each other, there are also some differences, e.g. the greater range of EPR values obtained from aerial photographs, different patterns of change at the parts of the sites identified as sensitive to coastal change. Results obtained from the two proxies are not directly comparable. Both proxies can provide useful information about how the coastline has evolved; movement in the position of MHWOST is related to changes in the beach profile and the volume of sediment on the beach, while movement in the vegetation line is related to height above tide levels, inundation frequency, the nature of the sediment, and is generally more dynamic that other shoreline proxies (Montreuil and Bullard, 2012). Neither proxy provides a comprehensive understanding of how the coastline changes, and it is possible for the two proxies to show conflicting results.

In Chapter 6 it was estimated that the errors associated with historic maps were of the order of 4-20 m, and were expected to be nearer to the lower end of this range due to the relatively small scale, georectification, and same source of the material. Net shoreline change measured from maps ranged from 0-30 m. Errors associated with aerial photographs were expected to be between 3.8-8.8 m. Net shoreline change measured from photographs ranged from 0-40 m. The differences between many of the intervening periods investigated for both data sources were smaller than the net changes. For data obtained from historic maps many of the measurements are similar to or within the range of error values. All efforts were made to minimise error (e.g. using small scale maps, use of MHWOST rather than MLWOST). For data obtained from photographs, the difference between error values and measured values is greater; therefore the results obtained from photographs may be treated with more confidence. While photogrammetrically orthorectified images would be preferred, the simple polynomial rectification method (used due to lack of flight information which is required for full orthorectification) appears to have produced reasonable results, probably due to the relatively small areas investigated (James et al., 2012).

Apart from *ad hoc* sand and gravel extraction from the foreshore and agricultural use of the coastal grasslands, the machair coast has evolved with relatively few anthropogenic modifications over the period studied compared to other sites in the

UK which have experienced extensive coastal management in the form of seawalls and revetments, etc. This simplifies interpretation of the results to some degree as measured changes can be largely assumed to be related to gradual natural changes in sediment dynamics, climate, and sea-level as opposed to reflecting a sudden change in sediment dynamics caused by, for example, the erection of cross-shore groynes (Brooks, 2010).

6. 5 Key Findings

6.5.1 Staoinebrig

Evidence from historic maps shows that Staoinebrig has experienced a net retreat in the position of the shoreline (as indicated by the position of MHWOST) between 1878-2002. The rate of change was variable, with seawards movement of MHWOST occurring between 1878-1965, and the majority of retreat occurring between 1905-1965. The most recent period (1965-2002) studied using maps shows that the shoreline indicator has been almost stable (NSM and EPR ~ 0). The northern end of the site appears to have greater shoreline retreat than the southern end.

Evidence from historic photographs shows that Staoinebrig has a slight net seawards movement in the position of the shoreline (as indicated by the position of the vegetation line) between 1948-2005. The rate of seawards movement decreased with time, with large parts of the 2005 shoreline having returned to a position similar to the shoreline in 1948. The most recent period (1987-2005) had the lowest NSM and EPR values. The northern end of the site does not appear to have experienced significantly different changes in shoreline position from the southern end of the site.

6.5.2 Milton

Historic maps show that the position of MHWOST at Milton has a net seawards movement between 1878-2002. While shoreline retreat occurred between 1989-1905, a positive EPR was measured between 1905-2002, with higher rates from 1905-1965 than in the most recent period. Seaward movement of the shoreline indicator was greatest at the centre of the site. The net positive shoreline movement and EPR values between 1878 and 2005 suggest that this site provides an appropriate comparison to Cille

Pheadair and Stoneybridge, which have been investigated due to their perceived sensitivity to coastal erosion.

6.5.3 Cille Pheadair

At Cille Pheadair historic maps indicate that the position of MHWOST has a net retreat from 1878-2002. This is despite a slight seawards movement of the shoreline indicator from 1878-1905. High negative EPR rates were measured from 1905-1965, and the most recent period from 1965-2002 has also been characterised by negative EPR rates, although slightly lower than those measured for the preceding period. The majority of the site at Cille Pheadair has experienced significant retreat (> 10 m), although there are some relatively small areas to the north and south of the headland which have experienced either less retreat, or a slightly positive EPR rate.

6.5.4 General

Historic maps suggest that Cille Pheadair and Staoinebrig have experienced a similar shoreline change from 1878-2002, while Milton shows contrasting changes. Cille Pheadair and Staoinebrig both show net shoreline retreat, while Milton has experienced a net seawards movement in shoreline position. Cille Pheadair has experienced the highest mean retreat. For all three sites, the most recent period from 1965-2002 appears to be the most stable.

CHAPTER 7
ANALYSIS OF TRENDS AND VARIATIONS IN SHORT-MEDIUM TERM COASTAL CHANGE

Synopsis:

This chapter details the methodology and results for investigations of coastal change over short-medium timescales between November 2005 and March 2014 using RTK-dGPS surveys and an aerial LiDAR dataset.

7.1 Introduction

7.1.1 Background

Despite the acknowledged sensitivity of the machair to marine erosion (Angus and Elliot, 1992; Hansom and Angus, 2001), as discussed in Chapter 2, there is little quantitative information on rates and volumes of erosion. Furthermore, while it is expected that the machair coastline undergoes typical seasonal changes in beach profile (Angus and Rennie, 2008), it is uncertain how these changes compare to the sudden and dramatic change that occurs during storm events, or the on-going gradual retreat of the coastline due to relative sea-level rise. This is despite calls for increased research into machair coastal sediment budgets (JNCC, 1999), which are generally assumed to be negative (e.g. Crawford, 1997), and the importance of understanding sediment dynamics to inform appropriate management in the coastal zone, e.g. an understanding of the differences between short-term fluctuations and long-term trends in coastal change is essential (Srinavasan, 2006). In a broader sense, the importance of coastal monitoring, and the systematic collection of information about coastal morphology through time, are acknowledged as crucial to adequately assess coastal hazards (Baptista et al., 2008). Furthermore, the Intergovernmental Panel on Climate Change (2007) has identified monitoring changes in coastal geomorphology over multiple timescales as critical to understanding how changes in oceanic and atmospheric conditions will impact vulnerable coastal zones (Nicholls et al., 2007).

7.1.2 Aims

This chapter aims:

i) to quantitively and qualitatively describe coastal change between November 2005 and March 2014;

ii) to identify spatial and temporal variations in the measured rates of change;

iii) to provide a context for interpreting the changes associated with the January 2005 storm by comparison with changes and fluctuations occurring over tidal, seasonal, and annual timescales;

iv) and to investigate whether the three sites have been characterised by positive, negative, or balanced sediment budgets since 2005.

7.2 Methods

7.2.1 Qualitative methods

During each field visit qualitative information on the coastal zone was recorded to supplement the data-sets collected using real time kinematic differential global positioning system (RTK-dGPS) equipment. Photographs were taken to illustrate changes occurring in the coastal zone, and detailed field notes were taken at each site. These were structured to include the following information:

- atmospheric conditions during survey (wind speed, temperature, rainfall, cloud cover);
- tidal conditions during survey (timing and height of high and low tide);
- beach classification (sand, shingle, or mixed);
- land-use and management in the coastal zone.

Notes also reported on any visible changes in the coastal zone, particularly with reference to: erosion of the dunes; damage to coastal defences; exposure of solid geology on the shore-face; changes in beach sediments, or their distribution within the beach; and evidence for overtopping of coastal defences or the dunes and machair front.

Photographs and observations made during field visits are included in the results section (section 7.4) where appropriate.

7.2.2 Quantitative data sources

Two sources of elevation data were used in this study: i) direct acquisition of elevation data using RTK-dGPS, collected during the field visits listed in Table 7.1, and ii) airborne LiDAR data, obtained from SNH on behalf of the Western Isles Data Partnership, from a remote survey flown in November 2005.

7.2.3 Direct Acquisition of Elevation Data Using RTK-dGPS

RTK-dGPS equipment was used to collect elevation data due to: i) the technique's high accuracy and ability to detect short-term changes of small magnitude (e.g. Mitasova et al., 2005; Pardo-Pascual et al., 2005; Harley et al., 2011); ii) the low cost (e.g. relative to airborne LiDAR); iii) rapid, high density data collection (Harley et al., 2011) relative to lower cost techniques such as total station; and iv) the requirement for dGPS established ground control points to accurately georeference LiDAR data, aerial photographs, and historic maps to a single geodatabase for quantitative comparison between data files.

All RTK-dGPS position and elevation data were collected using a Leica GPS1200+ Series base station and rover. Points were measured manually, using the 30 s epoch rate which is compatible with the Ordnance Survey's (OS) Active GPS network. This makes it possible to process data using OS receiver independent exchange (RINEX) format data which provides greater accuracy (~ 1 cm horizontal accuracy, ~ 2-3 cm vertical accuracy) than using the RTK-dGPS base station (~ 1-5 cm horizontal accuracy, ~ 1-20 cm vertical accuracy).

7.2.3.1 Survey design

At each site, the beach surface was fully surveyed to create digital terrain models (DTMs), which would allow direct comparisons of sediment volume - and the identification of areas of erosion and accretion - to be made between RTK-dGPS surveys and with the LiDAR dataset over the time frame 2005-2014. Beach surveys were at low tide to ensure the maximum possible coverage of the beach surface. The limits of the surveyed area were the position of low tide, and the break of slope

corresponding to the base of dunes or machair front (after Baptista et al., 2008). The surveys were conducted in a series of cross-shore profiles. In general, the density of data point collection advised in Rogers et al. (2010) for the development of coastal DTMs was adopted (~ 5 m cross-shore point spacing, ≤ 50 m alongshore spacing of profiles), which produces a regular grid of data points and matches the profile spacing normally identified as appropriate for analysing short-medium term coastal change (e.g. Murray-Hicks et al., 2002; Swales, 2002; Bertoni and Sarti, 2011). However, a degree of survey bias was deliberately introduced to capture variations in surface morphology (e.g. Baptista et al., 2008). The cross-shore density of point collection was increased where topographic complexity was greater and/or changes in elevation occurred over distances < 5 m, and the along-shore spacing of profiles was also reduced to accommodate beach curvature (particularly at Cille Pheadair), and to allow for variations in alongshore topography. A relatively low point density is acceptable due to the low topographic complexity of the beach face (see section 7.3.2.1). Baptista et al. (2008) found that increasing point density beyond a threshold led to only insignificant increases in the quality of the final DTM, and unnecessarily increased field work costs. Aguilar et al. (2005) found that terrain morphology was the largest source of error in DTM generation, followed by survey point density, and then interpolation method used (see section 7.3.2). This is confirmed by Swales (2002) who established that while an increase in profile spacing did lead to reduced accuracy in beach face DTMs, the effect was relatively small; in this case, 3-6 % overestimation of beach volume when increasing alongshore profile spacing from 30 m to 125 m. Outcrops of bedrock in the inter-tidal zone were outlined but not surveyed regularly.

At each site changes in the position of a linear feature indicative of coastal change were measured. The feature surveyed varied slightly with site morphology. At Staoinebrig the crest of the machair front/vegetation line was surveyed at the north of the site, and the seaward crest of the artificial shingle ridge was surveyed at the south. At Milton the dune crest/fixed vegetation line was surveyed. At Cille Pheadair the dune crest/vegetation line was surveyed at the north of the site, and the machair front/vegetation line was surveyed at the south of the site. These features have been identified as good indicators of coastal erosion (Boak and Turner, 2005). In general, these features were readily identifiable by major breaks of slope and the presence/absence of vegetation

Ten control points were recorded on each re-survey for all sites to allow the error between RTK-dGPS surveys, and the error between RTK-dGPS surveys and the LiDAR dataset to be quantified. Control points were located in stable, readily identifiable locations, such as at the corners of fields, at road intersections, or by signs. These points also provided ground control points for geo-referencing aerial photographs used in Chapter 6.

7.2.3.2 Survey timing

Surveys were planned to capture coastal change over the following timescales:

- Tidal cycle
  - Daily surveys over two weeks covering the period from HWN-HWS.
  - One survey at HWN at the beginning of a full 29.5 day tidal cycle, and one survey at HWN at the end of the cycle.
- Seasonal
  - 4 surveys conducted in spring, summer, autumn, and winter.
- Annual
  - 3 surveys conducted in the month of March in 2012, 2013, and 2014.
- Post-storm
  - Unplanned trips to re-survey the sites following any major storm events.

Additionally, coastal change between the 2005 LiDAR survey and the RTK-dGPS data was assessed. The survey schedule is in Table 7.1, and was designed to accommodate surveys on the above-listed timescales while taking into account other considerations. These included: the use of the RTK-dGPS by other University students and staff, ensuring coincidence of low tide with daylight hours (particularly during winter months, when daylight may be < 7 hours), finding times when another student or a family member could assist for health and safety reasons, and other work commitments.

Table 7.1. Dates and aims of field surveys.

Survey	Dates	Purpose
1	22-29 October 2011	autumn survey
2	19-23 March 2012	spring survey/annual survey
3	7-21 June 2012	summer survey/tidal cycle (HWN-HWS daily)
4	16-20 January 2013	winter survey
5	25 February – 1 March 2013	tidal cycle (HWN beginning of cycle)/post-storm
6	28 March – 1 April 2013	tidal cycle (HWN end of cycle)/annual survey
7	October-November 2013	autumn survey/pre-storm season survey
8	March 2014	annual survey/post-storm season survey

7.2.4 Data processing

Raw survey data was imported to the Leica GeoOffice Complete software package, and processed using RINEX data. RINEX data was downloaded from the Ordnance Survey active GPS network RINEX data server for the three stations closest to the field sites (Benbecula: NF7855 67.172 m O.D.; Barra: NL6598 70.332 m O.D.; Tiree: NL9944 70.801 m O.D.). Data was then exported to an Excel file format for further processing.

Control point data required no further processing and was stored in Excel file format for use in error quantification (see section 7.2.5). The datasets for the beach surveys needed to be changed to a format suitable for DTM creation, and were imported to ArcMap as XY datafiles, which were then converted to point shapefiles. Data for linear features was also added to ArcGIS and converted to polyline shapefiles.

7.2.4.1 DTM generation

DTM's were generated from the beach survey data points using the kriging method of geostatistical estimation and a 1 m^2 output cell size to match the cell size of the 2005 LiDAR dataset. Kriging is a geostatistical technique which relies on the basic geographic principle that the similarity between any two points on a surface is likely to decrease with increasing distance between the points, common to all interpolation and

geostatistical methods of estimating a surface (Clark and Harper, 2008). A surface is produced by estimating the elevation at all points across the area of interest using weighted averages of the data available, with greater weighting given to data points which are closer to the point being estimated. In contrast to methods relying solely on interpolation, kriging also accounts for the geospatial arrangement of data points. Kriging was used as it has been identified as a highly accurate method of estimating beach surfaces from survey point data (e.g. Swales, 2002; Baptista et al., 2008), and is a recognised means of obtaining surfaces from survey data in geomorphology (Bell, 2012). For this work, kriging was found to produce lower errors between predicted and actual elevation values relative to other methods for producing a 3D surface from point data, e.g. natural neighbour, inverse distance weighting, etc. (see section 7.3.2).

The weighting of data points is dependent on the model fitted to the semi-variogram (Fig. 7.1). This is a chart which plots semi-variance against separation distance between points. Due to the large number of data points frequently used to construct a DTM, points are grouped to 'lags', which are ranges of separation distance. At a point separation distance of 0, the data point is compared with itself, and hence, has a semi-variance of 0, and is therefore located on the origin of the graph. As the distance between data points increases, the variation between data values also increases (unless there is no spatial dependence), until there is no relationship between data points, and the semi-variogram levels off to an approximately horizontal 'sill'. The separation distance at which the sill occurs is called the 'range', and the semi-variance at the sill is identified as the 'scale' of the semi-variogram where there is no 'nugget value' (a step up in semi-variance very close to the origin which occurs in situations where there are relatively large differences between data points separated by small distances). The range identifies the separation distance within which data points provide information about elevation at un-sampled locations. Due to the discrete number of data points, and therefore the limited number of comparisons of variance with separation distance, it is necessary to fit a model to the plotted points to estimate elevation values for unmeasured parts of the surface grid. In this work, the spherical model was used as Swales (2002) found it provided a close fit to the semi-variogram for beach surface data. This was confirmed by comparison with other commonly used models for the RTK-dGPS survey data (see section 7.3.2).

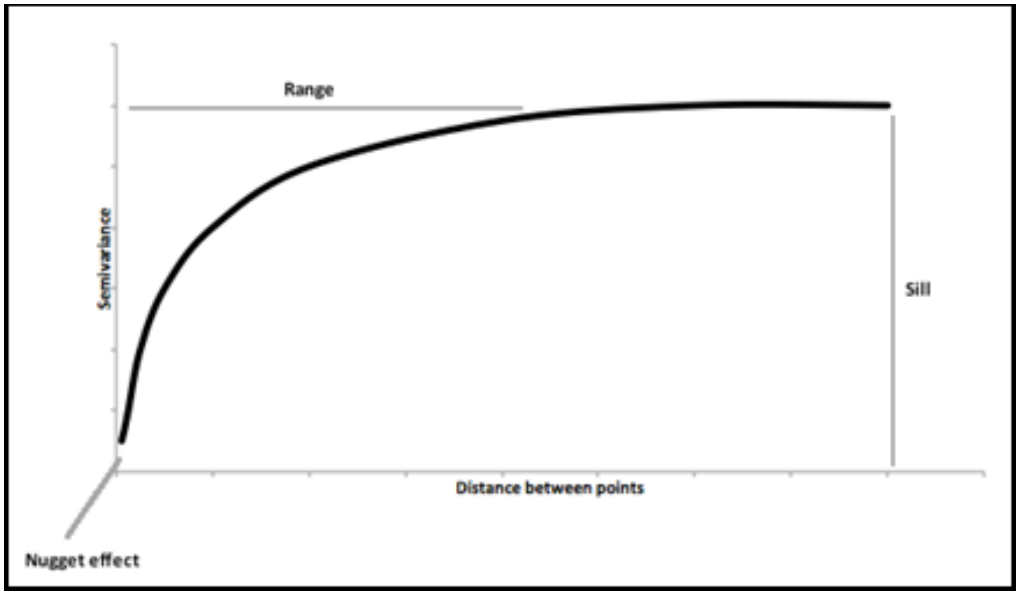

Figure 7.1. Idealised semi-variogram with key features annotated.

A further consideration in semi-variogram modelling is that on a beach surface, change in elevation is greater and occurs over shorter distances in the cross-shore direction relative to the longshore direction. This produces anisotropy in the elevation, i.e. if a directional semi-variogram is calculated for both longshore and cross-shore directions, the range and sill values are significantly different, and a higher accuracy DTM can be generated by taking this difference into consideration, which is achieved by altering the weighting of data points depending on the directional location relative to the point for which elevation is being estimated.

An additional advantage of kriging over other methods for creating DTMs is that estimates of error are automatically produced as part of the kriging process.

7.2.5 Data analysis

7.2.5.1 Planimetric change

Planimetric change in the position of linear features was characterised qualitatively and quantitatively. Qualitative analysis consisted of mapping subsequent resurveys of linear features and overlaying these on aerial imagery of the field sites to visually assess changes in the position of these features. Quantitative analysis involved

plotting landward and seaward changes between pairs of datasets at 10 m intervals along the length of the feature using the DSAS (see chapter 6).

7.2.5.2 Volumetric change

Volumetric change was calculated by creating 'DEMs of difference', (DoDs) which involves subtracting the older survey surface from the more recent survey to create a new DTM surface mapping elevation change between the two survey dates (Williams, 2012). The 'cut/fill' method (e.g. Pepe and Coutu, 2008) was applied to subsequent survey DTMs to quantify changes in beach sediment volume, which were then related to a theoretical total beach volume assuming a minimum elevation horizontal plane as the sand base to provide percentage changes in total beach volume.

7.2.6 Statistical analysis

Maximum, minimum, and mean rates of planimetric and vertical change were calculated for change over all timescales. Changes in sediment volume were expressed as percentages.

7.2.6.1 Student's T-test

The Student's T-test was used to statistically assess differences in beach survey datasets between consecutive RTK-dGPS surveys.

7.3 Error Quantification

The sources of error in this investigation can be grouped into three categories: i) errors arising through the surveying process; ii) errors arising through the DTM generation process, and iii) errors arising through the comparison between different datasets. The errors associated with these sources were quantified, combined, and used to establish a threshold value of change, below which results may be attributable to error.

7.3.1 Survey error

Maximum achievable RTK-dGPS survey accuracy using RINEX base station data for post-processing is ~ 2-3 cm vertically, and ~ 1 cm planimetrically. However, the accuracy may be decreased during the survey process by high wind speeds, low satellite coverage, and periods of high solar activity. The RTK functionality of the dGPS makes it possible to assess and record information about the quality of the position and height data recorded, and a data column is generated during post-processing that specifies the accuracy of each datum. Data with unusually low quality were rejected (Fig. 7.2). Mean data quality were calculated for each site survey (Table 7.2).

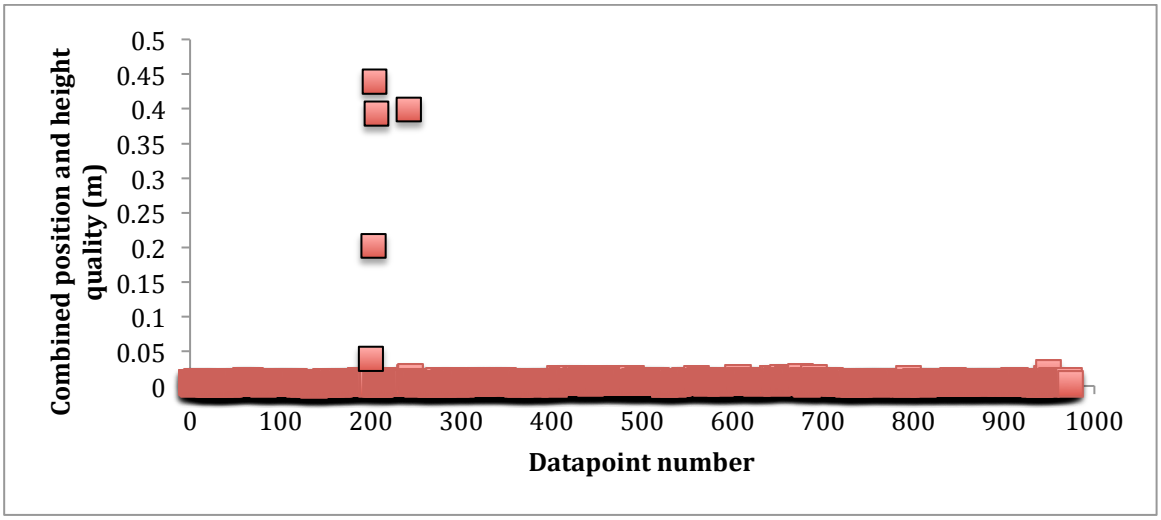

Figure 7.2. Combined position and height data quality against datum number. Outliers (outlined in black) were removed prior to DTM creation. This dataset is from the beach survey of Cille Pheadair, conducted in October 2011. N = 960.

Table 7.2. Mean data quality (combined position and height) values and standard deviations for all surveys.

Date	Site	Mean data quality (m)	Standard deviation
Oct 11	CP	0.009	0.030
	M	0.009	0.044
	SB	0.013	0.040
Mar 12	CP	0.012	0.003
	M	0.023	0.073
	SB	0.020	0.041
Jun 12	CP	0.042	0.131
	M	0.065	0.091
	SB	0.047	0.063
Jan 13	CP	0.031	0.016
	M	0.052	0.113
	SB	0.051	0.151
Feb-Mar 13	CP	0.028	0.010
	M	0.068	0.087
	SB	0.128	0.107
Mar-Apr 13	CP	0.066	0.069
	M	0.056	0.072
	SB	0.104	0.160

Table 7.2 shows that data quality was generally slightly lower than those achievable using RTK-dGPS equipment during optimum conditions. Sub-optimal performance is probably due to the exposed location of the sites, and the high wind speeds during some surveys, making it difficult to keep the rover pole vertical while taking measurements. However, accuracy is still fairly high (~ 1-7 cm). Some of the earlier surveys, particularly in October 2011, achieved centimetre-level accuracy. The slight decline in accuracy with time may have occurred as the RTK-dGPS equipment became due for servicing.

7.3.2 DTM error

Error is inevitable in DTM generation – a caveat in all studies using this approach - as creating a 3D surface from data points relies on interpolation or geostatistical methods to estimate elevation where no data are available. DTM accuracy depends on,: i) terrain morphology; ii) point density, and iii) the method used to create a DTM (Young, 2012). Aguilar et al. (2005) found terrain morphology was the largest source of error, then survey point density, and choice of interpolation method having the smallest effect on surface grid error. Terrain morphology is predetermined, but the associated error is likely to be low due to the topographic simplicity of coastal environments, particularly on the beach face. The effects of point density and the method used to generate a DTM from the data points were investigated.

7.3.2.1 Point density

The initial field surveys in October 2011 had a denser profile spacing than advised by Rogers (2010) (~ 50 m) to test the effects of decreasing point density on accuracy, and use this to inform field work plans. The dataset from Cille Pheadair was analysed as the most complex beach shape of the three sites, and therefore likely to have the highest error values. The dataset was used to test decreasing alongshore profile density on DTM accuracy by removing profile sets to produce 4 input grids with profile spacings of 10 m, 25 m, 50 m, and 100 m. To assess accuracy, 20 randomly selected points were removed from the dataset used to generate the DTM for each of the 4 profile spacings. Survey accuracy was assessed by calculating the difference between the measured values for these points and the values predicted for these points from a DTM generated via kriging from each of the 4 profile spacings. This approach is based on the RMSE method used by Baptista et al. (2008) and Bell (2012) to investigate variations in the accuracy of DTMs generated by different interpolation methods.

The results in Table 7.3 agree with the recommendation of Rogers (2010) that ~ 50 m alongshore profile spacing is sufficient to accurately capture the beach surface; 10 m, 25 m, and 50 m spacing all have similar RMS errors, and it appears a 10 m spacing does not benefit the maximum difference between actual and estimated surface elevations. Increasing alongshore profile spacing to 100 m significantly increased error,

with the maximum difference between estimated and actual values being ~ 7 times the other profile spacings. Additionally, the RMS error for this profile spacing is an order of magnitude greater than the other profile spacings. This profile spacing appeared unable to capture the shape of the headland.

Table 7.3. Mean, maximum, and minimum differences between actual data and estimated values, and root-mean-square error, for each profile spacing tested. Maximum and minimum difference values indicate maximum and minimum error, and disregard the sign of the difference.

Spacing (m)	Mean difference (m)	Max. difference (m)	Min. difference (m)	RMS error
10	-0.005	0.111	0.001	0.039
25	-0.001	0.175	0.000	0.043
50	-0.003	0.097	0.001	0.042
100	-0.003	0.762	0.160	0.430

Following this analysis, an alongshore profile spacing of 25-50 m was adopted for all future surveys to maximise productivity and accuracy. Profile spacing was increased towards 50 m on stretches of beach with little apparent topographical variation alongshore, and decreased to 25 m on beach with greater apparent alongshore variation.

7.3.2.2 Interpolation/geostatistical technique

The error introduced by interpolation of a DTM from survey data was investigated for five common methods: triangulated irregular network (TIN), inverse distance weighting (IDW), kriging, natural neighbour (NN), and spline. As with the error assessment for point density in section 7.3.2.1, and based on Baptista et al. (2008), the accuracy of each method was determined by assessing the difference between the actual and estimated values for 20 points. These points were random across the survey and were not in the data used for DTM creation. The dataset used was the same as in the effects of varying point density (Cille Pheadair, October 2011 – 7.3.2.1). Note that the kriging process automatically analyses error by systematically removing each data point and then estimating elevation based on the remaining data. However, for consistency error was manually estimated error for all five methods listed, as the non-kriging methods had no error estimation.

Table 7.4 shows the spline and IDW techniques introduce the greatest error, with maximum differences between actual and estimated values of ~ 1 m, and RMS errors of tens of centimetres. TIN and NN methods provide greater accuracy, with maximum differences between actual and estimated values in the order of 25-30 cm, and RMS errors of ~ 10 cm. Kriging provides the best estimates of surface elevations, with the maximum difference between actual and estimated values being ~ 11 cm, and a RMS error of ~ 4 cm.

Table 7.4. Mean, maximum, and minimum differences between actual data and estimated values, and root-mean-square error, for each interpolation method. Maximum and minimum difference values indicate maximum and minimum error, and disregard the sign of the difference.

Method	Mean difference (m)	Max. difference (m)	Min. difference (m)	RMS error
TIN	0.004	0.274	0.000	0.097
IDW	-0.007	0.969	0.002	0.312
kriging	-0.005	0.111	0.001	0.039
NN	-0.070	0.251	0.003	0.096
Spline	-0.097	1.168	0.000	0.319

With kriging the optimal method of DTM creation, it was necessary to determine which model best fitted the semi-variogram. As kriging provides an error summary as part of the surface creation, it was not necessary to test accuracy manually. Four commonly used models (spherical, circular, exponential, and Gaussian) were compared to the results obtaining using the default model (linear) for kriging in ArcGIS's geostatistical analyst tool. This test was also carried out on the Cille Pheadair (October 2011) dataset to determine which model best fitted the modelled data, and therefore gave the least error.

Table 7.5 shows the narrow range of RMS errors indicating the model fitted to the semi-variogram has a relatively low influence on the accuracy of the DTM surface created. As the spherical model produces the lowest RMS errors (2.3 cm), and the lowest maximum difference between actual and estimated values (5.4 cm) this model was used for the kriging.

Table 7.5. Mean, maximum, and minimum differences between actual data and estimated values, and root-mean-square error for each model. Maximum and minimum difference values indicate maximum and minimum error, and disregard the sign of the difference.

Model	Mean difference (m)	Max. difference (m)	Min. difference (m)	RMS error
spherical	-0.002	0.054	0.001	0.023
circular	0.000	0.059	0.003	0.030
exponential	-0.004	0.085	0.002	0.041
Gaussian	0.004	0.074	0.004	0.042
linear	-0.005	0.111	0.001	0.039

7.3.3 Error between surveys

Section 7.3.1 shows RTK-dGPS survey provides elevation data with very high relative accuracy (Table 7.5). However, absolute accuracy is also important for quantitative comparisons between surveys and other datasets. Errors from minor changes in the base station position should be avoided by using a fixed, continuously recording base stations via the RINEX network. However, minor errors may arise due to atmospheric conditions, solar activity, and variations in satellite configuration. Additionally, accuracy relative to control points must be established to facilitate comparisons, and quantify error, when comparing different RTK-dGPS datasets, and comparing RTK-dGPS data to other datasets.

At each site 10 ground control points were chosen at stable locations, unlikely to experience change in position or elevation, e.g. fence posts, corners of road intersections, etc. Two additional criteria helped select control points: i) that the control point had to be readily identifiable on the LiDAR dataset through comparison with georerferenced, high resolution aerial photography collected with the LiDAR dataset to allow comparisons between RTK-dGPS and LiDAR data; and ii) the controls points had to be distributed in such a way to allow comparison with, and georeferencing of historic aerial photographs, i.e. the ground control points had to be as evenly distributed across the site as possible.

Error between surveys at each site was determined by calculating the mean difference between the elevation of measured control points for each combination of

two survey datasets (RTK-dGPS and 2005 LiDAR). The largest error values obtained from this process are then used to indicate the maximum error arising between subsequent surveys (Table 7.6). The sign of the differences was disregarded to prevent positive and negative errors from cancelling. This may provide an overestimation of error in some cases as the majority of comparisons between two subsequent surveys will be associated with lower mean differences between control points. For example, the mean difference between control points measured in June 2012 and January 2013 at Staoinebrig is 0.11 m, much less than the maximum mean difference of 0.51 m. Furthermore, the maximum values reflect the lack of suitable ground control points within the machair; observation and measurement suggested some ground control points may have moved or changed elevation during the study. For example, the cemented base of a road sign was a ground control point at Staoinebrig. However, between January and February 2013 this sign was unearthed and the concrete base now rests on the ground surface, rendering this sign unsuitable for further measurements. At other GCP's large seasonal differences in vegetation height and density, and slight ground subsidence due to water-logging also appear to have affected GCP elevation.

Table 7.6. Maximum difference between the mean elevation values for all ten control points for any combination of two survey datasets.

Site	Max. mean difference between control points
SB	0.51
M	0.40
CP	0.46

7.3.4 Total elevation error

The total error for comparisons between beach surveys is a combination of the RTK-dGPS survey quality and DTM generation error for each survey in the comparison, the accuracy of the LiDAR data, – for which a conservative estimate of 0.15 m is quoted in the metadata - plus the mean difference between control points for the surveys being compared. As the uncertainty arising from the maximum differences

between control points between surveys are an order of magnitude greater than errors from survey data quality and the DTM generation process, and approximately three times the estimate of LiDAR data accuracy - the values in Table 7.6 are a reasonable, and probably conservative, estimate of the overall method error. These values are minimum change detections when interpreting DTM's of difference DoDs (Williams, 2012), an approach providing conservative estimates of error (Brasington et al., 2003; Wheaton et al., 2010; Williams, 2012).

7.3.5 Volumetric error

Uncertainty in volume calculations was quantified using the total maximum uncertainty in elevations for each site (from section 7.3.4). As the input data have an approximately normal distribution and a non-biased estimate of the surface is produced by the kriging process - i.e. the mean error is close to 0 - a sum of squares calculation quantified error (after Williams, 2012). This approach is based on the Central Limit Theory, e.g. the assumption that for some cells in the DTM an overestimation of elevation up to the maximum uncertainty in elevation will be made, while for an approximately equivalent number of cells an underestimation of elevation up to the maximum uncertainty in elevation will be made, with the result that many of the volume errors will cancel each other out and the output volume calculated will tend to converge on the mean over the full extent of the surface. Following this approach, equation 7.1 quantified volumetric uncertainty at each site.

Equation 7.1

$$\delta V = \sqrt{((\delta e)^2)\ x\ A}$$

where δV = the total volumetric DTM uncertainty in m^3; δe = the volumetric uncertainty per DTM cell in m^3; and A = the area of the DTM in m^2. δe in cubic metres is calculated per 1 m^2 cell, using the total elevation uncertainty values for each site from Table 7.6 using Equation 7.2.

Equation 7.2.

$$\delta e = U \text{ x } 1 \text{ x } 1$$

where U = the total elevation uncertainty, and is 0.51 m for Staoinebrig, 0.40 m for Milton, and 0.46 m for Cille Pheadair.

To compare two DTMs, the resulting uncertainty can be calculated using the sum of squares approach. In this case Equation 7.3 is used.

Equation 7.3.

$$\delta V_{change} = \sqrt{(\delta V)^2 + (\delta V)^2}$$

where δV_{change} = the uncertainty associated with any comparison between any two DTMs at each site.

Table 7.7 shows δV and δV_{change} for each site. This error quantification assumes the underlying errors quantified in sections 7.3.1-7.3.5 are uncorrelated and random, i.e. that probabilistic treatment of errors based on a normal distribution is appropriate.

Table 7.7. Table showing the area, δe, and δV values for each site.

Site	Area (m^2)	δe (m^3)	δV (m^3)	δV_{change} (m^3)
SB	43,930	0.51	106.89	151.17
M	105,833	0.40	130.13	184.03
CP	72,426	0.46	123.80	175.07

7.4 Results

Results are presented by site. For all sites, planimetric and volumetric changes over a tidal cycle – daily measurements, and beginning and end of the cycle – were less than the method error.

7.4.1 Staoinebrig

7.4.1.1 General summary of visual observations

Changes are summarised in Figure 7.3. The machair front extending along the northern third of the site showed evidence of on-going erosion. Here the machair front is an erosive scarp with evidence for wave undercutting. Organic rich layers exposed

by coastal retreat suggest a history of retreat. Throughout the study substantial erosion occurred during the winters, with sections of machair front (up to 30 cm x 30 cm x 100 cm) ripped up and deposited several metres inland, and sections of grass slumping and collapsing due to wave undercutting. Seaweed and shingle deposits inland from the machair front after every winter are evidence for overtopping. There was some evidence for accretion of sand along the scarped machair front during summers. Winter 2013-14 showed the most extreme visual changes, with sand and shingle deposited across the machair as far as the road; sand deposited behind the boulder wall; and evidence for water flowing across the machair (flattened grass, rivulets in the sand deposited), indicating that the machair front was over-topped.

The shingle ridge appeared very dynamic and was active throughout the study. The shingle bund was designed to be overtopped during severe storms, and the overtopping appeared to happen during all winters, leading to a flattening of the ridge top and the deposition of seaweed, shingle and sand between the ridge and the boulder wall. During winter 2012-13 and winter 2013-14 there was visual evidence for erosion of the sand bund beneath the northern end of the shingle ridge, particularly on the inland side of the ridge top. Longshore drift appeared to redistribute some of the shingle towards the northern end of the site where it was deposited along the base of the eroding machair front. There was some evidence for the formation of a transitory berm feature approximately half way from the base of the ridge. This was most defined at the southern end of the site.

Figure 7.3. Photographs from Stoneybridge., A. October, 2011. B. March 2012, C. June 2012, D. February 2013, E. March 2013, F. November 2013, G. March 2014. Photographs from the January 2013 surveys are omitted due to poor image quality caused by inclement weather. Similarly, only two photos are included from the October 2011 visit due to heavy rain.

October 2011

B. March, 2012.

C. June, 2012.

E. February, 2013

F. March, 2013

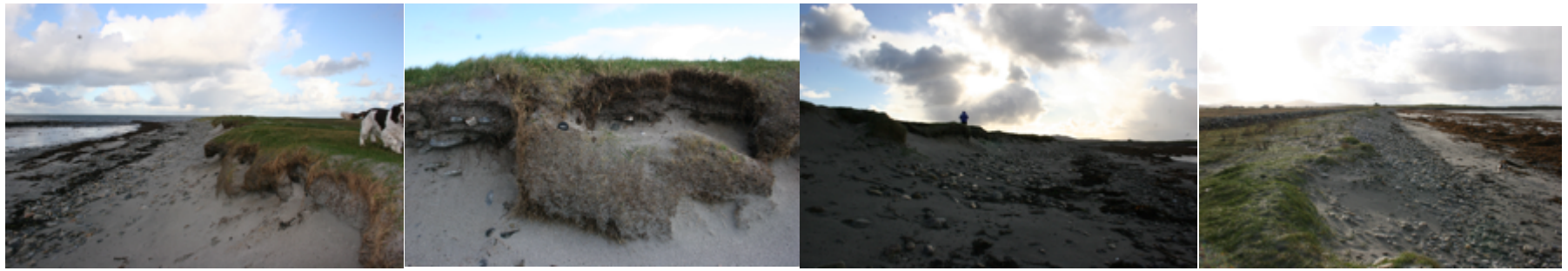

G. November, 2013

H. March, 2014.

7.4.1.2 Crest position

From 2005 to 2013 the crest at Staoinebrig retreated with the eroding machair front at the northern end, and showed a combination of retreat and progression of the ridge at the southern end (Fig. 7.4). Maximum retreat and progression are ~ 6.4 m (EPR of ~0.7 m/yr) and ~ 6 m (EPR of ~0.65 m/yr), respectively, with the mean NSM being ~ -1 m (EPR ~ -0.1 m/yr). Mean NSM along the machair front is ~ -2.4 m (EPR of ~0.25 m/yr), while mean NSM along the shingle ridge is ~ -0.3 m (EPR of ~ 0.05 m/yr). Of the 71 positions along the crest where change was measured, 18 show progression (mostly along the shingle ridge), 3 show no change, and 50 show retreat. There is considerable spatial variability, with the amount and nature of change varying along the crest line.

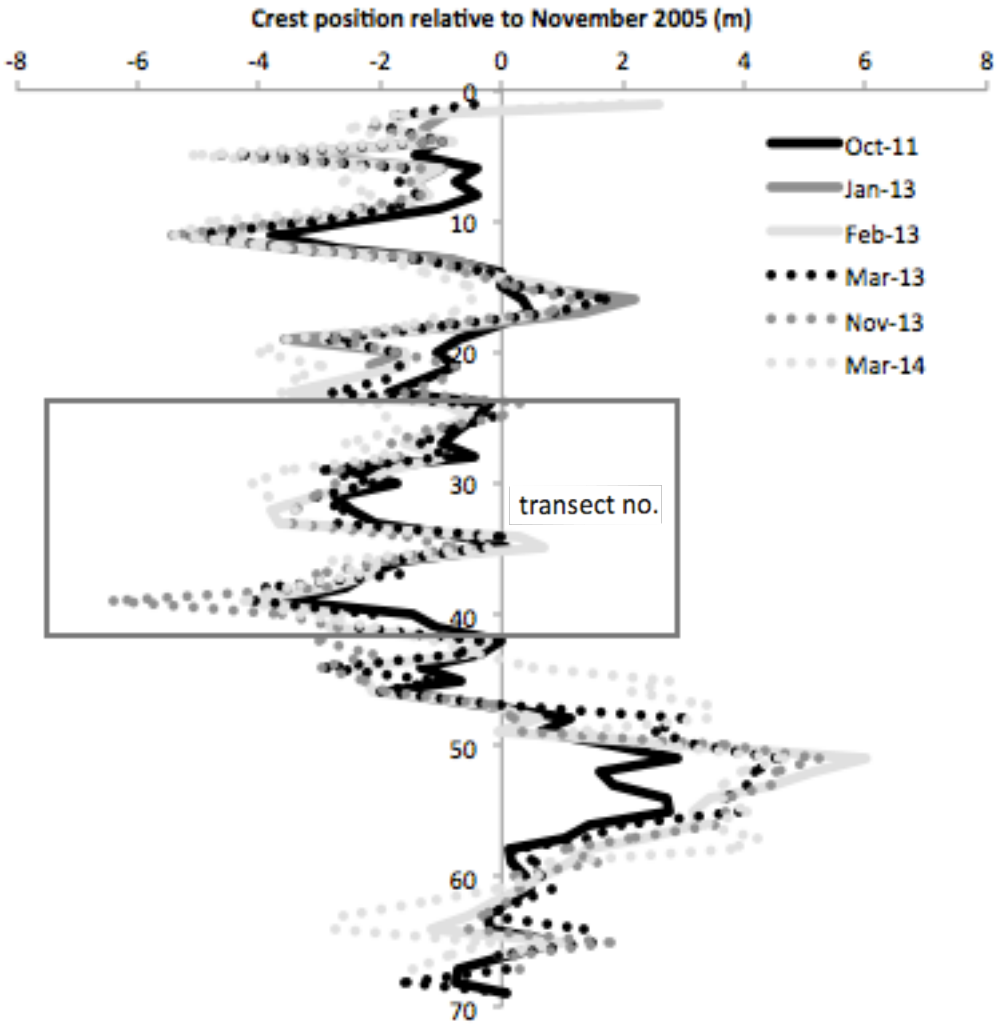

Figure 7.4. Planimetric change in the machair front and crest of the shingle ridge between 2005 and March 2014. Vertical axis indicates transect number, numbered from north-south of site (spaced at 10 m alongshore intervals). The grey box indicates likely greater error (up to ~ 2 m) due to break down of the shingle ridge.

The considerable seawards movement of the crest measured along the shingle ridge from 480-580 m should be interpreted with caution; following the January 2005 storm the shingle ridge has been anthropogenicaly modified. During initial clearance of debris the shingle ridge was bulldozed into an artificial, knife-edge shape (Richards and Phipps, 2007). LiDAR imagery and aerial photography from 2005 support this, with a narrow area of high elevation terminating abruptly, and different from the morphology of the ridge to the south (Fig. 7.5). Further alterations to the shingle ridge in 2009 and 2010, included reshaping and raising as part of coastal protection in the southern Outer Hebrides (David Muir, personal communication). Therefore changes along the shingle

ridge between November 2005 and October 2011 are a combination of anthropogenic and marine actions.

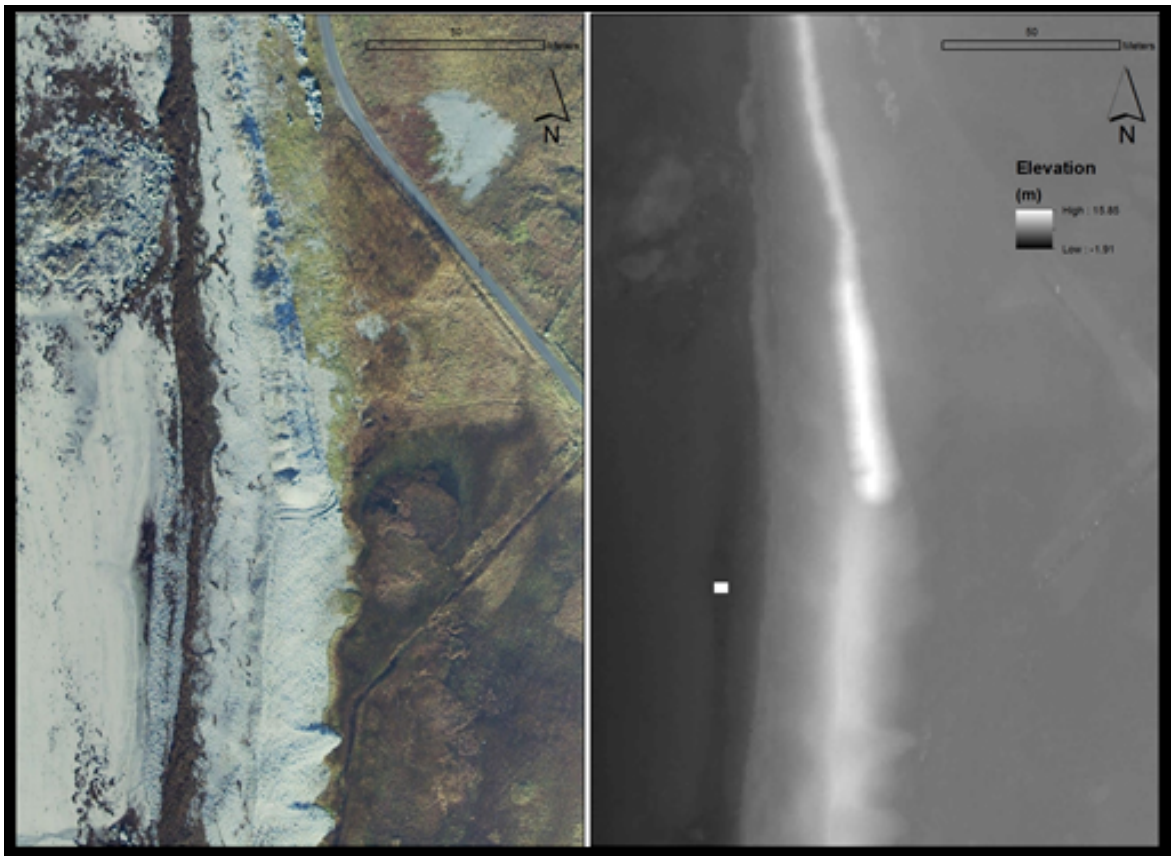

Figure 7.5. Aerial photograph (left) and LiDAR derived DTM (right) of Staoinebrig in November 2005. Area corresponds to 450 m to 630 m from the northern end in Fig 7.4. Note the area of high elevation in the centre of the lower image which terminates abruptly.

Along the northern section, characterised by the eroding machair front, changes in the position of the crest along the machair front are predominantly negative, i.e. indicating retreat. Evident from Figure 7.4 the majority of the change occurred between November 2005 and October 2011. Subsequently some of the crest experienced further progression or retreat, while other parts have been more stable.

Some changes in the crest position of the shingle ridge are larger than those along the machair front. These larger changes are probably due to changes in the shape of the crest (e.g. from a 'knife edge', to a flattened crest); the shingles making the ridge had a large diameter (~5-20 cm) and were unconsolidated such that movement of a few shingles caused a fairly large change in the crest position and hence the larger associated change. The central section (transects 25-40) became increasingly

challenging to map accurately over time as between October 2011 and March 2014 the gradual breakdown of the defined shingle ridge spread shingles north across the machair front. Accordingly, the results for this section of the site are likely to be less accurate.

In contrast to the northern section there is no pattern of retreat along the shingle ridge in the central section. Instead, it appears that the northern and southern ends of the shingle ridge experienced retreat, while the centre experienced progression. This pattern has held even after the anthropogenic modification discussed above. The net change of the ridge crest is a product of considerable fluctuation, with many measured positions exhibiting retreat at one time and progression at another.

Differences in the position of the eroding machair front and the shingle ridge crest are quantified in Table 7.8 demonstrating the machair front has experienced more and faster retreat than the shingle ridge ($p < 0.01$).

Table 7.8. Comparison of EPR and NSM for the machair front and shingle ridge.

Part of site	Transect no's.	mean EPR (m/yr)	mean NSM (m)
machair front	1-33	-0.26	-2.40
shingle ridge	34-71	-0.03	-0.31

At Staoinebrig the MHWN, and particularly MHWS, are very close to the eroding machair front/shingle ridge crest, much closer than at the other sites (Fig. 7.6). The minimum distance between MHWS and the machair front is ~ 15 m at Staoinebrig, and the minimum distance between MHWN and the machair front is ~ 50 m. Along the southern section of the site, the minimum distance between MHWS and the shingle ridge crest is ~ 15 m, and the minimum distance between MHWN and the shingle crest is ~ 30 m. Transient berms and high tide debris were seen part way up the ridge on each visit. This indicates that the base of the shingle ridge has been continually active under high tide conditions.

Figure 7.6. Aerial photograph of Staoinebrig showing the position of MHWN (seaward black line) and MHWS (landward black line). Note the proximity of MHWS to the crest, and the proximity between MHWS and MHWN in the southern section of the beach.

7.4.1.3 Beach elevation and volume change

The area of beach face over which elevation and volume changes were measured at Staoinebrig was 43,930 m^2. Net change over the study (November 2005 to March

2014) (Fig 7.7), shows the majority of the beach face has lost elevation. Table 7.8 shows the majority of elevation change is from no change to reduction in elevation of up to 1 m (mean elevation change = -0.80 m; standard deviation = 0.59). Areas of greatest reduction in elevation are largely found close to the southern and central sections of beach, surrounding the rock outcrop, and along the upper beach along the base of the ridge.

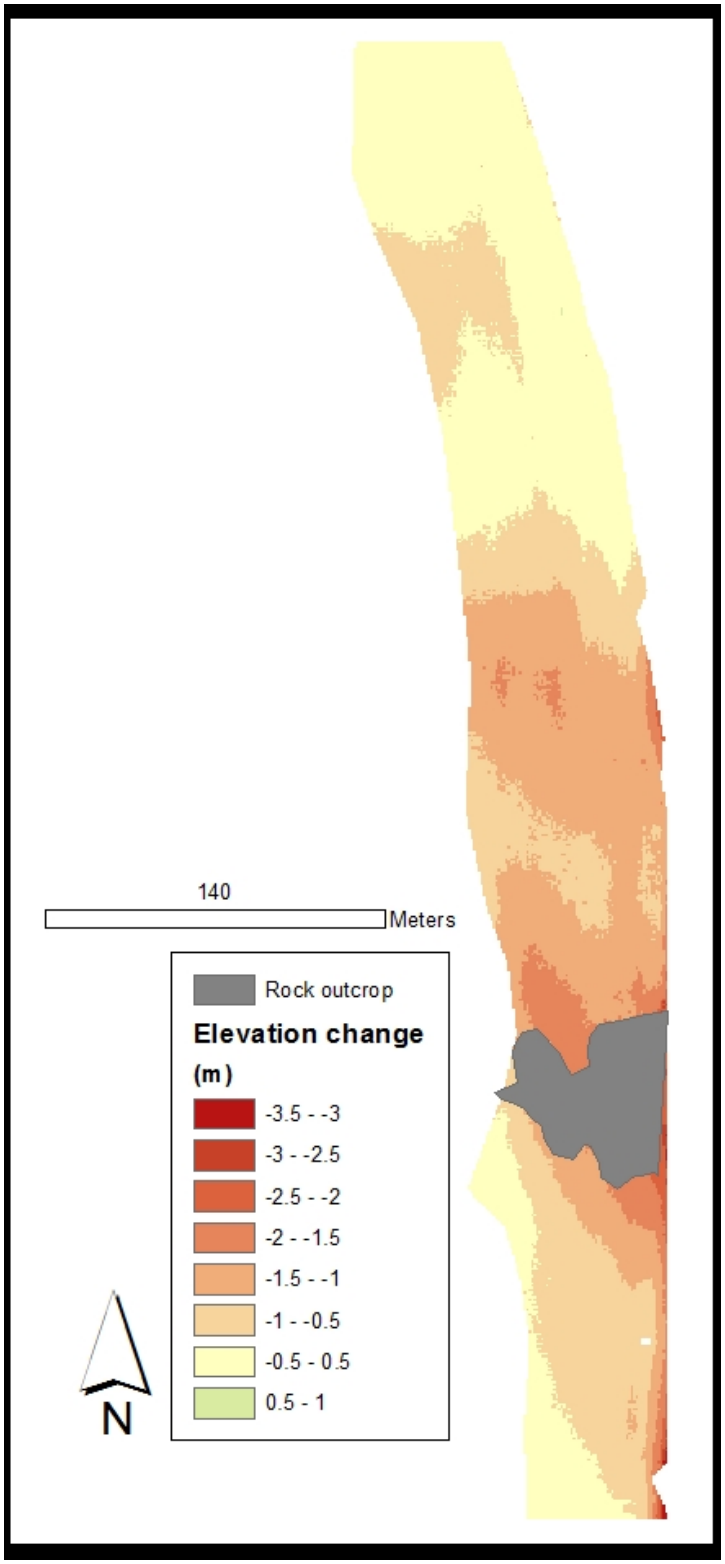

Figure 7.7. Changes in beach face elevation at Staoinebrig between November 2005 and March 2014. Green areas indicate accretion and red areas indicate erosion. The grey section indicates intertidal rock outcrop.

Changes in elevation over the beach face at Staoinebrig surveyed between November 2005 and March 2014 are shown in Figure 7.8. Elevation change between November 2005 and October 2011 is almost entirely negative. As with the net changes shown in Figure 7.7, the areas of minimal change in elevation and increases in elevation are along the upper beach. Along the section of beach north of the intertidal rocks, loss of elevation appears greatest in the middle section of the beach. The far southern section of the beach is slightly different, with a lens of accretion on the upper beach, and less loss of elevation than elsewhere along the beach. Between October 2011 and March 2012, the majority of the beach face lost elevation (possibly associated with spring tides). However the pattern of change is different, with little change in the middle beach, and more erosion along the upper beach and lower beach. The area previously characterised by high erosion at the far southern end of the beach is now characterised by accretion. From March 2012 to June 2012 most of the beach face experiences an increase in elevation, with the largest changes occurring on the upper beach. From June 2012 to January 2013 beach elevation is nearly constant, with the majority of the beach face experiencing elevation loss or gain of < 0.5 m. Accretion is along the upper beach at the north end, while erosion is along the upper beach in the central section of the site. From January 2013 to February 2013, the beach experienced little change in elevation. However unlike some periods there are some patches of high elevation change. The intertidal rock outcrop divides areas with high erosion immediately to the north on the lower and middle beach, and high accretion immediately to the south on the lower beach.

From February to March 2013 patchy areas of high erosion and accretion are distributed across much of the beach face. The areas of previous high erosion and accretion experience a reversal. Additionally there are some areas of erosion towards the northern end of the beach. From March to November 2013 most of the beach is little changed apart from some accretion up to 1 m isolated lenses of erosion in the southern section. In the final period studied between November 2013 and March 2014 the central section of the beach experienced a net loss of elevation up to 2 m, with relatively little change occurring in the northern and southern thirds. On several occasions the rock outcrop divides the beach with north of the outcrop experiencing different erosion/accretion patterns than the beach to the south (e.g. June 2012-January 2013, March 2013-November 2013, November 2013 to March 2014).

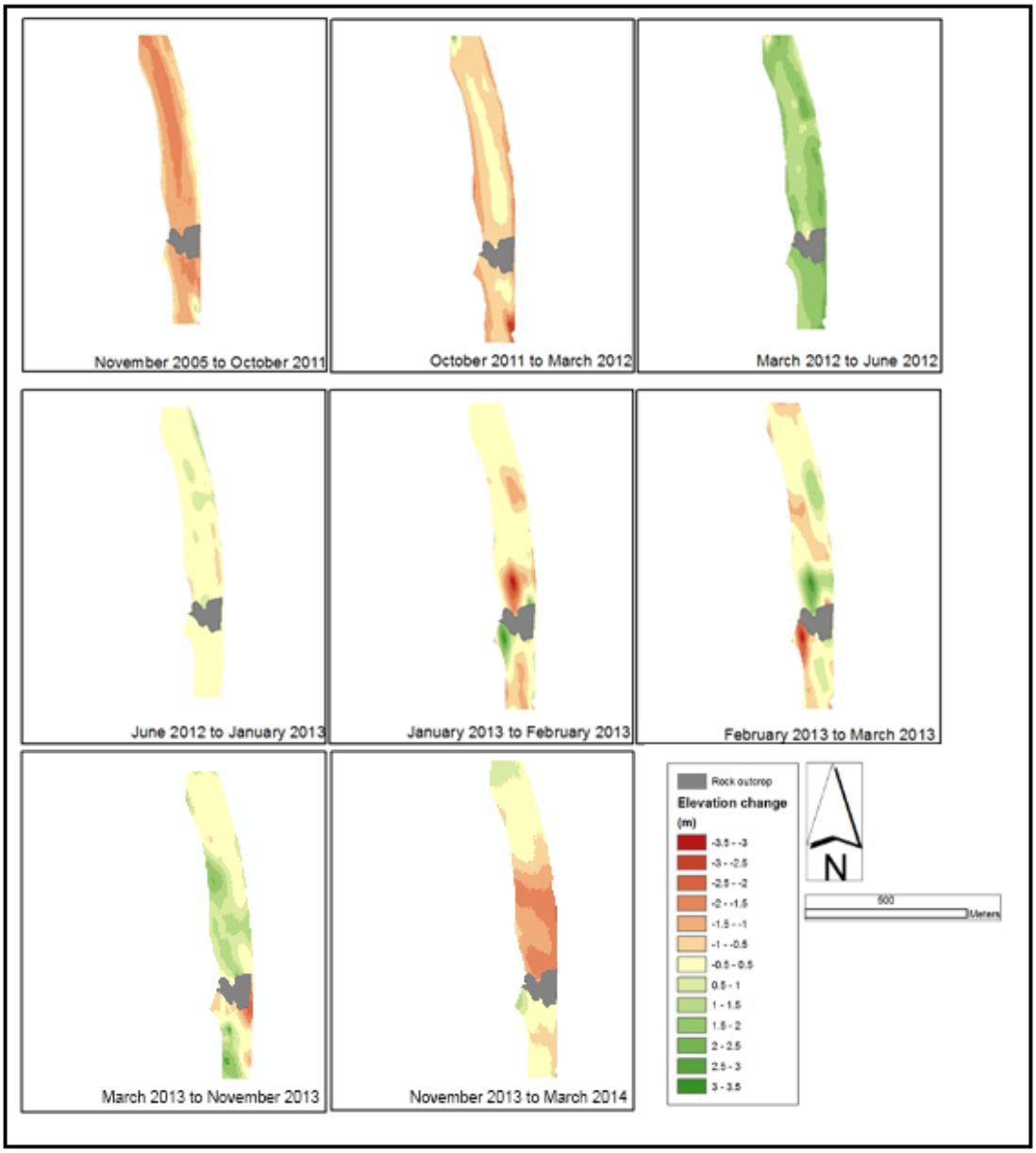

Figure 7.8. DoDs showing changes in elevation between each subsequent survey.

Changes in elevation and volume are summarised in Tables 7.9 and 7.10. The statistical significance of changes in elevation between each survey is given in Table 7.11. The largest changes in elevation appear in some of the shortest times studied – January to February 2013, and February to March 2013 – while the longest interval studied – November 2005 to October 2011 - has a comparatively low value for maximum change in elevation, and a moderate value for minimum change in elevation. The values for standard deviation all indicate that the majority of changes occurring during any time period are within ~ 1 m of the mean value for change.

Table 7.9. Numerical summary of elevation changes occurring at Staoinebrig.

Period	Max. (m)	Min. (m)	Mean (m)	St.Dev.
Nov05-Oct11	1.13	-2.57	-1.19	0.42
Oct11-Mar12	2.32	-3.13	-0.78	0.39
Mar12-Jun12	2.55	-1.23	1.54	0.35
Jun12-Jan13	1.77	-0.71	0.08	0.33
Jan13-Feb13	3.35	-3.51	-0.25	0.77
Feb13-Mar13	3.37	-3.43	0.03	0.86
Mar13-Nov13	2.58	-2.32	0.42	0.75
Nov13-Mar14	1.23	-2.19	-0.63	0.76
NET	0.56	-3.43	-0.80	0.59

Between October 2011 and March 2014 beach volume fluctuated considerably. However, the net change occurring between November 2005 and March 2014, is less than some of the volume changes occurring in intermediate times. The largest change in volume occurred from March to June 2012, when the beach face accreted ~ 68,000 m^3 of sediment. The significant loss of sediment over winter 2011-12 (loss of ~ 52,000 m^3 of sand) was not repeated in winter 2012-13 (loss of ~ 6,000 m^3,) with the erosion principally during the stormy period from the end of January 2013 to the beginning of February 2013. During the rest of the winter, a slight increase in sediment volume is indicated. During winter 2013-14 an intermediate amount of sediment was lost (~ 27,000 m^3). The highest beach volume is recorded for November 2005 (although this was almost matched in November 2013), while the lowest beach volume was recorded in March 2012. The net change is beach volume is loss of ~ 33,000 m^3 (~ 18% of the November 2005 beach volume).

Table 7.10. Numerical summary of volumetric changes at Staoinebrig. Volumes are measured relative to a planar surface set at the minimum measured elevation (-3.5 m in February 2013). Percentage change is calculated relative to previous beach volume.

Period	Volume ($m^{3)}$	Volume Change			Net Change ($m^{3)}$
		m^3	m^3/m^2	%	
November 05	182,631	n/a	n/a	n/a	0
October 11	130,543	-52,088	-1.19	-29	-52,088
March 12	96,127	-34,416	-0.78	-26	-86,504
June 12	164,149	+68,022	+1.55	+71	-18,482
January 13	166,463	+2,314	+0.05	+1	-16,168
February 13	155,753	-10,710	-0.24	-6	-26,878
March 13	158,490	+2,917	+0.07	+2	-23,961
November 13	176,471	+17,981	+0.41	+11	-5,980
March 14	149,203	-27,268	-0.61	-15	-33,248

A Student's T-test on the elevation data collected using the RTK-dGPS method during each survey shows that all changes in elevation measured are significant at the 99 % confidence level (p-values < 0.01) (Table 7.11), with one exception - the changes between February and March 2013, which are not statistically significant.

Table 7.11. Results of Student's T-test (two tailed, unequal variance) for each RTK-dGPS survey interval.

Period	p-value
oct11-mar12	1.43×10^{-31}
mar12-jun12	4.90×10^{-29}
jun12-jan13	8.08×10^{-7}
jan13-feb13	7.72×10^{-10}
feb13-mar13	0.47
mar13-nov13	8.35×10^{-3}
nov13-mar14	2.26×10^{-4}
net (oct11-mar14)	3.08×10^{4}

7.4.2 Milton

7.4.2.1 General summary of visual observations

Changes are summarised visually in Figure 7.9. Milton appeared relatively stable throughout the study with little visual evidence for change. There were no changes to the high dune ridge. Between March 2012 and June 2012 some sand accrued around the embryo dune ridge. Erosion was only noticeable following winter 2013-14 when the embryo dune ridge experienced substantial marine erosion, leaving a scarped face 1-1.5 m high along the site.

Figure 7.9. Photographs from Milton., A. October 2011, B. March 2012, C. June 2012, D. January 2013, E. February 2013, F. March 2013, G. March 2014. Due to technical problems with the RTK-dGPS there was insufficient daylight time to photograph Milton during the November 2013 field visit.

October 2011

March 2012

June 2012

January 2013

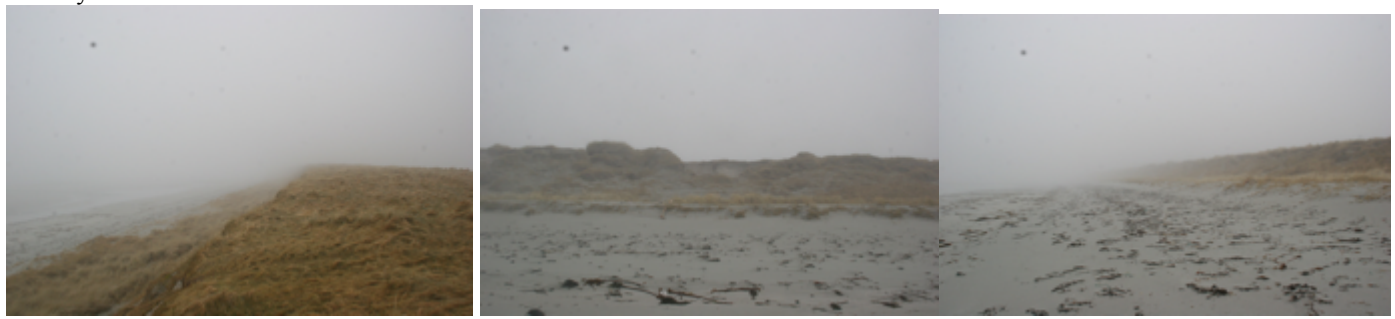

February 2013

March 2013

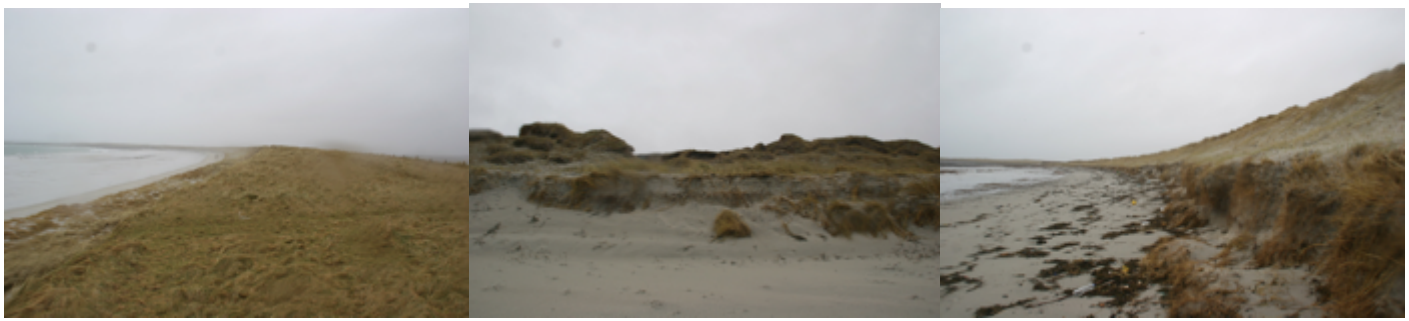

March 2014

7.4.2.2 Crest position

For most of the dune crest at Milton no change greater than the method error was measured between November 2005 and March 2014 (Fig. 7.10). However, a ~ 100 m stretch towards the southern end of the site experienced considerable crest retreat. The maximum NSM measured is -6.86 m, which equates to a maximum EPR of -0.76 m/yr. However, results from the RTK-dGPS surveys indicate minimal (within error) change in the position of the dune crest between October 2011 and March 2014, i.e. all of the change occurred between November 2005 and October 2011. This suggests that erosion may have occurred as a discrete episode rather than as an on-going, gradual change. The visual evidence for a discrete erosive episode in Fig. 7.9 shows two large blowouts towards the top of the high dunes. The blowout positions are well above normal high tide level, and erosion appears to have been initiated at the top of the dune crest as there is no evidence for wave undercutting. It is possible that erosion was initiated by vehicles using a track, shown in aerial imagery from November 2005 (Fig 7.11), along the dune crest. On the initial site visit in October 2011, parts of the track had been lost to the blowouts, and there was evidence (Fig. 7.9) for vehicle traffic creating a new track several metres inland from the previous track.

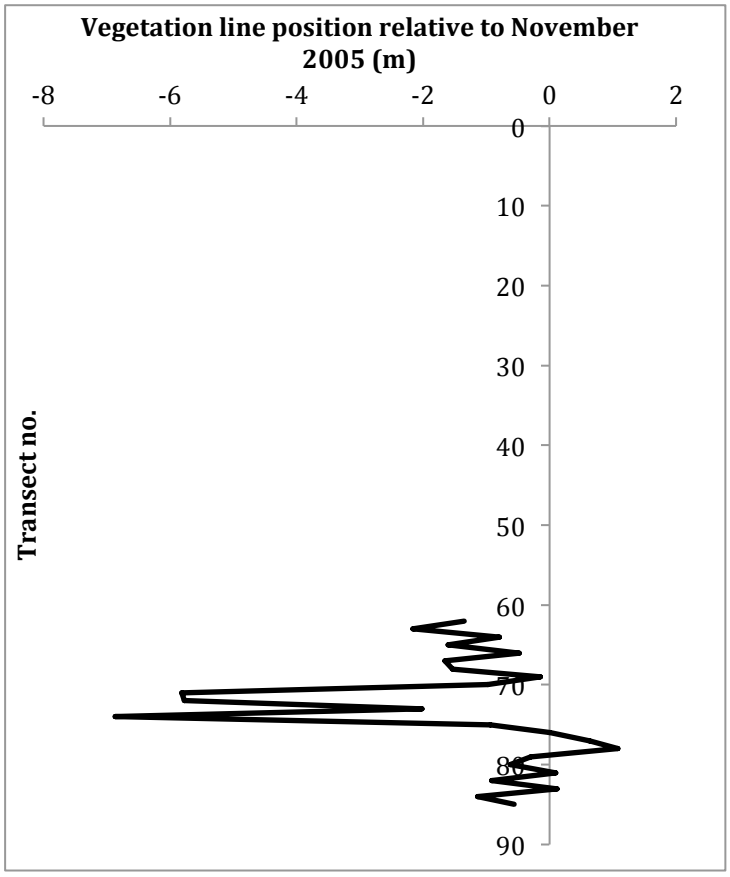

Figure 7.10 Position of the dune crest in March 2014 relative to the November 2005 position. Changes from transect 1-61 were less than the method error.

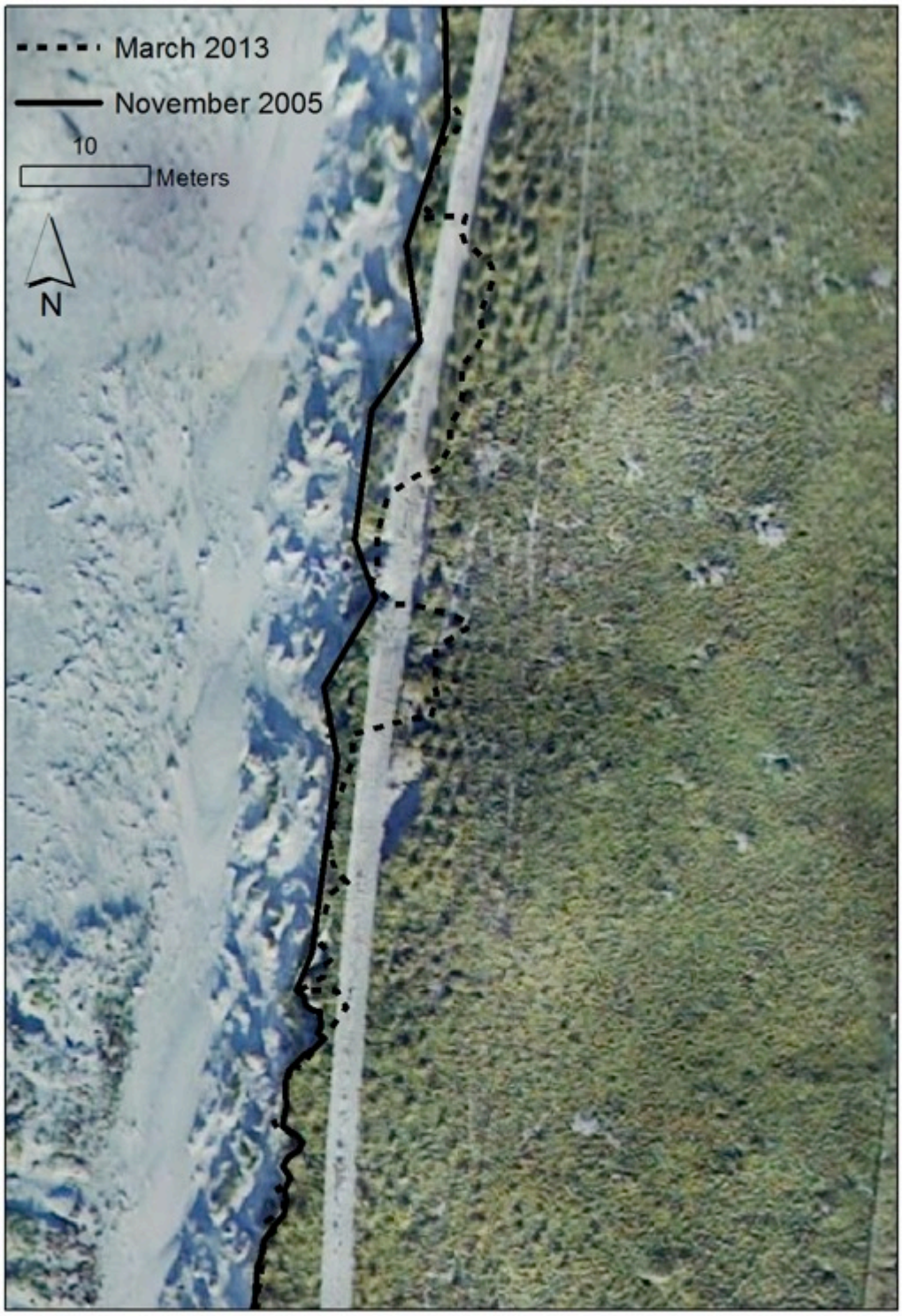

Figure 7.11. Position of the dune crest at the southern end of Milton in November 2005 and March 2013, superimposed on aerial photography of the site © SNH on behalf of the Western Isles Data Partnership.

Within method error the position of the dune crest was unchanged at Milton between October 2011 and March 2014. As expected from the initial analysis of

Milton's vulnerability to flooding in Chapter 4, there was no evidence of wave action reaching the dune crest, despite the extreme wave conditions experienced in February 2013.

Compared to Staoinebrig the distance between MHWS and MHWN and the dune crest is large (Fig. 7.12); the minimum distance between MHWS and the dune crest is ~ 45 m, and the minimum distance between MHWN and the dune crest is ~ 90 m.

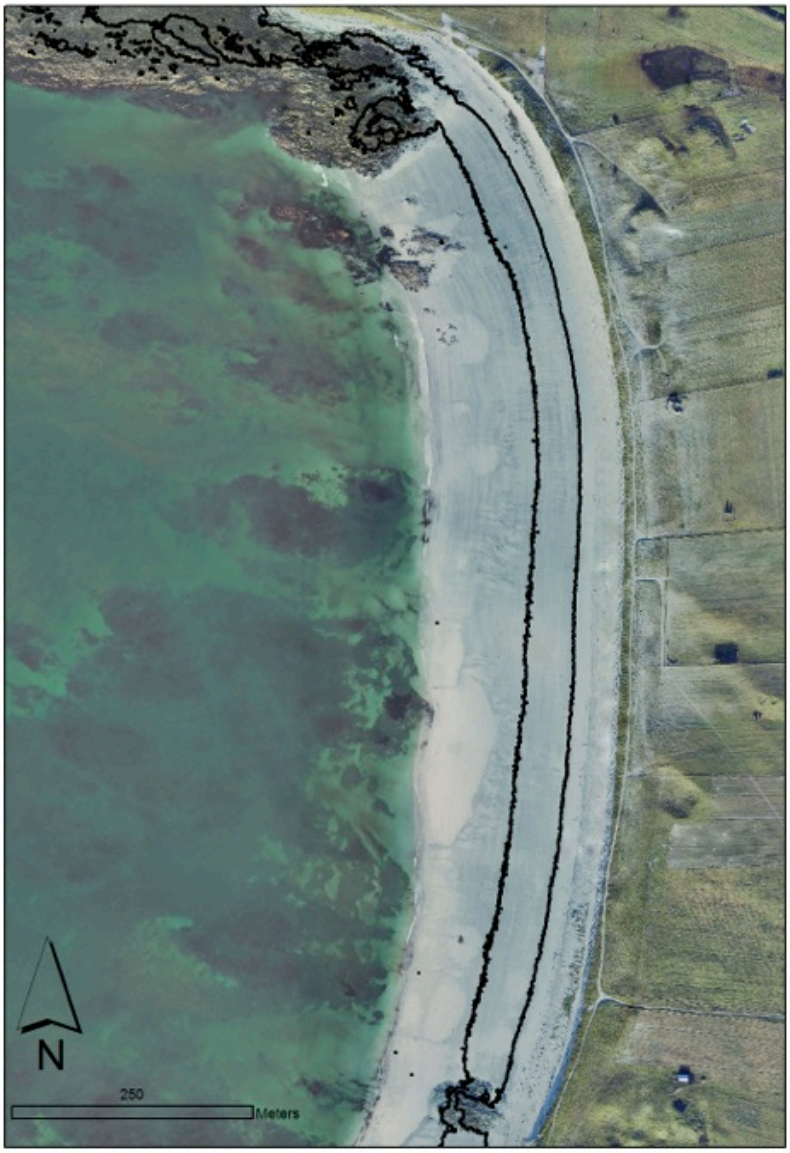

Figure 7.12. Aerial photography of Milton showing the MHWN (seaward black line) and MHWS (landward black line).

7.4.2.3 Beach elevation and volume change

The area of beach face over which elevation and volume changes were measured at Milton was 61,963 m^2. The DTM generated from the October 2011 dataset is omitted from calculations due to abnormally high error values that prevent reliable conclusions being drawn from this dataset. The errors may be due to high solar activity during the surveying period.

Net change between November 2005 and March 2014 (Figure 7.13) shows the majority of the beach face has experienced either a slight net loss of elevation or relatively small changes (between -0.5 to + 0.5 m elevation). Table 7.12 shows that, as at Staoinebrig, the majority of elevation changes are less than 1 m, whether positive or negative. The area of beach face experiencing a net increase in elevation is small, and appears restricted to the upper beach at the southern end of the site. Areas of net decrease in elevation are focused along two bands, one along the lower beach, and one in the middle of the beach. The location of these areas appears coincident with a channel and bar feature. The greatest decreases in elevation are associated with small lenses of change mostly focused along the channel feature.

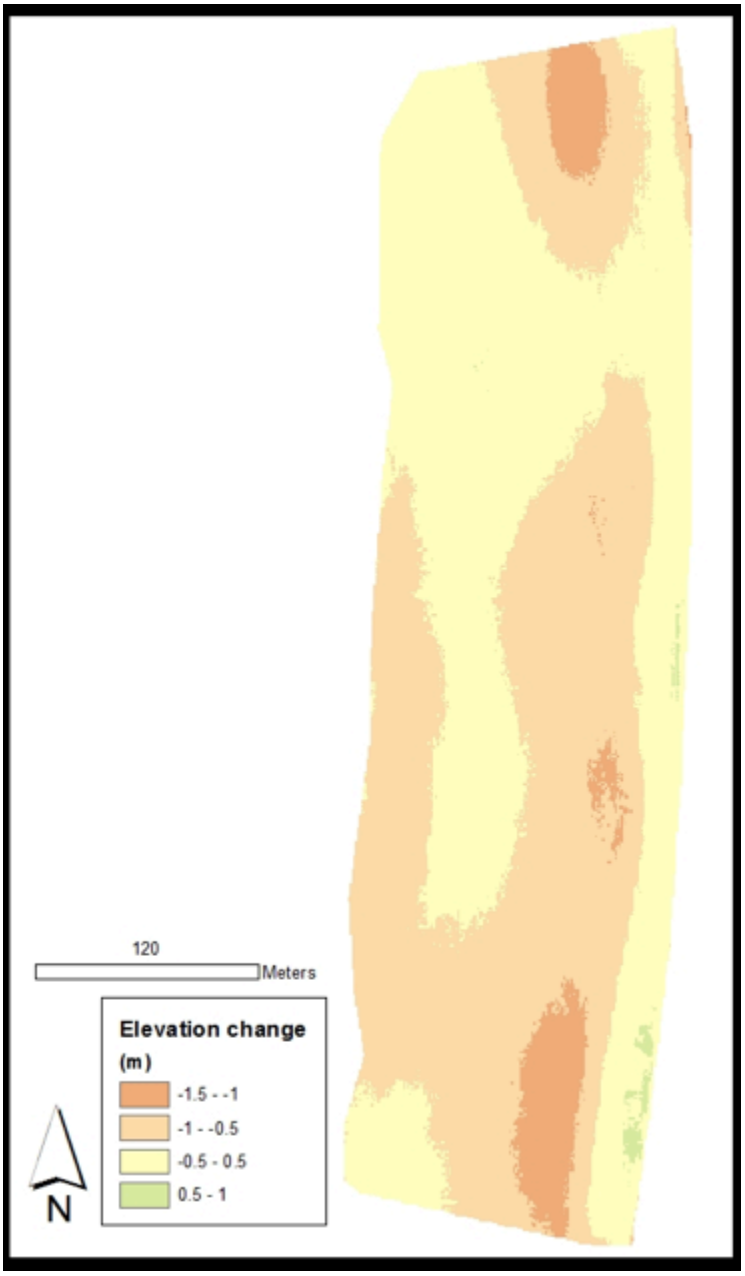

Figure 7.13. Map of changes in beach face elevation at Milton between November 2005 and March 2014. Green areas initiate accretion and red areas indicate erosion.

Figure 7.14 shows changes in elevation over the beach face at Milton in the intervening periods. In general, large areas of the beach face at Milton experience only small changes in elevation throughout much of the study, as indicated by the pale yellow shading. From November 2005 to March 2012 the main change is the development of a channel and bar feature, with the formation of the channel indicated by the linear red shaded section in the middle of the beach face indicating loss of elevation. Evidence for some accretion along the upper beach, possibly related to the

accumulation of sand seaward of the line of embryo dunes, is shown in Fig. 7.14. Between March and June 2012 the only notable change is an area of accretion on the lower and middle beach at the northern end of the section surveyed. From June 2012 to January 2013, this area experienced a loss of elevation, roughly equivalent to the previous gain with further accumulation of sand along the upper beach. As at Staoinebrig, some larger changes in elevation appear during relatively short times; between January and February 2013 a loss of elevation up to -2.5 m is focused on the lower beach, but is also along the upper beach where previously the elevation had increased. Some sand appears to be deposited in the channel feature during this period. From February to March 2013 some of the changes in the preceding interval seem reversed, e.g. with patchy loss of elevation along the channel feature, and increases in elevation in a lens on the lower beach at the northern end of the survey area, and also occurring linearly along the upper beach next to the embryo dunes. From March 2013 to November 2013, the changes again appear patchy, with the elevation of much of the beach face relatively unchanged. Areas of accretion are on the lower beach and the northern end of the site, while erosion appears confined to the middle and upper beach in southern and central parts of the beach.

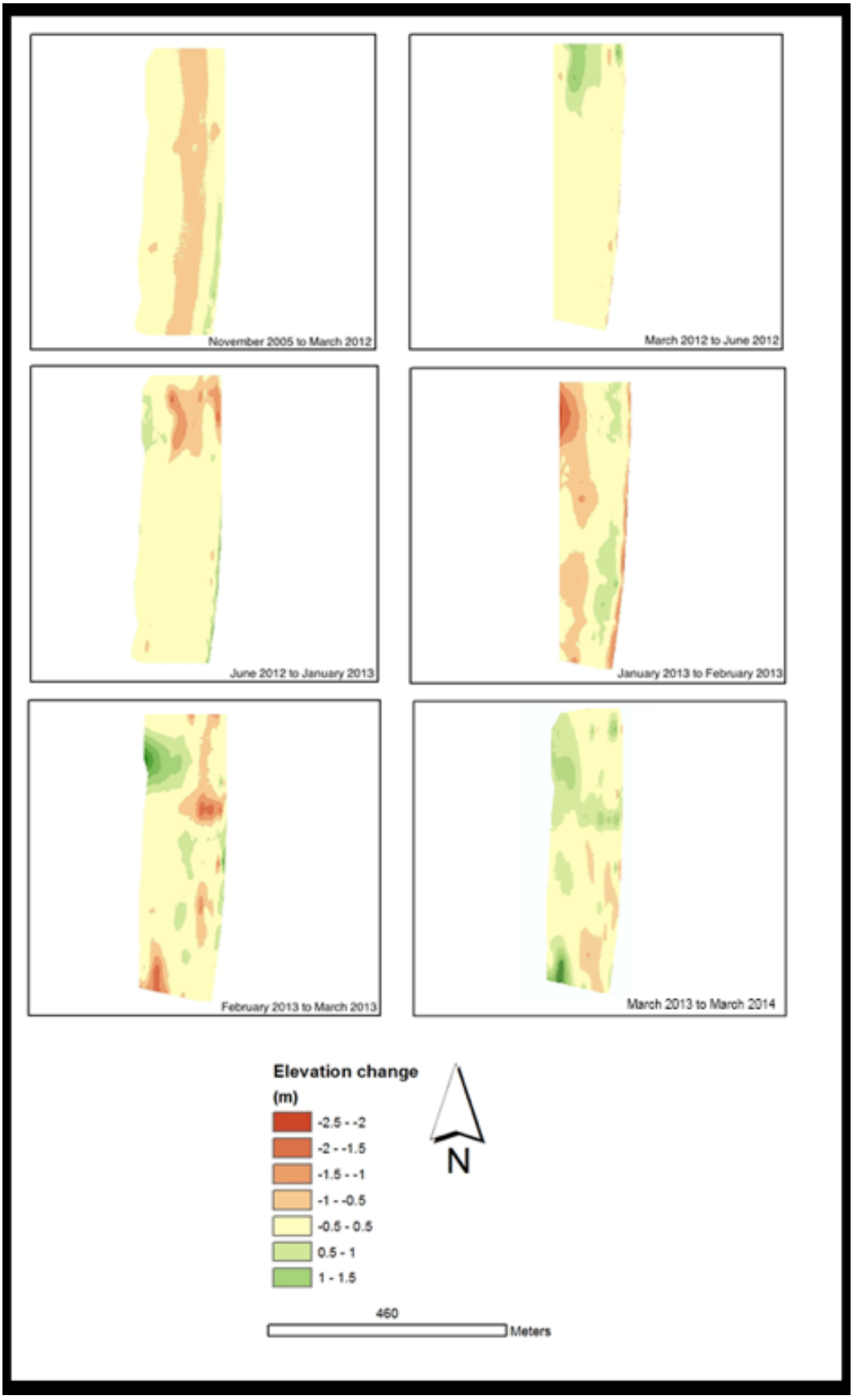

Figure 7.14 Changes in elevation between each subsequent survey.

Tables 7.12 and 7.13 are numerical summaries of changes in elevation and volume, respectively. Table 7.12 shows that during most time periods studied the average change in elevation was slightly negative. Maximum increases in elevation occurred from March 2013 to March 2014, and maximum losses from January to February 2013. The latter interval included the storms at the end of January and beginning of February 2013.

Table 7.12. Summary of elevation changes at Milton.

Period	Max. (m)	Min. (m)	Mean (m)	St.Dev.
Nov05-Mar12	0.92	-1.06	-0.38	0.27
Mar12-Jun12	0.75	-1.94	-0.11	0.35
Jun12-Jan13	1.64	-0.99	0.16	0.36
Jan13-Feb13	1.13	-2.18	-0.20	0.58
Feb13-Mar13	1.90	-1.90	-0.03	0.54
Mar13-Mar14	2.44	-2.02	0.23	0.55
NET	0.77	-1.30	-0.47	0.38

As at Staoinebrig, the amount and direction of changes in sediment volume vary significantly at Milton (Table 7.13). There is a net volume loss of ~ 5,000 m^3 of sediment above -4.83 m (only ~ 1% of the original beach volume in November 2005), indicating high overall stability in the beach face. A small loss of sediment was measured for all times apart from June 2012 to January 2013, and March 2013 to March 2014. In general the relative changes in sediment volume are much lower at Milton than the other two sites, with the maximum percentage change in volume being a loss of 7% from June 2012 to January 2013 and a gain of ~ 7 % between March 2013 and March 2014. The largest changes in beach volume occurred between March 2013 and March 2014.

Table 7.13. Summary of volumetric changes at Milton. Volumes are relative to a planar surface set at the minimum measured elevation (-4.83 m in February 2013). Percentage change is calculated relative to previous beach volume.

Period	Volume (m^3)	Volume Change			Net Change (m^3)
		m^3/m^2	%	m^3	
November 05	362,096	n/a	n/a	n/a	0
March 12	338,277	-23,819	-0.38	-7	-23,819
June 12	331,687	-6,590	+0.11	-2	-30,409
January 13	342,131	+10,444	+0.17	+3	-19,965
February 13	329,480	-12,651	-0.20	-4	-32,616
March 13	325,966	-3,514	-0.06	-1	-36,130
March 14	350,102	+24, 136	+0.39	+7	-11,994

Table 7.14 shows the statistical significance of changes in elevation between each survey interval. In contrast to Staoinebrig, half of the time periods studied at Milton show no statistically significant changes in elevation ($p < 0.01$). However, the net changes between 2012 and 2014 are statistically significant ($p < 0.01$).

Table 7.14. Results of Student's T-test (two tailed, unequal variance) for each RTK-dGPS survey interval.

Period	p-value
mar12-jun12	3.44×10^{-6}
jun12-jan13	2.45×10^{-11}
jan13-feb13	0.06
feb13-mar13	0.10
mar13-mar14	0.19
net (mar12-mar14)	1.68×10^{-3}

7.4.3 Cille Pheadair

7.4.3.1 General summary of visual observations

Changes are summarised in Figure 7.15. The northern end of the site, characterised by high dunes, experienced some retreat, which appears due to slumping and collapse of overhanging sections of grassland. In November 2013, cows used the

scarped dune crest as a ‘scratching post’, lifting and overturning sections of the overhanging turf. Furthermore, cattle and sheep were regularly seen walking on the dunes, and are likely to be the primary cause of crest retreat occurring in the dunes, as the dune crest is situated above the height of wave action. During winter 2013-14 severe erosion occurred at the base of the dunes, removing wedges of sand from the dune toe, and leaving eroded scarps 1-2 m high.

The artificial ridge maintained the planimetric position of the crest, however eroded noticeably each winter, with eroded cusps forming on the seaward side of the bund, particularly towards the northern end of the feature. The crest also appears to have been overtopped during winter 2012-13 and winter 2013-14 as the southern end of the ridge appeared eroded and pitted following these seasons, with vegetation removed. During the summer the ridge became fixed by vegetation and there was evidence for sediment accretion seaward of the ridge base. South of the artificial ridge the gently sloping machair grassland runs directly into the beach without the erosive scarp that characterised the northern end of the Staoinebrig site. This southern area shows very little geomorphological change from the initial survey. However, the vegetation line appears to be a very dynamic and an ephemeral feature, with colonisation of the upper beach during the summer months, and removal and/or die-back of vegetation during winter storms.

Figure 7.15. Photographs from Cille Pheadair., A. October 2011, B. March, 2012, C. June, 2012, D. January 2013, E. February 2013, F. March, 2013, G. November 2013, H. March 2014.

October 2011

March 2012

June 2012

January 2013

February, 2013

March 2013

November 2013

March 2014

7.4.3.2 Crest position

Planimetric change in the position of dune crest and machair front between November 2005 and March 2014 is shown in Figure 7.16. Mean NSM over this period is ~ +0.5 m (max. NSM = 5.63 m; min. NSM = -3.49 m); equivalent to an EPR of ~ +0.05 m/yr. The character of the coastline varies considerably between the northern and southern ends of the site, and is reflected in the pattern of change (Table 7.15). The northern end (0-330 m) is characterised by a high ridge; geomorphologically like a linear dune ridge. It lacks fixed dune vegetation; with vegetation absent to seaward, and low grassland extending landward from the dune crest (Fig. 7.15). Although variable, movement of the dune crest over the northern section is consistent with retreat. The retreat is greatest to the north, decreasing towards the northern end of the ridge. The mean NSM over this part of the site is -1.72 m. Changes in the central section of the site are largely attributed to the construction of an artificial shingle bund over the existing machair front. The bund was built in 2011 after the November 2005 LiDAR dataset was collected; preventing any conclusions about how this section of coast evolved between 2005 and 2011. The southern end of the site (410-680 m) is characterised by a low-lying machair front (the grassland elevation decreases gradually to the fixed vegetation line) (Fig. 7.15) which lacks the erosive scarp present at Staoinebrig. This section of the site is characterised by progression of the vegetation line at most points where change was measured, with some areas of 'no change'. The mean NSM over this section of the site is +0.93 m.

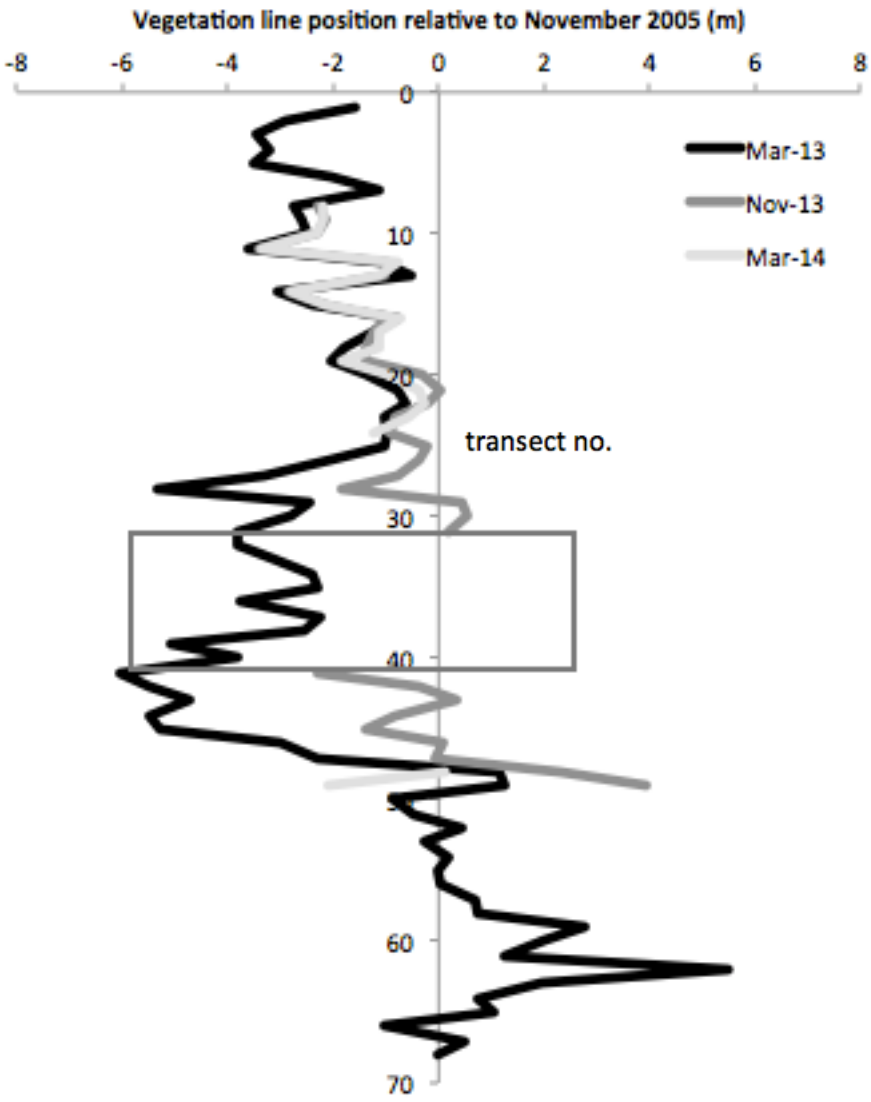

Figure 7.16. Planimetric change in the position of the vegetation line relative to the November 2005 position. The grey box indicates the position of the artificial bund.

Table 7.15. Mean NSM and EPR for the parts of Cille Pheadair located north and south of the artificial ridge.

part of site	Transect no's.	mean NSM (m)	mean EPR (m/yr)
north	1-33	-1.72	-0.20
south	41-68	+0.93	+0.10

Changes in the position of the crest along the machair front are consistently negative, i.e. indicative of retreat, although some measurements indicated a slight seawards movement (generally similar to the error tolerance for planimetric change). By far the greatest distance of retreat occurred between November 2005 and October

2011, which is also by far the longest survey interval. The majority of the other time periods studied showed no detectable change, although some measurements indicated a slightly positive NSM between October 2011 and March 2014, particularly transects immediately north of the bund. The majority of retreat between October 2011 and March 2014 periods is close to or below the threshold for error.

The artificial shingle ridge was banked up over the original machair front, and all changes indicated in Figure 7.16 occurred between November 2005 and October 2011 – the period during which the ridge was built. The ridge crest appears maintained in the 2005 planimetric position of the eroding machair front. However, the ridge profile changed noticeably between October 2011 and March 2013. Changes included sand accumulation at the base of the ridge between March 2012 and June 2012 (Figs. 7.15) and severe erosion during the storms from late January to early February 2013. As a result of these storms, the previously shallow cusps on the seaward side of the ridge (particularly at the northern end of the ridge) became pronounced.(Figs. 7.15). At the southern end of the shingle ridge there was evidence of overtopping and the removal of vegetation resulting in localised loss of crest height during both winters (Figs. 7.15).

Figure 7.16 shows that the majority of the machair front south of the shingle ridge experienced net seawards movement, with the greatest movement occurring across the centre of the section. As with the crest line north of the ridge, changes to the position of the machair front were seldom quantified (i.e. changes less than error) (Table 7.15). The most significant change occurred between November 2005 and October 2011 (seawards movement of the machair front).

Compared with Staoinebrig the distance between MHWS and MHWN and the dune crest/artificial ridge/machair front is large, particularly to the north of the headland (Fig. 7.17); the minimum distance between MHWS and the crest is ~ 40 m (at the centre of the headland), and the minimum distance between MHWN and the crest is ~ 70 m (to the north of the headland, and at the southern side of the headland).

Figure 7.17. Aerial photograph of Cille Pheadair showing the position of MHWN (seaward black line) and MHWS (landward black line). Note the proximity of MHWS to the crest at the headland, compared to the relative distance of MHWN at this point. North of the headland the position of MHWS appears to have been affected by densely packed seaweed in the intertidal zone.

7.4.3.3 Beach elevation and volume change

The area over which volume and elevation change was assessed at Cille Pheadair was 65,316 m^2. However several issues with data from Cille Pheadair

necessitated rejection of some or all of three datasets. The October 2011 survey covers only the beach south of the coastal defence ridge because large quantities of seaweed, deposited on the central and northern sections of the beach (Fig. 7.18) and which appeared to be up to ~ 1 m thick over much of the sub aerial beach face made survey impractical. In February 2013 the entire site was surveyed but results for only the beach north of the coastal defence ridge are presented. The data quality for the central and southern sections of the beach was extremely low, making meaningful conclusions impossible from this part of the dataset. The cause of this exceptionally low data quality is unknown, although high solar activity is a possibility. Furthermore, survey data from the entire March 2012 beach survey also had extremely low data quality. The data for these surveys has not been used.

Figure 7.18. The beach north of the coastal defence ridge at Cille Pheadair showing accumulated seaweed across the majority of the sub aerial beach face. In places the seaweed is sufficiently densely packed that pools of water have formed on the surface. View to the north, October 2011.

Unfortunately, the reliability of the November 2005 LiDAR dataset for the northern section of the beach is also questionable with aerial imagery showing large accumulations of seaweed (Fig. 7.19). Examination of the DTM and cross-shore profiles extracted (Fig. 7.20) suggest that the surface of the seaweed rather than the beach face may have been detected by the LiDAR.

Figure 7.19. Aerial photography of Cille Pheadair from November 2005. Note the large quantities of seaweed on the northern section of the beach.

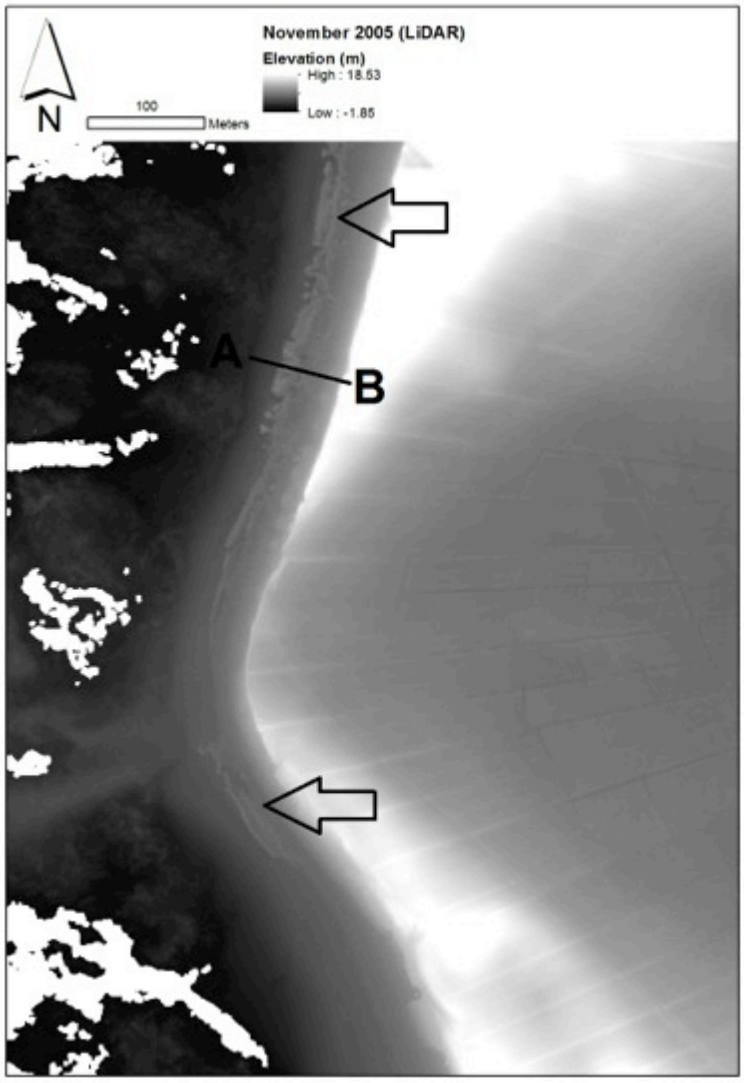

A.

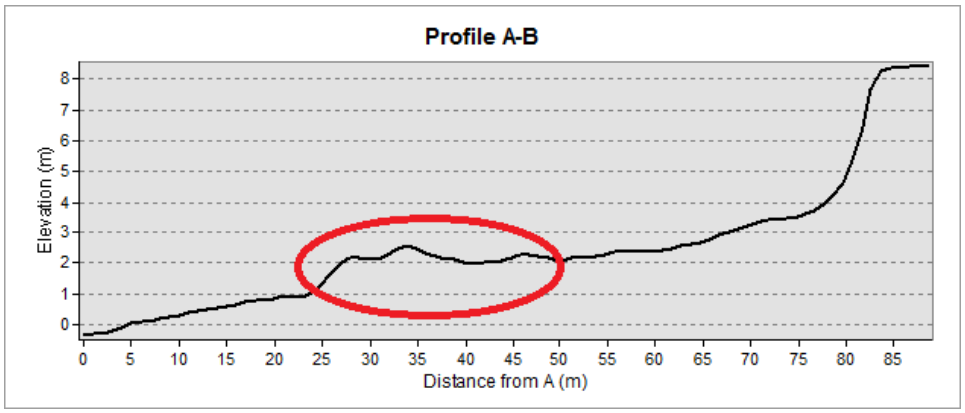

B.

Figure 7.20. a) LiDAR-derived DTM of Cille Pheadair from November 2005. Reflections apparently coinciding with the seaweed accumulations shown in Figure 5.36 are indicated by arrows. b) Cross-shore profile (location marked by line A-B on Figure 5.37a) with elevations which may be derived from reflections from seaweed circled in red.

Net change between November 2005 and March 2014 is shown in Figure 7.21, from which it is evident that the majority of the beach face has experienced either little change (-0.5 m to 0.5 m) or a slight net loss of elevation. Table 7.16 shows the majority of elevation change is between zero and 1 m loss of elevation (mean elevation change = -0.49 m; standard deviation = 0.53). Net accretion appears limited to the upper beach to the north and south of the artificial bund, while greatest erosion is on the middle beach in the northern section, and along the beach-dune margin along the southern and central sections of the site. In contrast to the northern and central sections of the site, the southern part has experienced less net elevation loss. The high spatial variability over short (1-5 m) distances (particularly visible at the northern end of the beach) compared to the other sites may be due to the effect of the densely packed seaweed which appears to have been incorporated in the LiDAR-derived DTM.

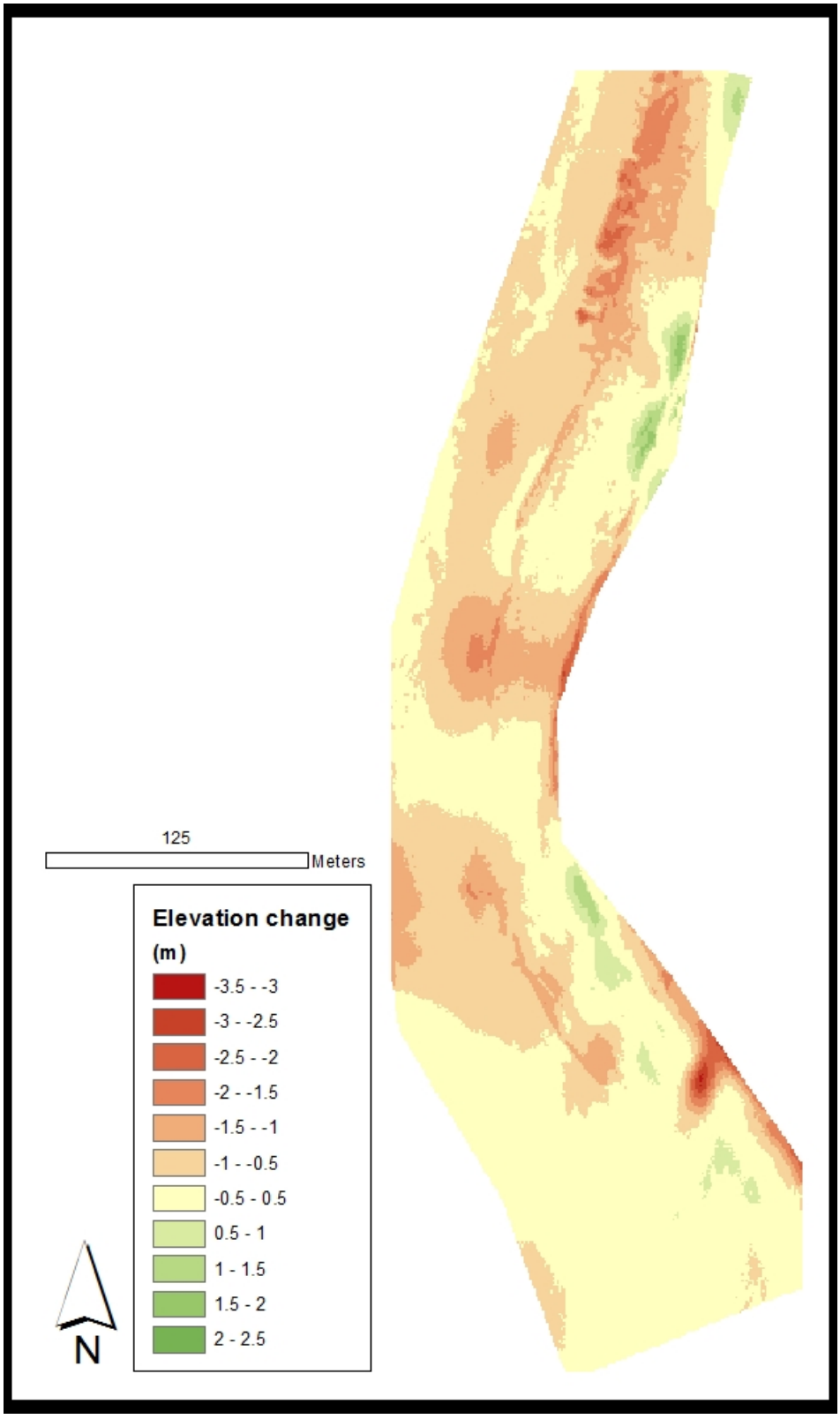

Figure 7.21. Changes in beach face elevation at Cille Pheadair between November 2005 and March 2014. Green indicates accretion and red indicates erosion.

The sequence of elevation changes over the beach face at Cille Pheadair from surveys between November 2005 and March 2013 are shown in Figure 7.22. Elevation change between November 2005 and June 2012 is generally small (plus or minus 0.5 m), although there is a band of elevation loss along the middle of the beach face, that may be associated with the formation of a channel feature, similar to that seen at Milton. There also appears to be some erosion close to the machair front along the southern section of the beach face. As at the other two sites, from June 2012 to January 2013 there is very little change in elevation. The few, small changes are along the extreme upper and lower beach, with accretion along the lower beach at the southern section of the site, and loss of elevation elsewhere. The most drastic changes occur from January to March 2013, coincident with storms in late January and early February. The changes are spatially variable, with the middle and lower beaches relatively unchanged, and the extreme upper beach gaining elevation, particularly along the central section of the beach in front of the bund. Observation suggests the elevation gain may be the deposition of shingle from the ridge across some of the upper beach. Unfortunately a significant edge effect occurs at the northern end of the site in the comparisons March to November 2013, and November 2013 to March 2014. The edge effect is due to low data quality for points taken on the northernmost transect surveyed in November 2013, and analysis of this section of the beach is unlikely to be reliable. For the rest of the beach surface, changes between March and November 2013 have a similar pattern to that from January 2013 to March 2013, with little change/erosion on the lower and middle beach and accretion on the upper beach. From March 2013 to March 2014 this pattern is reversed, with much of the beach gaining sediment (generally focused on the lower and middle beach), with erosion along much of the upper beach.

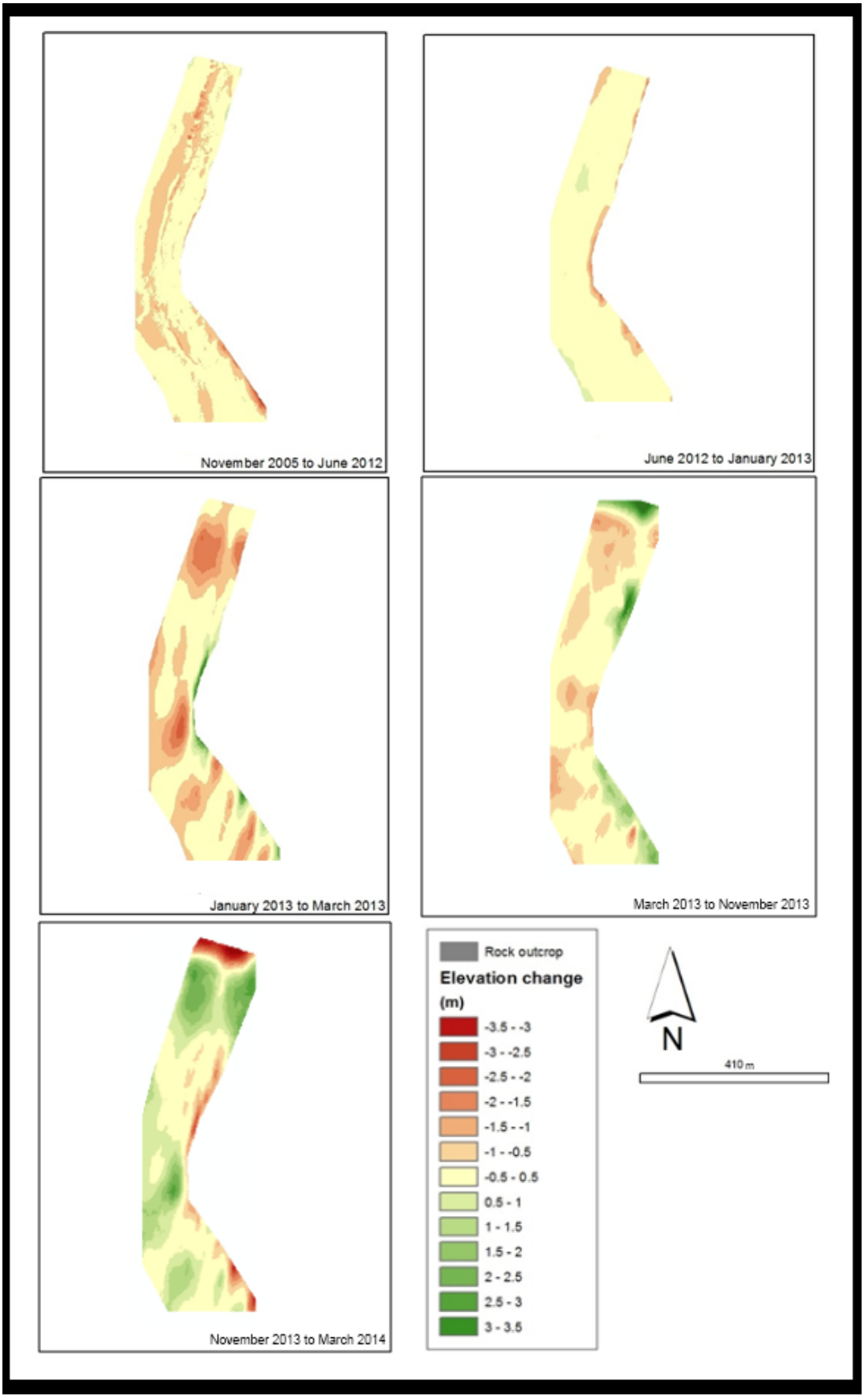

Figure 7.22. Changes in elevation between subsequent surveys.

Changes in elevation and volume are summarised in Tables 7.16 and 7.17. The statistical significance of changes in elevation between each survey is given in Table 7.18. The elevation changes between November 2005 and March 2014 are not significantly larger than those in the intervening times, and indeed, are smaller than many of the changes measured in intermediate periods. Most mean changes are negative, apart from between June 2012 and January 2013 (a period with very little elevation change, Figure 7.22), which had very close to zero change, and from March to November 2013. The greatest positive and negative changes in elevation were recorded between November 2013 and March 2014, and March 2013 and November 2013, respectively. However these values should be interpreted with caution due to a strong edge effect in the raster.

Table 7.16. Numerical summary of elevation changes occurring at Cille Pheadair.

Period	Max. (m)	Min. (m)	Mean (m)	St.Dev.
Nov05-Jun12	1.33	-3.08	-0.34	0.32
Jun12-Jan13	1.04	-1.98	6.70×10^{-2}	0.34
Jan13-Mar13	3.01	-2.33	-0.48	0.68
Mar13-Nov13	3.09	-4.05	0.42	1.06
Nov13-Mar14	4.66	-2.06	-0.08	0.87
NET	2.01	-3.12	-0.49	0.53

Compared with Staoinebrig the beach volume above the minimum elevation plane (in this case -2.18 m) changes considerably less over the intervals studied, with the maximum percentage change being < 15 %. This change is associated with the shortest time interval (2 months between January and March 2013). The overall change in volume is a net loss of ~ 32,000 m^3 (~ 13% of the original beach volume), which is greater than the net loss at Milton (~ 1%), but less than that at Staoinebrig (~ 18%).

Table 7.17. Summary of volumetric changes at Cille Pheadair. Volumes are relative to a planar surface set at the minimum measured elevation (-2.18 m in March 2013). Percentage change is relative to previous beach volume.

Period	Volume (m^3)	Volume change			Net change (m^3)
		m^3	m^3/m^2	%	
November 05	242,240	-	-	-	-
June 12	218,188	-24,052	-0.37	-10	- 24,052
January 13	221,740	+3,552	+0.05	+2	- 20,500
March 13	190,374	-31,366	-0.48	-14	- 51,866
November 13	214,685	+24,311	+0.37	+12	- 27,555
March 14	210,207	-4,478	-0.07	-2	- 31,933

A Student's T-test on the elevation data collected using the RTK-dGPS during each survey show that 60% changes in elevation are significant ($p < 0.01$).

Table 7.18. Results of Student's T-test (two tailed, unequal variance) for each RTK-dGPS survey interval.

Period	p-value
Jun12-Jan13	4.24×10^{-14}
Jan13-Mar13	2.02×10^{-17}
Mar13-Nov13	0.08
Nov13-Mar14	4.69×10^{12}
net (Jun12-Mar14)	0.08

7.4.4 Inter-site comparisons of change

Comparisons of change in the position of linear features, elevation, and volume for each site over the study period are shown in Figures 7.23 to 7.28.

Boxplots of EPR and NSM from the three sites are shown in Figure 7.23. These indicate that stability decreases in the order: Milton > Cille Pheadair > Staoinebrig (as indicated by the range of EPR and NSM). Median EPR and NSM values are negative for all sites, with Staoinebrig being most strongly negative. However, a Student's T-test shows no statistically significant difference for either NSM or EPR between Milton and other sites, and the difference between Cille Pheadair and Staoinebrig is only significant at the $p < 0.1$ level.

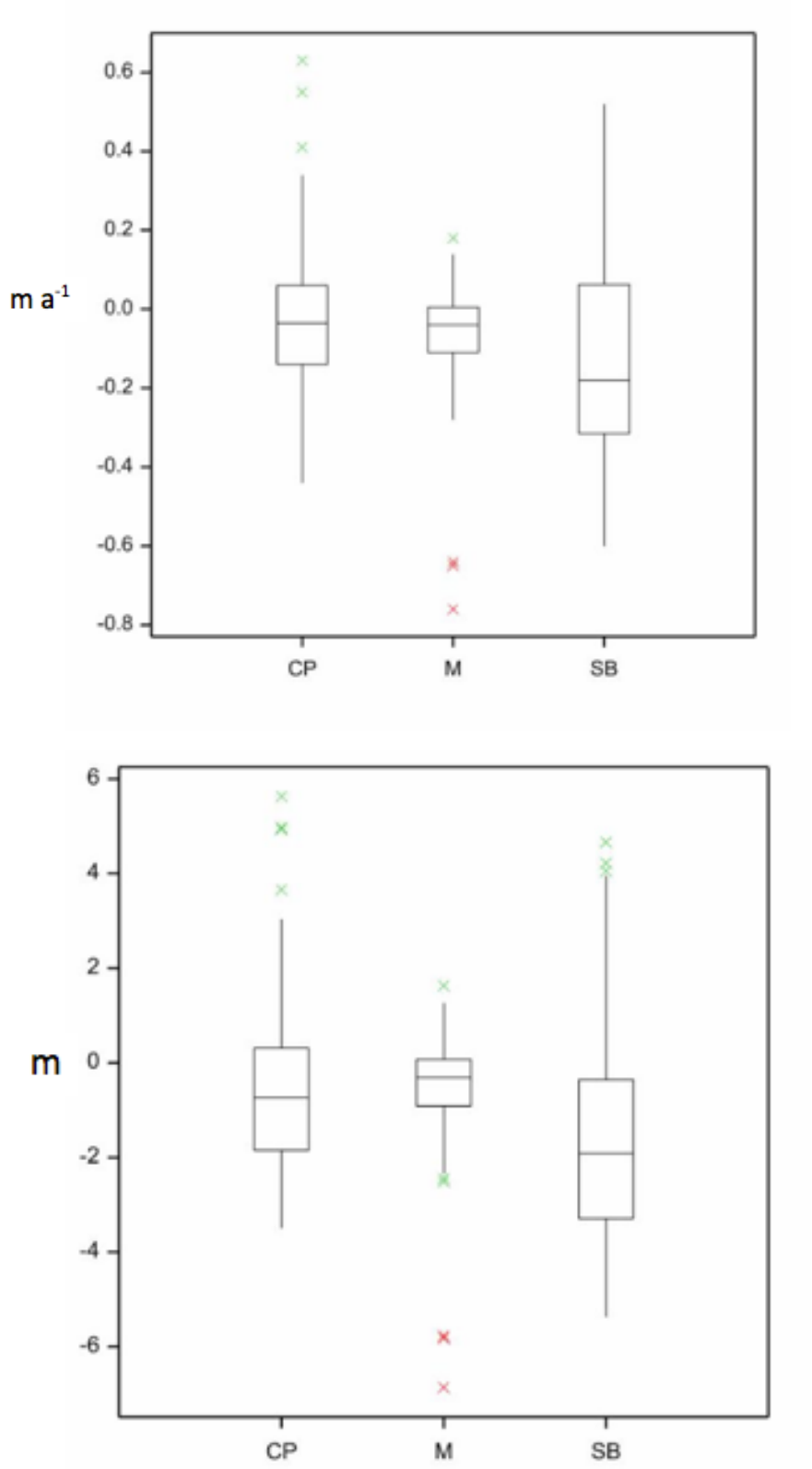

Figure 7.23. Boxplots comparing A) EPR, and B) NSM, between the three sites (November 2005-March 2014). Green crosses indicate outliers; red crosses indicate far outliers.

Changes in volume are summarised in Figure 7.24-27 and show high inter-site variability in the relative changes in sediment volume. Figure 7.24 indicates that Staoinebrig has larger fluctuations in beach volume than the other sites. There is a slight negative trend in beach volume at all three sites between 2005 and 2014, and within this evidence that all beaches gain volume during summer(March to October), and lose volume over winter. However, fluctuations in beach volume during interim periods are sometimes larger than the net volume change (particularly at Staoinebrig). As would be expected, the amount of volume change positively correlates with time interval of the survey. For example, monthly and post-storm changes measured between January and March 2013 are relatively small compared to changes measured over long time periods, particularly for Staoinebrig and Milton. However, there are exceptions, e.g. changes from June 2012 to January 2013 are amongst the smallest measured despite this being one of the longer time periods surveyed (8 months inclusive). Half of the volume changes measured at Staoinebrig were larger than the net volume changes, and at Milton almost all of the interim volume changes were larger than the relatively small net volume change (Fig. 7.27). In contrast, at Cille Pheadair, all interim volume changes were smaller than the net volume change (Fig. 7.27.

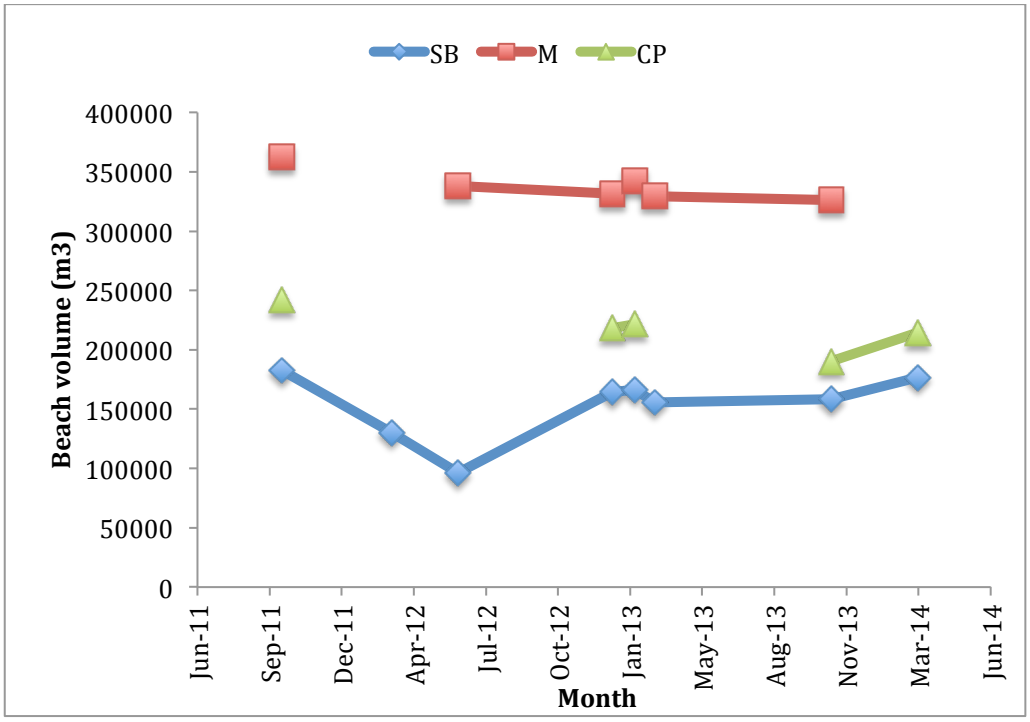

Figure 7.24. Changes in beach volume above minimum elevation planes from November 2011 to March 2014.

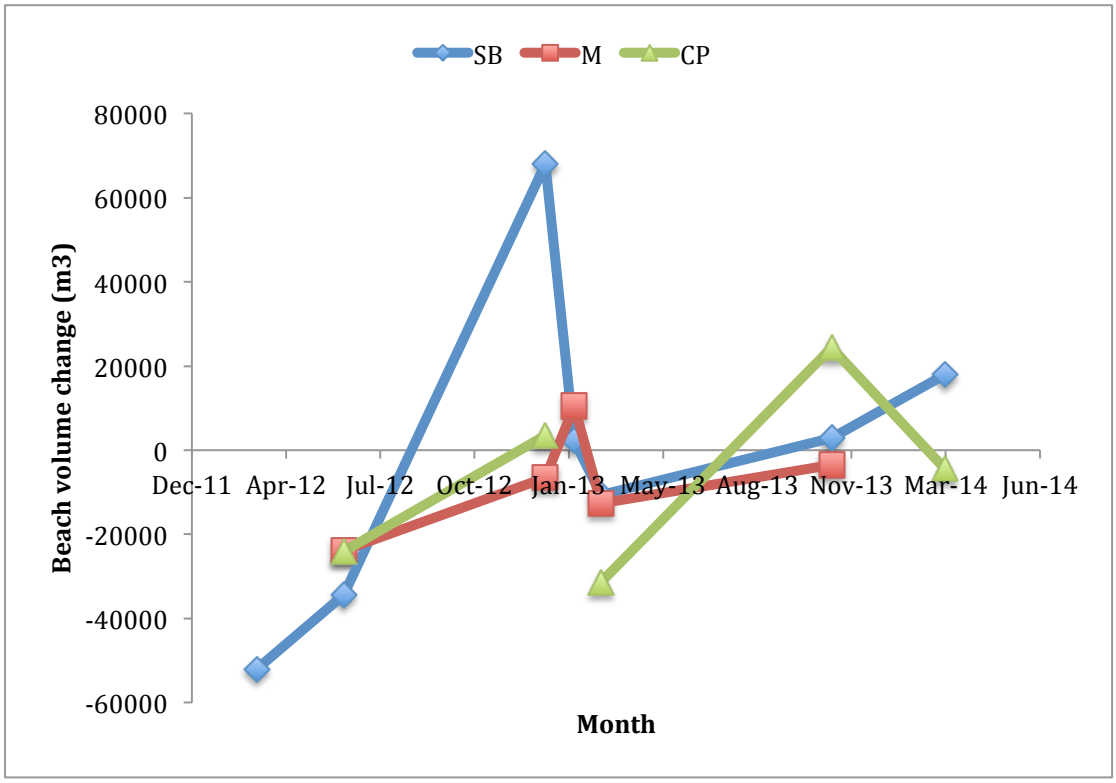

Figure 7.25. Beach volume change at all three sites from November 2011 to March 2014.

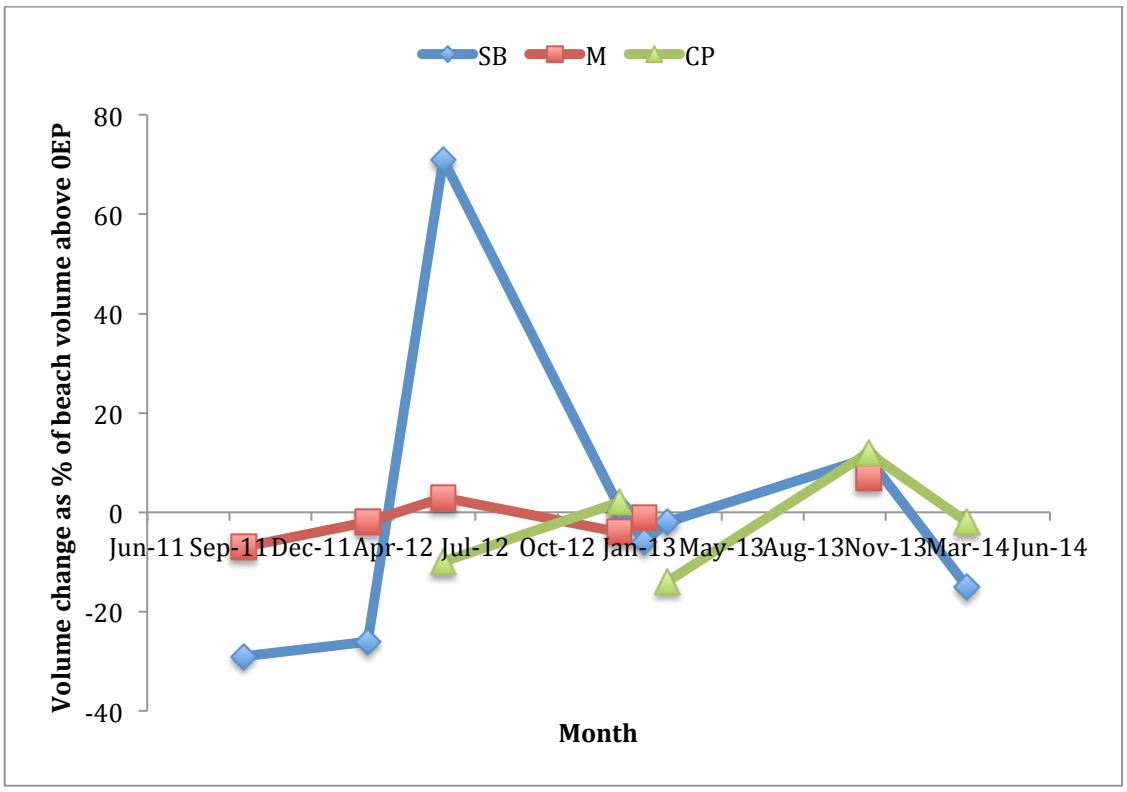

Figure 7.26. Volume change as a percentage of net volume change above the lowest elevation planes for each site.

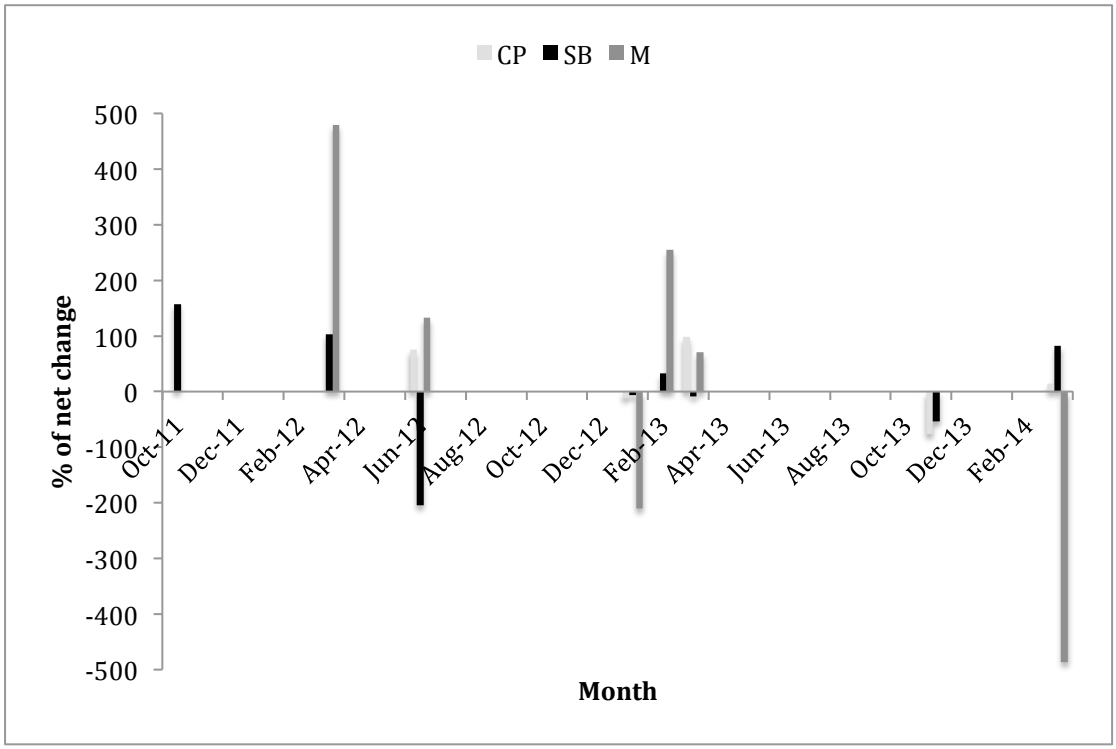

Figure 7.27. Changes in volume as a percentage of net volume change from November 2005 to March 2014. The sign (positive or negative) of the bars indicates whether change over each interim period was in the same direction (loss or gain of volume) as net change.

7.5 Interpretations

Local perceptions about sediment loss from the machair coastline suggested that the sediment budget would be negative (Crawford, 1997), and that loss of sediment and retreat of linear features would be greater at Staoinebrig and Cille Pheadair than at Milton. It was unclear from the literature how measured changes might compare with those of the January 2005 storm. Angus and Rennie (2008) suggested that along many parts of the coast changes associated with the January 2005 storm were not noticeably greater than those occurring during a typical winter season, while Dawson et al. (2007a) reported widespread coastal change associated with the January 2005 event.

The results (Tables 7.9, 7.12, and 7.16) indicated that the sediment budget between 2005 and 2014 was negative, but that net loss was similar or less than many of the volume changes measured during intervening periods. Milton is the most stable site; as expected, Cille Pheadair and Staoinebrig show higher rates of crest retreat, and Staoinebrig in particular, shows very high variability in beach volume. The effects of the January 2005 storm have not been equalled in any single event since, maximum net

retreat from 2005-2014 Cille Pheadair and Staoinebrig was of a similar magnitude. Similarly, while the visible geomorphological changes at the sites were not equivalent in severity and extent to those reported after the January 2005 storm (Dawson et al., 2007a), the same type of effects were seen, particularly at Staoinebrig e.g. overtopping of the shingle ridge and machair front, distribution of shingle and sand plumes, undercutting and slumping of dunes and machair front, etc.

7.5.1 Spatial and temporal variations in coastal change

In general, spatial variations in coastal change, particularly the position of linear features were as expected. Crest retreat was greatest along the eroding machair front at the north end of Staoinebrig and at and to the north of the headland at Cille Pheadair. However, there was also evidence for some progression of the vegetation line south of the headland at Cille Pheadair and the shingle ridge at the south of Staoinebrig during some time periods. At Milton, the crest line remained stable for most of the study, although erosion occurred and was associated with a vehicle track at the southern end of the site between November 2005 and October 2011. Mean NSM and EPR rates show that Milton was the most stable site, and Staoinebrig least. Similarly changes in beach volume show Milton most stable, with large parts of the beach face experiencing little to no change during many of the intervening study periods. The patterns of change vary from site to site. For example, net changes in volume at Staoinebrig show the northern end of the site had no detectable change, while the central and southern sections are characterised by loss of sediment – mostly along-shore. At Milton, net changes in volume show cross-shore banding with no change to slight accretion along the upper beach, and a band of erosion along the mid-beach, corresponding to a tidal channel. At Cille Pheadair, a mix of cross- and along-shore effects is seen with erosion at the north and centre of the site. There is also a distinct cross-shore factor, with any evidence for accretion being limited to the upper beach, and a band of higher erosion extending along much of the mid-beach. The high variability in the results from all sites suggests that site specific factors dominate sediment dynamics on the western coastline of South Uist, as opposed to factors applicable to all sites, e.g. longshore drift.

At the three sites investigated there was variability in the direction as well as the magnitude of change for large parts of the study area. While linear features for some

parts of the coastline showed consistent movement in one direction (e.g. crest retreat of the eroding machair front at the north end of Staoinebrig), other parts of the linear features were extremely dynamic. For example, the crest of the shingle ridge at Staoinebrig and the vegetation line at the southern end of Cille Pheadair both showed evidence for retreat and progression over different time periods. The same is true of beach volumes. Although there was a slight net loss of sediment at all sites (Cille Pheadair (-13%), Staoinebrig (-18%), Milton (-3%)), there was no clear trend in volume, as percentage changes in both directions of similar magnitudes were recorded at Cille Pheadair during intervening periods, and greater changes were recorded at Milton and Staoinebrig. Again, Milton was the most stable site, with all volume changes limited to < 10% of the preceding beach volume.

Annual and seasonal signals are indistinct. For example, volume measurements taken in March of 2012, 2013, and 2014 at Staoinebrig and Milton, and March 2013 and 2014 at Cille Pheadair differ from each other by 5-40%. The typical offshore movement of sediment and the formation of nearshore sandbars associated with stormier conditions (Angus and Rennie, 2008; Baptista et al., 2008; Backstrom et al., 2008) suggested that beach volume would be lower during the winter (October-March) than summer (April-September). On this basis beach levels would be highest in late summer/early autumn after months of accretion and lowest in late winter/early spring after the winter storm season. Results from Staoinebrig largely follow this trend, e.g. the two greatest beach volumes are during November 2005 and 2013, and the lowest beach volume in March 2012. However, there are some discrepancies, e.g. a high beach volume in January 2013, and a low beach volume in October 2011. The same is true for Cille Pheadair, where apart from an anomalously high beach volume in January 2013, higher beach volumes correspond to summer/autumn surveys, and lower volumes to spring/winter surveys. The results from Milton do not appear to follow the expected trend, with three of the highest four beach volumes recorded between January and March. The small fluctuations in beach volume at Milton relative to original volume and the lack of a seasonal component to volume change indicate stability and resilience to change, while Staoinebrig and Cille Pheadair are more susceptible to seasonal changes. The variation in responses to seasonal forcing may be attributed to factors including slight differences in beach orientation, differences in exposure to waves

(influenced by proximity to headlands, and offshore geomorphology and geology), and shore-face morphology, etc. (Backstrom et al., 2008).

The results cannot confirm or reject the perception that the beaches have a negative sediment budget (Crawford, 1997; JNCC, 1999). While the slight net loss of volume at all three sites may support this hypothesis, the loss could be attributed to the seasonal signal in the data, based on the timing of the first and last survey months (November and March, respectively). Furthermore, comparison of the magnitude of the net volume change to interim volume changes suggests that the net change may be indicative of a typical short-term fluctuation rather than indicating a negative trend in the sediment budget (Tables 7.9, 7.12, and 7.16). Continuation of the study over a longer time period might have elucidated this issue further. Aside from general loss of sediment from the beaches, beach lowering at the southern end of Staoinebrig is a particular concern for local residents (David Muir, personal communication). The results (Fig. 7.8) indicate that variability is very high over this part of the beach, and there is a greater net loss of sediment in the southern and central parts of the beach compared to the northern end of the site. This may be partly due to the steepness of the beach; results indicated that the position of both MHWOST and MLWOST are very close to the base of the shingle ridge for this part of the beach (see Figure 7.6), indicating that all of the beach profile will be active under almost all tidal conditions for this part of the site.

7.5.2 Comparison of measured change and climate data

The RTK-dGPS data spanned three winters (October-March, inclusive), 2011-2012, 2012-2013, and 2013-2014; most negative coastal change of the machair coastline was expected in winter (Angus and Rennie, 2008). Table 7.19 shows climate data for these winters. While there were no extreme storms similar to the January 2005 event, the maximum significant wave height recorded in February 2013 (16.39 m) is similar to the modelled 1 in 50 year wave height (Wolf, 2007). Winters 2011-2012 and 2013-2014 had moderate numbers of gale and storm days (18), compared to the 1876-2014 average (19), while 2012-2013 had a very low number of gale and storm days (8).

Table 7.19. Climatic and coastal change data for the three winter seasons investigated. Mean Atm. P = mean atmospheric pressure; mean WS = mean wind-speed. Bold text indicates the value in each column indicative of highest storminess.

Season	No. storms/gales	mean Atm.P (hPa)	mean WS (m/s)	max. Hs (m)	mean NAO
11-12	**18**	1010.8	**16.1**	14.48	1.05
12-13	8	1007.7	11.6	**16.39**	-0.93
13-14	**18**	**999.1**	15.2	15.87	0.45

Results from chapter 7 show no obvious relationship with the conditions listed in Table 7.19. For example, at Staoinebrig volume loss in winter 2011-2012 was -26 % and only -15% in winter 2013-2014, despite the two winters having similar storm numbers. The net loss is less over winter 2012-2013 (-3 %). Furthermore, at Cille Pheadair results show greater volume loss from June 2012 and March 2013 (-12 %), than from November 2013 to March 2014 (-2 %), despite the low storminess in the former interval. This difference in relative responses between sites is further evidence that the beaches are responding differently to similar external forces, and of the complexity of the sediment system on the machair coastline of South Uist

Relationships between beach volumes and monthly climatic parameters are shown in Table 7.20. The significant positive relationships between beach volume and many of the parameters linked to storminess are surprising, as increased storminess is generally linked to lowering of beach volumes and coastal erosion (e.g. Thomas et al., 2010; 2011a; 2011b). At Cille Pheadair and Milton all indicators of storminess are positive correlated with beach volume, while at Staoinebrig the relationships are mixed, with wind-speed and NAO negatively correlated with beach volume. Most relationships for Staoinebrig are not statistically significant. An explanation for the unexpected findings could be the release of sediment from the dunes at Cille Pheadair and Milton during storms, i.e. erosion of the dune toe deposits material on the beach face with a net gain of sediment to the beach face. There was visible evidence for this at both of these sites (see photos of coastal change in Chapter 7), and DoD's revealed that the majority of sediment accretion was on the upper beach, close to the dune toe. The difference in response apparent at Staoinebrig may be due to the lack of an equivalent sediment bank at this site.

Table 7.20. Relationships (r-value) between climatic parameters and beach volumes. SB (Staoinebrig), M (Milton), and CP (Cille Pheadair) are relationships to data from each site. 'All' refers to relationships between climatic factors and data from all sites, normalised to prevent differences in the original size of the beach affecting the relationships. + indicates positive relationship; - indicates negative relationship. Significance of relationship is : *** ($p < 0.01$); ** ($p < 0.05$); * ($p < 0.01$).

Climatic Parameter	Relationships			
	SB	M	CP	All
No. gale/storm days	+ 0.20	+ 0.75***	+ 0.68**	+ 0.22**
Mean wind-speed	- 0.07	+ 0.63**	+ 0.42*	0.00
Mean atm. pressure	- 0.34**	- 0.12	- 0.28	- 0.19**
Highest wind-speed	+ 0.11	+ 0.83***	+ 0.63**	+ 0.18**
NAO	- 0.17	+ 0.31*	+ 0.07	- 0.03

7.5.3 Influence of short-medium term analysis of change on interpretation of long-term change analysis, and vice-versa

Comparison of the rates of crest movement from short and long term analyses are in Table 7.21. The results indicate that EPR is a similar magnitude for both long and short timescales, although values obtained from short-term analysis of change are higher. Boxplots showed a trend of decreasing mean EPR between 1948-2005 (see Figure 6.9) at Staoinebrig, while data on short-term change indicates the trend may have reversed from 2005-2014. It is probable that the constructed shingle ridge (Richards and Phipps, 2007) has contributed to this reversal. At Cille Pheadair, the EPR from 2005-2014 is less than the value for 1948-2005, suggesting a trend of increasingly negative EPR values over time. The results indicate that the rate of coastal retreat has increased at these sites from 1948 to the present.

Table 7.21. Mean EPR values obtained from analysis of change in the position of the vegetation line/crest over short (2005-2014) and long (1948-2005) timescales.

Timescale	Mean EPR (m/yr)		
	SB	M	CP
short	+ 0.10	+ 0.12	- 0.23
long	+ 0.06		- 0.10

Short-term analysis of change showed very high variability in the position of linear features and beach volume (Figs. 7.4, 7.10, and 7.16). While some of the changes appear to be seasonal, fluctuations over the three year survey are considerable, particularly at Staoinebrig and Milton where interim changes in beach volume were frequently > 100% of the net volume change measured from 2005-2014 (Fig. 7.28). The position of MHWOST (derived by adding contours at the appropriate datum (1.51 m O.D.) to DTMs) was also highly variable. At Cille Pheadair and Staoinebrig variability was on the order of ~ ±25 m, while at Milton it was ~ ±15 m. These fluctuations are close to the magnitude of changes in the long-term analysis of MHWOST, with implications for the interpretation of long term change results (discussed below).

The 'signal-to-noise' ratio in detecting geomorphic change is generally used to test whether measured change is likely to be genuine or attributable to measurement error (James et al., 2012; Williams, 2012). However, apparent from the above comparison of long term and short term change in the machair coastline, a trend (or 'signal') in coastal change could be concealed by the high short-term variability (or 'noise'). For example, the trend in beach volume from 2005-2014 could be significantly altered by using survey data measured in January or June 2014, instead of March, i.e. rates of change over short periods of time may be to 'either side' of a longer term trend (Cambers, 1976). By investigating short-term fluctuations in coastal geomorphology, this chapter enabled consideration of the amount of 'noise' expected from seasonal, annual, and decadal changes in the coastal zone (many of which appear to be readily reversible) and of the more commonly quantified errors arising from measurement and DTM use (Wheaton et al., 2010; James et al., 2012; Williams, 2012). The high variability in beach volume and the position of the vegetation line identified between subsequent surveys in March of 2012, 2013, and 2014 suggest that even matching survey times and tidal conditions may be insufficient to prevent 'noise' from short-term variability and highlight the limitations associated with using 'snapshot' data (e.g. a photograph or map) for long-term geomorphic change analysis. It is probable that pre-conditioning (over a range of timescales) contributes to variations in coastal response and configuration, even when surveys are conducted at similar tidal and seasonal settings (e.g. as discussed in Brunsden, 1993; Phillips, 2009). Cambers (1976) discussed this concept, identifying high spatial and temporal variability in cliff retreat

rates over short time periods, which averaged to a more uniform pattern over longer times.

The significance of the January 2005 storm is placed in a clearer context by comparison with short and long term data. Up to 5 m of crest retreat occurred at Cille Pheadair within 48 hours during this event. This approximates to one-eighth of maximum long-term NSM from 1878-2005 (-41.48 m) at Cille Pheadair, suggesting that the maximum retreat associated with the storm was equivalent to ~7 years of gradual change at the most sensitive parts of the coastline. Compared with short-term change in the vegetation line/crest, the maximum magnitude of retreat associated with the January 2005 storm appears to be similar to maximum NSM values for Cille Pheadair between 2005-2014 (~ 3.5 m, see Figure 7.16), suggesting that over this shorter timescale the storm damage was equivalent to ~12 years of change. The higher significance of the event for shorter times is consistent with Cambers (1976) who proposed that the severity of an event was a function of the timescale over which it was considered.

7.5.4 Critique

A key limitation to the analysis of short term change in isolation is that the volumetric measurements are restricted to the beach face, and the nearshore environment was not investigated planimetrically or volumetrically. These limitations may explain the comparatively high sediment fluxes over the beach face relative to other studies that incorporate the nearshore environment and/or the dunes in volumetric analysis (e.g. Murray-Hicks et al., 2002; Wang and Roberts, 2012), as sediment will often transfer within the elements of a coastal geomorphic system. This internal transfer can lead to high variability in sediment volumes within each part of the system, while the net volume of the system as a whole remains relatively constant. However, due to the high interconnectivity between nearshore, beach face, and dune components of a coastal geomorphic system, useful information can be obtained from analysis about component parts where access to information about the whole system is limited by financial, practical, and logistical considerations. For example, an on-going net loss of sediment from the beach face would have implications for coastal management regardless of the changes occurring in other parts of the system. This is most relevant

for areas with a lack of sediment budget quantification as is the case for the machair coast of the Outer Hebrides (JNCC, 1999).

In contrast to the results from analysis of long-term change, the majority of volumetric and planimetric results of short-term analysis are all significantly larger (often by orders of magnitude) than the error associated with the methodology. The choice of presentation for results from DoD's – i.e. considering elevation changes < 0.5 m as indicative of no change – is conservative, as using a 0.5 m error threshold is likely to overestimate error, due to the scarcity of suitable control points on the machair. For this reason the results for short-term change analysis can be attributed to real geomorphic change rather than error with relatively high confidence. Additionally, the range of conditions and temporal scales over which surveying took place (tidal, seasonal, post-storm, annual) and the nature of the weather during the study period (typical in terms of storminess) suggests the results are a reasonable indication of the variability in the coastal zone that is recoverable (in terms of beach volume, and movement of the shingle ridge at Staoinebrig, and the vegetation line at the south of Cille Pheadair) under normal conditions.

The implications of short-term variability in the position of MHWOST and the vegetation line on long term analysis of change are that much of the measured change is attributable to short-term fluctuations. This is particularly the case for the position of MHWOST and the vegetation line where it does not coincide with a distinct geomorphological scarp, as these features appear highly mobile in both directions. Conversely, results for changes in linear features that only show evidence for movement in a negative direction (e.g. high dunes at Milton and north of Cille Pheadair, eroding machair scarp at the north end of Staoinebrig) more likely indicate longer term trends rather than fluctuations. These findings suggest that the position of MHWOST, and the position of the vegetation line are not necessarily appropriate proxies for investigating shoreline change despite their widespread use as such (e.g. Boak and Turner, 2005), particularly where short-term variability in these features has not been quantified. The results of long-term change analysis should be treated with caution, but the agreement of the nature and magnitudes of rates of change with: i) the findings of Dawson et al. (2007b, 2012); ii) expected changes associated with known sea-level rise, iii) mean rates of change from 2005-2014, and, iv) local perceptions of on-going retreat and

coastal sensitivity at Staoinebrig and Cille Pheadair (Richards and Phipps, 2007; David Muir, personal communication) increases their credibility.

7.6 Key Findings

- Change in crest position fell into three categories: i) stable (Milton); ii) consistent retreat (machair front at Staoinebrig and high machair front at Cille Pheadair); and iii) variable/dynamic (shingle ridge at Staoinebrig and low machair front at Cille Pheadair);
- Beach volume and elevation are more variable at Staoinebrig than at other sites. MHWS and MHWN are also closer to the crest at Staoinebrig than at the other sites, particularly at the southern end of the beach;
- A similar range of elevation changes was measured for most survey intervals. However the distribution of elevation changes varied considerably;
- There was some evidence for rapid but localised changes in elevation during the stormy period from January to February 2013, and evidence for rapid recovery of this between February and March 2013, particularly at Staoinebrig;
- At all three sites there is a small net loss of sediment volume; however, at Staoinebrig the net loss is less than some of the interim changes in sediment volume, and at Milton and Cille Pheadair the net loss is of a similar magnitude to interim changes. All three sites experienced sediment gain during some surveyed intervals;
- Unlike crest position, changes in sediment volume happen gradually (e.g. relatively small changes in volume in stormy period from January to February 2013);
- There was no evidence throughout the study for extreme changes such as were recorded during the January 2005 storm, (e.g. 5 m of coastal retreat in one event recorded at Cille Pheadair);
- Maximum net change in crest position between November 2005 and March 2013 (a 7.5 year period) was: i) 5.53 m at Cille Pheadair, equivalent to 111% of the maximum recorded change during the January 2005 storm; ii) 6.68 m at Milton, equivalent to 134% of the maximum record change during the January 2005 storm; and iii) 4.6 m at Staoinebrig, equivalent to 92% of the maximum

record change during the January 2005 storm (changes at Milton over the 7.5 years are unlikely to be caused by marine action);

- Mean net change in crest position between November 2005 and March 2013 was i) 0.7 m at Cille Pheadair, equivalent to 14% of the maximum recorded change during the January 2005 storm; ii) 0.44 m at Milton, equivalent to 9% of the maximum record change during the January 2005 storm; and iii) 0.1 m at Staoinebrig, equivalent to 2% of the maximum record change during the January 2005 storm.

CHAPTER 8
VARIATIONS AND TRENDS IN THE SENSITIVITY OF MACHAIR SOILS TO AEOLIAN DEFLATION

8.1 Introduction

8.1.1 Background

In the preceding chapters the sensitivity of machair landforms to erosion via coastal processes has been investigated. In this chapter, the second major mechanism of erosion in the machair landscape is considered; namely, aeolian deflation of the machair grasslands. While wave erosion and aeolian deflation are separate physical processes, both represent key parts of the currently accepted model of machair formation and evolution (e.g. Ritchie, 1967; 1979) (discussed in Chapter 2). There are also potential feedbacks between the two processes. For example, blowouts or sandblow near the dune cordon/machair front may increase susceptibility to sediment removal by storm waves. Furthermore, excessive deflation of the grasslands may lead to further reductions in the altitude of the machair grassland surface – already at or close to MHWOST in many areas (e.g. see Chapter 4).

The machair is considered to be esepcially susceptible to aeolian erosion (Mate, 1992; Ritchie et al., 2001), due to a sandy texture and low concentration of organic matter (both of which contribute to poor aggregate stability), and frequent exposure to high wind speeds (see Chapter 5). Poor agricultural management has been linked to localised destabilisation and wind erosion (Seaton, 1968; Ritchie, 1971; Angus, 2001; MacDonald, 2011), which has on some occasions been severe enough to disrupt agriculture (Seaton, 1968) and endanger or damage archaeological sites (Moore et al., 2005). Further, it is thought that rabbit burrowing, stock trampling, and tourism may also initiate or exacerbate erosion on the dunes and grasslands (Mather and Ritchie, 1977).

It should be noted that aeolian erosion is only possible when soil is bare. On the cultivated machair grasslands bare soil is only present in certain circumstances: i) after ploughing and before crops are big enough provide sufficient cover to reduce wind

erosion; ii) where rabbit burrowing and scraping has removed vegetation; and iii) where overgrazing has occurred. Furthermore, during winter the water table is generally high enough that it provides some protection against wind erosion; consequently, late spring and early summer represent the period when wind erosion is most likely to be problematic (see section 2.3.1.1).

Several traditional agricultural methods have been promoted and/or subsidised by conservation groups, the Scottish Government, and the European Union to promote the conservation of the idealised machair landscape and ecosystem. For example, shallow ploughing to a depth of ~10 cm is subsidised by the Scottish Government (Scottish Government, 2012) in preference to deep ploughing (~20 cm depth), as it is thought this reduces erosion and encourages more rapid vegetation regrowth (Crawford, 1990). The practices recommended are often promoted based on casual observations, or the perception that traditional management techniques are 'better' than modern methods. There is limited scientific evidence that these methods will improve soil stability, e.g. Thorsen et al. (2010) found that the use of seaweed as fertilisers had no beneficial effects on aggregate stability or microbial activity when compared to synthetic fertilisers. Traditional management methods tend to be promoted on a 'blanket' basis, aimed at the machair as a whole. This is despite evidence for considerable variation in machair soil properties on moving inland from the coastal dunes to the 'blacklands' (Ritchie, 1974; Randall, 2004; Angus, 2006). It is probable that the full range of variation in soil properties may be found across a typical machair field, as cultivated strips are generally long and narrow, with the long side perpendicular to the coast. The orientation of cultivated strips on the machair is a continuation of historic agricultural practices during the 19th Century, when the land was divided in this way to ensure that each crofter's land included access to the beach (for extraction of seaweed and sand/gravel), free draining grassland (for cropping), and 'blacklands' (for seasonal cattle grazing) (Caird, 1979). In many areas, the cultivated areas extend from within a few metres of the dune crest to the 'blacklands' transition zone.

8.1.2 Aims

Previous studies of the machair identified trends in soil properties with distance from the coast (see section 2.1.4). However, there has been little quantitative research

into the quality of machair soils and the factors that influence this, with the exception of the work of Thorsen et al. (2010). The aims of this study are to:

i) investigate spatial variations in the sensitivity of the cultivated machair soils to wind erosion, with particular emphasis on cultivation of the back dunes, that are a key landform on the machair coast, acting as topographical barrier to marine flooding of the low-lying grasslands;

ii) to determine which soil properties, if any, are correlated with wind abrasion resistance;

iii) to establish whether there are chemical and/or physical differences between erodible and non-erodible soil fractions;

iv) and to consider the implications of the results with regards to management of the machair grasslands.

8.2 Methods

8.2.1 Sample collection

Samples were collected in June 2012 from three recently cultivated plots in the 1st year of their fallow period. One cultivated strip was selected at each of the field sites at which coastal change was investigated: at Cille Pheadair the strip is ~100 m north of the centre of the headland; at Milton the strip is at the southernmost end of the section of coast surveyed; the machair at Stoneybridge is not currently used for cultivation (although historic aerial photography shows a history of cultivation) so a strip was selected at Tobha Mor, ~2.5 km northeast of Stoneybridge beach. At each site, sampling was along a transect perpendicular to the coastline with samples collected at 10-13 loci along a distance of 250-450 m (Fig. 8.1). At each loci on the transects 4 further samples were taken along lines perpendicular to the transect to equally cover the width of the cultivated plot. Bulk topsoil samples weighing ~ 100 g, and topsoil cores (depth = 4 cm, volume = 100 cm^3), were collected at each loci. After collection samples were refrigerated at 5 °C until needed.

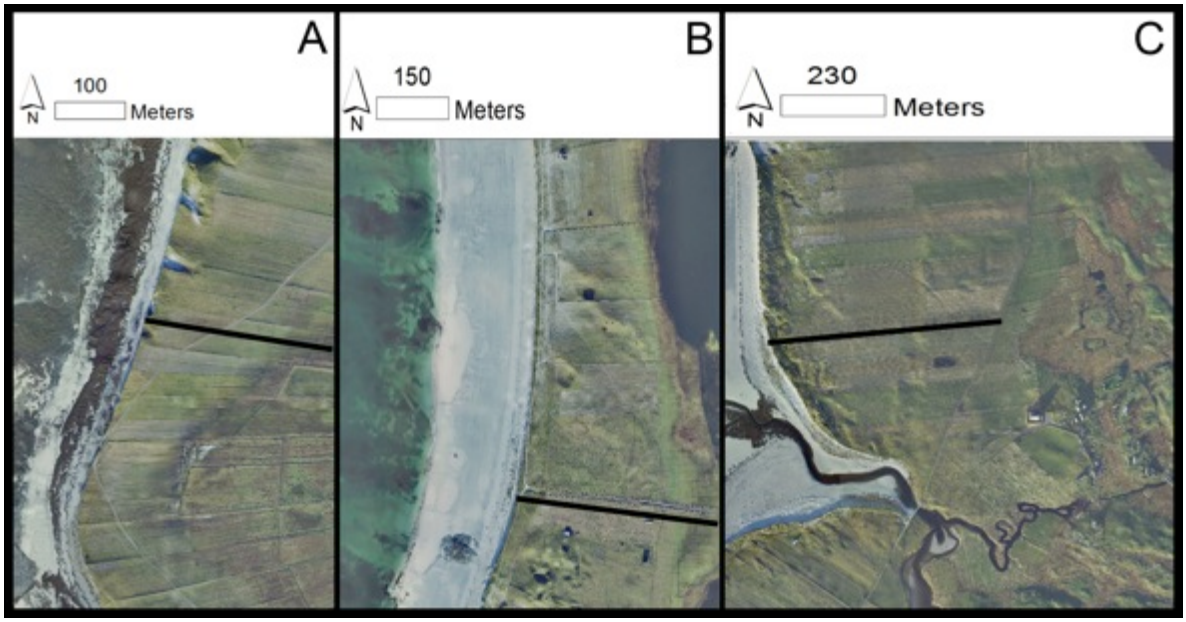

Figure 8.1. Aerial photographs of the three sites showing the sampled transects. A. Cille Pheadair. B. Milton. C. Tobha Mor. Black lines indicate the positions of sampled transects.

Samples are labelled CP (Cille Pheadair), M (Milton), or TB (Tobha Mor), according to the transect from which they are taken. Samples are numbered in increasing order with distance from the coast. The letters a-d indicate samples taken perpendicular to the main transect.

Weather conditions prior to sampling had been unusually dry. Total rainfall for the period from April-June 2012 was 74 mm – substantially lower than the mean rainfall values for these months (195 mm – see Figure 2.1, section 2.2.1.1).

8.2.2 Measurement of wind abrasion resistance

The sensitivity of a soil to wind erosion is negatively correlated with the mass of soil aggregates > 840 μm in diameter (Chepil, 1953), and a soil which consists of > 40 % air-dry aggregates > 840 μm is considered to be non-erodible by wind (Leys et al., 1996). This is due to the resistance large particles and aggregates have to entrainment. If aggregates are resistant to abrasion, they cannot be eroded by aeolian processes. Nelson (1998) used a rotary sieve to establish both the abrasion resistance of soils (determined by separating soil particles and aggregates < 850 μm in diameter from particles and aggregates > 850 μm in diameter), and rates of abrasion of aggregates > 850 μm in diameter (determined by rotary sieving soil samples for 300 s).

In this chapter a rotary sieve with mesh size of 850 μm was used to simulate wind abrasion (Fig. 8.2.), following the methods of Nelson (1998) and Tisdall et al. (2012). Samples were air dried for 48 hours prior to rotary sieving. Forty grams of soil was transferred to the barrel of the rotary sieve. The rotary sieve was then rotated for 300 s at 7 rpm. Material passing through the sieve was collected on a balance. The balance reading was recorded every 10 s for the first 40 s, and every 20 s from 40-300 s. Measurements were conducted in duplicate for each main transect loci. Additionally, two further measurements were made on samples from sub-loci to either side of the main transect and combined with the measurements from the main transect sample to provide a mean and standard deviation. This was based on the assumption that the dominant direction of variation in wind abrasion resistance would be perpendicular, rather than parallel, to the coastline; consistent with other soil physical characteristics (Ritchie, 1974; Randall, 2004; Angus, 2006).

Rotary sieving divided the sample into 3 fractions: sediment passing through the sieve within the first 40 s was collected and classified as 'erodible' (E); sediment passing through the sieve between 41 s and 300 s was collected and classified as 'potentially erodible' (PE); sediment remaining on the rotary sieve after 300 s was collected and classified as 'non-erodible' (NE). The selection of 40 s as the cut-off time between E and PE soil fractions was based on wind abrasion curves from Tisdall et al. (2012), which showed a significant reduction in the rate of aggregate abrasion at 30-50 s. Additionally, the mass of sediment remaining on the sieve at 14 s was considered an indication of the overall wind abrasion resistance (WAR) of the soil aggregates (after Tisdall et al., 2012). The maximum possible value for WAR is 40, which would indicate that no material passed through the sieve within 14 s.

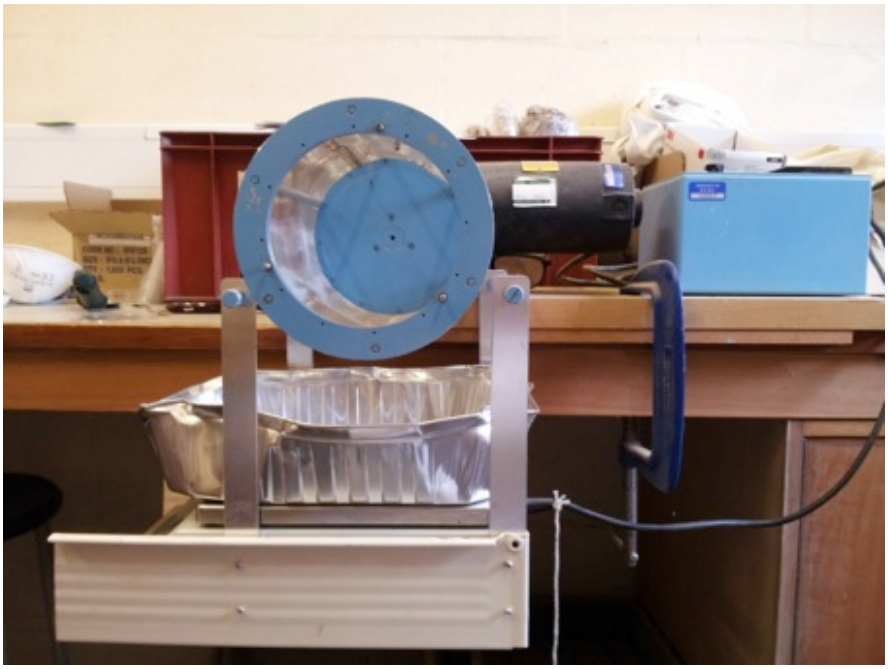

Figure 8.2. Rotary sieve after the design of Tisdall et al. 2012.

8.2.3 Measurement of soil properties related to WAR

The soil properties analysed were generally selected due to their potential to influence soil erodibility by wind (e.g. particle size, organic matter content, water repellency). However, some additional soil properties were also measured as a 'by product' of other analyses. For example, a review of the literature on machair soils suggested that the ratio of carbonate to silicate sands, and the use of seaweed fertiliser (with high arsenic concentration) might indicate changed susceptibility to wind erosion. The techniques used to assess these properties (Fourier transform infrared spectroscopy and X-ray fluorescence, respectively) generated other data related to different minerals and elements which were also assessed due to the ready availability of this information.

8.2.3.1 Particle size analysis

Particle size analysis by laser granulometry was conducted on each main transect sample used for rotary sieving using a Beckman Coulter LS 13 320 Laser Diffraction Particle Size Analyser (e.g. Rowan et al., 2012). Samples from each transect were run in triplicate to indicate variation. Results were analysed to establish the

percentage of each sample with a particle size > 850 μm, i.e. the percentage of each sample which would be expected to remain on the sieve.

8.2.3.2 Fourier transform infrared analysis

Fourier transform infrared (FTIR) analysis was used to investigate mineralogical differences between samples. Bulk samples M: 1, 4, 8, 9-12, TB: 1, 6, 10, and CP: 1-5, 7-11, and the corresponding sub-samples representing E, PE, and NE fractions of the soil (as separated by rotary sieving) were prepared for FTIR analysis. Samples were selected to cover the variation in wind abrasion resistance found along the transects (see section 8.3.1). Three grams (± 0.1 g) of each sample or sub-sample was ground to a fine powder by milling for 12 minutes using a Glen Creston McCrone micronising mill with agate grinding elements prior to analysis.

8.2.3.3 X-ray fluorescence analysis

X-ray fluorescence (XRF) analysis was used to investigate chemical differences between soil samples, specifically variations in the concentration of potassium (K), calcium (Ca), titanium (Ti), chromium (Cr), manganese (Mg), iron (Fe), cobalt (Co), copper (Cu), zinc (Zn), arsenic (As), and strontium (Sr). XRF analysis was carried out on the same samples analysed by FTIR. Samples were prepared for XRF analysis by ball milling ~ 2-4 g of soil at an amplitude of 30 for 6 minutes using a Glen Creston MM 2000 ball mill.

8.2.3.4 Water repellency

Water repellency was measured using the method of Hallett and Young (1999). In this method capillary tubes link a bottle of distilled, degassed water to a sponge tip (diameter 4 mm). The sponge tip is maintained at a negative pressure head of 2 cm. The surface of each field-moist soil-core is brought into contact with the sponge tip for 180 s. Over this period, the mass of water lost from the bottle is recorded every 5 s using an Ohaus Explorer balance (accurate to 0.001 g) and logging software. This is repeated three times for each core.

The determination is repeated using ethanol instead of water. Through comparison of the infiltration rates for water and ethanol (two liquids with different solid-liquid contact angles), it was possible to assess the repellency of the soil using the water repellence index (Equation 8.1) developed by Hallett and Young (1999):

$$WR = 1.95\left(\frac{S_e}{S_w}\right)$$

Equation 8.1.

Where S_e is the sorptivity of ethanol, and S_w is the sorptivity of pure water. Using this index, a soil with a WR value of 1 is non-repellent. The greater the WR value, the more repellent the soil.

8.2.3.5 Water drop penetration time

The persistency, or stability, of water repellence was characterised by the water drop penetration time (WDPT) method (Krammes and Debano, 1965; Doerr et al., 2006). Three 50 µl drops of distilled water were placed on the surface of each soil-core and the time taken in seconds for each drop to completely infiltrate the soil recorded up to a maximum of 5 hours, after which time it is expected that evaporation will influence any results obtained (Doerr et al., 2006).

The WDPT classification system of Doerr et al. (2006) was used to analyse results. This system uses 10 classes to describe the persistency of water repellence, and 4 textual ratings (Table. 8.1).

Table 8.1. WDPT classes and ratings for the severity of water repellency along with the associated penetration time classes. Modified from Doerr et al. (2006). t(s) indicates time in seconds.

Class	0	1	2	3	4	5	6	7	8	9	10
t(s)	≤5	6-10	11-30	31-60	61-180	181-300	301-600	601-900	901-3600	3600-18000	> 18000
rating	none	slight			moderate			severe		extreme	

8.2.3.6 Loss-on-ignition

The organic carbon concentration (C_{org}) of all bulk samples was investigated by loss-on-ignition (LOI). This method relies on the principal that the organic matter in soil samples undergoes complete combustion at lower temperatures than mineral material. The temperature and length of heating required to remove organic matter is dependent on the characteristics of the soil sample. (Wang et al., 2011). For example, the time needed to combust organic matter increases with increasing organic matter concentration. At temperatures above 500-600° C it is also possible for weight loss to occur due to loss of structural water from clay minerals (Sun et al. 2009), and for incomplete combustion of inorganic carbon (C_{inorg}), e.g. carbonates, to occur (Chatterjee et al., 2009; Szarva-Kovats, 2009). Due to the high carbonate content and low organic matter content of machair soils a moderate burn temperature of 550 ° C and a short burn duration of 1 hour were selected to prevent partial combustion of C_{inorg}. As there is no specific conversion factor for machair sediments to calculate the % weight loss due to C_{org} during combustion of soil organic matter, data are presented as the percentage of the sample consisting of organic matter. This is likely to be approximately twice the percentage of C_{org} in the soil, as in general, 40-60% of organic matter loss by weight is attributable to C_{org} (Abbott, 2005).

Approximately 2 g of each sample (pre-dried at 105° C for 48 hours to remove water) was heated at 550° C for 1 hour in a muffle furnace. Samples were re-weighed following combustion, and the percentage organic matter content (SOM%) of the sample calculated using equation 8.2, where W_1 indicates the weight of the sample prior to burning, and W_2 indicates the weight of the sample post burning:

$$SOM\% = \frac{(W_1 - W_2)}{W_1}\ x\ 100$$

Equation 8.2

8.2.3.7 Bulk density and water content

Bulk density and water content were calculated by weighing the bulk soil samples before and after drying at 105 °C for 24 hours. Bulk density was determined

by dividing the dry weight of the soil by the volume of the soil (100 cm^3). Water content was determined using Equation 8.3.

$$Water(\%)by\ mass = \frac{(wet\ mass - dry\ mass)}{(dry\ mass)} \text{ x } 100$$

Equation 8.3

8.2.3.8 pH

The pH of all topsoil cores was measured using a Hanna H1 99121 soil pH meter. Due to the low water content of the soil samples, cores were moistened using HI 7051 aqueous preparation solution prior to measurement.

8.2.4 Statistical analysis

Linear regressions for wind abrasion resistance (WAR) against all measured soil variables (apart from FTIR data) were carried out using the Pearson product moment correlation coefficient in Microsoft Excel 2011 to indicate the strength of correlations. R^2 values were calculated to indicate the ability of soil properties to predict to WAR. Principal component analysis (PCA) was used to statistically assess inter- and intra- site variability between FTIR spectra, and to consider the relationship between FTIR spectra and WAR. A regression tree was constructed to predict WAR, using the 19 bulk samples which were included in XRF and FTIR analysis. Regression trees are a form of predictive model, the purpose of which is to predict an unknown target variable from the values of known variables, and to output this prediction in a numerical form. In this case, the goal was to predict WAR using physical and chemical soil characteristics as the known variables. The original tree was pruned to predict WAR on the basis of four variables: As levels, WDPT class, WC, and mean PS. The regression tree's ability to predict WAR was tested using two further batches of soil samples containing 13 and 11 samples. Jim McNicol, an associate of Biomathematics and Statistics Scotland (BioSS) based at the James Hutton Institute, Invergowrie, was consulted regarding the appropriate statistical tests to use in this chapter, and assisted with PCA and regression tree analysis.

8.3 Results

8.3.1 Wind abrasion resistance (WAR)

The results from simulating wind abrasion using the modified rotary sieve show considerable intra- and inter-site variation. At CP, there is a steady increase in WAR moving inland (Fig. 8.3). This is evident from the reduced mass of soil passing through the sieve with increased distance from the coast. The increase in WAR is almost linear against distance from the coast, with the greatest mass of soil passing through the sieve for the sample closest to the coast (distance from coast = 0 m), and the least mass of soil passing through the sieve for the sample furthest from the coast (distance from the coast = 255 m) (Figure 8.4). WAR (Table 8.2) shows that when the samples are ranked according to WAR the samples have similar rankings for distance from the coast and abrasion resistance, with the maximum difference between rankings being two places. There is a very strong positive relationship WAR and distance from the coast at this site ($R^2 = 0.85$, $p < 0.01$).

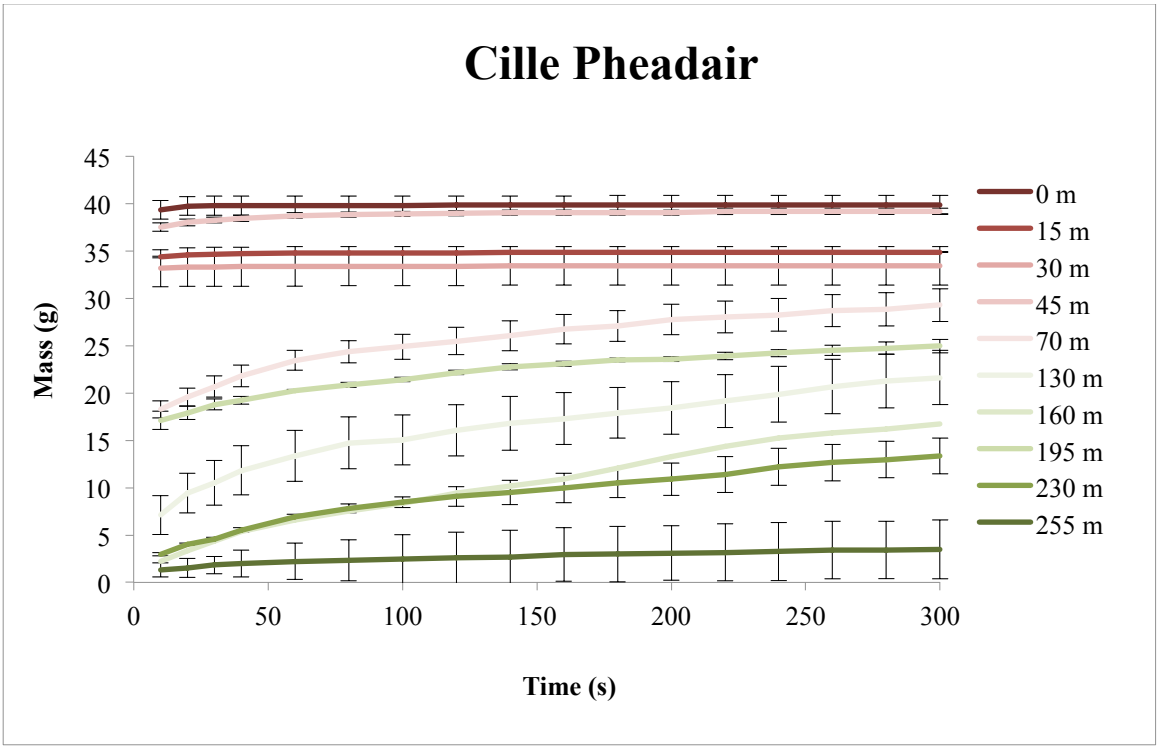

Figure 8.3. Mass (g) of air-dried soil passing through the rotary sieve over 300 s for samples from CP. Labels indicate the distance of the sample from the coast. Error bars indicate 2 x SE.

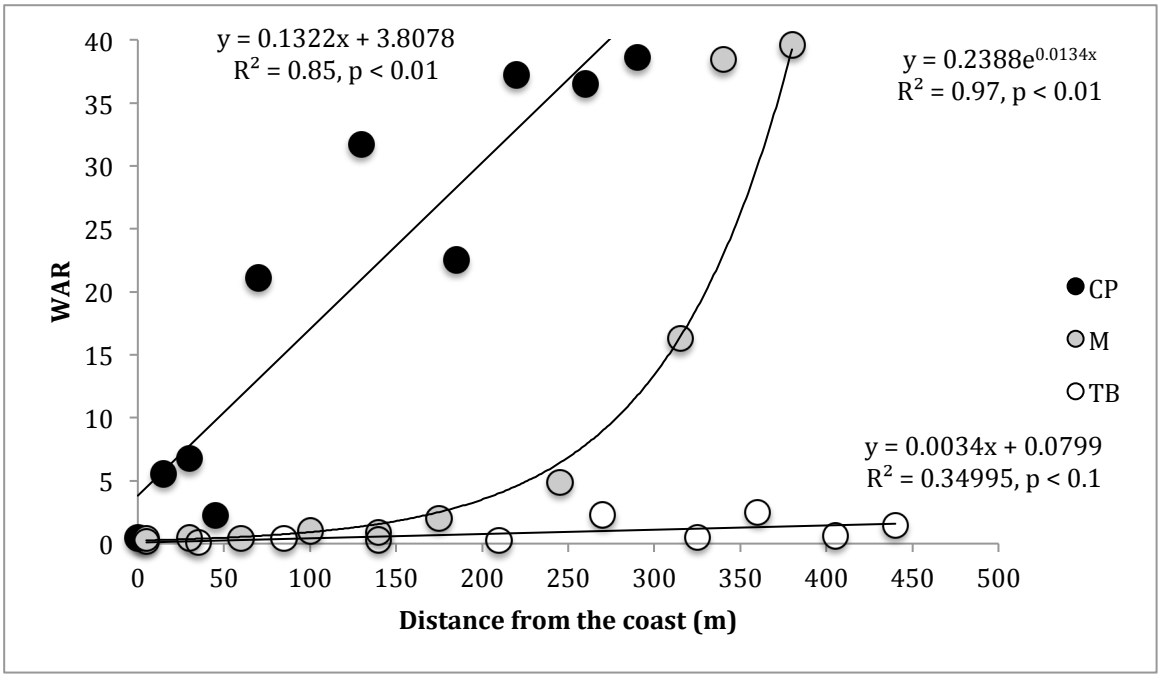

Figure 8.4. Regression of mean WAR values for each sample against distance from the coast for Cille Pheadair, Milton, and Tobha Mor. Note that the maximum possible value for WAR is 40.

Table 8.2 Wind abrasion resistance of each sample, and rankings for the samples in terms of distance from the coast (ranked closest to furthest) and abrasion resistance (ranked lowest to highest) at CP.

Sample distance from the coast (m)	mean WAR	Rank – distance from the coast	Rank – WAR
0	0.47	1	1
15	5.55	2	3
30	6.78	3	4
45	2.25	4	2
70	21.1	5	5
130	31.74	6	7
160	22.5	7	6
195	37.23	8	9
230	36.51	9	8
255	38.59	10	10

At M, there is also an increase in WAR with distance from the coast; however the pattern is different to that seen at CP: there is little change in WAR between 0-250 m, and then a rapid increase from ~ 250-400 m (Figs. 8.4-8.5). The greatest change in WAR occurs between 260 m (WAR = 16.24) and 340 m (WAR = 38.42) from the coast.

A vehicle track crosses the site at a distance of ~ 310 m, although there does not appear to be any visible difference in management on either side of the track. At this distance (260-340 m) from the coast, there are also noticeable changes in WDPT class (≥ 3 from 0-250 m, ≤ 2 from 250-400 m); pH (≥ 8.3 from 0-250 m, ≤ 8.3 from 250-400 m); and water content (≥ 7 from 300-400 m, ≤ 6 from 0-300 m). A split-line regression analysis identifies a break point within this range at 261.6 m from the coast, corresponding to a WAR value of 4.02 ($p < 0.05$). As with CP, the samples closest to the coast have very low abrasion resistance, with all the soil passing through the sieve within 40 s. A similar maximum WAR to that found at CP is reached by the end of the transect, with < 5 g of soil passing through the sieve in 300 s. At M, there is also a very strongly positive relationship between wind abrasion resistance and distance from the coast ($R^2 = 0.97$, $p < 0.01$) (Fig. 8.4, Table 8.3).

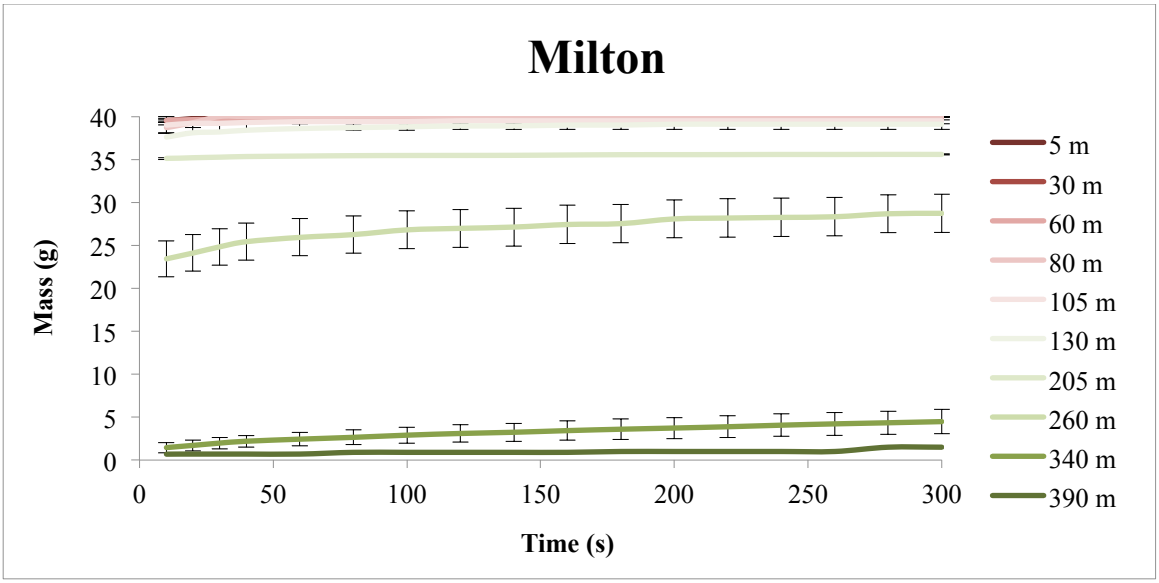

Figure 8.5. M (g) of air-dried soil passing through the rotary sieve over 300 s for samples from M. Labels indicate the distance of the sample from the coast. Error bars indicate 2 x SE.

Table 8.3 Wind abrasion resistance of each sample, and rankings for the samples in terms of distance from the coast (ranked closest to furthest) and abrasion resistance (ranked lowest to highest) at M.

Sample distance from the coast (m)	mean WAR	Rank – distance from the coast	Rank – WAR
5	0.39	1	1
30	0.45	2	3
60	0.42	3	2
80	1.01	4	5
105	0.91	5	4
130	2.03	6	6
205	4.86	7	7
260	16.24	8	8
340	38.42	9	9
390	39.58	10	10

At TB, no relationship is apparent between WAR and distance from the coast (Fig. 8.6). All soils have very low WAR, similar to the WAR of coastal samples at CP and M, with more than 35 g of soil passing through the sieve within 300 s for all samples measured. However, statistical analysis shows a weak positive relationship between WAR and distance from the coast at TB ($R^2 = 0.35$, $p < 0.1$) (Table 8.4, Fig. 8.4), albeit the increase in wind abrasion resistance is of a much lower magnitude than at CP and M.

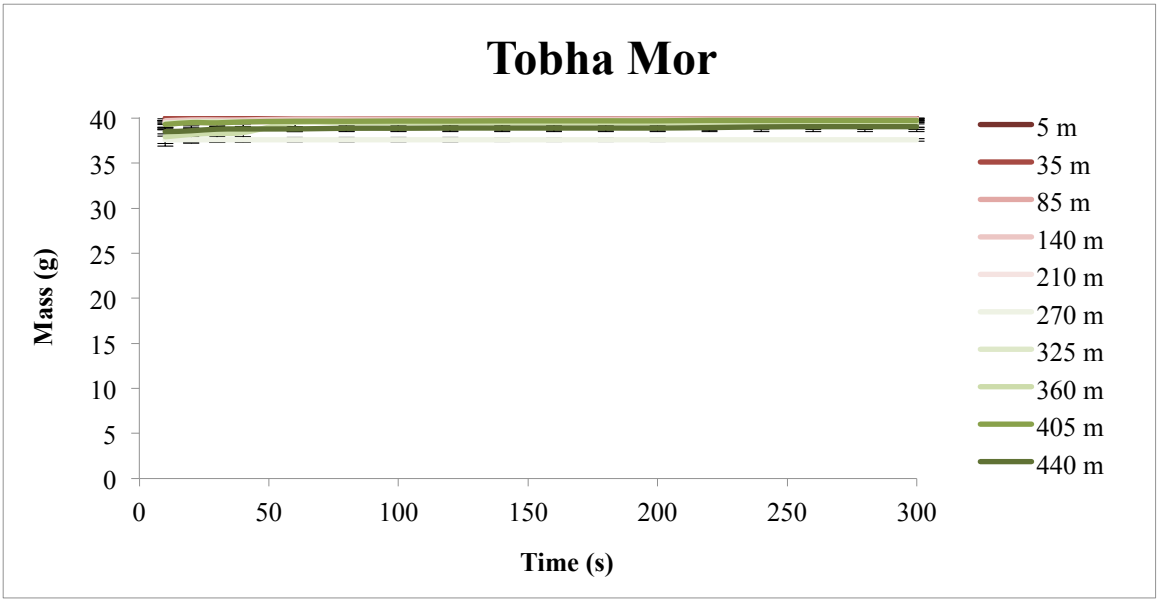

Figure 8.6. Mass (g) of air-dried soil passing through the rotary sieve over 300 s for samples from TB. Labels indicate the distance of the sample from the coast. Error bars indicate 2 x SE.

Table 8.4 Wind abrasion resistance of each sample, and rankings for the samples in terms of distance from the coast (ranked closest to furthest) and abrasion resistance (ranked lowest to highest) at M.

Sample distance from the coast (m)	WAR	Rank – distance from the coast	Rank – WAR
5	0.18	1	2
35	0.08	2	1
85	0.41	3	5
140	0.28	4	4
210	0.25	5	3
270	2.3	6	9
325	0.49	7	6
360	2.5	8	10
405	0.6	9	7
440	1.46	10	8

The shape of the WAR-distance curves supports the decision to classify soil into E and PE fractions, using 40 s as the boundary between these fractions, as in most samples the rate of soil passing was highest in the first 30-50 s. Samples with very low WAR passed through the sieve in as little as 10 s. For some samples from CP and M, abrasion of soil was still continuing after 300 s of sieving.

The high inter- and intra-site variability is evident from box plots of the WAR data (Fig. 8.7). CP and M have similar ranges of WAR, both covering the full range from the minimum (0 g) to maximum (40 g) potential values for wind abrasion resistance. However, the mean WAR at CP is approximately twice that at M, and the majority of samples at M have lower WAR values than at CP. Samples from TB have both a much smaller range of WAR values, and a lower mean value ($p < 0.01$ when compared with CP mean; $p < 0.1$ when compared with M mean). As with CP and M, the minimum WAR at TB is close to the minimum possible value, but the maximum is also close to the minimum possible value, at 2.5 g.

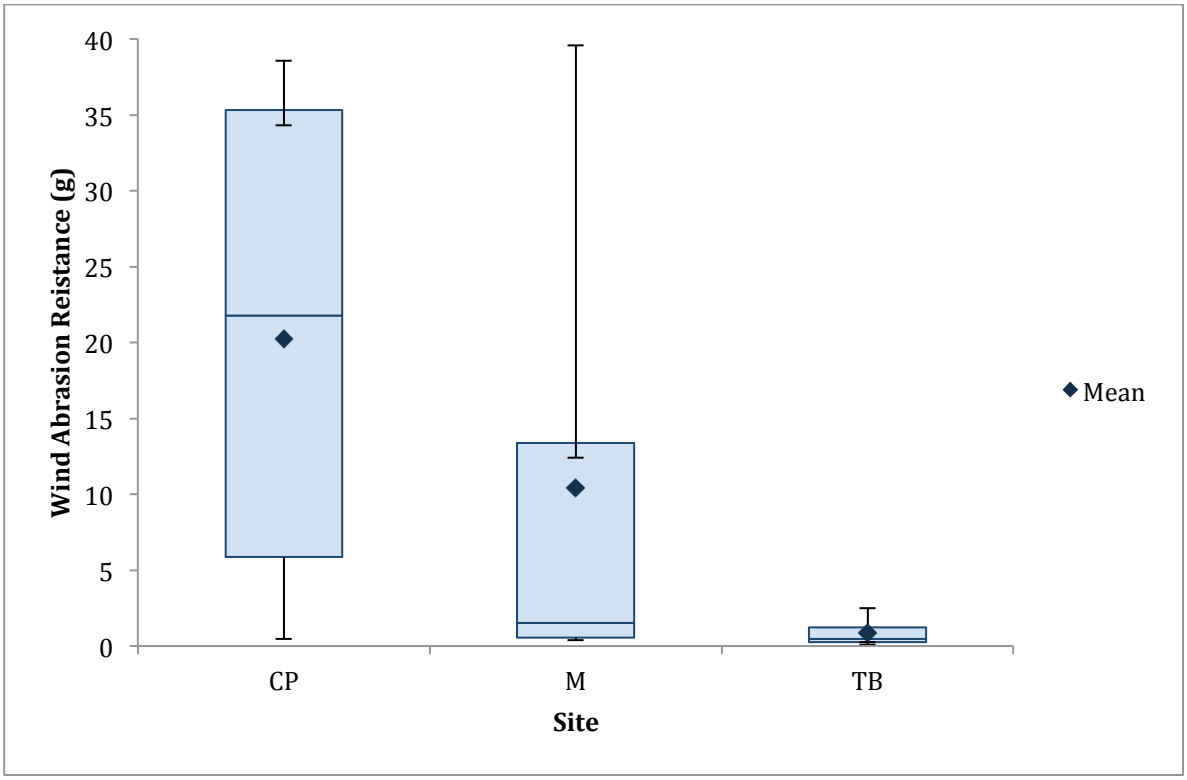

Figure 8.7. Box plot of Wind Abrasion Resistance data from CP, M, and TB showing mean, median and standard deviation.

Note that the transects at M and TB extended for ~ 400 m and ~ 450 m, respectively, while the transect at CP was ~ 250 m. The implications for different distances are discussed in section 8.3.1.1.

8.3.1.1. Erodible, potentially erodible, and non-erodible fractions

At CP, the erodible fraction decreases almost linearly ($R^2 = 0.85$) from ~ 100 % near the coast, to < 10% at the end of the transect (Fig. 8.8). This corresponds to the non-erodible fraction of the soil increasing from < 10% of the sample at the coast to > 90% at the end of the transect. This shift from soil that is predominantly erodible to soil that is predominantly non-erodible occurs gradually over the transect, ~ 250 m. PE material makes up ~ 10-25 % of the sample along the majority of the transect, although the first and final samples are either all erodible or all non-erodible.

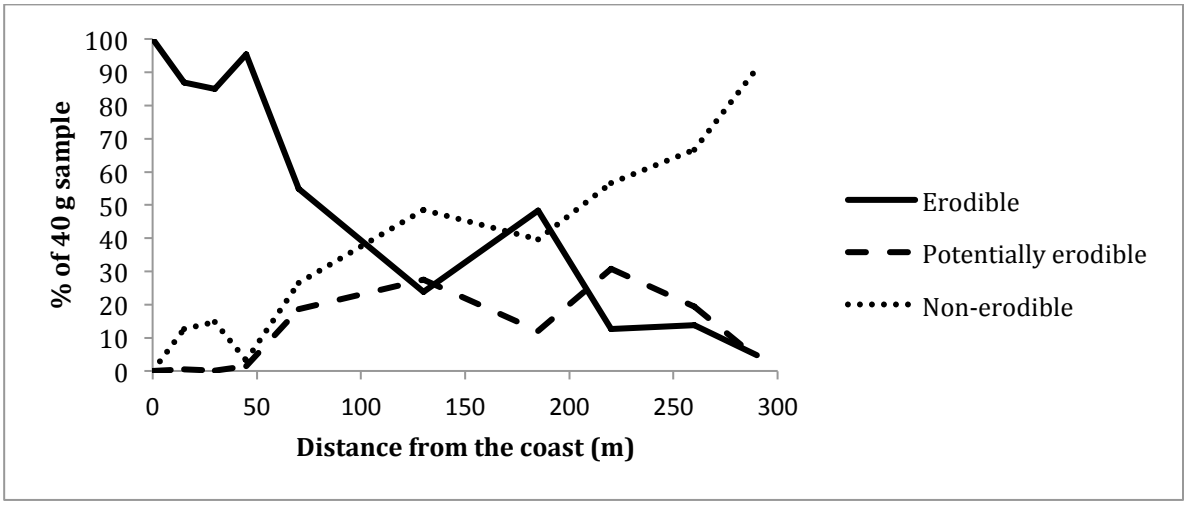

Figure 8.8. Percentage of each 40 g sample that was erodible, potentially erodible, and non-erodible, with distance from the coast at CP.

As at CP, at M there is a switch from samples which are > 90% erodible near the coast to samples which are > 90 % non-erodible at the end of the transect (Fig. 8.9). Although the pattern of change in WAR with relation to distance is different from that at CP (see Fig. 8.4), the key change occurs at approximately the same distance from the coast (~125-175 m). Potentially erodible material is < 10 % at all points along the transect, and is < 5% for the first ~ 250 m.

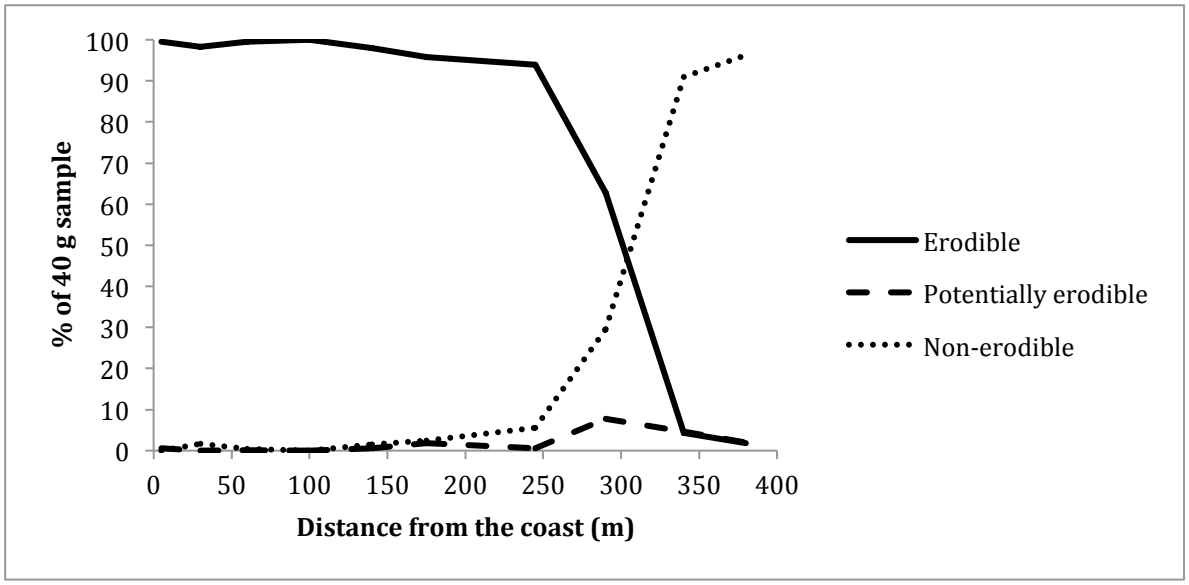

Figure 8.9 Percentage of each 40 g sample that was erodible, potentially erodible, and non-erodible, with distance from the coast at M.

Results from TB show a different pattern from CP and M. At TB there is no switch from predominantly erodible to predominantly non-erodible soil. Samples from all loci along the transect are made up of > 90% erodible material, and no relationship is apparent between the ratios of the three soil fractions to distance from the coast (Fig. 8.10). As at M, there is very little potentially erodible material present in any of the samples, with one sample including ~ 3 % potentially erodible material, and all other samples having < 1 % potentially erodible material.

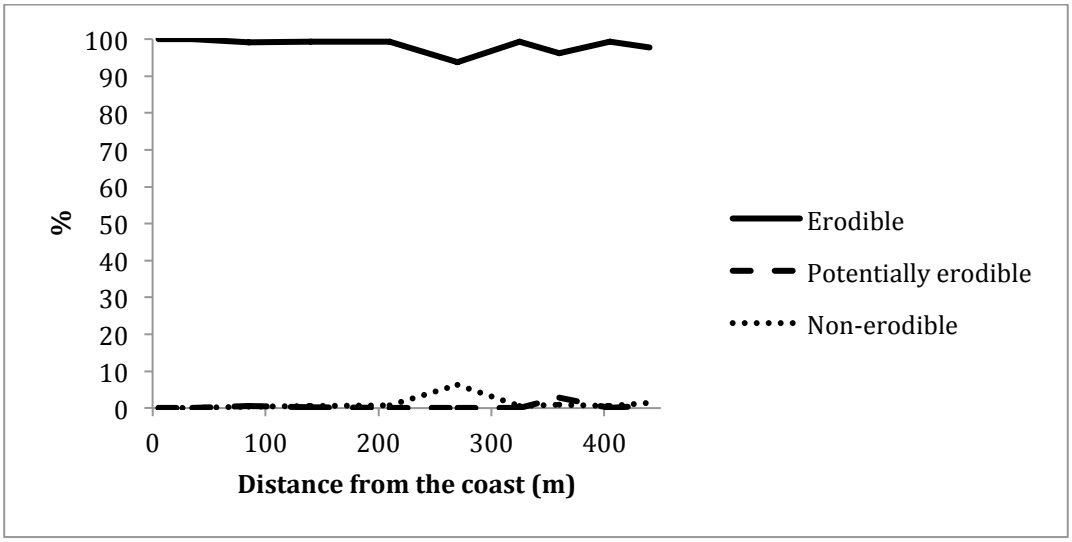

Figure 8.10. Percentage of each 40 g sample that was erodible, potentially erodible, and non-erodible, with distance from the coast at TB.

While results from CP and M show a similar overall trend, there are differences between the transects. The distance along the transect at which the switch from soils which are predominantly erodible to soils which are predominantly non-erodible is ~ 100 m inland at CP, while at M the transition occurs much further inland, at ~ 325 m inland. This does not appear to be a factor of the transect lengths as the transition occurs over a longer distance at CP compared to M, with the non-erodible fraction increasing gradually between 0-300 m inland. At M, the mass of non-erodible material doesn't noticeably increase until ~250 m inland, and reaches > 90% of the sample mass by ~350 m, approximately one third of the distance over which the non-erodible fractions increases at CP. Transect length was dictated by the width of the machair habitat at each site (which varies from a few hundred metres to 2 km), i.e. the full range of variation in soil properties might be expected to occur at all sites as each transect extended from the coastal dunes to the 'blacklands' transition zone.

All sites and samples have very limited PE material. The most PE material is found in samples from CP, peaking at ~ 30 % of the sample mass in samples from the middle of the transect where the switch from soils which consist of predominantly E material to soils which consist of predominantly NE material occurs. At M, the highest proportion of PE material is also found at the distance where the switch from E dominated to NE dominated soil occurs, although this peak is considerably lower than at CP, ~ 8 %. All other samples from M, and all samples from TB, include < 5 % PE material.

8.3.1.2. Particle size analysis (PSA)

While PSA was used to assess whether there was any relationship between particle size and WAR, the percentage of each sieved sample made up of particles > 850 μm was also quantified. This was investigated to determine whether material remaining on the sieve after 300 s (and therefore, classified as NE material) was due to a high aggregate stability or un-aggregated particles with dimensions greater than the sieve mesh size.

The particle size analysis shows that for all samples, > 85 % of the sample by mass consists of particles < 850 μm in diameter, and for most samples (24 out of 30), > 95 % of the sample is made up of particles < 850 μm in diameter (Fig. 8.11). This

demonstrates that the reduction in the mass of soil passing through the sieve with increased distance inland for samples at CP and M is largely attributable to improved aggregation, with particles > 850 μm in diameter accounting for a relatively small proportion of the material remaining on the sieve at the inland ends of the transects at CP and M. For some samples, the amount of sediment passing through the sieve is greater than the percentage of the sample < 850 μm. This may be due to the irregular shapes of calcium carbonate particles, which may be > 850 μm in one dimension, but < 850 μm in others.

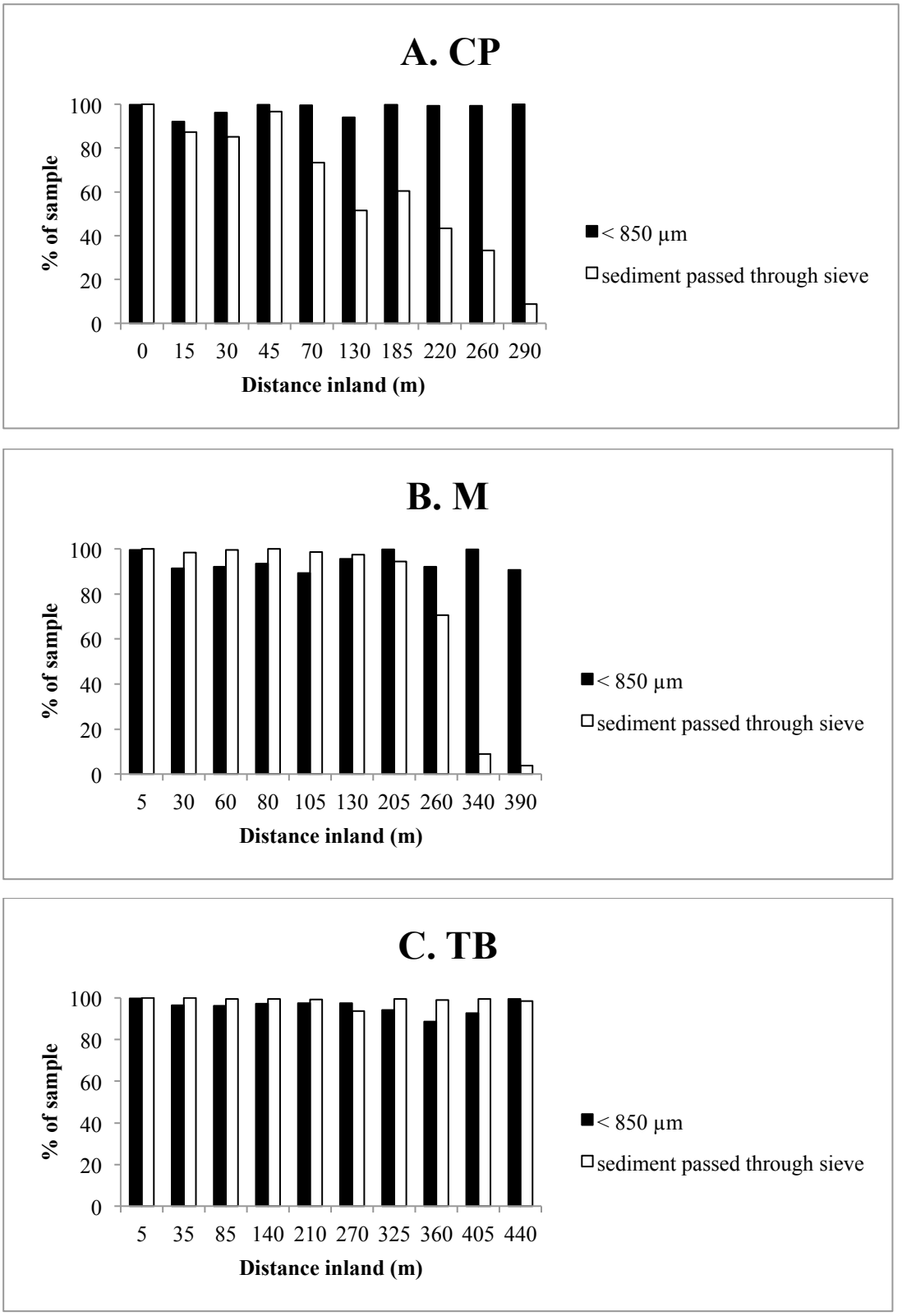

Fig. 8.11. Proportion (by mass) of sample material < 850 µm in diameter to the proportion (by mass) of sample material which passed through the rotary sieve with mesh size 850 µm. A. CP. B. M. C. TB.

8.3.2 Correlations between WAR and other soil properties

Table 8.5 shows correlation values (R) for WAR and all measured soil properties. Very strong positive correlations exist between WAR and Zn, LOI, water content, and As (Fig. 8.12). Weaker, but still statistically significant, positive correlations exists between WAR and Co, distance from the coast, and PS (skewness) (Fig. 8.12). Very strong negative correlations exist between WAR and PS (mean), Sr, and Ca, with weaker, but still statistically significant negative correlations, between WAR and WDPT (class), bulk density, Cr, and Cu (Fig. 8.14). No statistically significant correlation exists for elevation, PS (kurtosis), WDPT (mean time), water repellency, pH, K, Ti, Mn, and Fe (Fig. 8.14).

Figures 8.12-8.14 show considerable inter-site variability in correlations. For example, WAR is very strongly correlated with elevation for samples from CP ($R = -0.96$, $p < 0.01$), while the correlation between WAR and elevation is not statistically significant for samples from TB ($R = 0.22$) (Fig. 8.14a). While some of the soil properties investigated show no clear site effect, other variables show evidence for strong inter-site variation in the range and/or trend of the measured variable. For example, Figure 8.12f showing the relationship between WAR and distance from the coast, shows the same relationship at all sites (positive correlation), but with markedly different gradients for each site. A similar pattern is seen for cobalt (Fig. 8.12e), strontium (Fig. 8.14b), calcium (Fig. 8.13c), bulk density (Fig. 8.13e), manganese (Fig. 8.14g), and iron (Fig. 8.14h). For several of the soil properties, the range of values measured from soil from TB are limited compared to ranges from CP and M, e.g. LOI (Fig. 8.12b), water content (Fig. 8.12c), and strontium (Fig. 8.13b). While several of the correlated variables indicate an approximately linear relationship between the measured variable and WAR, some of the graphs indicate that the relationships may be better characterised by exponential curves (e.g. Figs. 8.12b, 8.14b and 8.14c).

Table 8.5. R values for linear regressions of soil variables against WAR for samples from all sites. Statistical significance (2-tailed T-test) is indicated by asterisks ($p < 0.1$ = *, $p < 0.05$ = **, $p < 0.01$ = ***)

Variable	R	Variable	R^2
Elevation	-0.30	K	0.28
Distance from the coast	0.36*	Ca	-0.71***
WDPT (mean time)	0.02	Sr	-0.79***
WDPT (class)	-0.41**	Ti	-0.24
Water repellency	0.29	Cr	-0.46**
Water content	0.63***	Mn	-0.16
Bulk density	0.42**	Fe	-0.16
PS (mean)	-0.56***	Co	0.44**
PS (skewness)	0.42**	Cu	-0.37**
PS (kurtosis)	0.25	Zn	0.57***
pH	-0.27	As	0.62***
LOI	0.66***		

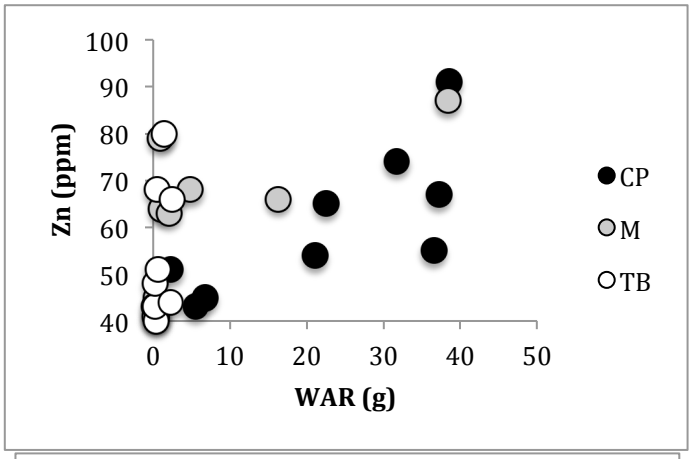
Zn (ppm)
100
90
80
70
60
50
40
0
10
20
30
40
50
WAR (g)
CP
M
TB

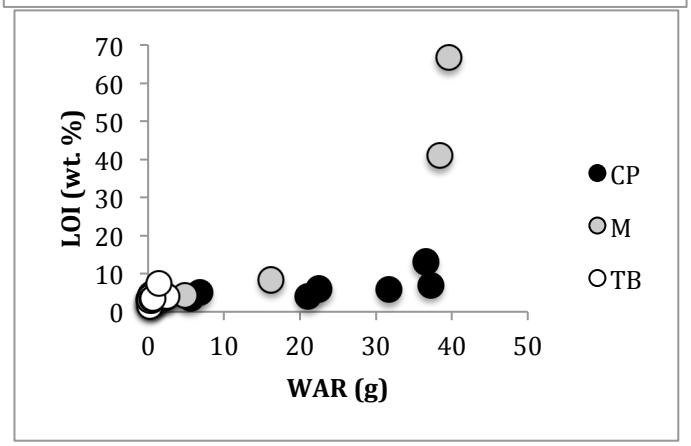
LOI (wt. %)
70
60
50
40
30
20
10
0
0
10
20
30
40
50
WAR (g)
CP
M
TB

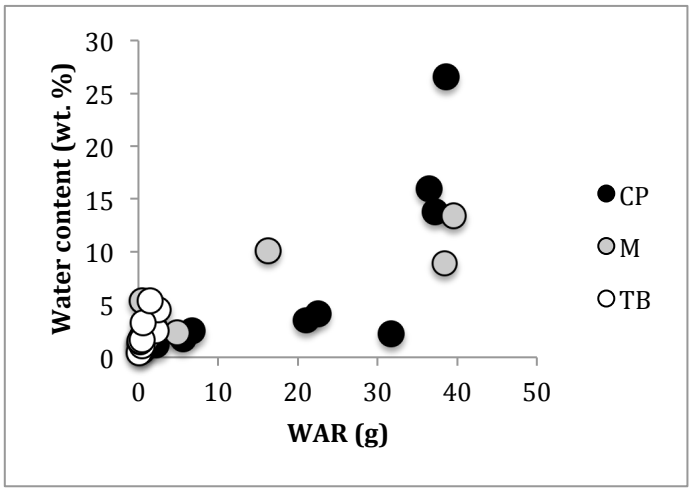
Water content (wt. %)
30
25
20
15
10
5
0
0
10
20
30
40
50
WAR (g)
CP
M
TB

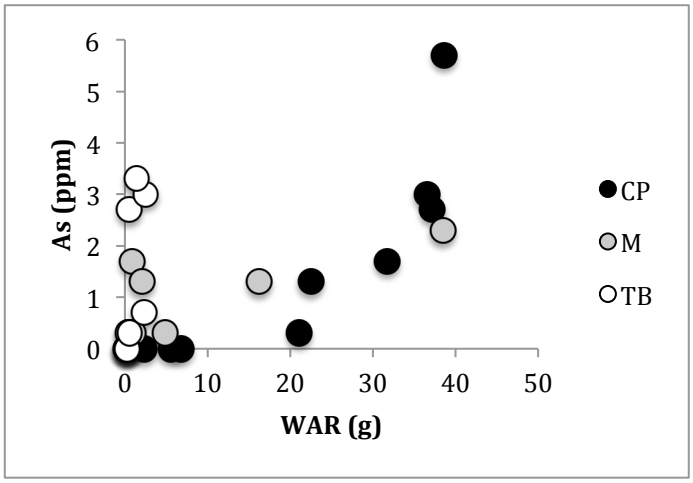
As (ppm)
WAR (g)
CP
M
TB

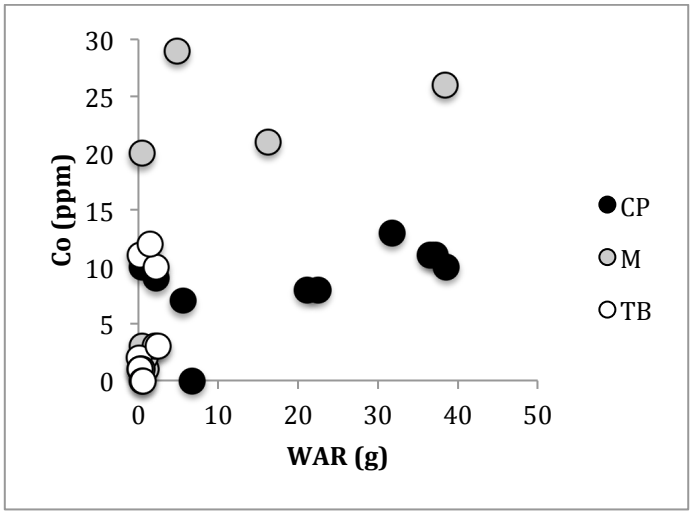
Co (ppm)
WAR (g)
CP
M
TB

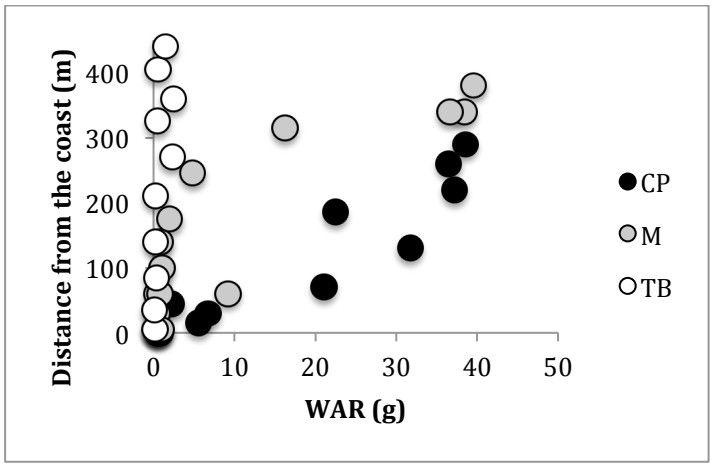
Distance from the coast (m)
WAR (g)
CP
M
TB

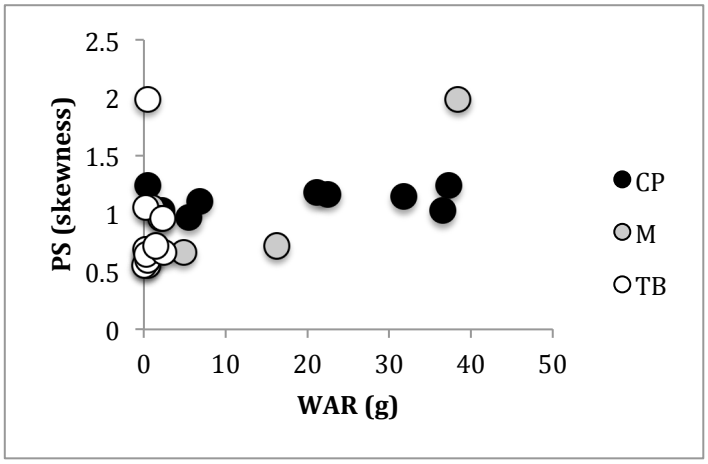

Figure 8.12. Scatterplots of soil properties against WAR for soil properties with statistically significant positive relationships with WAR. a)Zinc, b) LOI, c) water content, d) As, e) Co, f) distance from the coast, g) PS (skewness).

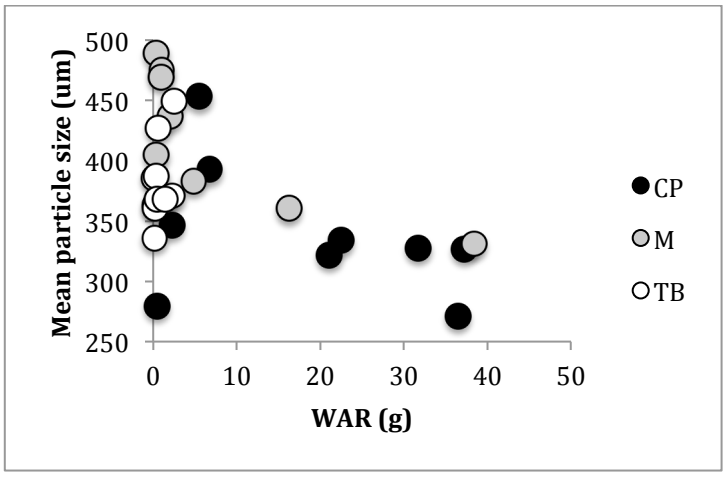

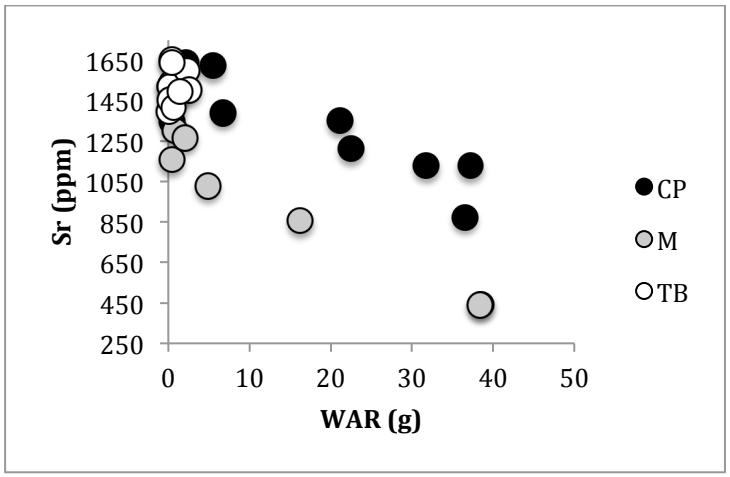

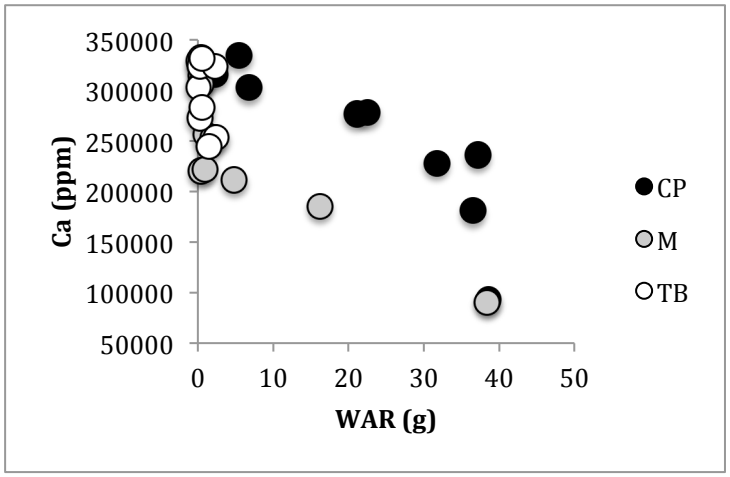
350000
300000
250000
200000
150000
100000
50000
Ca (ppm)
0
10
20
30
40
50
WAR (g)
CP
M
TB

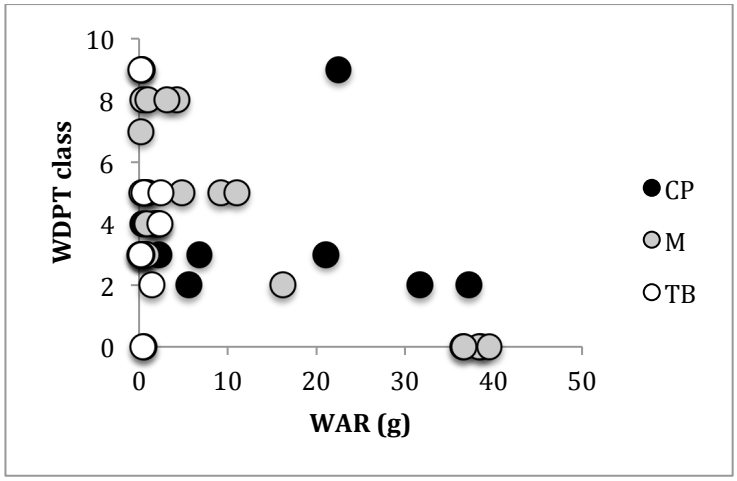
10
8
6
4
2
0
WDPT class
0
10
20
30
40
50
WAR (g)
CP
M
TB

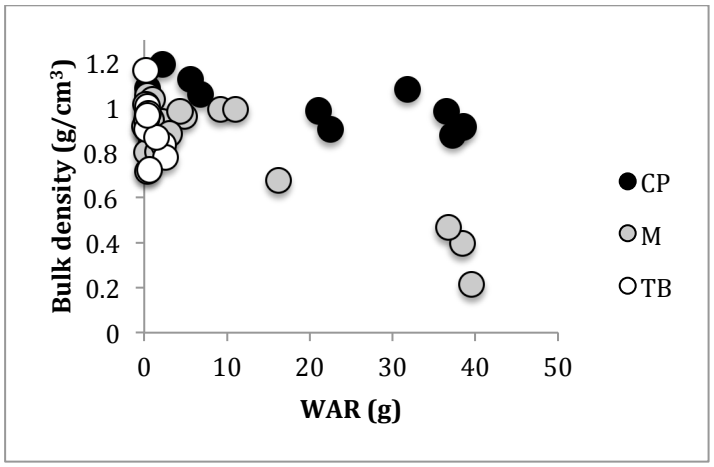
1.2
1
0.8
0.6
0.4
0.2
0
Bulk density (g/cm³)
0
10
20
30
40
50
WAR (g)
CP
M
TB

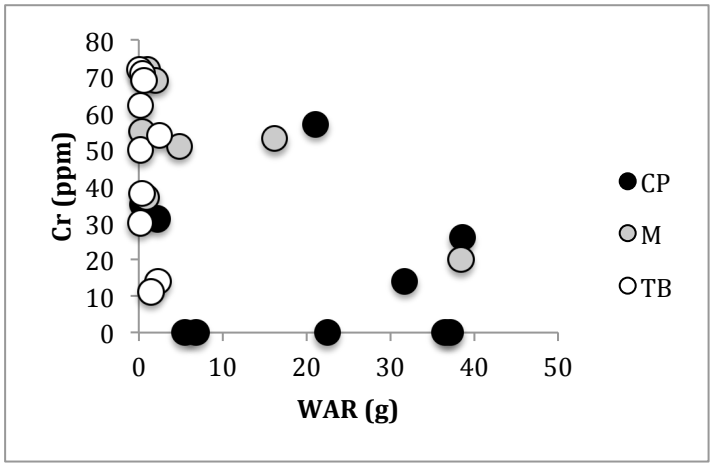

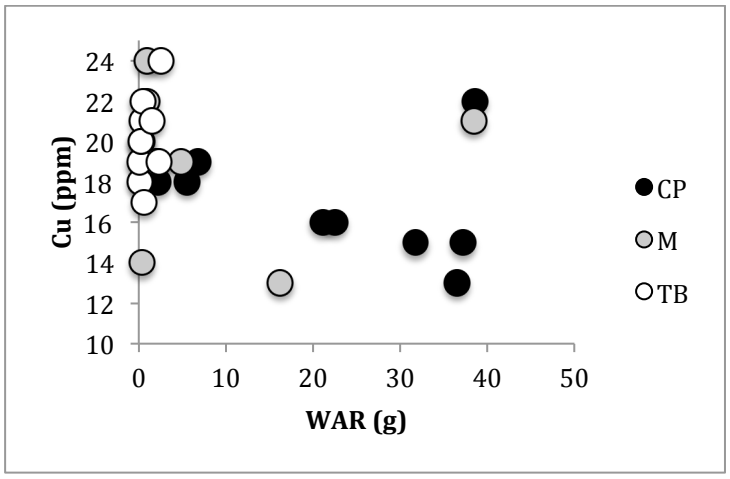

Figure 8.13. Scatterplots of soil properties against WAR for soil properties with statistically significant negative relationships with WAR. a) PS, b) Sr, c) Ca, d) WDPT class, e) bulk density, f) Cr, g) Cu.

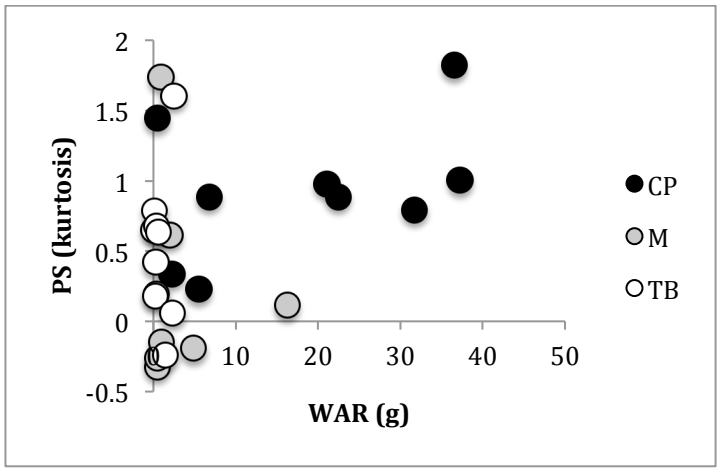

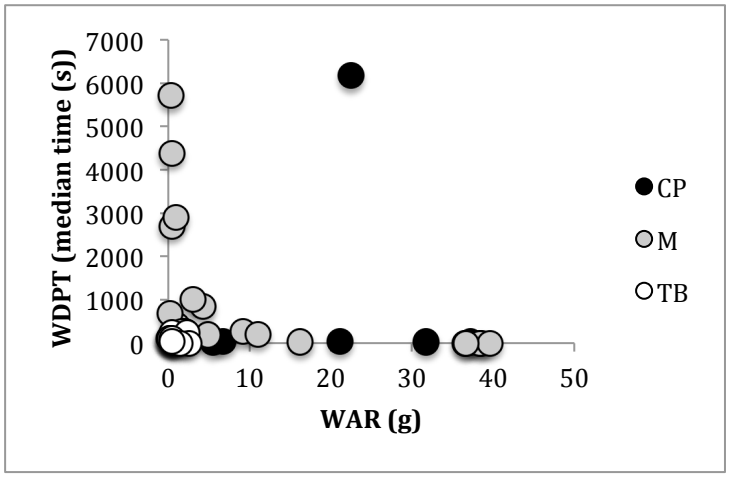
WDPT (median time (s))
7000
6000
5000
4000
3000
2000
1000
0
0
10
20
30
40
50
WAR (g)
CP
M
TB

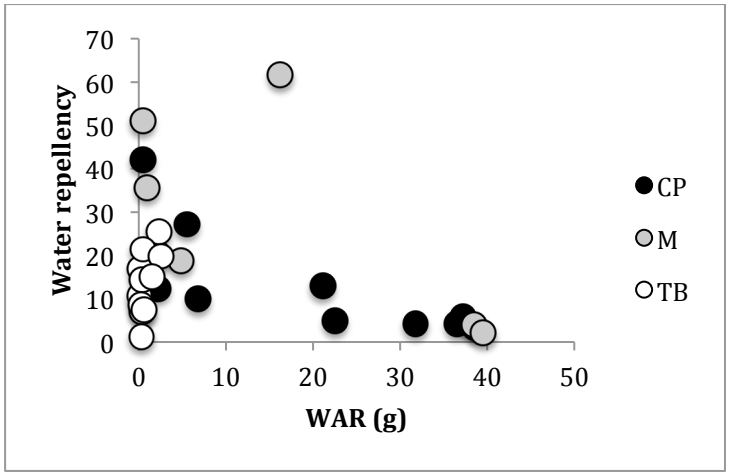
Water repellency
70
60
50
40
30
20
10
0
0
10
20
30
40
50
WAR (g)
CP
M
TB

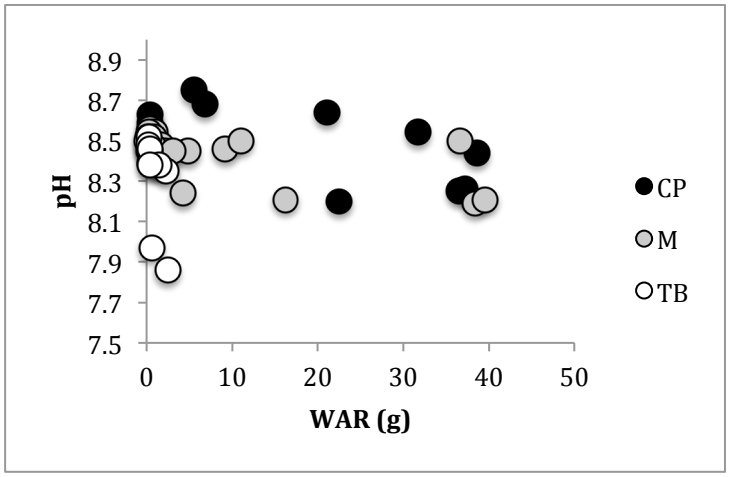
pH
8.9
8.7
8.5
8.3
8.1
7.9
7.7
7.5
0
10
20
30
40
50
WAR (g)
CP
M
TB

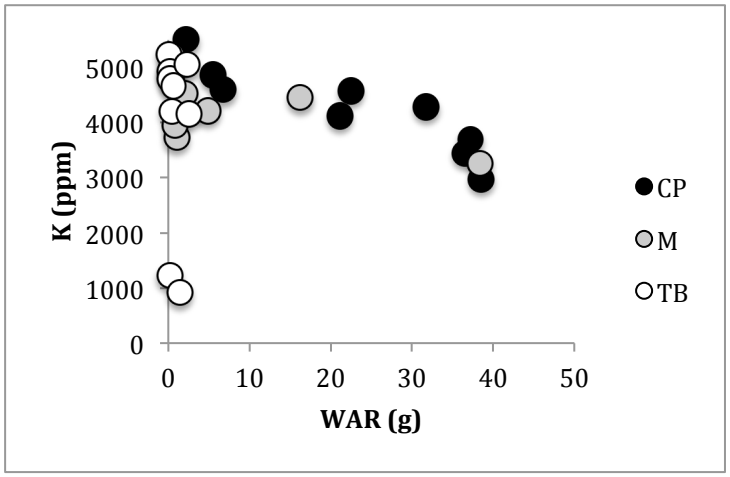
5000
4000
3000
2000
1000
0
K (ppm)
0
10
20
30
40
50
WAR (g)
CP
M
TB

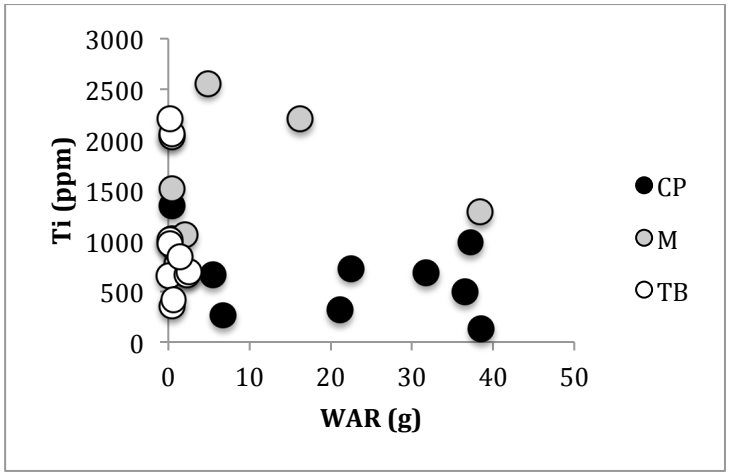
3000
2500
2000
1500
1000
500
0
Ti (ppm)
0
10
20
30
40
50
WAR (g)
CP
M
TB

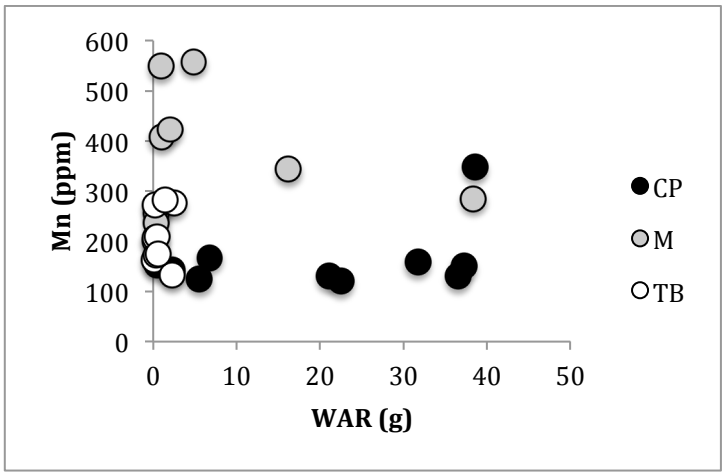
600
500
400
300
200
100
0
Mn (ppm)
0
10
20
30
40
50
WAR (g)
CP
M
TB

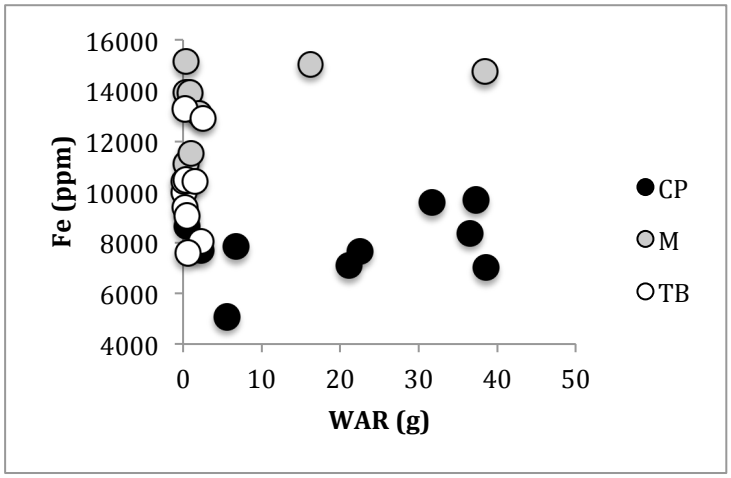

Figure 8.14. Scatterplots of soil properties against WAR for soil properties with no statistically significant relationship with WAR. a) PS (kurtosis), b) WDPT (mean time), c) water repellency, d) pH, e) K, f) Ti, g) Mn, h) Fe.

8.3.3 FTIR

FTIR analysis showed that the base mineralogy for samples from all sites was similar. The composition of all samples was dominated by carbonate and siliceous sands, with low organic matter content, and very low clay mineral content (generally < 1%). For samples from Milton and Cille Pheadair the influence of coastal material (calcareous sands) decreases with distance from the coast, with the mineralogy of inland samples being progressively more influenced by peat soils and the silicate bedrock (Figs. 8.15a and b). This is not the case at Tobha Mor, where the influence of coastal sediments is dominant for all samples (Figs. 8.15a and b).

A.

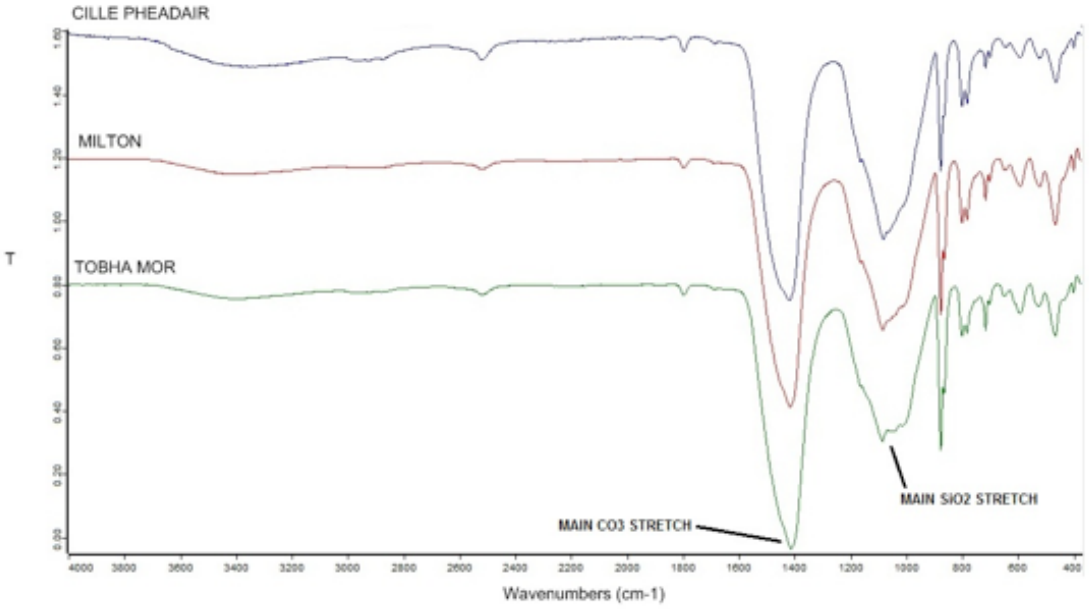

B.

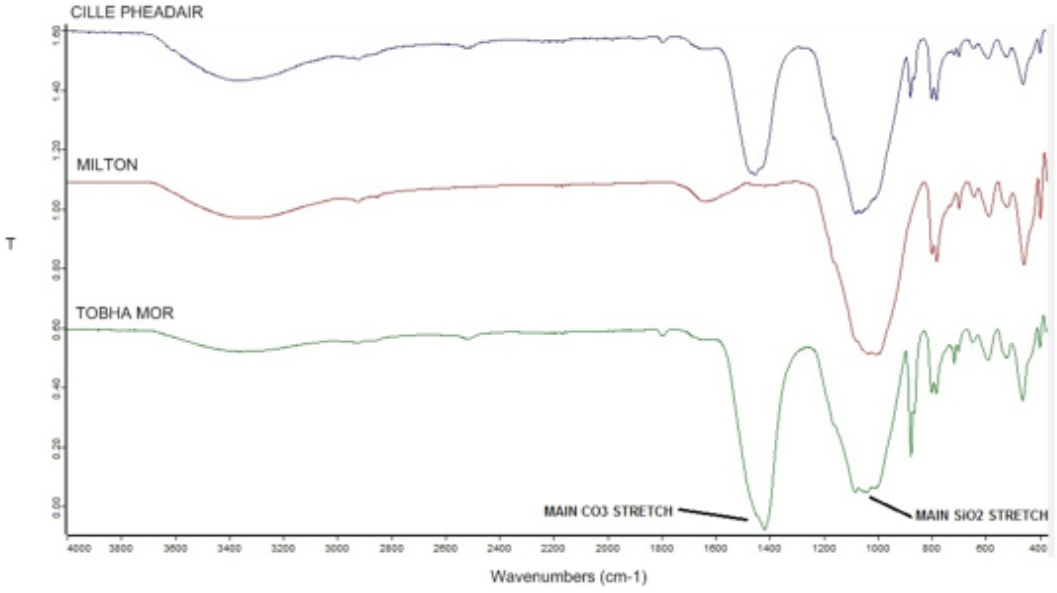

Figure 8.15. FTIR data showing a) spectra for the most coastal sample from each site, and b) spectra for the most inland sample from each site. The main carbonate stretch is located from ~1400-1500 cm^{-1}, while the main silicate stretch is from ~1000-1200 cm^{-1}. A T-shift has been applied to separate the spectra for better visibility.

Samples from the length of the transect at Tobha Mor all have a similar mineralogy, that is predominantly carbonate, although the ratio of carbonate to silicate material drops slightly on moving inland (Figs. 8.15a and b). Organic matter

concentration is very low for all samples as shown by T-values close to 0 from 1700-3800 cm^{-1} for both Tobha Mor spectra in Figure 8.15. At Milton, samples closest to the coast have a dominantly carbonate mineralogy and very little organic carbon (Fig. 8.15a). At the inland end of the transect, samples have very little carbonate, a higher proportion of silicate sand, and higher organic carbon content, with no detectable carbonate material in the sample furthest from the coast (Fig. 8.15b). At Cille Pheadair there is a gradual transition from samples which are predominantly carbonate at the coastal end of the transect (Fig. 8.15a) to samples which are predominantly silicate at the inland of the transect (Fig. 8.15b). Unlike at Milton, there is still some carbonate present in the samples furthest from the coast. There is also an increase in organic carbon with distance from the coast, but this is much less pronounced than the increase seen in samples from Milton.

8.3.3.1 Erodible, potentially-erodible, and non-erodible fractions

Due to the very small amounts of soil which passed through the rotary sieve in the time interval classified as 'potentially erodible', there was insufficient material to analyse the mineralogy of potentially erodible material. However, a subtle but consistent difference is noted between the spectra of E and NE soil fractions for samples from Cille Pheadair (the site which provided the greatest number of comparable E and NE sub-samples). The E fractions have lower silicate to carbonate ratios, and concurrently, the NE fractions have higher silicate to carbonate ratios. The difference appears to be on the order of 5-10% of the absorption band in the spectra. This relationship is seen consistently in samples with organic matter concentrations below 10%, but becomes less obvious for samples with concentrations in excess of 20%. Additionally, E fractions appear to have higher aragonite content than NE fractions. At Milton, the most significant characteristic of the NE fraction is the high organic carbon content when compared to E fractions.

8.3.4 Principal component analysis

Principal component analysis (PCA) was used to investigate which parts of the FTIR spectra i) explained variance between samples, and ii) were correlated with WAR.

It was found that the first, second, and third principal components accounted for 77.7%, 14.2%, and 6.3% of the variance between spectra, respectively. Spectra for principal components 1-3 are shown in Figure 8.16. These highlight at which wavelengths the majority of variation between samples occur. Figure 8.16a shows highest variance at wavelengths ~1400-1550, equivalent to the main carbonate stretch, and some variance at wavelengths ~2500-3750, part of the spectra representing organic carbon, and 0-1250, representing silicate material. Figure 8.16b shows the highest variance for the silicate stretch of the spectra, with some variance at the organic carbon and carbonate parts of the spectra. Figure 8.16c shows the highest variance for the organic carbon stretch, with some variance at the carbonate and silicate stretches.

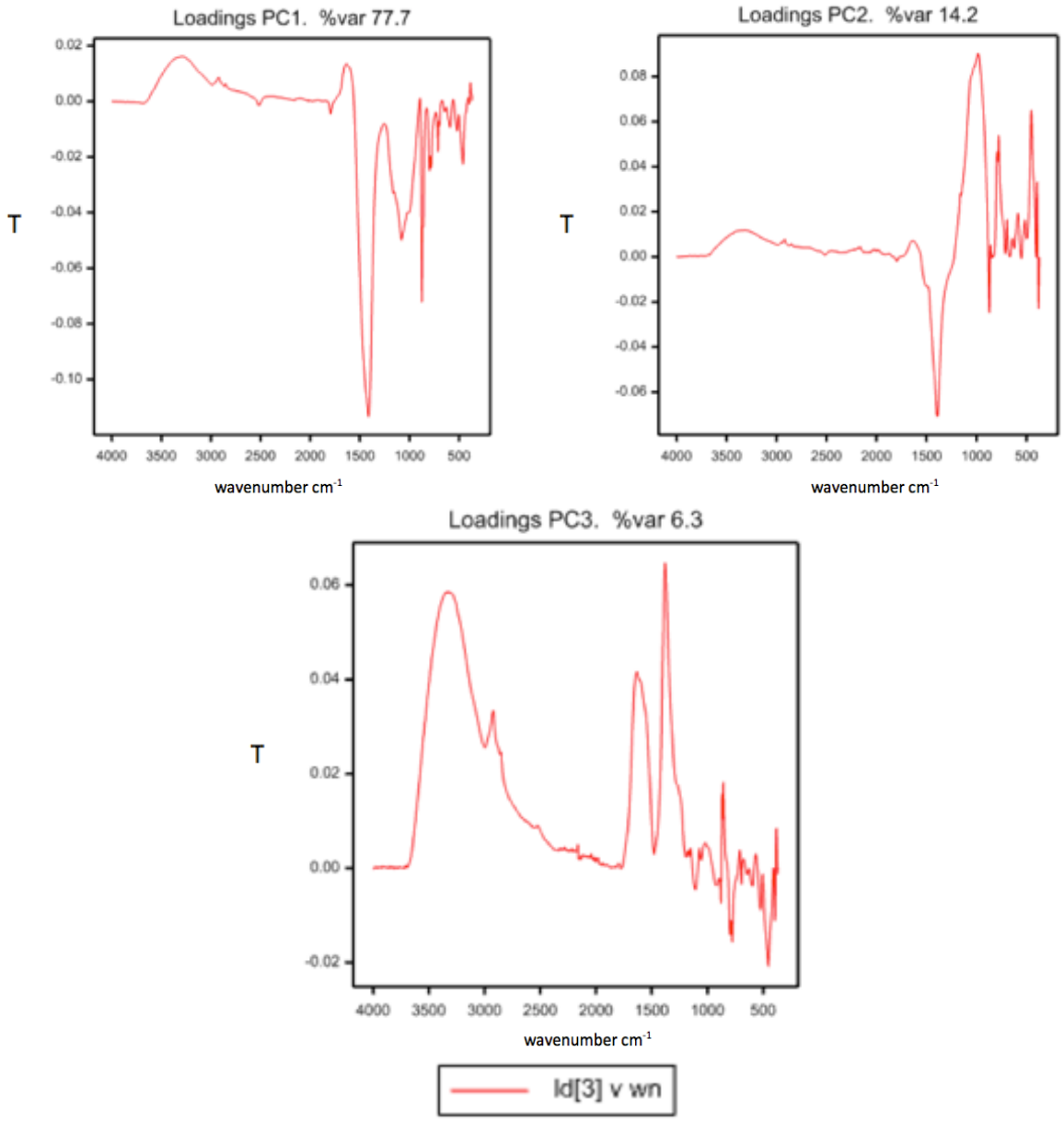

Figure 8.16. Spectra for a) principal component 1, b) principal component 2, c) principal component 3, derived from FTIR spectra for all 19 main transect samples analysed using FTIR.

Regression analysis using the principal components indicated that best predictions of WAR were made using principal components 1-3, and 5. Principal component 4 was not used as it was found to have a lower correlation with WAR than principal component 5, and therefore did not contribute to the regression in terms of accounting for WAR variance. The results of this are shown in Figure 8.17 (adj R^2 = 65.98), and indicate that predicted WAR appears to be closer to actual WAR for lower observed WAR values.

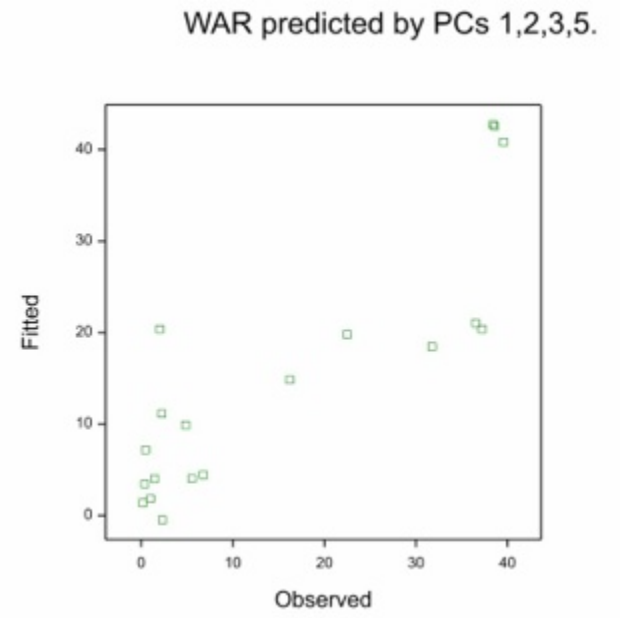

Figure 8.17. Comparison of observed WAR values, and WAR values predicted by principal components 1-3, and 5, derived from FTIR spectra.

8.3.5 Regression analysis

Due to the limited number of samples for which FTIR and XRF data were available (19 main sample transects), a pruned regression tree was generated (as opposed to conducting multiple regression analysis). To prevent over fitting (due to the decreasing size of sub-samples used on moving down the tree), the original regression tree was pruned to predict WAR using four key variables (WDPT class, mean particle size, As content, and water content) which provided minimum error with the dataset the tree was generated from (Fig. 8.18).

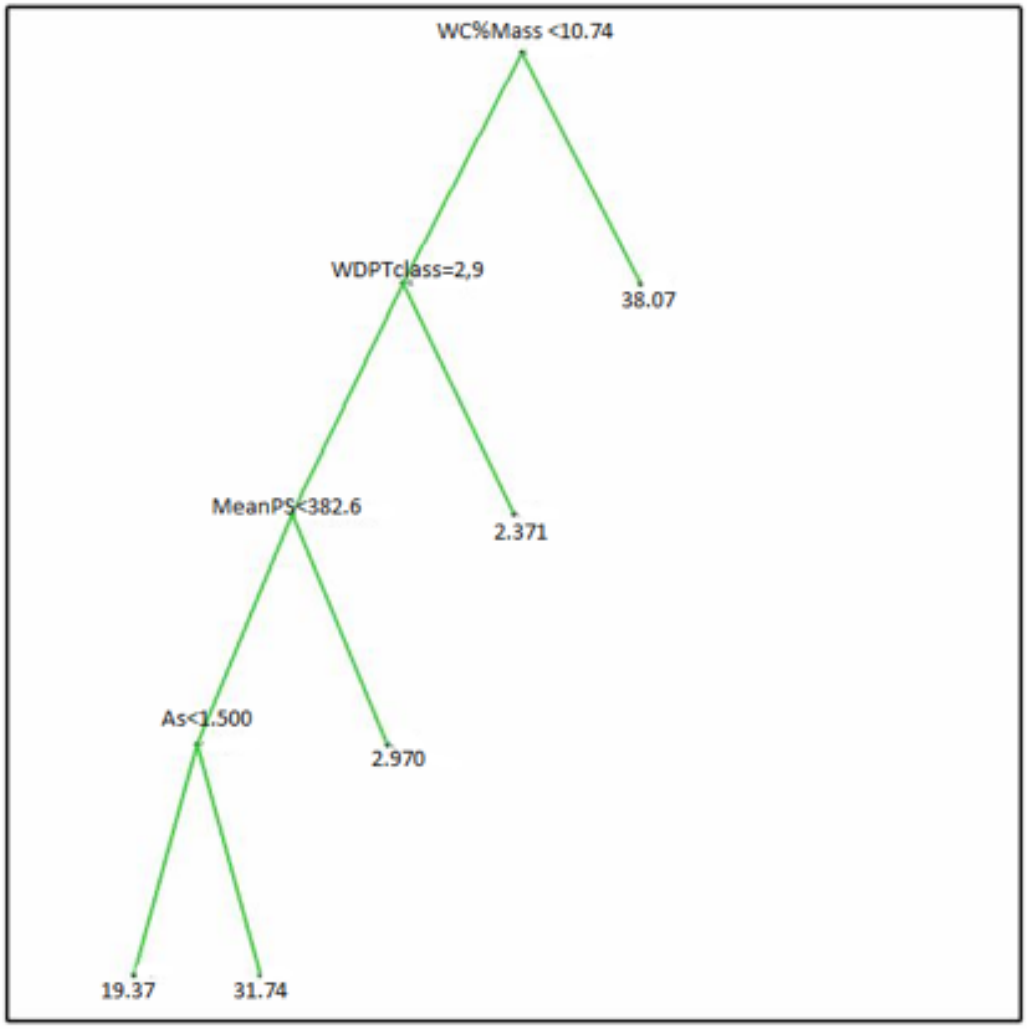

Figure 8.18. The pruned regression tree using to predict WAR from WDPT class, water content (% by mass), As content (ppm), and mean particle size (μm).

The ability of the regression tree to predict WAR was then tested using two further sample sets, one containing 13 samples which had low WAR values (< 5), and one containing 11 samples which had low, medium, and high WAR values (0-40). The regression tree was found to be incapable of accurately predicting WAR for the 13 samples which had low WAR values. When samples with a range of WAR values were used to test the tree it was found that the pruned regression tree was capable of predicting whether a sample would have low (WAR < 15), medium (15 < WAR < 35), or high WAR (WAR > 35) (Fig. 8.19). However, the pruned tree is not capable of predicting variations within these three bands. This may be due to the limited number of samples available to generate the model (due to limitations on the number of samples for which full physical and chemical analysis – including FTIR and XRF – could be

conducted), and the poor coverage of WAR values measured in the samples (e.g. the majority of samples measured had low or high WAR values, with very few samples falling into the 'medium' category of WAR).

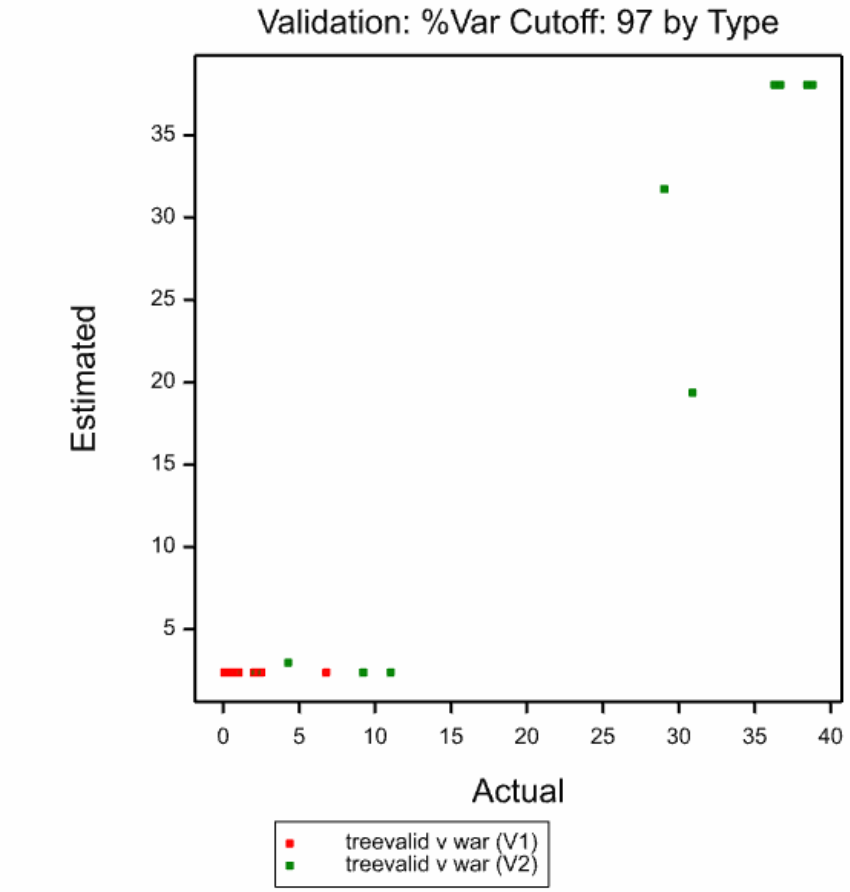

Figure 8.19. Comparison of measured and predicted WAR values. V1 = initial samples used for validation; V2 = additional samples used for validation. N = 24.

8.4 Interpretations

This chapter investigated and quantified spatial variability of wind abrasion resistance (WAR) as a surrogate for the sensitivity of machair soils to wind erosion. To be consistent with documented changes in machair soil properties with distance from

the coast (e.g. Randall, 2004), it was expected that WAR would be lowest at the coastal ends of cultivated strips, and highest at the inland ends. The properties that were correlated with WAR were also investigated. The literature review suggested that organic matter concentration and the proportions of carbonate to silicate sand would influence WAR; the former widely acknowledged as influencing soil erodibility (e.g. Chepil, 1954, 1955), and the latter discussed specifically in relation to machair soils (e.g. Randall, 2004), as well as in the wider soil science literature (e.g. Chepil, 1954). Generally, where organic matter concentration is low and carbonate content is high, WAR was predicted to be highest, and *vice versa*. Chemical and physical differences between erodible (E), non-erodible (NE), and potentially erodible (PE) material (as determined by rotary sieving) were also characterised. The implications for management - particularly in relation to dunes and back dunes which are key areas for coastal change – are also discussed.

8.4.1 Sensitivity of machair soils to wind erosion

At two of the investigated sites, CP and M, WAR was, as expected, positively correlated with distance from the coast. At the third site, TB, no relationship was found between WAR and distance from the coast. Statistical analysis showed a positive correlation at TB, but the increase in WAR was an order of magnitude higher at CP and M. At CP and M, WAR values ranged from close to the minimum (0) to close to the maximum possible values (40), indicating a dramatic change in WAR on moving inland. At TB, all values were close to the minimum. The nature of the relationship between WAR and distance from the coast was also different between CP (approximately linear) and M (broken stick or exponential increase to maximum value).

The above results partially support the perception that the machair grasslands are susceptible to wind erosion (Mate, 1992; Ritchie et al., 2001). However, there are significant inland sections of CP and M that have considerable WAR. Soils are considered non-erodible by wind if the mass of air-dry aggregates > 850 μm exceeds 40% of the mass (Leys et al., 1996). Applying this to the machair soil samples would indicate that any sample which retained ≥ 16 g on the sieve would be classified as non-erodible by wind. On this basis, at CP soils > 130 m and at M soils > 340 m inland from the coast would be considered non-erodible by wind. While at TB the majority of

samples appear to have very low WAR, at CP and M, as well as the soils which would be classified as non-erodible, many of the samples have intermediate values of WAR, indicating that over large parts of the machair soils have some resistance to wind abrasion. Of particular significance are the findings presented in section 8.3.1.2, which indicate that higher WAR is attributable to aggregation rather than larger particle size. Further investigation of aggregation processes in machair soils would be beneficial to enhance management strategies aimed at increasing aggregation. It should be noted that results relate to the topsoil only; where the subsoil is exposed (e.g. by rabbit burrowing, ploughing), WAR is likely to be lower than measured values due to lower organic matter concentration with depth.

The significant differences between trends in WAR at the three sites investigated makes it difficult to draw conclusions about the WAR of machair soils as whole. Evidently there is significant variation between machair systems within one island. Without further investigation of other machair systems in South Uist and other areas of Scotland and Ireland, it is not possible to determine which relationship between WAR and distance from the coast is more typical of the machair, or whether high variability between systems would be found throughout other machair areas.

During rotary sieving, samples were split into erodible (E), potentially erodible (PE), and non-erodible (NE) categories. As a result of this, it was found that all of the soil samples contained relatively little material that was classified as PE. At M and TB, PE material consistently accounted for $< 10\%$ of the sample mass. At CP there was slightly more PE material ($\leq 30\%$), particularly over the transition between erodible and non-erodible soils. At M, the highest percentages of PE material are also found over the transition area. Little PE material at TB, most of M, and either end of CP suggest that most machair soils are almost entirely composed of non-erodible material or erodible material, and that wind abrasion has limited potential to break down non-erodible material to form erodible material. However, in the case of the machair soils, the decrease occurs abruptly rather than gradually for the majority of samples. It is only at CP that there is much evidence for breakdown of aggregates by wind abrasion.

8.4.2 Soil properties related to WAR and prediction of WAR

Since a range of relationships between WAR and distance from the coast were found, determining which soil properties were correlated with WAR was pursued as a means to predict WAR. Statistically strong regression coefficients were found between WAR and mean particle size, field-moist water content, organic matter concentration, zinc, arsenic, strontium, and calcium. Principal component analysis (PCA) of Fourier transform infrared (FTIR) spectra indicated that carbonate, silicate, and organic matter were correlated with WAR. Using a pruned regression tree to predict WAR, mean particle size, water drop penetration time (WDPT), water content, and arsenic concentration were identified as the soil properties that might best predict WAR.

A strong positive correlation between WAR and organic matter concentration was expected as improved aggregate formation is observed with higher organic matter concentrations (Chepil 1954, 1955). The relative concentrations of carbonate and silicate based sand were also expected to affect sensitivity to wind erosion due to the different shapes, sizes, and densities of particles of carbonate and silicate sand, and the effects of these variations on entrainment and transport (Ritchie, 1974). The results from FTIR analysis suggest that higher ratios of carbonate to silicate material are correlated with lower WAR. However, the method used to assess sensitivity to wind erosion by assessing WAR does not test for preferential entrainment or duration of transport. This suggests that the carbonate/silicate ratio affects aggregate strength and/or formation, as well as potentially influencing transport dynamics. Previous studies have found mixed relationships between carbonate and WAR. Black and Chanasyk (1989) found that adding carbonate to soil at concentrations < 10% decreased WAR, while Chepil (1954) found that increasing calcium carbonate from 3% to 10% led to an increase WAR in a highly erodible soil. The former finding is more consistent with the FTIR results from Chapter 8, that indicate for soil samples with low organic matter concentration (i.e. generally more susceptible to wind erosion), higher ratios of carbonate to silicate were correlated with lower WAR, while at higher soil organic matter concentrations the ratio had no apparent effect, and soil organic matter was the dominant control on WAR. The predictions of WAR using PCA were generally more accurate at lower actual values of WAR (< 15). This may be due to the significance of carbonate (PC1) and silicate (PC2) wavelengths in the predictions; which appear, from

the FTIR data to influence WAR where organic matter concentrations are low (< 10%). Furthermore, FTIR analysis showed that non-erodible soil fractions generally contained slightly less carbonate material than their erodible counterparts (typically 5-10% less).

That mean particle size was negatively correlated with WAR may be linked to the results for carbonate by differences in the shape, size, and density of carbonate particles relative to silicate particles. However, the relationship between coarser soil texture and low WAR is widely acknowledged (e.g. Chepil, 1958; Black and Chanasyk, 1998), and appears to be generally true for a range of soil mineralogies.

The results for soil properties related to water are also in agreement with previous findings. An increased water content generally improves wind abrasion resistance by enhancing cohesion between particles and aggregates (Chepil, 1953). This may be related to the strong positive correlation found between water content and WAR; increased water content in samples prior to drying may be linked to water held in clay, or may be related to organic matter concentration. Regression tree analysis also identified WDPT class as a key property for predicting WAR. WDPT is a measure of the persistence of water repellence. For the machair soils, more persistent water repellence was correlated with lower WAR. The effect of water repellency on erosion is more frequently considered with relation to erosion by water, where water repellency is generally correlated with increased erosion by water due to low infiltration, leading to low water contents, reduced cohesion, and greater susceptibility to topsoil erosion during overland flow events (e.g. Wessel, 2006). The same mechanism is likely to increase sensitivity to wind erosion; lower water infiltration may lead to reduced cohesion between particles.

Some of the significant correlations between WAR and elements (investigated using XRF analysis) are unexpected. While the strong negative correlation between calcium and WAR is to be expected as a consequence of presence of calcium in calcium carbonate, the strong positive correlations between WAR and zinc and arsenic, and the strong negative correlation between WAR and strontium are harder to explain. The relationship with arsenic may be due to the use of seaweed fertiliser on the machair, which is linked to high soil arsenic concentrations (Castlehouse et al., 2003). This would imply that the use of seaweed fertiliser may improve soil wind abrasion resistance. This is in contrast with the findings of Thorsen et al. (2010), who showed that the application of kelp to machair soils did not improve soil aggregation, but in

agreement with local perceptions that using seaweed as fertiliser reduces soil erosion by wind (Angus, 2001). It should be noted that plotting arsenic against WAR indicates that there is no relationship between arsenic and WAR at Tobha Mor, and the relationship appears to be strongest at Cille Pheadair. This suggests that the relationship between arsenic and wind abrasion resistance may be complicated, and possibly dependent on other soil properties, e.g. mineralogy, or management factors, e.g. the historic application of seaweed fertiliser. It is difficult to provide a rationale for the relationships between zinc and strontium and WAR, as these elements seem unlikely to influence WAR. The apparent relationship between WAR and these elements may be a product of changing concentrations of these elements with distance from the coast and a subsequent change in parent material, coastal/marine influence, etc. (e.g. Randall (2004) showed changes in potassium, magnesium, and sodium with distance from the coast on soils from the Monach Isles). This is supported by the data from TB, which shows an increase in zinc concentrations (sometimes used as an addition to fertiliser to promote increased plant growth) and a decrease in strontium concentrations with distance from the coast, despite showing no change in WAR values.

The two approaches used to predict WAR (PCA, regression tree) indicated that the concentrations of carbonate, silicate, and organic matter (PCA prediction of WAR), and WDPT class, mean particle size, water content, and arsenic (regression tree prediction of WAR) were key variables to estimate wind abrasion resistance. For each of these a mechanism of action can be proposed. However, the absence of organic matter from the latter set of properties, and its relatively low significance in the former (PC3, explaining 6.3% of variance) is surprising given that the relationship between organic matter and WAR is widely recognised and generally strong. However, the concentrations of organic matter here are very low (< 5%) for many of the soils samples and hence may not be present in sufficient concentrations to significantly improve WAR, with the results that other soil properties may have more influence.

8.4.3 Implications for management

The results for trends and variations in WAR and other soil properties are consistent with findings that show considerable variation in soil character on moving across the cultivated machair from the coast to the blacklands (e.g. Ritchie, 1974;

Randall, 2004; Angus, 2006). However, they also indicate considerable inter-site variation in the trends observed, the range of WAR values, and the distances over which changes in erodibility occur. The implications of these finding are that a 'blanket' approach for improving soil stability may not be appropriate; instead, management may need to be tailored to conditions found at specific sites. For example, soil properties and erodibility 250 m from the coast vary dramatically between sites; at this distance from the coast at CP WAR is reasonably high, and there may be no need for intervention to improve WAR, while at TB and M, WAR is very low at this distance, and could usefully be improved.

Some of the properties identified as corresponding to high WAR can be roughly estimated relatively easily in the field, for example, the amount of soil organic matter, water content, and the relative abundance of silicate and carbonate sand. Although the methods used to model WAR were unable to accurately predict WAR values from soil properties, they provided reasonable estimations of whether WAR was high, intermediate, or low which may be more useful in terms of management than an exact value given the large range of WAR values found.

With regards to the proximity of cultivation to the dune crest, the results clearly indicate that at all sites erodibility is very low at this end of the cultivated strips. This is of particular concern at Cille Pheadair, where cultivated land stretches to within a few metres of the eroding dune crest. During several site visits sand entrainment was visible, with sand being transported from the ploughed fields and blown inland. While the transfer of sand is a natural part of machair sediment dynamics, the lack of dune vegetation at Cille Pheadair and the proximity of cultivation to the dune crest makes the replacement of lost sand unlikely. In contrast to Cille Pheadair, an area of dune vegetation (~ 20-30 m wide) is left uncultivated at Milton and Tobha Mor. It may be beneficial to leave such a margin at the coastal end of all cultivated areas where coastal erosion is a risk, and/or to maximise measures to prevent soil erosion over areas of low WAR close to the coast.

8.4.4 Critique

The results were from a set of soil samples taken at one time, and therefore it is possible that they may not represent soil conditions – and soil WAR – throughout the

year. Samples were taken in June 2012, following an unusually dry period of weather. Therefore, soil water content results are likely to be close to the minimum for machair soil, and WAR values may be lower than at other times due to the extremely dry nature of the soil at the time of sampling. Additionally, all samples were taken from cultivated areas of machair grassland that appeared to be in 1st or 2nd year fallow (this assumption was confirmed by crofters for two of the sites), i.e. it was without the scope of this investigation to consider variations in WAR and soil properties between different stages of cultivation. Results are therefore unlikely to have been influenced by the recent application of fertilisers, recent ploughing, etc., however it is acknowledged that different histories of management may have influenced results. The timing of soil sampling (early summer) does coincide with the period when machair soils are most likely to be at risk from wind erosion – soils are bare due to lack of crop growth following ploughing, and the water table is low due to the comparative dryness of sprin and summer.

The high inter-site variability in trends and ranges of WAR and other soil properties mean that further work would be needed to determine which trend is the norm for the machair grasslands, or whether there is a norm at all. The inclusion of cross-transect sampling confirmed that the majority of variation occurred on moving inland from the coast. However, cross-transect sampling was limited to the width of the strip being investigated, resulting in uncertainty as to how far up or down the machair trends in WAR and other soil properties would remain similar.

From the comparison of particles < 850 μm (see section 8.3.1.2) with material passing through the sieve it is evident that there is a slight mis-match, with the amount of sediment passing through the sieve exceeding the amount of material < 850 μm. The mis-match may be due to the irregular, platy shape of shell sand material, that may be able to pass through the sieve mesh in some orientations but not others.

The low amount of PE material from the majority of samples may indicate the limits of this concept with regards to machair soils. Indeed, for the majority of samples observation of the sieving process revealed that machair soil was composed of either i) readily erodible material (passing through the sieve in < 10 s), ii) aggregates with high resistance to abrasion (remaining on the sieve for 300 s), or iii) a combination of i) and ii), with relatively low amounts of material that could be broken down by sieving. However, as the full range of WAR measurement was used and applicable to soil

samples (i.e. WAR values from 0-40 were obtained) the general approach to assessing WAR appears to be robust and a good discriminator. Further analysis of the properties of PE material might reveal more information on the intermediate steps in the process of machair soil aggregation. It was not possible to conduct the majority of soil analyses on PE material due to the very low amounts of it obtained.

With regards to predicting WAR, it is evident that neither principal component analysis nor the pruned regression tree was able to accurately predict observed values of WAR from soil properties. However, both methods were able to provide a reasonable estimation of whether WAR would be low, medium, or high, and principal component analysis appeared to have a better ability to predict WAR at low actual values. This may be sufficient for management purposes. There are several possible reasons for the inaccuracy of the models. Firstly, the number of samples that could be analysed using FTIR analysis was limited so the number of main transect samples available for inclusion in the models was low, particularly as additional samples were required to validate the models. A second major issue is the relatively poor 'coverage' of WAR values measured, i.e. the majority of samples had either very low or very high WAR values; very few samples had intermediate values of WAR, and these were mostly from one site (Cille Pheadair). It is probable that the models' ability to predict WAR would be improved by increasing the input sample size, although whether this would provide any additional information of use in terms of management is debatable.

8.5 Key Findings

8.5.1 Sensitivity to wind erosion

There are significant intra- and inter-site variations in sensitivity to wind erosion. At one site studied (Tobha Mor), WAR shows no apparent relationship with distance from the coast, remaining low along the length of the transect. At the other two sites (Milton and Cille Pheadair), a positive relationship is demonstrated between WAR and distance from the coast. However, the shape of the relationship is different, with WAR increasing linearly at CP, and in a broken stick form at M. Dividing samples into erodible (E), potentially erodible (PE), and non-erodible (NE) material revealed that very little PE material was present in the majority of samples (generally < 20%).

8.5.2 Correlations between WAR and soil properties

WAR is strongly correlated with zinc concentration, organic matter content, water content, arsenic concentration, mean particle size, strontium concentration, and calcium concentration. Weaker, but still statistically significant, correlations exist between WAR and cobalt concentration, distance from the coast, the skewness of particle size distributions, WDPT class, bulk density, chromium concentration, and copper concentration. Elevation, kurtosis of particle size distribution, mean WDPT time, water repellency, pH, potassium concentration, titanium concentration, manganese concentration, and iron concentration show no statistically significant relationship with WAR. However, there are inter-site variations in the significance and gradient of relationships, and in the range of values observed for each soil property.

8.5.3 Predicting WAR

Results from FTIR analysis suggest that most significant differences between samples with high and low WAR values were related to the ratio of carbonaceous to siliceous material, and the organic matter concentration; a higher ratio of carbonaceous to siliceous material and a lower organic matter concentration appear to be linked to samples with lower WAR values. FTIR analysis of E and NE soil fractions indicated that NE material had slightly lower (5-10%) ratios of carbonaceous to siliceous material. Principal component analysis of the FTIR spectra was able to provide a reasonable estimation (R^2 = 65.98) of measured WAR values, with the principal mineralogical components being linked to carbonate, silicate, and organic material. The predictions appeared to be closer to measured values at lower WAR values.

Using pruned regression trees to predict WAR identified four key variables – mean particle size, WDPT class, arsenic concentration, and water content. Using these variables, it was possible to predict whether WAR was low (< 15), medium (> 15 and < 35), or high (> 35).

CHAPTER 9
DISCUSSION

9.1 Introduction

This thesis investigated and quantified spatial and temporal variations in the relative sensitivity of machair soils and landforms to erosion. Sensitivity was assessed at three sites within the machair of South Uist, two were identified as experiencing high rates of coastal erosion, and one appeared more stable. Differences in erodibility were quantified using a range of proxies to indicate sensitivity (e.g. shoreline position, beach sediment volume, soil wind abrasion resistance (WAR)), over nested temporal scales.

The sensitivity of the machair system to erosion is both spatially and temporally variable on inter- and intra-site levels. The high variability indicates the dynamic nature of the machair system, particularly evidenced by some indicators of sensitivity to erosion that fluctuated in both directions (i.e. accretion and erosion) over different timescales. Short- and long-term analysis of change highlighted the importance of characterising normal system variability to separate trends from fluctuations. All results indicate the hazards and drawbacks of 'snapshot' measurements to assess sensitivity, e.g. a single measure of soil WAR per site may lead to erroneous identification as sensitive/insensitive to wind erosion. Similarly, shoreline change from the position of mean high water at ordinary spring tide (MHWOST) with a temporal separation of decades between datasets, may indicate high net erosion or accretion, when the measured difference may be within seasonal or annual fluctuations. The high variability also leads to major differences in the magnitude and direction of change if the temporal scale is altered, indicating the importance of maximising both the duration of timescales, and the number of intervening datasets.

Figure 9.1 is a flowchart of the layout of this thesis, as well as showing relationships between chapters 4-8 and with other work. The questions raised in the flowchart are an index to assess the relative sensitivity of any given machair site to erosion (this will be further developed in section 9.4).

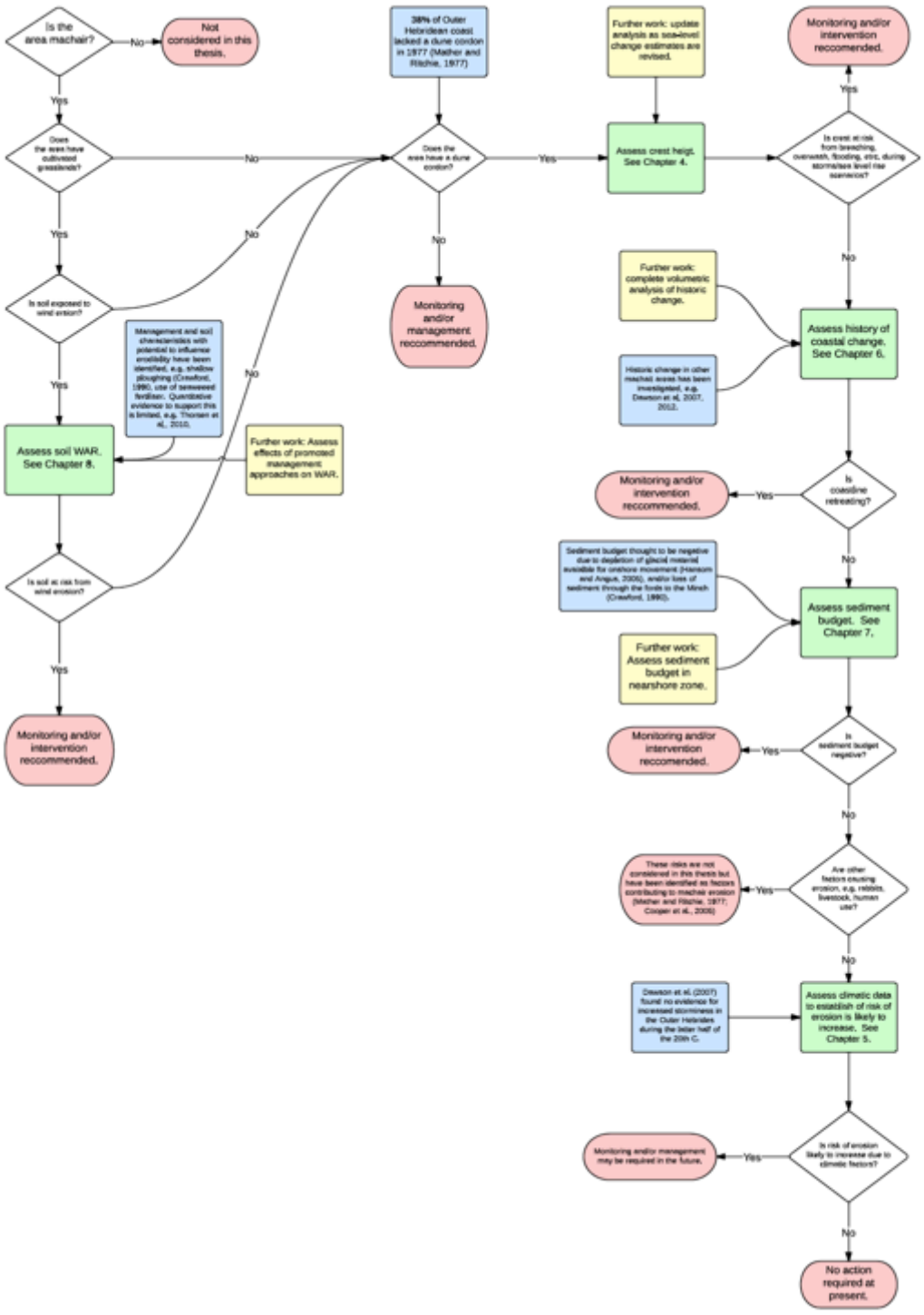

Figure 9.1. Flowchart of this thesis showing interconnections and relationships with other work. White boxes are 'yes/no' questions; red boxes are terminal nodes; green boxes refer to the chapters of this thesis; blue boxes refer to related research; yellow boxes indicate suggestions for further work.

This chapter discusses the results in relation to the broader themes of the machair system, and past and present coastal change. The significance of the thesis and its limitations are considered, and suggestions for further work provided.

9.2 The machair system

This research strengthens the suggestion that the machair system is currently in a phase of erosion and sediment recycling (e.g. as proposed by Hansom and McGlashan (2004)). The evidence here is that of few landforms indicating accretion (e.g. embryo dunes), the predominance of erosive features (e.g. scarps, blowouts), the results from beach volume calculations, and long-term rates of change in the position of linear features. However, the results provide limited support for an on-going net loss of sediment (as proposed by Crawford (1997)). While a slight net loss of sediment was quantified from some of the sites over the short-term beach volume surveys (2005-2014), these volume fluctuations were frequently significantly higher than the net changes. This suggests that the system is relatively stable and sediment recycling is capable of maintaining an approximately balanced sediment budget.

Support for the view that the machair is predominantly a system of sediment recycling is also provided by the dynamic nature of changes in the position of some linear features, e.g. the shingle ridge at the southern end of Staoinebrig, and the low machair front at the southern end of Cille Pheadair, both recorded seaward and landward movements over different times. In contrast, some other landforms showed consistent landwards movement, e.g. eroding dune and machair front scarps. While the lack of significant net change in beach volumes in front of these landforms suggests that the sediment from this erosion probably remains within the system, these landforms are clearly less resilient to erosion, with implications for human use of the landscape and the wider ecosystem.

Rates of coastal change for the machair coastline (e.g. this thesis; Dawson et al., 2012; Gomez et al., 2014) also support an understanding of machair system being comparatively stable and dominated by sediment recycling. However, there is also evidence for either accretion or rapid erosion (this thesis; Dawson et al., 2012; Gomez et al., 2014) along some of the coast, indicating relative stability is a broad generalisation and individual sites experiencing such changes should be investigated in

more detail. As discussed in Chapter 4, increases in r.s.l. will increase the frequency of over-topping and breaching, and expose more dunes and machair front to wave action. Changes in climate while difficult to predict may exacerbate erosion. For example, while changes in the NAO were considered in Chapter 5 and linked to changes in storminess and wind speed, there is no consensus among climatic scientists as to how anthropogenic activity will influence the NAO regime (e.g. compare Wang et al. (2004) with Sinclair and Watterson (2009)).

Rate of change results also question the generalization that the machair is a 'fragile' or 'vulnerable' system (e.g. Angus, 2014; Angus and Rennie, 2014). The apparent stability of much of the coastline suggests the machair system is not generally 'vulnerable' to change. However, some areas (e.g. the headland at Cille Pheadair), and some components (e.g. eroding machair front scarps, ecological and social aspects of the machair) of the system have higher 'vulnerability'. The understanding of the machair as a 'vulnerable' system is discussed in more detail in section 9.2, where the term 'sensitivity' is preferred to 'vulnerability' (as outlined in section 1.2) to prevent confusion with the social associations of the latter term.

As well as supporting the understanding that the current sedimentary regime is characterised by recycling, this thesis also addressed several untested hypotheses based on observations and local perceptions. Firstly – as mentioned in the above paragraphs – Crawford (1997) suggested that the machair coast might be experiencing an on-going net loss of sediment, with sediment leaving the system either through the Fords (and deposited in the deep Minch channel to the east of Uist), or by transport offshore during storms (and deposited on the continental shelf to the west of the Uists, below the depth at which wave action normally operates). As discussed above, results presented in Chapter 7 instead suggest that while beach volumes fluctuate widely over a range of timescales, net change between 2005-2014 is very low, supporting the suggestion by Angus and Rennie (2008) that the majority of sediment moved offshore during winter storms is deposited on nearshore bars and therefore not removed from the machair sedimentary system.

Secondly, Randall (2004) suggested that calcium carbonate sand might be more susceptible to aeolian erosion than silicate sand. Chapter 8 supports this hypothesis; strong negative correlations were found for WAR and calcium concentration and for WAR and mean particle size – the two measured properties indicative of calcium

carbonate content – and FTIR results indicated that samples with higher carbonate to silicate sand ratios were more susceptible to wind abrasion, although the mechanism for this is unclear.

Thirdly, IPCC (2007) provided evidence to show that storminess in the North Atlantic region has increased since the mid-20th C. This is also consistent with public perceptions that storminess is increasing (Matulla et al., 2008). Chapter 5 contrasts with this, in agreement with Dawson et al. (2007a), showing no evidence that storminess has increased since the 1950s. However, the results also indicated the variation in trends obtained by altering the start and end dates of the periods considered, e.g. an increase in storminess is shown when only data from 1910-2000 is considered, which may explain the conflicting results presented in the literature (e.g. compare Wolf and Woolf (2006) and Dawson et al. (2007a) with Phillips et al. (2013) and McClatchey et al. (2014)).

Fourthly, the severity of the January 2005 storm has been considered from a range of perspectives. For example, the people of the Outer Hebrides considered the January 2005 storm as 'the worst in living memory' (Richards and Phipps, 2007), while climatological data (Dawson et al., 2007a) suggests that the storm was severe but shows two other events with a similar maximum gust velocity between 1980 and 2007. Additionally, Angus and Rennie (2008) consider that from a geomorphological perspective the changes associated with the storm in most places were not significantly greater than those which would occur under typical winter conditions. Chapter 5 suggests that many climatic parameters associated with the January 2005 storm have a relatively short return period (1.5-15 years), with the duration of the storm being perhaps the single most 'severe' factor. Chapters 6 and 7 propose that changes associated with the January 2005 storm at Staoinebrig and Cille Pheadair are greater (visually and quantitatively) than those occurring during typical winters. Note that the sites studied in this thesis are sensitive to coastal change and experienced some of the most extreme changes during the January 2005 storm.

Fifthly, there are local concerns of beach lowering at the southern end of Staoinebrig (David Muir, personal communication). Results from 2005-2014 show that across the central and southern sections at Staoinebrig there was a net decrease in beach elevation. Results indicate that these sections experienced variable changes (including elevation gains) over different time periods. However, net elevation loss appears

greater and more spatially consistent at the central and southern sections of Staoinebrig than at the northern end of this site or at the other sites.

Finally, while this research did not directly investigate the influence of seaweed fertiliser on soil quality, results from Chapter 8 indicate that higher arsenic concentrations (potentially linked to the application of seaweed fertiliser (Castlehouse et al., 2003)) are strongly correlated with higher WAR values, and may also be used to predict soil WAR. Tangentially, this suggests that seaweed fertiliser may benefit machair soil stability.

Analysis in Chapter 4 highlights the already recognised importance of conserving a functioning dune cordon (e.g. Angus and Rennie, 2014). Preventing the erosion of dune cordon's – where they do exist – should be a management priority.

9.3 Coastal change – sensitivity, dynamic equilibrium, and thresholds

The concepts of dynamic equilibrium, sensitivity, thresholds, resilience, and resistance were introduced in section 1.2. Throughout the thesis, a range of proxies have been used to quantitatively study variations in the sensitivity to different factors of the three sites, e.g. in Chapters 6 and 7 rates of change in the position of linear coastal features were determined to identify variations in the sensitivity of coastal landforms to marine erosion, and in Chapter 8, the sensitivity of machair soils to wind erosion was investigated by quantifying trends in wind abrasion resistance. In this section the qualitative relations of these terms to the wider machair system are considered.

As in section 1.2, a system in equilibrium is one which maintains the same form (e.g. presence/absence of landforms, ecosystems, continuity of relative proportions of component system parts) and function (e.g. recreational, agricultural, ecological, etc.) (Schumm, 1979). Cambers (1976) consideration of cliff retreat on the English coast provided the observation that an erosive (or accretionary) system could still be in a state of dynamic equilibrium if the rate of retreat was approximately constant over long periods, e.g. cliff retreat is one of the 'normal' functions of an erosive coastline. This concept is equally applicable to the soft machair coastline of South Uist, which is recognised to have been an erosive system since ~ 6.5 ky (Hansom and Angus, 2001). Comparisons of rates of change, over a ~140 yr period, in the position of linear features presented in Chapter 6, and by Dawson et al. (2012), and Gomez et al. (2014) suggest

that, while there have been fluctuations in the measured rates of change, the order of magnitude of retreat has been fairly constant, with fluctuations occurring in both directions from the long-term average over intermediate periods. The work presented in this thesis does not indicate any clear trend of accelerating or decelerating erosion since 1878, suggesting that the machair system can be interpreted as being in a period of dynamic equilibrium as this concept was interpreted by Cambers (1976).

The concept of 'thresholds' was also introduced in section 1.2; the idea that once a system's resilience and resistance have been overcome by external forces it will shift across a threshold to a new equilibrium with differences in form and function. Although not directly studied in this thesis, the longer history of the machair system was considered in section 2.3.2. The key findings from Bennet et al. (1990), Ritchie and Whittington (1994), Gilbertson et al. (1996), Grattan et al. (1996), Ritchie et al. (2001), and Dawson et al. (2004) showed that throughout the Holocene the machair system has experienced periods of relative stability (characterised by stratigraphic layers enriched in organic matter, the machair stratification effect, and cultivation of the grasslands) and periods of widespread instability (characterised by sand dominated stratigraphic layers, and described in historic literature as periods of widespread sand blow and deposition). These two distinct states may represent the machair system shifting between positions of dynamic equilibrium; with changes in either external factors acting on the system (e.g. climate, anthropogenic activity) or internal properties of the system (e.g. sediment supply) leading to the threshold between the two states being crossed.

It is unclear from the literature which factor dominates in crossing the threshold between equilibrium states. For example, Gilbertson et al. (1999) suggests a link between increased cultivation and improved topsoil stability, while Brayshay and Edwards (1996) argue that periods of intensive grazing may have destabilised the machair. Dawson et al. (2004) indicate that climate changes have been the key factor driving changes in machair stability. For example, the last period when large parts of the machair were unstable was thought to occur from ~1400-1900 (Dawson et al., 2004; Hansom and Angus, 2005) and the end of this period corresponds to a dramatic decrease in the frequency of storms (see Dawson et al., 2007a and Chapter 5 of this thesis). It is possible that different causes, e.g. overgrazing, excessive sand/gravel extraction, increased storminess, etc., may have caused the threshold between the stable and non-

stable machair states to be crossed at different times throughout the Holocene, or that a combination of factors has been involved. It is also evident that anthropogenic factors operate over generally smaller temporal and spatial scales than climatic factors.

The range of anthropogenic and climatic change that the machair is resilient and/or resistant to in its current stable state are important. This thesis has begun to address this issue by quantifying some of the variation in change in coastal landforms and erodibility of soils that are experienced within the current stable machair state. Some of the results indicate greater capacity for resilience (e.g. fluctuations in the position of shingle ridge at Staoinebrig, low machair front at Cille Pheadair, and the position of mean high water at ordinary spring tide (MHWOST) occur in both directions (retreat and progression) and indicate recovery from changes caused by external factors) or resistance (e.g. lack of retreat in coastal features at Milton, high wind abrasion resistance of inland soils at Milton and Cille Pheadair) within some parts of the machair system than at others (e.g. on-going net retreat of the exposed machair front at Staoinebrig). While all changes measured in this thesis appear within normal operating capacities of the machair in its stable state, the lower resistance and resilience of some sites may indicate closer proximity to a threshold (e.g. lower crest heights at parts of Cille Pheadair and Staoinebrig are more susceptible to erosion, overwash, and flooding, that may lead to changes in characteristic landforms and functions). For example, at Cille Pheadair it is probable that without the erection of a coastal bund, the low machair front at the centre of the headland would be more frequently inundated following the January 2005 storm. Historic evidence indicates that the stability of the machair may lack regional synchronicity (Ritchie and Whittington, 1994; Ritchie et al., 2001), i.e. some parts of the South Uist machair may be stable while others are unstable.

Comparison of results from Chapters 6 and 7 indicate that while the changes in the position of linear features associated with this event were 1-2 orders of magnitude higher than typical annual changes, there is no clear evidence for a subsequent increased rate of change. While the visible effects of the storm were dramatic (e.g. Moore et al., 2005; Dawson et al., 2007a), many of the changes are now amalgamated into the landscape with no qualitative change in the form or function of the coastline. This suggests that while severe, the January 2005 storm, is within the boundaries of storminess to which stable machair is resilient/resistant, and agrees in part with Angus and Rennie (2008) who considered the effects of the storm to be not significantly

greater than those caused by typical winter conditions. This is consistent with the results of climate data analysis in Chapter 5 and presented in Dawson et al. (2007a); several storms of a similar magnitude have been identified within the recent historical period (1800-2000), and there is no evidence for a net increase in the severity or frequency of storm events during the 20th or early 21st Centuries. The severity of the event and the recovery of many parts of the coastline (visibly, and with regards to quantitative rates of change) supports Angus and Rennie's (2008) suggestion that the machair is a relatively resilient system.

Interpretation of the January 2005 storm is complicated by human intervention. For example, at Staoinebrig the shingle ridge was artificially reshaped and shingle deposits cleared from the road; without intervention the social function of this site as an access route would have changed, and it is probable that rates of erosion at the southern end of the site would have increased in the absence of a defined shingle ridge. Similarly, at Cille Pheadair, the artificial bund has raised the crest height along the lowest lying section of machair front. Without intervention it is possible than on-going erosion would have further reduced crest height at this site, leading to flooding of parts of the grasslands.

Will the machair remain stable? Angus (2001) and Cooper and Pile (2014) suggest that the machair system is capable of 'roll-back', i.e. the landforms and habitats of the machair system will retreat landwards without any net change to the proportions of each physical component of the system. However, Cooper and Pile. (2014) also acknowledge the possibility that rates of erosion may increase in response to rising sea-level, and some physical features may be lost or reorganised. Phillips (2009) suggests that thresholds can be crossed either due to a large scale change in external forces or an on-going, gradual preconditioning of the internal properties of the system (i.e. high frequency, low intensity events lower system resistance of resilience, so that a comparatively minor storm event may have a large impact on system dynamics). This implies that the shift from stable to non-stable states could be precipitated by either a sudden shift in the factors influencing the system (e.g. a rapid increase in the rate of sea-level rise, or a sudden increase in the frequency and/or severity of storms), or gradual on-going changes which reduce the resilience or resistance of the system (e.g. the on-going marine undercutting of the machair front and lowering of crest height), and then allow a relatively minor shift in external factors to tip the system across a threshold. It

is unclear whether storminess is likely to change, however the rate of sea-level rise is predicted to increase through the remainder of the 21st century, and that may potentially reorganise landforms constituting a shift in equilibrium associated with gradual change in external factors. Alternatively, some parts of the coastal zone are experiencing on-going preconditioning, e.g. the continual gradual retreat of parts of the coast lacking a protective dune cordon. At these sites, a shift to non-stable conditions may not be associated with a change in external conditions but with the cumulative effect of on-going coastal processes on parts of the system lacking sufficient resilience or resistance to withstand them, e.g. on-going erosion of the machair scarp at Staoinebrig may lead to more frequent deposition of sand across a larger area inland from the crest.

Note that the above discussion refers solely to the physical components. The social, economic, and cultural sensitivity, or 'vulnerability' of the machair system is not necessarily similar to the physical sensitivity. For example, the physical machair system can accommodate some realignment and erosion without significant qualitative change to its form and function. However, the effects of on-going erosion may have a serious effect on the people, e.g. loss of agricultural land may reduce the economic viability of a croft, leading to land being taken out of cultivation, with potentially negative 'knock-on' effects on the machair ecosystem. It is possible that the adaptive capacity of the social and cultural aspects of the machair is lower than the capacity of the physical system to respond to change. However, the interlinked nature of the components means that crossing a threshold in one part of the system may trigger other parts of the system to change form or function.

The conceptual model of the machair as a system moving between two states of dynamic equilibrium is illustrated in Figure 9.2.

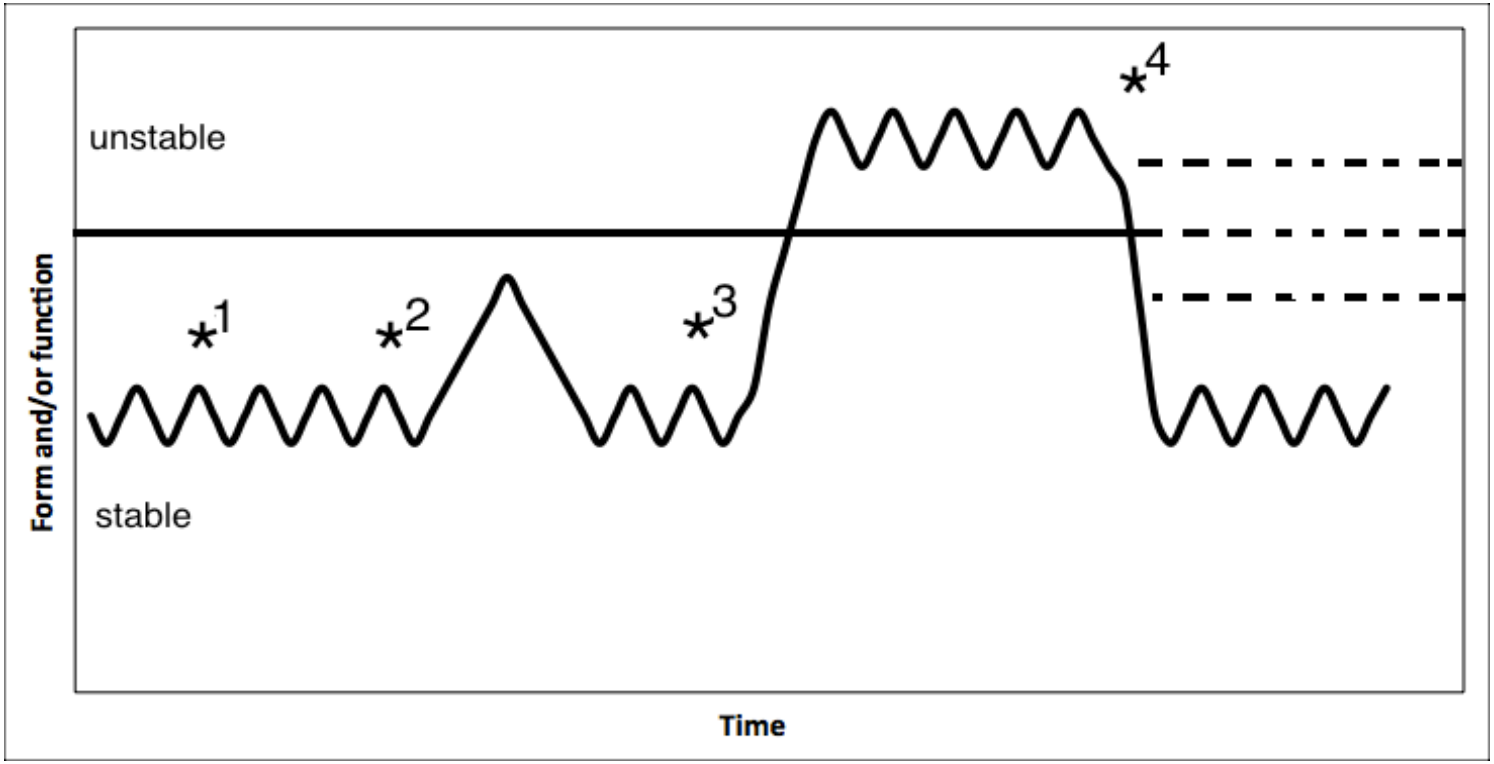

Figure 9.2. Diagram illustrating the conceptual model of the machair as a system between two states of dynamic equilibrium. The irregular black line indicates the status of the machair, with crests and troughs representing minor fluctuations in the system. The horizontal black line represents the threshold between the stable form and function (below) and the unstable form and function (above). The stars indicate changes in the external or internal properties of the machair system, numbered to indicate different responses (dependent on the magnitude of change): 1 = resistance; 2 = resilience; 3) and 4) = shifts in equilibrium position due to a threshold being crossed. The three horizontal dashed black lines which replace the horizontal solid black line to the right of change 4 indicate possible new positions for the threshold between stable and unstable forms.

9.4 Significance of results

The key contribution of this thesis is the quantification of the range of variability in the sensitivity of coastal soils and landforms (as investigated through rates of change in linear features, beach volumes, visual analysis, soil characteristics, etc.). The results demonstrate the high variability inherent in the machair under normal conditions, and suggest that studies that depend on temporally isolated datasets to quantify change may not be reliable. For example, the position of MHWOST is frequently used as a proxy for investigating long-term (decadal-centennial) coastal change. For the three sites studied, MHWOST varied by as much as 25 m on a seasonal basis an amount similar to the net change for many parts of the sites over ~ 140 years. The very dynamic nature of many coastal features such as the shingle ridge at Staoinebrig and the low machair front at Cille Pheadair is evidence of considerable retreat and progression over different periods. The dynamism also suggests extreme caution is needed when interpreting results from widely spaced temporal datasets. Furthermore, results from Chapter 7 indicated that using datasets taken during the same season or tidal conditions are not by themselves sufficient to remove error associated with short-term cyclical fluctuations, e.g. beach volumes measured every March were no more similar to each other than to beach volumes taken at other months during the year. This thesis therefore contributes to separating trends from fluctuations in assessing coastal change on the machair coast by investigating what happens 'between the snapshots'.

The use of different shoreline proxies suggested that the position of MHWOST as an indicator of shoreline change is inappropriate, except where shoreline change is extreme, and even in then the error to signal ratio is likely to be very high. This finding is agrees with the work of Valentin (1954), Shalowitz (1964), Morton and Speed (1998), Moore (2000), and Pye and Blott (2006) who drew attention to the high error associated with the position of MHWOST as a shoreline indicator.

The vegetation line is a widely used shoreline proxy (Boak and Turner, 2005) and is commonly extracted from aerial photography. However, on the machair, the vegetation line along the low machair front at Cille Pheadair was an ephemeral feature not linked to a specific geomorphological feature of datum and moved in both directions, while the vegetation lines along the high dunes at Milton and to the north of Cille Pheadair were tied to the dune crest with change in position indicating the gradual

erosion of the underlying geomorphology. This highlights the importance of visual and qualitative monitoring of sites to interpret measured changes and the need for different shoreline proxies to be used for different landforms to minimise error and confirm change.

For the South Uist machair this research provides baseline data on soil properties and coastal geomorphology for three sites, two of which have been identified as sensitive to further coastal change (e.g. Richards and Phipps, 2007). Several hypotheses and assumptions have also been tested, as discussed in section 9.1 and the results of these have several implications for management of the machair system. For example, much of the erosion measured along the high dune crest north of Cille Pheadair and damage to the nearby coastal defence bund appeared to be attributable to livestock rather than marine action. Erosion at this sight might be controlled by restricting livestock access, allowing the dunes and bund to re-vegetate and thus reducing the rate of crest retreat. The very low wind abrasion resistance of soils close to the dune crest may also contribute to crest height lowering where land very close to the dune crest is cultivated and highly erodible soil is exposed to aeolian action (e.g. at Cille Pheadair). The exposure of the soil by vegetation removal also makes it more susceptible to livestock damage. At Milton, a ~15 m wide strip along the dune crest is fenced to exclude grazing and cultivation, allowing dense vegetation to fix the dunes and provide a degree of protection from erosion. This study also identified some coastal features that may show considerable retreat over short times (e.g. shingle ridge, low machair front) but are in fact dynamic features with resilience to marine action, and therefore unlikely to require management intervention. The results presented in Chapters 4, 6, 7, and 8 quantify the high variability of sensitivity within the machair landscape, indicating that targeted management may be required to maximise efficiency. It is recognised that recommendations relating to the physical components of the machair system may not be feasible from a socio-economic or cultural perspective (e.g. Muir, 2014). However, Angus and Rennie (2014) observed that funding to local communities may be reduced or removed if the conservation value of the machair sites is not preserved.

As mentioned in section 9.1, the flowchart Figure 9.1 is a crude index of machair coastal sensitivity to erosion based on the answers to the key ‘yes/no’ boxes for individual machair sites. Tables 9.1 and 9.2 demonstrate this use for the three sites

investigated in this thesis. To assign numeric values to indicators of coastal sensitivity in Table 9.2 the following values were used: i) cultivation: < 10 m from dune crest (1), > 10 m from dune crest (0); ii) wind abrasion resistance (WAR) values: low (2), low-high (1), high (0); iii) coastal morphology: low machair front (2), mixed (1), high dunes (0); iv) % dune crest (DC) < water level (WL): 75-100 (4), 50-74 (3), 25-49 (2), 1-24 (1), 0 (0); v) historic shoreline change: retreat (3), variable (mainly retreat) (2), variable (1), no change/progression (0); vi) sediment budget: > - 50% and greater loss (5), -40 to 49% (4), -30 to -39% (3), -20 to -29% (2), -10 to -19% (1), 0 to -10% (0); other factors: numbers assigned based on visual assessment of severity of other factors contributing to erosion. For the amalgamated total values (T), it is proposed that a total value of 0-3 indicates low sensitivity to coastal change, values from 4-7 indicate moderate sensitivity to coastal change, and values > 8 indicate high sensitivity to coastal change. In the case of the three sites investigated, this index would assign Milton a low sensitivity value (3), while Staoinebrig and Cille Pheadair would be assigned high sensitivity values (8 and 9, respectively), which agrees with qualitative and quantitative analysis of these sites. This framework could be tested at other machair sites with a view to prioritising management resources.

Table 9.1. Key factors from Figure 9.1that inform an index of machair coastal sensitivity, and description of each factor for each site. '% DC<WL' refers to the length of crest below current MHWOST (as investigated in Chapter 4). The number in brackets indicates the percentage of crest below water levels under the most extreme high water scenario investigated in Chapter 4. 'Sediment budget' is the net volume change between 2005-2014.

SITE	Cultivation	WAR values	Coastal morphology	% DC<WL	Historic shoreline change	Sediment budget	Other factors
SB	> 10 m from DC	low	low machair front	0 (12)	variable (mainly retreat)	- 18 %	n/a
M	> 10 m from DC	low-high	high dunes	0 (0)	variable	- 3 %	vehicle track
CP	< 10 m from DC	low-high	low machair front/dunes	0 (17)	variable (mainly retreat)	- 13 %	livestock trampling

Table 9.2. Descriptive results from Table 9.1 assigned numerical values to provide an index of machair sensitivity. T indicates total for each site and provides a relative indication of the sites sensitivity. Higher values indicate higher sensitivity.

SITE	Cultivation	WAR values	Coastal morphology	% DC<WL	Historic shoreline change	Sediment budget	Other factors	T
SB	0	2	2	1	2	1	0	8
M	0	1	0	0	1	0	1	3
CP	1	1	1	1	2	1	2	9

9.5 Limitations

The individual limitations of work presented in each chapter are discussed in the relevant 'critique' sections of each chapter. This section focuses on the more holistic limitations of the research project.

Perhaps the most significant limitation of this work is that it is restricted to three sites within the South Uist machair; the relevance of the work to the rest of the machair coast, in South Uist, and elsewhere in Scotland and Ireland, has yet to be confirmed. For the obvious practical reasons, it was implausible to conduct detailed quantitative work along the entire extent of the South Uist machair. However, some aspects of the work could be extended to a greater area (see section 9.5). Based on previous research, effort was made to select two sites with anticipated high sensitivity to coastal change (Staoinebrig and Cille Pheadair), and one site with anticipated low sensitivity to coastal change (Milton); the results support the original assumptions about the sites. Furthermore, the full range of soft coast geomorphological variation found on the machair was captured within the three sites. For these reasons, it is expected that the broad qualitative trends found with each geomorphology type may be extrapolated to other areas within the machair, although significant quantitative variation in rates and amounts of change could be expected from the work in this thesis and in Dawson et al. (2007b) and Gomez et al. (2014). Additionally, the analysis of soil properties showed that the full range of variation for WAR was measured between the three sites, indicating that the three sites selected provide a good indication of the range of variation in soil properties to be expected elsewhere on the machair.

A second key limitation is the lack of comprehensive quantitative data on coastal change related to a severe storm causing similar effects to the January 2005 event. Quantitative information related to the January 2005 storm is limited, making it challenging to draw conclusions about the storm's significance in comparison to long and short term coastal change. While eight storm-force events (excluding the January 2005 storm) were recorded between 2005-2014 (with 2 during regular monitoring in 2011-2014) none caused similar change to of the January 2005 event. However, it is acknowledged that even if such a storm had occurred during the RTK-dGPS surveying period, quantitative information alone provides a limited picture of the storm's impact. The qualitative descriptions of storm damage (with some quantitative information)

provided by Moore et al. (2005), Dawson et al. (2007a), and Angus and Rennie (2008, 2014) present a range of indications of the storm's severity that would be difficult to compare quantitatively, e.g. distribution of debris plumes, damage to vegetation caused by flooding, the movement of sections of bedrock, undercutting, etc. are not typically features investigated quantitatively when assessing coastal change.

The study was also limited by technological and practical constraints, e.g. efficiency, cost, availability, and accuracy of equipment. For example, the RTK-dGPS equipment used in the survey is part of a range of spatial analysis techniques that have revolutionised the study of the physical environment. However the RTK-dGPS method is likely to be increasingly replaced by airborne and terrestrial LiDAR, and photogrammetric techniques, as these become cheaper, more widely available, and more accurate with technological advances. Despite this, the data collected in this study will remain valid and useful as a highly accurate quantitative data source for investigating coastal change at the sites investigated.

9.6 Suggestions for further work

Due to the exploration of different aspects of the machair and the use of different methodologies in each of the chapters of this thesis, there are numerous directions for further work. To further enhance understanding of the machair sediment budget, volumetric analysis could be beneficially extended spatially to the nearshore environment and the dunes, and temporally extended by stereographic photogrammetry. Unfortunately the potential for the latter is uncertain due to the limited availability of flight data for historic aerial photographs. Spatially, quantifying volumetric changes in the nearshore zone would further investigate the end fate of sediment removed during storms. Ideally, surveying would be timed to take place before and after a major storm. Quantification of volume change in the dune area of the machair could be usefully linked to further historic analysis of this critical part of the machair geomorphology, e.g. analysis of historic photographs to investigate dune erosion and vegetation from the 1940s to the present to assess rates of dune erosion, and changes in the sensitivity of this landform.

Some of the methods used in this research could be applied to other parts of the machair coast relatively easily, e.g. the analysis of sensitivity to flooding, breaching,

and overwash presented in Chapter 4 could be extended along the western coastline of South Uist and Benbecula using the SNH/Western Isles Partnership 2005 LiDAR dataset. This would help to identify areas that may be at risk to marine erosion, flooding, etc. with rising sea-levels, with the analysis being updated to reflect refinements in sea-level change predictions. Similarly, GIS analysis of coastal change from historic maps can be carried out for other machair sites relatively efficiently due to the availability of historic maps in a GIS-ready format through Digimap. However, the results from Chapter 7 indicate that long term change results obtained from historic maps should be interpreted with extreme caution where data on short term fluctuations are not available.

The results from Chapter 8 have implications for management and could therefore usefully be developed further, e.g. investigation of methods to improve WAR scores (such as the comparison of artificial and seaweed fertiliser by Thorsen et al. (2012), refinement of models for predicting WAR by further sampling, etc.

CHAPTER 10
CONCLUSIONS

The overall purpose of this thesis was to quantify variations in the sensitivity of the coastal machair landscape to erosion, using a range of proxies to indicate sensitivity for different aspects of the sediments and landforms. This purpose has been addressed using three field sites, representing the range of variation in coastal machair geomorphologies, to study sediment budgets, shoreline positions, soil properties, and the climatic data corresponding to the periods investigated. How the individual aims of the thesis, outlined in section 2.4, are met are briefly discussed below.

- **Aim i)** – *Quantify long term trends in planimetric coastal evolution using historic maps and aerial photography.*

Chapter 6 presented historic changes of the shoreline position as indicated by the vegetation line (derived from aerial photographs) and the position of Mean High Water at Ordinary Spring Tides (derived from maps). The results indicated high variability in the nature and rates of change, with Stoneybridge and Cille Pheadair showing evidence for net retreat and a similar pattern of change, and Milton showing evidence for net progression and a pattern of change different from the other sites. The results illustrated that rates of shoreline change have been lowest in the most recent periods analysed using both methods (1987-2005 for photographs; 1965-2002 for maps).

- **Aim ii)** – *Quantify short-medium term trends in planimetric and volumetric coastal change using RTK-dGPS and LiDAR data.*

Chapter 7 quantified short-medium term coastal change using the position of the dune crest (equivalent to the position of the vegetation line investigated in Chapter 6) as an indicator of planimetric change, and the sediment budget of the beach as an indicator of volumetric change. The results indicated high temporal and spatial variability between and within sites, with net change from 2005-2014 frequently being exceeded in intervening time periods. As with the results from Chapter 6, Cille Pheadair and Stoneybridge showed higher sensitivity to erosion than Milton. The results from this

chapter support the higher error estimates associated with historic shoreline change techniques supporting the interpretation in Chapter 6.

- **Aim iii)** – *Provide a context for interpreting the significance of erosion during severe storms (such as the January 2005 event) relative to gradual, on-going coastal erosion.*

Chapters 6 and 7, combined with the crest height analysis conducted in Chapter 4, and the historic climatological data presented in Chapter 5 were used to analyse the changes associated with the January 2005 storm. During the short-medium term study of coastal change from November 2005 to March 2014, no storm events or winter seasons approached the severity of qualitative effects recorded during the January 2005 storm, e.g. fragmentation of bedrock, widespread deposition of debris plumes, etc. (recorded in Dawson et al., 2007, and Angus and Rennie, 2008). The results in Chapter 7 also indicated that the quantitative changes in crest position in sensitive areas recorded during the storm (up to 5-10 m of retreat) were not equalled during the entirety of the short-term study period. Over very localised scales (< 10% of transects investigated using the Digital Shoreline Analysis System – see Chapter 7), retreat of 1-3 m from 2005-2014 was recorded. However, for the majority of transects, retreat was considerably less than this.

Analysis of long-term change presented in Chapter 6 suggests that the change occurring at sensitive sites during the January 2005 storm is of the same magnitude as the mean net shoreline movement from 1948-2005 at Cille Pheadair. This emphasises the severity of this event.

The analysis of climatic factors associated with the January 2005 storm (see Chapter 5) surprisingly found short return periods (< 20 yrs) for all measured parameters of storm severity associated with this event. This indicates only a weak connection between the *climatological* and the *geomorphological* significance of an event (possibly due to the cumulative effect of pre-conditioning by previous storms), and/or individual parameters of storminess (e.g. max. wind-speed, minimum pressure, etc.) are poor indicators of a storm's climatological severity.

- **Aim iv)** – *Investigate whether storminess has increased in the southern Outer Hebrides since 1867, and to consider the implications of these findings for coastal change over this period.*

Chapter 5 shows no evidence for a sustained increase in storminess from 1867-2014; indeed, current storminess appears moderate compared with high storminess from 1867-1910, and a low storminess from 1910-1950. The results provide a strong caution to use the longest timescales possible for assessing climatological change. Altering the period for which changes in climate were investigated significantly impacted on the nature and strength of trends identified. Additionally, comparison of results from Chapters 5 and 6 showed unclear relationships between storminess and weather, and rates of shoreline change.

- **Aim v)** – *Determine if there are spatial trends in the wind abrasion resistance (WAR) of machair soils with relation to distance from the coast, and to establish which soil properties can be correlated with this.*

Chapter 8 demonstrated evidence of an increase in WAR with distance from the coast at two of the three sites investigated. Analysis of soil properties demonstrated that WAR was correlated with a range of physical and chemical soil characteristics, and that some of these properties (FTIR spectra, arsenic content, water content, mean particle size, and water drop penetration class) could predict WAR acceptably using principal component analysis and regression trees.

The aims addressed as in the preceding paragraphs were synthesised in Chapter 9 to: i) address several unaddressed hypotheses related to machair erosion, ii) consider management implications, and iii) to develop a conceptual model of the machair as a recycling-dominated system in dynamic equilibrium. This model interprets the machair as moving between states of relative stability and instability as thresholds in climatic and/or anthropogenic processes affecting machair stability are crossed. The quantitative work presented in this thesis contributes to the model by beginning to establish the climatic and geomorphological fluctuations that can be accommodated within the machair's two proposed states.

REFERENCES

Abbott, R. 2005. **Loss on ignition (LOI) procedures**. Standard Operating Procedures. University of Pittsburgh.

Aguilar, F.J., Agüera, F., Aguilar, M.A., Carvajal, F. 2005. Effects of terrain morphology, sampling density and interpolation methods on grid DEM accuracy. **Photogrammetric Engineering and Remote Sensing 71**, 805-816.

Allan, R., Tett, S., Alexander, L. 2008. Fluctuations in autumn-winter severe storms over the British Isles: 1920 to present. **International Journal of Climatology 29**, 357-371.

Angus, S., Elliot, M.M. 1992. Problems of erosion in Scottish machair with particular reference to the Outer Hebrides. In: Carter, R.W.G., Curtis, T.G.F., Sheehy-Skeffington, M.J. (Eds.), **Coastal Dunes: Geomorphology, Ecology and Management for Conservation**. A.A. Balkema, Rotterdam, pp. 93-112.

Angus, S. 1994. The conservation importance of machair systems in the Scottish islands, with particular reference to the Outer Hebrides. In: Baxter, J.M., Usher, M.B. (Eds.), **The Islands of Scotland: A Living Marine Heritage**. HMSO, Edinburgh, pp. 95-120.

Angus, S. 1996. Natural heritage conservation in the southern Outer Hebrides. In: Gilbertson, D., Kent, M., Grattan, J. (Eds.), **The Outer Hebrides: The Last 14,000 Years**. Sheffield Academic Press, Sheffield, pp. 227-250.

Angus, S. 1999. The state of the maritime natural heritage: machair in Scotland. In: Baxter, J.M., Duncan, K., Atkins, S.M., Lees, G. (Eds.), **Scotland's Living Coastline.** HMSO, London, pp. 166-172.

Angus, S. 2001. **The Outer Hebrides: Moor and Machair**. The White Horse Press, Cambridge.

Angus, S. 2014. The implications of climate change for coastal habitats in the Uists, Outer Hebrides. **Ocean and Coastal Management 94**, 38-43.

Angus, S., Dargie, T. 2002. The UK Machair Habitat Action Plan: Progress and problems. **Botanical Journal of Scotland 54**, 63-74.

Angus, S., Hansom, J.D. 2004. Tir a'mhachair, tir nan loch? Climate change scenarios for Scottish machair systems: a wet future? In: **Proceedings Vol. 2, Littoral**

2004. Delivering Sustainable Coasts: Connecting science and policy. Cambridge Publications, pp. 565-569.

Angus, S. 2006. De tha machair? Towards a machair definition. **Sand Dune Machair 4**, 7-22.

Angus, S., Rennie, A.F. 2008. **An Ataireachd Ard: The great sea surge. The natural heritage impact of the storm of 11 January 2005 in the Uists and Barra, Outer Hebrides**. Commissioned report for Scottish Natural Heritage. Scottish Natural Heritage, Inverness.

Angus, S., Rennie, A.F., 2014. An Ataireachd Aird: The storm of January 2005 in the Uists, Scotland. **Ocean and Coastal Management 94**, 22-29.

Backstrom, J.T., Jackson, D.W.T., Cooper, J.A.G., Malvárez, G.C. 2008. Storm-driven shoreface morphodynamics on a low-wave energy delta: The role of nearshore topography and shoreline orientation. **Journal of Coastal Research 24**, 1379-1387.

Baily, B. 2009. **An analysis of old tide-line mapping for coastal zone management**. History seminar – session 3. FIG Working Week 2009. Surveyors Key Role in Accelerated Development. Eliat, Israel, 3-8 May 2009.

Baptista, P., Bastos, L., Bernardes, C., Cunha, T., Dias, J. 2008. Monitoring sandy shores morphologies by DGPS – A practical tool to generate digital elevation models. **Journal of Coastal Research 24**, 1516-1528.

Bagnold, R.A. 1948. **The Physics of Blown Sand and Desert Dunes**. Methuen, London.

Bell, A.D. 2012. Section 2.3.1. Creating DEMs from survey data: Interpolation methods and determination of accuracy. In: Clarke, L.E., Nield, J.M. (Eds.), **Geomorphological Techniques (online edition)**, British Society for Geomorphology, London. ISSN: 2047-0371.

Belly, A.P. 1964. **Sand Movement by Wind**. Technical Memo 1, Coastal Engineering Research Centre.

Bennet, K.D., Fossitt, J.A., Sharp, M.J., Switsur, V.R. 1990. Holocene vegetational and environmental history at Loch Lang, South Uist, Western Isles, Scotland. **New Phytologist 114**, 281-298.

Bertoni, D., Sarti, G. 2011. On the profile evolution of three artificial pebble beaches at Marina di Pisa, Italy. **Geomorphology 130**, 244-254.

Black, J.M.W., Chanasyk, D.S. 1989. The wind erodibility of some Alberta soils after seeding: aggregation in relation to field parameters. **Canadian Journal of Soil Science 69**, 835-847.

Boak, E.H., Turner, I.L. 2005. Shoreline definition and detection: A review. **Journal of Coastal Research 21**, 688-703.

Bondevik, S., Mangerud, J., Lohne, Ø., Dawson, S., Dawson, A. 2005. Evidence for three North Sea tsunamis at the Shetland Islands between 8000 and 1500 years ago. **Quaternary Science Reviews 24**, 1757-1775.

Boorman, L.A. 1977. Sand dunes. In: Barnes, R.S.K. (Ed.), **The Coastline: A contribution to our understanding of its ecology and physiography in relation to land-use and management and the pressures to which it is subject**. Wiley, Chichester, pp. 161-197.

Brasington, J., Langham, J., Rumsby, B. 2003. Methodological sensitivity of morphometric estimates of coarse fluvial sediment transport. **Geomorphology 53**, 299-316.

Brayshay, B., Edwards, K. 1996. Late glacial and Holocene vegetational history of South Uist and Barra. In: Gilbertson, D., Kent, M., Grattan, J. (Eds.), **The Outer Hebrides: The Last 14,000 Years.** Sheffield Academic Press, Sheffield, pp. 13-26.

Brennan, M.J., Hennon, C.C., Knabb, R.D. 2009. The operational use of QuikSCAT ocean surface vector winds at the National Hurricane Centre. **Weather Forecasting 24**, 612-645.

Brooks, S.M. 2010. **Coastal changes in historic times: Linking offshore bathymetry changes and cliff recession in Suffolk**. Marine Estate Research Report. London, UK: The Crown Estate, pp. 88.

Brown, J., Jorgenson, M.T., Smith, O.P., Lee, W. 2003. Long-term rates of coastal erosion and carbon input, Elson Lagoon, Barrow, Alaska. **Proceedings of the 8th International Conference on Permafrost**, Zurich.

Brunsden, D. 1993. Barriers to geomorphological change. In: Thomas, D.S.G., Allison, R.J. (Eds.), **Landscape Senstivity**. Wiley & Sons, pp. 7-12.

Brunsden, D. 2001. A critical assessment of the sensivitity concept in geomorphology. **Catena 42**, 99-123.

Burningham, H., French, J. 2013. Is the NAO winter index a reliable proxy for wind climate and storminess in northwest Europe? **International Journal of Climatology 33**, 2036-2049.

Caird, J.B. 1979. Land use in the Uists since 1800. **Proceedings of the Royal Society of Edinburgh 77b**, 505-526.

Cambers, G., 1976. Temporal scales in coastal erosion systems. **Transactions of the Institute of British Geographers ns1**, 246-256.

Castlehouse, H., Smith, C., Raab, A., Deacon, C., Meharg, A.A., Feldmann, J. 2003. Biotransformation and accumulation of arsenic in soil amended with seaweed. **Environmental Science and Technology 37**, 951-957.

Carr, A.P. 1962. Cartographic record and historical accuracy. **Geography 47**, 135-144.

Chatterjee, A., Lal, R., Wielopolski, L., Martin, M.Z., Ebinger, M.H. 2009. Evaluation of different soil carbon determination methods. **Critical Reviews in Plant Sciences 28**, 164-178.

Chepil, W.S. 1953. Factors that influence clod structure and erodibility of soil by wind: I. Soil texture. **Soil Science 75**, 473-483.

Chepil, W.S. 1954. Factors that influence clod structure and erodibility of soil by wind: III. Calcium carbonate and decomposed organic matter. **Soil Science 77**, 473-480.

Chepil, W.S. 1955. Factors that influence clod structure and erodibility of soil by wind: V. Organic matter at various stages of decomposition. **Soil Science 80**, 413-421.

Chepil, W.S. 1958. Soil conditions that influence wind erosion. **USDA-ARS**, Technical Bulletin no. 1158. U.S. Government Print Office, Washington D.C..

Clark, I., Harper, W.V. 2008. **Practical Geostatistics 2000**. Geostokos (Ecosse) Limited, Scotland, pp. 430.

Clarke, M.L., Rendell, H.M. 2009. The impact of North Atlantic storminess on western European coasts: A review. **Quaternary International 195**, 31-41.

Cooper, A.T., McCann, T., Ballard, E. 2005. The effects of livestock grazing and recreation on Irish machair grassland vegetation. **Plant Ecology 181**, 255-267.

Cooper, J.A.G., Jackson, D.W.T., Dawson, A.G., Dawson, S., Bates, C.R., Ritchie, W. 2012. Barrier islands on bedrock: A new landform type demonstrating the role of antecedent topography on barrier form and evolution. **Geology 40**, pp. 823-826.

Cooper, J.A.G., Pile, J. 2014. The adaptatin-resistance spectrum: A classification of contemporary adaptation approaches to climate-related coastal change. **Ocean and Coastal Management 94**, 90-98.

Crawford, I. 1990. Agriculture, weeds, and the Western Isles machair. **Botanical Society of Edinburgh Transactions 45**, 483-492.

Crawford, I. 1997. The conservation and management of machair. **Botanical Journal of Scotland 49**, 433-439.

Dawson, A.G., Smith, D.E., Dawson, S. 2001. **Potential impacts of climate change on sea levels around Scotland**. Scottish Natural Heritage Research, Survey, and Monitoring Report No. 178. Scottish Natural Heritage, Perth.

Dawson, A.G., Hickey, K., Holt, T., Elliott, L., Dawson, S., Foster, I.D.L., Wadhams, P., Jonsdottir, I., Wilkinson, J., McKenna, J. Davis, N.R., Smith, D.E. 2002. Complex North Atlantic Oscillation (NAO) index signal of historic North Atlantic storm track changes. **The Holocene 12**, 363-369.

Dawson, A.G., Elliot, L., Noone, S., Hickey, K., Holt, T., Wadhams, P., Foster, I. 2004. Historical storminess and climate 'see-saws' in the North Atlantic region. **Marine Geology 210**, 247-259.

Dawson, A.G., Dawson, S. and Ritchie, W. 2007a. Historical climatology and coastal change associated with the 'Great Storm' of January 2005, South Uist and Benbecula, Scottish Outer Hebrides. **Scottish Geographical Journal 123**, 135-149.

Dawson, A.G., Ritchie, W., Green, D.R., Wright, R., Gomez, C., Taylor, A. 2007b. **Assessment of the rates and causes of change in Scotland's beaches and dunes – Phase 2**. SNH Commissioned Report.

Dawson, A.G., McIlveny, J., Warren, J. 2010. Winter gale day frequency in Shetland and Faeroes, AD 1866-1905: Links to sea ice history and the North Atlantic Oscillation. **Scottish Geographical Journal 126**, 141-152.

Dawson, A.G., Warren, J., Gomez, C., Ritchie, W. 2011. **Weather and Coastal Flooding History: The Uists and Benbecula.** Commissioned report for Comhairle nan Eilean Siar, South Ford Hydrodynamic Study.

Dawson, A.G., Gomez, C., Ritchie, W., Batstone, C., Lawless, M., Rowan, J.S., Dawson, S., McIlveny, J., Bates, R., Muir, D. 2012. Barrier island geomorphology, hydrodynamic modelling, and historical shoreline changes: An

example from South Uist and Benbecula, Scottish Outer Hebrides. **Journal of Coastal Research 28**, 1462-1476.

Dawson, S., Smith, D.E., Jordan, J., Dawson, A.G. 2004. Late Holocene coastal sand movements in the Outer Hebrides, N.W. Scotland. **Marine Geology 210**, 281-306.

Dawson, S., Powell, V.A. 2012. Chapter 4. Relative sea level rise. In: Ghimire, S. (Ed.), **Coastal Flooding in Scotland: A guidance document for coastal practitioners**. CREW, pp. 27-31.

Dawson, S., Powell, V.A., Duck, R.W., McGlashan, D.J. 2013. Discussion of Rennie, A.F. and Hansom, J.D. 2011. Sea level trend reversal: Land uplift outpaced by sea level rise on Scotland's coast. Geomorphology 125, 193-202.

De la Vega-Leinert, A.C., Nicholls, R.J., 2008. Potential implications of sea-level rise for Great Britain. **Journal of Coastal Research 24**, 342-357.

Dickinson, G. 1975. Man and machair soil ecosystems. In: Ranwell, D.S. (Ed.), **Sand Dune Machair 2**, NERC, Aberdeen, pp. 5-6.

Doerr, S.H., Shaeksby, R.A., Blake, W.H., Humphreys, G.S., Chafer, C. and Wallbrink, P.J. 2006. Occurrence, prediction and hydrological effects of water repellency amongst major soil and land use types in a humid temperate climate. **European Journal of Soil Science 57**, 741-754.

Emery, K.O., Aubrey, D.G. 1991. **Sea Levels, Land Levels and Tide Gauges.** Springer-Verlag, New York, p. 237.

Firth, C.R., Smith, D.E., Hansom, J.D., Pearson, S.G. 1995. Holocene spit development on a regressive shoreline, Dornoch Firth, Scotland. **Marine Geology 124**, 203-214.

Gilbertson, D.D., Grattan, J., Pyatt, B. 1996a. A reconnaissance of the potential 'coastal-erosion archaeological-hazard' on the islands of Barra, Vatersay, Sandray, and Mingulay. In: Gilbertson, D.D., Kent, M., Grattan, J. (Eds.), **The Outer Hebrides: The Last 14,000 Years**. Sheffield Academic Press, Sheffield, pp. 103-122.

Gilbertson, D.D., Grattan, J., Pyatt, B., Schwenninger, J.-L. 1996b. The Quaternary geology of the coasts of the islands of the southern Outer Hebrides. In: Gilbertson, D.D., Kent, M., Grattan, J. (Eds.), **The Outer Hebrides: The Last 14,000 Years**. Sheffield Academic Press, Sheffield, pp. 59-103.

Gilbertson, D.D., Schwenninger, J.-L., Kemp, R.A., Rhodes, E.J. 1999. Sand-drift and soil formation along an exposed North Atlantic coastline: 14,000 years of diverse geomorphological, climatic, and human impacts. **Journal of Archaeological Science 26**, 439-469.

Gómez, C., Wulder, M.A., Dawson, A.G., Ritchie, W., Green, D.R. 2014. Shoreline change and coastal vulnerability characterisation with Landsat imagery: A case study in the Outer Hebrides, Scotland. **Scottish Geographical Journal**, DOI: 10.1080/14702541.2014.923579.

Gordon, J.E., Bruneau, P.M.C., Brazier, V. 2014. Valuing the soil: Connecting land, people, and nature in Scotland. In: Churchman, G.J., Landa, E.R. (Eds.), **The Soil Underfoot: Infinite possibilities for a finite resource**. CRC Press, Boca Raton, FL, pp. 337-350.

Grattan, J., Gilbertson, D.D., Pyatt, B. 1996. Geochemical investigations of environmental change in the Outer Hebrides. In: Gilbertson, D.D., Kent, M., Grattan, J. (Eds), **The Outer Hebrides: The Last 14,000 Years**. Sheffield Academic Press Ltd., Sheffield, pp. 27-44.

Hall, A. 1996. Quaternary geomorphology of the Outer Hebrides. In: Gilbertson, D., Kent, M., Grattan, J. (Eds.), **The Outer Hebrides: The Last 14,000 Years**. Sheffield Academic Press, Sheffield, pp. 5-12.

Hallett, P.D., Young, I.M. 1999. Changes to water repellence of soil aggregates caused by substrate-induced microbial activity. **European Journal of Soil Science 50**, 35-40.

Hansom J.D., Angus, S. 2001. Tir a'mhachair (Land of the machair): Sediment supply and climate change scenarios for the future of the Outer Hebrides machair. In: Gordon, J.E., Leys, K.F. (Eds.), **Earth Science and the Natural Heritage: Interactions and Integrated Management**. The Stationary Office, Edinburgh, pp. 68-81.

Hansom, J.D., McGlashan, D.J. 2004. Scotland's coast: Understanding past and present processes for sustainable management. **Scottish Geographical Journal 120**, 99-116.

Hansom, J.D., Angus, S. 2005. Machair nan Eilean Siar (Machair of the Western Isles). **Scottish Geographical Journal 121**, 401-411.

Harley, M.D., Turner, I.L., Short, A.D., Ranasinghe, R. 2011. Assessment and integration of conventional, RTK-dGPS and image-derived beach survey methods for daily to decadal coastal monitoring. **Coastal Engineering 58**, 194-205.

Himmelstoss, E.A. 2009. DSAS installation instructions and user guide. In: Thieler, E.R., Himmelstoss, E.A., Zichichi, J.L., Ergul, A. (Authors), **Digital Shoreline Analysis System (DSAS) version 4.0 – An ArcGIS extension for calculating shoreline change.** U.S. Geological Survey open-file report 2008-1278.

Hughes, M.L., McDowell, P.F., Marcus, W.A. 2006. Accuracy assessment of georectified aerial photos: implications for measuring lateral channel movement in a GIS. **Geomorphology 74**, 1-16.

Hurrell, J.W. 1995. Decadal trends in North Atlantic Oscillation and relationships to regional temperature and precipitation. **Science 269**, 676-679.

IPCC (Intergovernmental Panel on Climate Change), 2007. Contribution of working group II to the fourth assessment report of the Intergovernmental Panel on Climate Change. Parry, M.L., Canziani, O.F., Palutikof, J.P., van der Linden, P.J., Hanson, C.E. (Eds.). Cambridge University Press, Cambridge.

IPCC, 2013. Summary for Policymakers. Stocker, T.F., Qin, D., Plattner, G-K., Tignor, M.M.B., Allen, S.K., Boschung, J., Nauels, A., Xia, Y., Bex, V., Midgley, P.M. (Eds.). Working group 1 contribution to the fifth assessment report of the Intergovernmental Panel on Climate Change. IPCC, Switzerland.

James, L.A., Hodgson, M.E., Ghoshal, S., Latiolais, M.M. 2012. Geomorphic change detection using historic maps and DEM differencing: The temporal dimension of geospatial analysis. **Geomorphology 137**, 181-198.

JNCC (Joint Nature Conservation Committee) 2007. **Conservation Status Assessment for Habitat: H21A0 – Machairs**. http://jncc.defra.gov.uk/pdf/Article17/FCS2007-H21A0-Final.pdf (accessed December 27, 2011).

Jones, P.D., Jónsson, T., Wheeler, D. 1997. Extension to the North Atlantic Oscillation using early instrumental pressure observations from Gibraltar and South-West Iceland. **International Journal of Climatology 17**, 1433-1450.

Jordan, J.T., Dawson, S., Dawson, A.G. 2004. Late Holocene coastal dune evolution, Lewis and Harris, Scottish Outer Hebrides. In: Angus, S., Ritchie, W. (Eds.), **Littoral**. Aberdeen Institute for Coastal Science and Management, Aberdeen.

Judge, E.K., Overton, M.F., Fisher, J.S. 2003. Vulnerability indicators for coastal dunes. **Journal of Waterway, Port, Coastal, and Ocean Engineering 129**, 270-278.

Knox, A.J. 1974. Agricultural use of machair. In: Ranwell, D.S. (Ed.), **Sand Dune Machair**. Monks Wood Experimental Station: Institute of Terrestrial Ecology.

Krammes, J.S., Debano, L.F. 1965. Soil wettability: A neglected factor in watershed management. **Water Resources Research 1**, 283-286.

Lambert, S.J., Fyfe, J.C. 2006. Changes in winter cyclone frequencies and strengths simulated in enhanced greenhouse warming experiments: results from the models participating in the IPCC diagnositic exercise. **Climate Dynamics 26**, 713-728.

Lewis, R.J., Marrs, R.H., Pakeman, R.J. 2014. Inferring temporal shifts in landuse intensity from functional response traits and functional diversity patterns: a study of Scotland's machair grassland. **OIKOS 123**, 334-344.

Leys, J., Koen, T., McTanish, G. 1996. The effect of dry aggregation and percentage clay on sediment flux as measured by a portable field wind tunnel. **Australian Journal of Soil Reseach 34**, 849-861.

MacDonald, A. A. 2011. Leave crofters to deal with the machair. **The Scottish Farmer**. [online] Available at: http://www.thescottishfarmer.co.uk/leave-crofters-to-deal-with-the-machair. (Accessed 26 March 2013).

Mate, I.D. 1992. The theoretical development of machair in the Hebrides. **Scottish Geographical Magazine 108**, 35-38.

Mather, A.S., Ritchie, W. 1977. **The Beaches of the Highlands and Islands of Scotland**. Commissioned report for the Countryside Commission for Scotland, Battleby.

Matulla, C., Schöner, Alexandersson, H., von Storch, H., Wang, X.L. 2008. European storminess: Late nineteenth century to present. **Climate Dynamics 31**, 125-130.

McClatchey, J., Devoy, R., Woolf, D., Bremner, B., James, N. 2014. Climate change and adaptation in the coastal areas of Europe's northern periphery region. **Ocean and Coastal Management 94,** 9-21.

Meteorlogical Office. 2010. Monthly mean station data for South Uist Range from 2005-2010.

Miller, T.L., Fletcher, C.H. 2003. Waikiki: Historical analysis of an engineered shoreline. **Journal of Coastal Research 19**, 1026-1043.

Milne, F., Dong, P., Davidson, M. 2012. Natural variability and anthropogenic effects on the morphodynamics of a beach-dune system at Montrose Bay, Scotland. **Journal of Coastal Research 28**, 375-388.

Mitasova, H., Overton, M., Harmon, R.S. 2005. Geospatial analysis of a coastal sand dune field evolution: Jockey's Ridge, North Carolina. **Geomorphology 72**, 204-221.

Montreuil, A-L., Bullard, J.E., 2012. A 150-year record of coastline dynamics within a sediment cell: Eastern England. **Geomorphology 179**, 168-185.

Moore, H., Wilson, G., Dawson, A.G., Dawson, S. 2005. **Western Isles (South) Coastal Zone Assessment Survey, Grimsay, Benbecula and South Uist**. Commissioned report for Historic Scotland and Scottish Coastal Archaeology and the Problem of Erosion. EASE Archaeological Consultants, Edinburgh.

Moore, L.J. 2000. Shoreline mapping techniques. **Journal of Coastal Research 16**, 111-124.

Mørk, G., Barstow, S., Kabuth, A., Pontes, M.T. 2010. Assessing the global wave energy potential. In: **Proceedings of OMAE2010**, 29th International Conference on Ocean, Offshore Mechanics, and Arctic Engineering, Shanghai. ASME.

Morton, R.A., Speed, F.M. 1998. Evaluation of shorelines and legal boundaries controlled by water levels on sandy beaches. **Journal of Coastal Research 14**, pp. 1373-1384.

Muir, D., Cooper, J.A.G., Pétursdóttir, G. 2014. Challenges and opportunities in climate change adaptation for communities in Europe's northern periphery. **Ocean and Coastal Management 94**, 1-8.

Murray-Hicks, D., Green, M.O., Smith, R.K., Swales, A., Ovenden, R., Walsh, J. 2002. Sand volume change and cross-shore sand transfer, Mangawhai Beach, New Zealand. **Journal of Coastal Research 18**, 760-775.

Nelson, S.E. 1998. **Soil fungi, soil stabilisation and implications for wind erosion**. PhD thesis. Department of Agricultural Sciences, La Trobe University, Victoria (Australia).

Nicholls, R., Wong, P., Burkett, V., Codignotto, J., Hay, J., McLean, R., Woodroffe, S.R.C. 2007. Coastal systems and low-lying areas. In: Parry, M., Canziani, O., Palutikof, J., Linden, P.V.D., Hanson, C. (Eds.), **Climate Change 2007: Impacts, Adaptation, and Vulnerability**. Contribution of Working Group II to the Fourth Assessment Report of the Intergovernmental Panel on Climate Change. Cambridge University Press, Cambridge.

Oades, J.M., Waters, A.G. 1991. Aggregate hierarchy in soils. **Australian Journal of Soil Research 29**, 815-828.

Oliver, R. 1993. **Ordnance Survey maps: A concise guide for historians**. Charles Close Society, London, pp. 192.

Owen, N., Kent, M., Dale, P. 2000. Ecological effects of cultivation on the machair sand dune systems of the Outer Hebrides, Scotland. **Journal of Coastal Conservation 6**, 155-170.

Pardo-Pascual, J.E., García-Asenjo, L., Palomar-Vásquez, J., Garrigues-Talens, P. 2005. New methods and tools to analyse beach-dune system evolution using a real-time kinematic global positioning system and geographic information systems. **Journal of Coastal Research SI 49**, 34-39.

Pepe, G., Coutu, G. 2008. Beach morphology change using ArcGIS spatial analyst. **Middle States Geographer 41**, 91-97.

Phillips, J.D. 2009. Changes, perturbations, and responses in geomorphic systems. **Progress in Physical Geography 33**, 17-30.

Phillips, M.R., Rees, E.F., Thomas, T. 2013. Winds, sea levels and North Atlantic Oscillation (NAO) influences: An evaluation. **Global and Planetary Change 100**, 145-152.

Pye, K., Blott, S.J. 2006. Coastal processes and morphological change in the Dunwich-Sizewell area, Suffolk, UK. **Journal of Coastal Research 22**, 453-473.

Randall, R. 2004. Soils of the Heisgeir machair complex, Outer Hebrides. In: Angus, S. Ritchie, W. (Eds.), **Littoral**, Aberdeen Institute for Coastal Science and Management, Aberdeen, pp. 49-60.

Rennie, A.F., Hansom, J.D. 2011. Sea level trend reversal: Land uplift outpaced by sea level rise on Scotland's coast. **Geomorphology 125**, 193-202.

Richards, L.A.R. and Phipps, P.J. 2007. Managing the impact of climate change on vulnerable areas: A case study of the Western Isles, UK. In: **Landslides and**

Climate Change – Challenges and Solutions, Centre for the Coastal Environment, Ventnor, May 2004.

Ritchie, W. 1966. The post-glacial rise in sea level and coastal changes in the Uists. **Transactions of the Institute of British Geographers 39**, 79-86.

Ritchie, W. 1967. The machair of South Uist. **Scottish Geographical Magazine 83**, 161-173.

Ritchie, W. 1971. **The beaches of Barra and the Uists.** A survey of the beach, dune and machair areas of Barra, South Uist, Benbecula, North Uist and Berneray. Commissioned report no. 047 for Scottish Natural Heritage. Aberdeen.

Ritchie, W. 1974. Spatial variation in shell sand content between and within machair systems. In: Ranwell, D.S. (Ed.), **Sand Dune Machair**. NERC, Norwich, pp. 9-12.

Ritchie, W. 1976. The meaning and definition of machair. **Transactions of the Botanical Society of Edinburgh 42**, 431-440.

Ritchie, W. 1979. Machair development and chronology in the Uists and adjacent islands. **Proceedings of the Royal Society of Edinburgh 77** (B), 107-122.

Ritchie, W., Whittington, G. 1994. Non-synchronous aeolian sand movements in the Uists: The evidence of the intertidal organic and sand deposits at Cladach Mór, North Uist. **Scottish Geographical Magazine 110**, 40-46.

Ritchie, W., Whittington, G., Edwards, K.J. 2001. Holocene changes in the physiography and vegetation of the Atlantic littoral of the Uists, Outer Hebrides, Scotland. **Transactions of the Royal Society of Edinburgh 92**, 121-136.

Rogers, J., Hamer, B., Brampton, A., Challinor, S., Glennerster, M., Brenton, P., Bradbury, A. 2010. **Beach Management Manual (second edition)**. CIRIA, London.

Rowan, J.S., Black, S., Franks, S.W. 2012. Sediment fingerprinting as an environmental forensics tool explaining cyanobacteria blooms in lakes. **Applied Geography 32**, 832-843.

Seaton, D. 1968. Bornish blow-out: a record of co-operation in overcoming machair and land erosion. **Scottish Agriculture 47**, 145-148.

Schumm, S.A. 1979. Geomorphic thresholds: The concept and its applications. **Transactions of the Institute of British Geographers NS4**, 485-515.

The Scottish Government 2012. **Cropped Machair**. Rural priorities, Scotland Rural Development Programme. [online] Available at: http://www.scotland.gov.uk/Topics/farmingrural/SRDP/RuralPriorities/Options/Managementcroppedmachair [Accessed 24 March 2013].

Shalowitz, A.L. 1964. Shoreline and sea boundaries: Washington D.C., U.S. Department of Commerce. **Coast and Geodetic Survey volume 1**, pp. 420.

Shennan, I., Milne, G., Bradley, S. 2012. Late Holocene vertical land motion and relative sea-level changes: lessons from the British Isles. **Journal of Quaternary Science 27**, 64-70.

Sinclair, M.R., Watterson, I.G. 1999. Objective assessment of extratropical weather systems in simulated climates. **Journal of Climate 12**, 3467-3485.

SNH (Scottish Natural Heritage) 2012. Machair. [online] Available at: http://www.snh.gov.uk/about-scotlands-nature/habitats-and-ecosystems/coasts-and-seas/coastal-habitats/machair/ [Accessed 13 February 2013].

Soil Survey of Scotland, 1985. Sheets 18-22. Macaulay Institute for Soil Research, Aberdeen.

Srinavasan, A. (Ed.). 2006. **Asian Aspirations for Climate Regime Beyond 2012.** Institute for Global Strategies. Hayama, Japan. pp. 77-100.

Stockdon, H.F., Doran, K.S., Sallenger Jr., A.H. 2009. Extraction of LiDAR-based dune-crest elevations for use in examining the vulnerability of beaches to inundation during hurricanes. **Journal of Coastal Research SI 53**, 59-65.

Sun, H., Nelson, M., Chen, F., Husch, J. 2009. Soil mineral structural water loss during loss on ignition analyses. **Canadian Journal of Soil Science 89**, 603-610.

Swales, A. 2002. Geostatistical estimation of short-term changes in beach morphology and sand budget. **Journal of Coastal Research 18**, 338-351.

Szava-Kovats, R. 2009. Re-analysis of the relationship between organic carbon and loss-on-ignition in soil. **Communications in Soil Science and Plant Analysis 40**, 2712-2724.

Thieler, E.R., Himmelstoss, E.A., Zichichi, J.L., Ayhan, E. 2009. **Digital Shoreline Analysis System (DSAS) version 4.0 – An ArcGIS extension for calculating shoreline change**. U.S. Geological Survey Open-file report 2008-1278.

Thomas, T., Phillips, M.R., Williams, A.T. 2010. Mesoscale evolution of a headland bay: Beach rotation processes. **Geomorphology 123**, 129-141.

Thomas, T., Phillips, M.R., Williams, A.T., Jenkins, R.E. 2011a. Short-term beach rotation, wave climate and the North Atlantic Oscillation (NAO). **Progress in Physical Geography 33**, 333-352.

Thomas, T., Phillips, M.R., Williams, A.T., Jenkins, R.E. 2011b. A multi-century record of linked nearshore and coastal change. **Earth Surface Processes and Landforms 36**, 995-1006.

Thorsen, M.K., Hopkins, D.W., Woodward, S., McKenzie, B.M. 2010. Resilience of microorganisms and aggregation of a sandy calcareous soil to amendment with organic and synthetic fertiliser. **Soil Use and Management 26**, 149-157.

Tisdall, J.M., Nelson, S.E., Wilkinson, K., Smith, S.E. and McKenzie, B.M. 2012. Stabilisation of soil against wind erosion by six saprotrophic fungi. **Soil Biology and Biochemistry 50**, 134-141.

Trewin, N.H. 2002. **The Geology of Scotland**. Geological Society of London, London, pp. 576.

Trouet, V., Scourse, J.D., Raible, C.C. 2012. North Atlantic storminess and Atlantic Meridional Overturning Circulation during the last Millennium: Reconciling contradictory proxy records of NAO variability. **Global and Planetary Change 84-85**, 48-55.

Tsimplis, M.N., Woolf, D.K., Osborn, T., Wakelin, S., Woodworth, P., Wolf, J., Flather, R., Blackman, D., Shaw, A.G.P., Pert, F., Challenor, P., Yan, Z. 2005. Towards a vulnerability assessment of the UK and northern European coasts: the role of regional climate variability. **Philosophical Transactions: Mathematical, Physical and Engineering Sciences**, doi:10.1098/rsta.2005.1571.

UK Climate Projections, 2009. Key findings for Scotland North. DEFRA http://ukclimateprojections.defra.gov.uk/content/view/2153/499/ (accessed September 19, 2011).

Valentin, H. 1954. Land loss at Holderness. Reprinted in 1971 in: Steers, J.A. (Ed.) **Applied Coastal Geomorphology**. Macmillan, London, pp. 116-137.

Von Ahn, J.M., Sienkiewicz, J.M., Chang, P.S. 2006. Operational impact of QuikSCAT winds at the NOAA Ocean Prediction Centre. **Weather Forecasting 21**, 523-539.

Wakelin, S.L., Woodworth, P.L., Flather, R.A., Williams, J.A. 2003. Sea-level dependence on the NAO over the NW European continental shelf. **Geophysical Research Letters 30**, 10.1029/2003GL017041.

Walton Jr., T.L. 1992. Interim guidance for prediction of wave run-up on beaches. **Ocean Engineering 19**, 199-207.

Wang, P., Roberts, T.M. 2012. Volume and shoreline changes along Pinellas County beaches during tropical storm Debby https://www.pinellascounty.org/environment/coastalMngmt/pdfs/Beaches-Tropical-Storm-Debby-Impacts-7-24-12.pdf (accesssed October 20, 2014)

Wang, Q., Li, Y., Wang, Y. 2011. Optimising the weight loss-on-ignition methodology to quantify organic and carbonate carbon of sediments from diverse sources. **Environmental Monitoring and Assessment 174**, 241-257.

Wang, X.L., Zwiers, F.W., Swail, V.R. 2004. North Atlantic Ocean wave climate change scenarios for the twenty-first century. **Journal of Climate 17**, 2368-2383.

Wavenet. 2012. Half-hourly wave buoy data from the West of Hebrides site, from 2009-2012. Centre for Environment, Fisheries, and Aquaculture Science.

Wessel, A.T. 2006. On using the effective contact angle and the water drop penetration time for classification of water repellency in dune soils. **Earth Surface Processes and Landforms 13**, 555-561.

Wheaton, J.M., Brasington, J., Darby, S.E., Sear, D. 2010. Accounting for uncertainty in DEMs from repeat topographic surveys: Improved sediment budgets. **Earth Surface Processes and Landforms 35**, 136-156.

Williams, R.D. 2012. DEMs of difference. In: Clarke, L., Nield, J. (Eds.), **Geomorphological Techniques (Online Edition)**; London, UK. ISSN: 2047-0371.

Wilson, P. 2002. Holocene coastal dune development on the South Erradale peninsula, Wester Ross, Scotland. **Scottish Journal of Geology 38**, 5-13.

Wolf, J. 2007. **Modelling of waves and set-up for the storm of 11-12 January 2005.** Internal document no. 181. Proudman Oceanographic Laboratory.

Wolf, J., Woolf, D.K. 2006. Waves and climate change in the north-east Atlantic. **Geophysical Research Letters 33**, doi: 10.1029/2005g1025113.

Woolf, D., Coll, J. 2013. Impacts of climate change on storms and waves. In: Buckley, P.J., Dye, S.R., Baxter, J.M. (Eds.), **Marine Climate Change Impacts Annual Report Card 2007-8.** Marine Climate Change Impacts Partnership, Lowestoft.

Young, E. 2012. Direct acquisition of elevation data using dGPS. In: Clarke, L. (Ed.) **Geomorphological Techniques** (online edition). British Society for Geomorphology. ISNN 2047-03

APPENDIX

Publications based on the work of this thesis:

Young, E.J., 2012. Section 2.1.3: Direct acquisition of elevation data using dGPS. In: Clarke, L.E., Nields, J.M. (Eds), **Geomorphological Techniques (Online edition)**. British Society for Geomorphology, London. ISSN: 2047-0371.

Young, E.J., Muir, D., Dawson, A., Dawson, S. 2014. Community driven coastal management: An example of the implementation of a coastal defence bund on South Uist, Scottish Outer Hebrides. **Ocean & Coastal Management 94**, 30-37.

Young, E.J., McKenzie, B.M., McNicol, J.W., Robertson, A.H.J., Wendler, R., Dawson, S. 2015 Spatial trends in the wind abrasion resistance of cultivated machair soil, South Uist, Scottish Outer Hebrides. **Catena 135**, 1-10.